PB86-219201

Numerical Simulations of Photochemical Air Pollution in the Northeastern United States ROM1 (Regional Oxident Model) Applications

(U.S.) Environmental Protection Agency
Research Triangle Park, NC

Jul 86

U.S. Department of Commerce
National Technical Information Service
NTIS

TECHNICAL REPORT DATA
(Please read Instructions on the reverse before completing)

1. REPORT NO. EPA/600/3-86/038	2.	3. RECIPIENT'S ACCESSION NO. PB86 219201/AS

4. TITLE AND SUBTITLE NUMERICAL SIMULATIONS OF PHOTOCHEMICAL AIR POLLUTION IN THE NORTHEASTERN UNITED STATES: ROM1 APPLICATIONS	5. REPORT DATE July 1986 6. PERFORMING ORGANIZATION CODE
7. AUTHOR(S) Robert G. Lamb	8. PERFORMING ORGANIZATION REPORT NO.
9. PERFORMING ORGANIZATION NAME AND ADDRESS Same as Block 12	10. PROGRAM ELEMENT NO. CDWA1A/02-1335 (FY-86) 11. CONTRACT/GRANT NO.
12. SPONSORING AGENCY NAME AND ADDRESS Atmospheric Sciences Research Laboratory -- RTP, NC Office of Research and Development U.S. Environmental Protection Agency Research Triangle Park, NC 27711	13. TYPE OF REPORT AND PERIOD COVERED Final 14. SPONSORING AGENCY CODE EPA/600/9

15. SUPPLEMENTARY NOTES

16. ABSTRACT

The first-generation Regional Oxidant Model (ROM1) was used to simulate pollutant concentrations during the nine-day period 23-31 July 1980. The one-hour and daily daylight (0900-1600 LST) averaged ozone concentrations produced in each of two simulations, one representing 1980 base emissions and the other projected 1987 emission, were compared to assess the effectiveness of the proposed emissions changes on air quality.

The analyses of the model results are prefaced by discussions of a number of basic issues on regional scale modeling, including model initialization, selection of meteorological data, effects of grid size on model performance, estimating long-term concentration statistics from short-period simulations, probabilistic vs. quasi-deterministic modes of model operation, uncertainty in emissions estimates, the characteristics of VOC and NO_x sources in the Northeast, and other topics. Preliminary results of analyses of the SAROAD monitoring data, which reveal the characteristics of the ozone problem in the northeastern United States, set the stage for the model simulations.

NCR

17. KEY WORDS AND DOCUMENT ANALYSIS

a. DESCRIPTORS	b. IDENTIFIERS/OPEN ENDED TERMS	c. COSATI Field/Group

18. DISTRIBUTION STATEMENT RELEASE TO PUBLIC	19. SECURITY CLASS *(This Report)* UNCLASSIFIED	21. NO. OF PAGES 175
	20. SECURITY CLASS *(This page)* UNCLASSIFIED	22. PRICE

EPA Form 2220-1 (Rev. 4-77) PREVIOUS EDITION IS OBSOLETE

PB86-219201

EPA/600/3-86-038
July 1986

NUMERICAL SIMULATIONS OF PHOTOCHEMICAL AIR POLLUTION IN THE NORTHEASTERN UNITED STATES: ROM1 APPLICATIONS

by

Robert G. Lamb
Meteorology and Assessment Division
Atmospheric Sciences Research Laboratory
Research Triangle Park, North Carolina 27711

ATMOSPHERIC SCIENCES RESEARCH LABORATORY
OFFICE OF RESEARCH AND DEVELOPMENT
U.S. ENVIRONMENTAL PROTECTION AGENCY
RESEARCH TRIANGLE PARK, NC 27711

REPRODUCED BY
NATIONAL TECHNICAL
INFORMATION SERVICE
U.S. DEPARTMENT OF COMMERCE
SPRINGFIELD, VA. 22161

NOTICE

The information in this document has been funded by the United States Environmental Protection Agency. It has been subject to the Agency's peer and administrative review, and it has been approved for publication as an EPA document. Mention of trade names or commercial products does not constitute endorsement or recommendation for use.

The author, Robert G. Lamb, is on assignment to the Atmospheric Sciences Research Laboratory, U.S. Environmental Protection Agency, from the National Oceanic and Atmospheric Administration, U.S. Department of Commerce.

ABSTRACT

The first-generation Regional Oxidant Model (ROM1) was used to simulate pollutant concentrations during the nine-day period 23-31 July 1980. Two simulations were performed. The first, which is considered to be the base case, used the 1980 NAPAP 4.2 inventory for all hydrocarbon and NO_x emission rates. The second simulation, or control case, was identical in all respects except that the county-by-county hydrocarbon and NO_x emissions rates were modified in accordance with baseline projections for 1987 contained in SIPs. The one-hour and daily daylight (0900-1600 LST) averaged ozone concentrations produced in each simulation were compared to assess the effectiveness of the proposed emissions changes on air quality.

It was found that ozone concentrations in the control case were everywhere lower than those in the base case, but the percentage reduction was not uniform in space. In areas near the major VOC and NO_x sources, the maximum one-hour averaged ozone levels were reduced by about 25% while in areas farther than 100 km from these sources peak values were only about 10% lower. Slightly smaller percentage reductions were found in the daily daylight averaged ozone concentrations. It was also found that the emissions reductions lowered peak ozone concentrations by considerably larger percentages than they reduced the median or mean concentration values.

The analyses of the model results are prefaced by discussions of a number of basic issues on regional scale modeling, including model

ABSTRACT

The first-generation Regional Oxidant Model (ROM1) was used to simulate pollutant concentrations during the nine-day period 23-31 July 1980. Two simulations were performed. The first, which is considered to be the base case, used the 1980 NAPAP 4.2 inventory for all hydrocarbon and NO_x emission rates. The second simulation, or control case, was identical in all respects except that the county-by-county hydrocarbon and NO_x emissions rates were modified in accordance with baseline projections for 1987 contained in SIPs. The one-hour and daily daylight (0900-1600 LST) averaged ozone concentrations produced in each simulation were compared to assess the effectiveness of the proposed emissions changes on air quality.

It was found that ozone concentrations in the control case were everywhere lower than those in the base case, but the percentage reduction was not uniform in space. In areas near the major VOC and NO_x sources, the maximum one-hour averaged ozone levels were reduced by about 25% while in areas farther than 100 km from these sources peak values were only about 10% lower. Slightly smaller percentage reductions were found in the daily daylight averaged ozone concentrations. It was also found that the emissions reductions lowered peak ozone concentrations by considerably larger percentages than they reduced the median or mean concentration values.

The analyses of the model results are prefaced by discussions of a number of basic issues on regional scale modeling, including model

initialization, selection of meteorological data, effects of grid size on model performance, estimating long-term concentration statistics from short-period simulations, probabilistic vs quasi-deterministic modes of model operation, uncertainty in emissions estimates, the characteristics of VOC and NO_x sources in the Northeast, and other topics. Preliminary results of analyses of the SAROAD monitoring data, which reveal the characteristics of the ozone problem in the northeastern United States, set the stage for the model simulations.

CONTENTS

Abstract iii
Figures vi
Tables x
Acknowledgments xi

1. Introduction 1
2. Overview of the Regional Oxidant Model 2
3. Characteristics of Observed Ozone Concentrations in the Northeastern United States 11
4. The Sources of Ozone Precursor Species in the Northeastern United States 26
    - The spatial scales of the VOC and NO_x sources 35
    - Uncertainty in gridded NO_x and VOC emissions 39
5. Definitions of Receptor Classes for Use in Analyzing Simulated Concentrations 47
6. Meteorology of the Test Period: 23 - 31 July 1980 58
7. The Control Strategy Emissions Inventory 72
8. Results of Model Simulations 81
    - Specification of input parameters for the model simulations 81
        - Initial and boundary conditions 82
        - Deposition velocities 84
        - Miscellaneous Fields 86
    - Comparison of predicted and observed ozone concentrations 86
    - Results of base emissions simulations 91
    - Simulated effects of emissions controls on ozone concentrations in the Northeast 100
9. Conclusions 119

References 125

Appendices

A. 127
B. 137
C. 146
D. 152

FIGURES

Number Page

2-1 Modeling domain treated in the present study. Each dot represents a grid cell 5

2-2 Illustration of the daytime (A) and nighttime (B) meteorological phenomena treated by the ROM and the vertical structure (C) used to simulate these processes 6

2-3 Schematic illustration of the network of processors and core module that compose the Regional Oxidant Model (ROM) . . . 7

3-1 Maximum hourly averaged ozone concentration (ppb) observed during July - September 1980 20

3-2 Locations and record lengths (in days) of hourly averaged ozone measurements during July - September 1980 21

3-3 Maximum hourly averaged ozone observed during an episode on 21 July 1980 22

3-4 Difference (ppb) between the maximum hourly averaged ozone concentration observed during the daytime (1000-1759 LST) at each monitoring station during June-August 1980 and the maximum value observed at night (2100-0959 LST) at the same station over the same 3-month period 23

3-5 Maximum hourly averaged ozone (ppb) observed during the nighttime hours (2100-0959 LST) during June - August 1980 . . . 24

3-6 Number of days in 1980 in which the maximum hourly averaged ozone exceeded 120 ppb 25

4-1 Locations of the 70 major source counties listed in Tables 4-1, 2. See Eq. 4.7 for definitions of "high VOC", "high NO_x", and "high VOC and NO_x" 43

4-2 Cumulative VOC and NO_x emissions densities vs. cumulative source area and characteristic length scale. See text, pages 36-37, for details 44

4-3 Comparison of NAPAP and NECRMP estimates of gridded VOC emissions for the 200 strongest source cells in the ROM grid network 45

4-4 Comparison of NAPAP and NECRMP estimates of gridded NO_x emissions for the 200 strongest source cells in the ROM grid network 46

Number Page

5-1 Locations of the 70 cells selected in each of the four receptor classes urban (U), suburban (S), rural (R) and wilderness (W) 53

5-2 Locations of the 70 major source counties, defined as "urban" type receptors 54

5-3 Non-major source Standard Metropolitan Statistical Areas (SMSAs) defined here as "suburban" type receptors 55

5-4 Non-major source, non-SMSA counties in which the predominant land use is in agricultural activities, defined here as "agricultural" type receptors 56

5-5 Counties in which forest and/or wetlands are the predominant land use, defined here as "natural" type receptors. 57

6-1 Quartile plot of the maximum hourly averaged ozone concentrations observed at some 200 SAROAD monitoring stations each day during the period June - August 1980. See text, page 60, for explanation of symbols. 67

6-2a Quantile - quantile comparisons of the cumulative frequency distributions of hourly ozone concentrations at a rural site in Connecticut (070570007). The ordinate (y-axis) represents the distribution observed during the meteorological scenario period 23-31 July 1980 while the abscissa (x-axis) represents the distribution observed over the entire summer, June - August 68

6-2b Same as 6-2a except data are from Whiteface Mountain, New York (33020002) 69

6-2c Same as 6-2a except data are from a New Jersey site (312750001) about 50 km east of Philadelphia. 70

6-3 Trajectories calculated from wind fields used in Layer 1 of the ROM for the 9-day meteorological scenario 23-31 July 1980 (Julian dates 205-213). Numbers along the trajectories refer to Julian date 71

7-1a VOC emissions in the control strategy expressed as a percentage reduction in the base emissions. (See Appendix B for details.) 75

7-1b NO_x emissions in the control strategy expressed as a percentage reduction in the base emissions. (See Appendix B for details.) 76

Number Page

7-2 Comparison of base and controlled emissions of VOC (moles/day) of the 200 strongest VOC emitting cells in the ROM domain, Canada excluded. (All point and area sources within each cell are combined.) 77

7-3 Comparison of base and controlled emissions of NO_x (moles/day) of the 200 strongest NO_x emitting cells in the ROM domain, Canada excluded. (All point and area sources within each cell are combined.) 78

7-4 Base vs. controlled VOC emissions (moles per km^2 per day) of the 70 major source counties listed in Tables 4-1,2 79

7-5 Base vs. controlled NO_x emissions (moles per km^2 per day) of the 70 major source counties listed in Tables 4-1,2 80

8-1 Maximum ozone concentration during the 9-day scenario simulated using the base emissions inventory. Isopleths are drawn at intervals of 40 ppb. Numbers beside isopleths are ppb/100 104

8-2 Maximum hourly averaged ozone concentration observed at SAROAD monitoring sites during the scenario period 23-31 July 1980 . . 105

8-3 Simulated ozone in Layer 1 at hour 1600 EST on the first day of the 9-day scenario, using the base emissions inventory . . . 106

8-4 Same as 8-3 except hour 1600 of day 2 of the scenario 107

8-5 Same as 8-3 except hour 1600 of day 3 of the scenario 108

8-6 Same as 8-3 except hour 1600 of day 4 of the scenario 109

8-7 Same as 8-3 except hour 1600 of day 5 of the scenario 110

8-8 Same as 8-3 except hour 1600 of day 6 of the scenario 111

8-9 Same as 8-3 except hour 1600 of day 7 of the scenario 112

8-10 Same as 8-3 except hour 1600 of day 8 of the scenario 113

8-11 Same as 8-3 except hour 1600 of day 9 of the scenario 114

8-12 Quartile plots of simulated base case daily daylight averaged (0900-1600 LST) ozone concentrations in each of the four county receptor classes defined in Section 5. See page 96 for explanation of symbols 115

8-13 Quartile plots of simulated base case hourly ozone concentration in each of the four receptor cell classes defined in Section 5. See page 96 for an explanation of the graphs. 116

Number Page

8-14 Simulated effects of emissions controls on daily daylight (0900-1600 LST) averaged ozone concentrations in each of the four county receptor classes. See page 101 for an explanation of the symbols 117

8-15 Simulated effect of emission controls on hourly averaged ozone concentrations in each of the four receptor cell classes. See page 101 for an explanation of the symbols. 118

9-1 Counties in which simulated one-hour averaged ozone concentrations exceeded 120 ppb during the 9-day scenario. Light shading denotes counties in which exceedance occurred only in the base case simulation. Dark shading indicates areas where exceedance occurred in both the base and control runs. 124

TABLES

Number		Page
2-1	Chemical reactions included in the Demerjian/Schere mechanism and the rate constants assumed for each	8
2-2	Comparison of the principal differences between the first generation regional oxidant model used in the present study and the second generation model currently in development. . . .	10
4-1	Major county sources of VOC ranked in order of source strength Q (= mass per area per time). Counties marked with an asterisk (*) are also major sources of NO_x (listed in Table 4-2)	41
4-2	Major county sources of NO_x ranked in order of source strength Q (= mass per area per time). Counties marked with an asterisk (*) are also major sources of VOC (listed in Table 4-1)	42
8-1	Values used for the initial and boundary concentrations in both the base and control ROM applications	85

ACKNOWLEDGEMENT

The work reported here is the product of the efforts of many people to whom the author is sincerely grateful. Joan Novak coordinated data acquisition, programming and computer operations with unprecedented thoroughness and efficiency. James Reagan provided timely, masterful analyses of the ozone monitoring data. Ken Schere managed the chemistry aspects of the model with skill and precision, and Barbara Hinton exhibited her usual patience and proficiency in typing the manuscript. I am also indebted to the following members of Computer Science Corporation for his or her special contribution to this work: Lucille Bender, Larry Bergman, Russ Bullock, Tony Griffin, Don Pelles, Ted Smith, Joe Vaughan, and Jeff Young.

SECTION 1

INTRODUCTION

The development of the Environmental Protection Agency's Regional Oxidant Model (ROM) began in the late 1970's as a part of the Northeast Corridor Regional Modeling Project (NECRMP). The NECRMP was initiated out of the recognition that the adverse ozone concentrations observed in the Northeastern United States are due in large part to the regional transport of ozone and its precursor species. The principal role envisioned for the ROM in this project was to assist the states in developing emissions control plans that would effect compliance with the Federal ozone air quality standards in the most equitable and cost effective way. This report describes the second of a series of applications of the Regional Oxidant Model in this role. It considers projected 1987 emissions, based on 1982 State Implementation Plans (SIPs), and compares the ozone concentrations simulated using these emissions with the corresponding concentrations predicted using 1980 emissions data. This study also examines the character of the ozone problem in the Northeast; the strengths and spatial distributions of the sources of the precursor species, namely hydrocarbons and NO_x; meteorology; and other factors important in interpreting model results and in developing a basic understanding of the relationship between observed ozone levels and source emissions. These analyses begin in Section 3 following a brief summary of the structure of the ROM in Section 2. The projected 1987 emissions are described in Section 7 and results of the model simulations are presented in Section 8.

SECTION 2

OVERVIEW OF THE REGIONAL OXIDANT MODEL

The ROM is a three-dimensional Eulerian model that simulates hourly averaged species concentrations over the geographical area shown in Figure 2-1 (page 5) with a spatial resolution, or grid size, of approximately 18 km. (The actual grid dimensions are 1/4 degree longitude by 1/6 degree latitude.) The model has 3 layers in the vertical in which species concentrations are treated prognostically and it has a shallow layer adjacent to the ground in which concentrations are handled diagnostically. The latter is used primarily to simulate dry deposition processes and subgrid scale chemistry phenomena associated with line and point source plumes.

Each of the three prognostic layers has a thickness that varies in space and time in a manner designed to keep track of the dominant meteorological processes within that layer. Both the processes and the model's layer structure are illustrated in Figure 2-2 (page 6).

Generally speaking, the lowest layer, Layer 1 (see Figure 2-2c), handles wind shear and marine layers by day and the radiation inversion layer by night. Layer 2 simulates the free convective subcloud mixed layer by day and the reservoir of aged species above the radiation inversion by night. And Layer 3 represents the convective cloud layer by day and the zone of cloud residue by night. At any given location, the elevation of the top of Layer 3 is equivalent to the elevation of the tops of convective clouds at that location, regardless of how high the clouds might be. The entrainment of stratospheric ozone into the lower atmosphere can be simulated by prescribing the ozone flux across the top surface of Layer 3. Complete details on the structure of the ROM can be found in Lamb (1983a).

All of the chemical and physical processes that occur within the four layers that we have discussed are described by a system of differential equations that constitute the basis of the model's predictions. Computer solvable analogues of these equations comprise what we refer to as the core model. All of the independent variables that enter these equations, such as wind velocities, layer thicknesses, emission rates, etc, are prepared by a network of peripheral processors or modules for input to the core model. The relationships among the processors and CORE are depicted in Figure 2-3 (page 7). By structuring the ROM in this modular fashion, we can change the method used to generate individual variables without having to overhaul the entire model. Note that even the chemical kinetics mechanism, which is a major component of any photochemical model, is among the interchangeable components. Thus, when we refer to a particular "generation" of the ROM, we are referring to the network of modules, including the kinetics scheme, that drive the CORE model. The CORE, as described briefly above and in detail in Lamb (1984), will remain fixed for all foreseeable generations of the ROM.

The model simulations that we have conducted to date, including the ones to be presented in this report, have used the Demerjian and Schere (1979) chemical mechanism described in Table 2-1 (page 8). This scheme treats 36 reactions among 23 species. The second-generation ROM will employ a condensed version of the CBM-IV chemical mechanism. Table 2-2 (page 10) summarizes the principal differences between the first generation ROM used in the present study and the second-generation model, which is presently undergoing tests.

Concerning the present status of our model verification studies, we have completed what we regard as tests of the necessary conditions for model validity. This work, described in Lamb and Laniak (1985), demonstrates that the solutions of the mathematical equations that constitute the CORE model (see Figure 2-3) are close facsimiles of the solutions of the corresponding differential equations that describe the chemistry and physics that the ROM is intended to simulate. It remains to be shown that the model satisfies the sufficient conditions for validity, namely that its predictions of species concentration statistics are acceptably close to the values one would measure under the meteorological and emissions conditions simulated. This final step of the verification process will be applied in a rigorous way only to the second-generation model. A partial verification of the first generation model, used in the present study, has been performed by Schere (1986). Some additional comparisons of the model's predictions with observations are presented in Section 8.

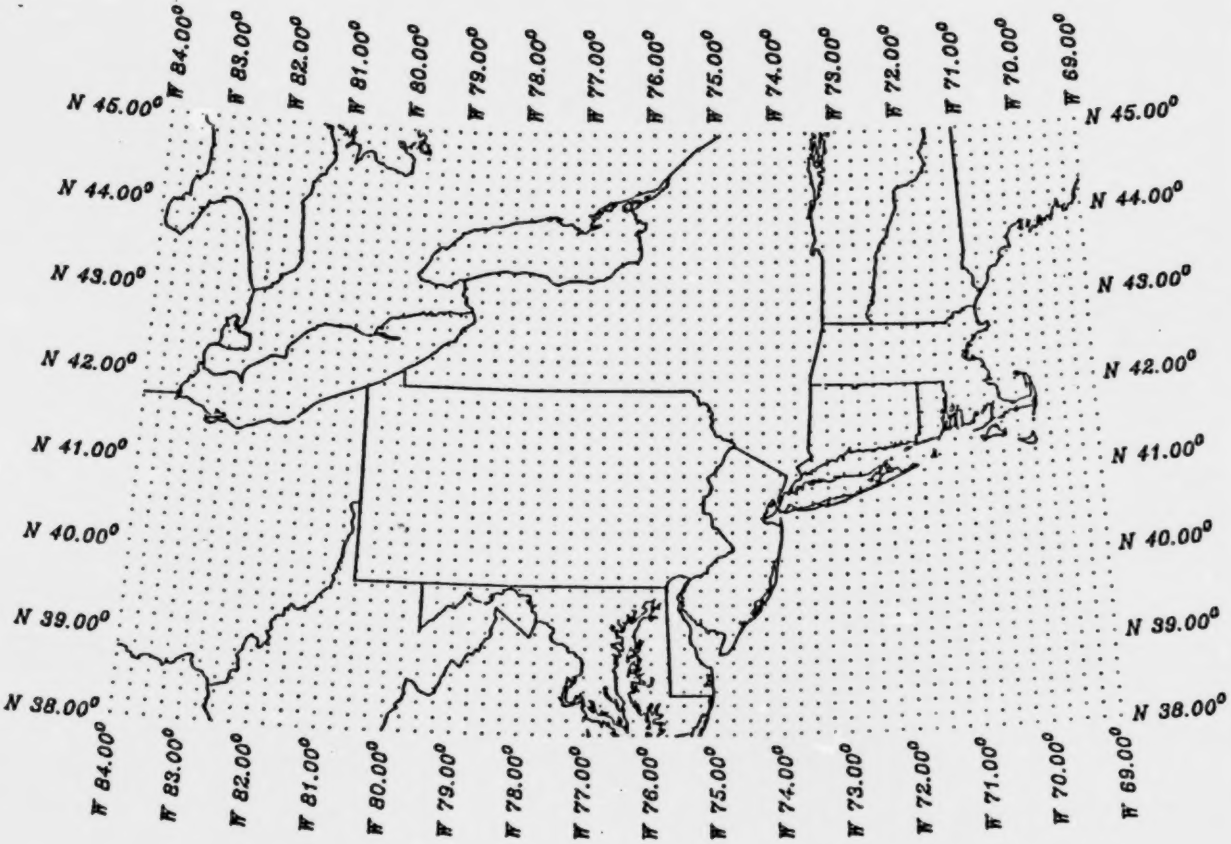

N 45.00°
N 44.00°
N 43.00°
N 42.00°
N 41.00°
N 40.00°
N 39.00°
N 38.00°
W 84.00°
W 83.00°
W 82.00°
W 81.00°
W 80.00°
W 79.00°
W 78.00°
W 77.00°
W 76.00°
W 75.00°
W 74.00°
W 73.00°
W 72.00°
W 71.00°
W 70.00°
W 69.00°

Figure 2-1. Modeling domain treated in the present study. Each dot represents a grid cell.

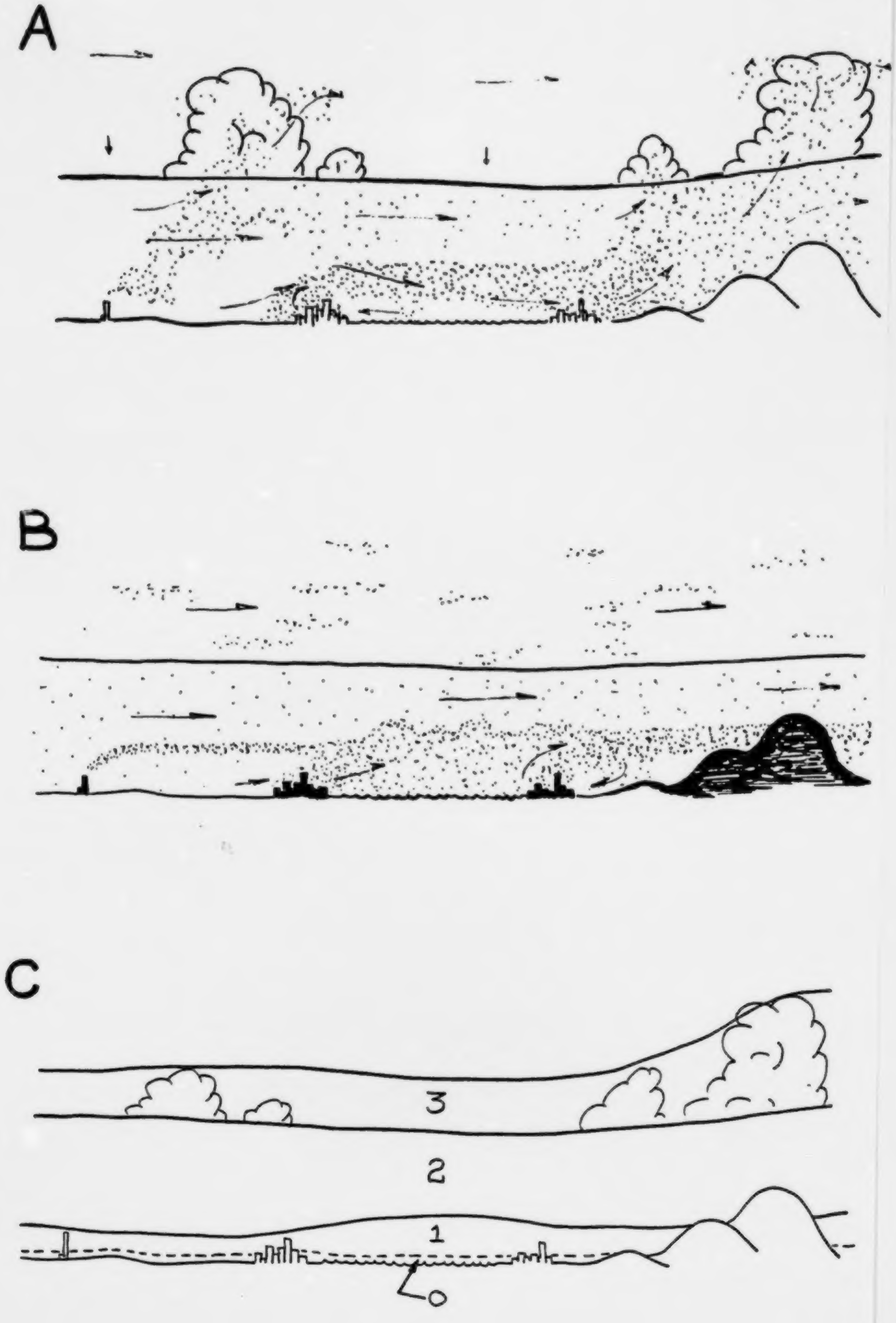

Figure 2-2. Illustration of the daytime (A) and nighttime (B) meteorological phenomena treated by the ROM and the vertical structure (C) used to simulate these processes.

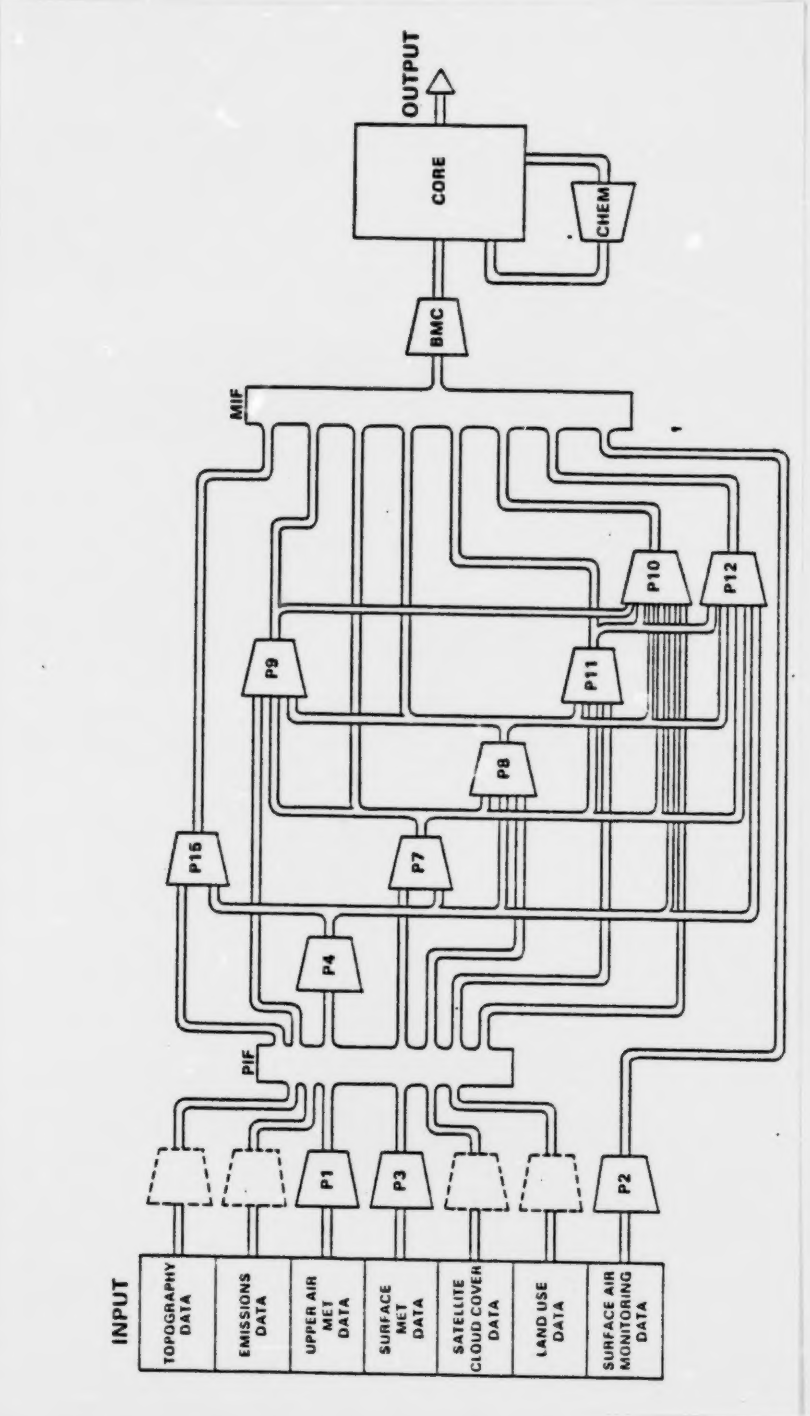
OUTPUT
CORE
CHEM
BMC
MIF
P10
P12
P9
P11
P8
P15
P7
P4
PIF
P1
P3
P2
INPUT
TOPOGRAPHY DATA
EMISSIONS DATA
UPPER AIR MET DATA
SURFACE MET DATA
SATELLITE CLOUD COVER DATA
LAND USE DATA
SURFACE AIR MONITORING DATA

Figure 2-3. Schematic illustration of the network of processors and core module that compose the Regional Oxidant Model (ROM).

Table 2-1. Chemical reactions included in the Demerjian/Schere mechanism and the rate constants assumed for each.

		Reaction		Rate Constant* (units[a])
1.	NO_2	$\xrightarrow{h\nu}$	$NO + O$	variable[d]
2.	$O + O_2 + M$	$\rightarrow$	$O_3 + M$	2.3×10^{-5} [c]
3.	$O_3 + NO$	$\rightarrow$	$NO_2 + O_2$	$2.7 \times 10^{+1}$
4.	$O_3 + NO_2$	$\rightarrow$	$NO_3 + O_2$	4.8×10^{-2}
5.	$NO_3 + NO$	$\rightarrow$	$2NO_2$	3.0×10^{4}
6.	$NO_3 + NO_2 + H_2O$	$\rightarrow$	$2HONO$	3.4×10^{-3} [c]
7.	$HONO$	$\xrightarrow{h\nu}$	$HO + NO$	variable[d]
8.	$HO + CO$	$\xrightarrow{(O_2)}$	$HO_2 + CO_2$	4.1×10^{2}
9.	$HO_2 + NO_2$	$\rightarrow$	$HONO + O_2$	4.4
10.	$HO_2 + NO$	$\rightarrow$	$HO + NO_2$	1.2×10^{4}
11.	$HO_2 + NO_2 + M$	$\rightarrow$	$HOONO_2 + M$	1.5×10^{-3} [c]
12.	$HOONO_2$	$\rightarrow$	$HO_2 + NO_2$	3.3
13.	$HO + HONO$	$\rightarrow$	$NO_2 + H_2O$	9.8×10^{3}
14.	$HO + NO_2 + M$	$\rightarrow$	$HONO_2 + M$	1.5×10^{-2} [c]
15.	$HO + NO + M$	$\rightarrow$	$HONO + M$	7.4×10^{-3} [c]
16.	$HO_2 + O_3$	$\rightarrow$	$HO + 2O_2$	3.0
17.	$HO + O_3$	$\rightarrow$	$HO_2 + O_2$	1.0×10^{2}
18.	$HO_2 + HO_2$	$\rightarrow$	$H_2O_2 + O_2$	3.7×10^{3}
19.	$OLEF + O$	$\rightarrow$	$RO_2 + ALD + HO_2$	5.1×10^{3}
20.	$OLEF + O_3$	$\rightarrow$	$RO_2 + ALD + HO_2$	1.4×10^{-2}
21.	$OLEF + HO$	$\rightarrow$	$RO_2 + ALD$	3.1×10^{4}
22.	$PARAF + HO$	$\rightarrow$	RO_2	5.0×10^{3}
23.	ALD	$\xrightarrow{h\nu}$	$0.5RO_2 + 1.5HO_2 + 1.0CO$	variable[d]

Table 2-1, continued

	Reaction	Rate Constant (units[a])
24.	$ALD + HO \rightarrow 0.3R1O_2 + 0.7HO_2 + 0.7CO$	1.4×10^4
25.	$RO_2 + NO \rightarrow RO + NO_2$	1.1×10^4
26.	$RO + O_2 \rightarrow ALD + HO_2$	9.0×10^{-1}
27.	$R1O_2 + NO_2 \rightarrow PAN$	8.9×10^3
28.	$RO + NO_2 \rightarrow RONO_2$	1.0×10^2
29.	$RO_2 + O_3 \rightarrow RO + 2O_2$	2.0
30.	$R1O_2 + NO \xrightarrow{(O_2)} RO_2 + NO_2$	4.0×10^3
31.	$PAN \rightarrow R1O_2 + NO_2$	1.4×10^{-1} b
32.	$AROM + HO \xrightarrow{(O_2)} R_2O_2 + 2ALD + CO$	2.3×10^4
33.	$R_2O_2 + NO \rightarrow R_2O + NO_2$	1.1×10^4
34.	$R_2O + O_2 \rightarrow ALD + HO_2 + 2CO$	8.9×10^{-1}
35.	$R_2O_2 + O_3 \rightarrow R_2O + 2O_2$	2.0
36.	$R1O_2 + O_3 \rightarrow RO_2 + 2O_2$	2.0

---

* Values of rate constants that vary by temperature are evaluated here for 298°K and 1 atm pressure.

[a] Rate constant units are ppm^{-1} min^{-1} unless otherwise noted.

[b] Units of rate constant are min^{-1}.

[c] Units of rate constant are ppm^{-2} min^{-1}.

[d] Photolysis rate constants are based on data compiled by Demerjian, Schere and Peterson (1980) and vary as a function of solar zenith angle.

Species definitions:

RNO_3	Alkyl Nitrate
HO2	Hydroperoxyl Radical
HO4N	Pernitric Acid
RO	Alkoxyl Radical
RO2	Alkylperoxy Radical
R2O	Alkoxy Radical
R1O2	Peroxyacyl Radical
R2O2	Peroxy Radical

Table 2-2. Comparison of the principal differences between the first generation regional oxidant model used in the present study and the second generation model currently in development.

	First Generation	Second Generation
Layers	Constant Thickness	Thicknesses variable in space and time
Winds	Nondivergent	Divergent
Chemistry	Demerjian-Schere	CBM-IV
Emissions	1980 NAPAP 4.2	1980 NAPAP 5. + Biogenic

SECTION 3

CHARACTERISTICS OF OBSERVED OZONE CONCENTRATIONS IN THE NORTHEASTERN UNITED STATES

Within the geographical area shown in Figure 2-1 that is presently simulated by the Regional Oxidant Model, i.e., the region that we refer to in this report as the Northeast, the highest ozone concentrations attributable to anthropogenic activities occur during the summer months. Isolated occurrences of extreme ozone levels are occasionally reported in other seasons, particularly the winter and spring, but these are more likely to be due to intrusions of stratospheric ozone than to photochemical reactions among anthropogenic emissions (see Lamb, 1977; Viezee et al, 1983).

The spatial distribution of maximum 1-hour averaged ozone concentrations observed during June through September 1980 is shown in Figure 3-1 (page 20). (We have excluded data from October through May to minimize the influence of stratospheric ozone.) The information presented in Figure 3-1 is based on data reported by some 200 SAROAD stations whose locations and record lengths are given in Figure 3-2 (page 21). Despite the relatively large number of monitoring sites, the spatial coverage is not adequate to resolve the full detail of the ozone distribution. Moreover, sizable areas of West Virginia and Pennsylvania contain no monitoring sites at all. For these reasons, the concentration isopleths shown in Figure 3-1 should be viewed qualitatively.

The data reveal five general subregions where ozone concentration in excess of the current primary standard, 120 ppb, occur. One is a vast area roughly parallel to the East Coast, extending from Virginia into southern Maine and extending inland from the coastline some 200 kilometers. Within this area is a zone roughly 100 km wide lying along the Eastern Corridor cities from Washington to Boston in which ozone concentrations greater than 160 ppb are observed. And in northern Long Island and southern Connecticut, it is not uncommon to observe ozone levels in excess of 240 ppb.

In the four other regions shown in Figure 3-1 where ozone concentrations exceed 120 ppb, only the region around Pittsburgh contains an area where values exceed 160 ppb, and even here the area is apparently rather small. The fact that ozone levels in the Detroit airshed are relatively low is surprising since the modeling studies we have conducted to date indicate that the VOC and NO_x emissions in that area are capable of producing ozone concentrations comparable to those produced by East Coast sources. The same is true of the simulated emissions from the Toronto area. We will return to this matter in Section 8 when we discuss the results of the model runs.

From the standpoint of model design, an important characteristic of the ozone distribution is the spatial scale of concentration variations. Figure 3-1 suggests that in the areas of highest concentration, the characteristic scale is less than 100 km. This is supported by the distribution of maximum hourly ozone values shown in Figure 3-3 (page 22) which were recorded during one of the major episodes observed in the Northeast in 1980. The concentrations vary markedly from station to station along the Eastern Corridor. For example, in southwestern Connecticut, maximum ozone values of 155 and 302 ppb were measured at sites within about 40 km of each other. Similar gradients can be seen in New Jersey. It has been known since aircraft observations of ozone in the Northeast were begun in the late 1970's that the highest ozone values occur within urban plumes several tens of kilometers wide that are often discernable up to 200 km downwind of the major sources of NO_x and VOC (see, for example, Alkezweeny, et al 1981; Clark and Clarke, 1984; and Westberg, 1985). The fact that emissions from urban areas are concentrated in relatively narrow plumes during the first day of their travel can be a significant factor in determining the fate of emissions. Because the higher the concentrations of chemical species, the faster are the reactions among them; and the longer the concentrations remain high, due to inefficient atmospheric mixing, the larger are the quantities of product species produced (such as ozone). Models with grid meshes larger than the lateral dimensions of urban plumes, i.e., several tens of kilometers, cannot simulate plume chemistry unless a scheme to approximate subgrid scale processes is incorporated. We will return to this point in the next section when we discuss the character of the hydrocarbon and NO_x sources in the Northeast.

One of the primary objectives of regional modeling is to identify those areas that are primarily sources of ozone and those that are primarily receptors. Information of this kind is essential in formulating the most equitable, cost effective emissions control plans. We can begin to form a picture of the source and receptor areas by analyzing the observed hourly ozone concentrations in light of the following basic fact: ozone is effectively generated only during daylight hours.

If one examines the chemical mechanisms that govern photochemical air pollution, one finds that the only source of ozone is the reaction

$$O + O_2 + M \rightarrow O_3 + M \quad , \tag{A}$$

with the principal source of atomic oxygen (O) being the photolysis of NO_2, namely

$$NO_2 + h\nu \rightarrow NO + O \tag{B}$$

where $h\nu$ represents a photon of sunlight. Reaction A is several orders of magnitude faster than B, and the vast majority of oxygen atoms produced by reaction B are removed by reaction A. Therefore, for all practical purposes reactions A and B can be combined in the form

$$NO_2 + O_2 + h\nu \rightarrow NO + O_3 \ . \tag{C}$$

The fact that this reaction is the only source of ozone implies the following premise:

> Ozone observed at any given location at night (when $h\nu = 0$) is ozone that was generated somewhere else. (P1)

Here we use the terms "night" and "somewhere else" in a general sense which we will make more specific shortly. Essentially, premise P1 provides a means of using ozone values measured during the hours of darkness to assess the extent to which distant sources affect the ozone burden at the measurement site. Premise P1 has the following corollary:

> The difference between the maximum ozone concentration observed at a given site during the day and the maximum ozone observed at the same location at night is a measure of the quantity of ozone generated in the vicinity of that site. (C1)

To implement P1 and C1 we adopt the following definitions of day and night:

$$\text{day} = 1000 - 1759 \text{ LST} \tag{3.1a}$$
$$\text{night} = 2100 - 0959 \text{ LST} \tag{3.1b}$$

The definition of "day" is intended to span the period in which reaction C is most effective in generating ozone. The definition of night, (3.1b), is intended to achieve two ends. First, by placing a gap between the end of the daytime period and the beginning of the period defined as night we minimize the extent to which locally generated ozone influences the values to which we ultimately apply premise P1. For example, under our definition (3.1), in which the gap between day and night is 3 hours, ozone generated within 30 km of a monitor would have no effect on the measured nighttime ozone levels under conditions of a 10 km/hr mean wind. Second, by extending the period defined as night to include several hours after sunrise, we capture the effects of ozone transported long distances that fumigates into the surface layer following the erosion of the nighttime radiation inversion. Let us now apply P1 and C1 to the SAROAD ozone data, using (3.1) as the definitions of day and night.

Figure 3-4 (page 23) shows isopleths of the difference between the maximum hourly daytime ozone measured throughout June-August 1980 and the corresponding maximum hourly nighttime value observed in the same three month period. According to C1, the areas of largest concentration differences are the areas of largest ozone production. We will refer to these areas as "virtual ozone sources" with the understanding that the ozone generated in these zones is likely due to hydrocarbon and nitrogen oxide emissions from sources outside these zones. On comparing Figures 3-4 and 3-1 (page 20) we find that the areas of highest apparent ozone generation coincide with the areas of highest observed ozone concentration. A relationship of this kind between source and concentration distributions is characteristic of species that undergo chemical transformation. The data presented in Figure 3-4 indicate that maximum daytime ozone concentrations are larger than the corresponding maximum nighttime values everywhere except portions of central Pennsylvania and northeastern New York. In these two areas the difference between the daytime and nighttime ozone maximum is actually negative, implying that these are predominantly areas of ozone destruction. The fact that both these areas are remote from the major urban source regions supports the validity of C1. Because after a mixture of ozone precursor species has been exposed to sunlight for a sufficiently long time, its ozone production potential is exhausted and the ozone that has been formed up to that time begins to disappear primarily through uptake by vegetation and soil. These particular removal mechanisms are most effective during the daytime when turbulence intensities are high enough to maintain a constant flux of ozone down to the earth's surface where removal processes are taking place. Thus, interpreting the data given in Figure 3-4 from the perspective of premise C1, we tentatively conclude that the bulk of the ozone attributable to anthropogenic sources is generated within about 100 km of the major urban areas; and that beyond distances of about 200 km, ozone is primarily in a state of decay.

Let us look now at the areas where ozone transported from source regions has the largest effect. Figure 3-5 (page 24) shows isopleths of the maximum nighttime ozone concentrations observed during June - August 1980, the same period represented by Figure 3-4 (page 23). Under premise P1 the concentration values shown in Figure 3-5 are a measure of the maximum ozone burden imposed on a site by distant sources, namely sources farther than about 30 km from the site in question. On comparing the locations of the zones of highest nighttime ozone shown in Figure 3-5 with the locations of the areas of highest ozone generation indicated in

Figure 3-4, we find that the former are displaced some 50 to 100 km from the latter. For example, a zone of nighttime ozone concentrations in excess of 120 ppb is evident in Southeastern Pennsylvania some 50 km north of the source areas associated with the Washington, DC to Philadelphia corridor. Similarly high nighttime ozone concentrations also occur in an area east and northwest of Boston. A check of the ozone data showed that the high concentrations in this area were observed around midnight on days when afternoon concentrations in the Connecticut virtual-source area, shown in Figure 3-4, were high.

The nighttime data suggest that the maximum ozone burden due to imported ozone exceeds 100 ppb within an elongated zone stretching along the eastern seaboard from Washington, DC to just northeast of Portland, Maine. Relatively small areas of similarly high burdens appear near Detroit, Pittsburgh and Buffalo. The data also indicate that nighttime ozone levels ranging from 100 ppb to just over 120 ppb occur throughout upstate New York and a large part of Vermont. The model simulations that we present later suggest that the high ozone concentrations observed in these areas are attributable to east coast sources with occasional contributions from ozone generated from Toronto emissions. If the influence zones delineated by the model are correct, we can deduce from the observations made at Whiteface Mountain in upstate New York that ozone concentrations slightly in excess of the current primary standard, 120 ppb, exist as far as 400 km downwind of the major source areas along the East Coast. This is not meant to imply, however, that values this high would be observed at all ground-level stations within 400 km of the major eastern cities. At sites near sources of NO_x, observed ozone values would be smaller due to scavenging by NO. At remote sites where the ozone plume arrives overhead during the predawn hours, surface ozone readings would remain well below 120 ppb if a strong enough radiation inversion were present to prevent turbulent transport of the ozone to the ground. It is reasonable to conclude, however, that within 400 km of the Eastern Corridor cities, the New York City area in particular, hourly averaged ozone concentrations as high as 120 ppb can occur at all elevations higher than the depth of the radiation inversion, i.e., elevations higher than 300-500 meters above the lowest local relief. This characteristic of the ozone distribution has a major bearing on the ozone exposures of forests in the Northeastern United States.

As we stated at the outset, the data analyses that we just presented provide only a qualitative description of the ozone problem in the Northeast, because the available data cover only a limited geographical area and the accuracies of some of the data themselves are questionable. Moreover, some of our results were based on the speculations embodied in premises P1 and C1. We presented this analysis in an effort to gain a general view of the areas in which ozone is generated and the areas into which it spreads. We believe that this knowledge is useful in formulating model experiments, in interpreting the results, and in designing the most effective emissions controls for ozone reduction. In the next section we use the information derived here to determine the locations of the ozone precursor species that have the largest effect on ozone concentrations.

As a final piece of information that illustrates the current ozone problem in the Northeast, we show in Figure 3-6 (page 25) the number of days during 1980 in which the maximum hourly ozone concentration exceeded

120 ppb. The areas in which the primary ozone standard was not attained, i.e., the area in which two or more exceedances were observed, correlates well with the areas of apparent ozone generation shown in Figure 3-4 (page 23). The close spacing of the frequency isopleths shown in Figure 3-6 also gives an indication of the difficulty that will be faced in reducing ozone concentrations below the current standard. That is, the data suggest that if emissions changes were adopted that reduced the number of exceedances of 120 ppb ozone by one-half everywhere, the geographical area in which the standard was not attained would be reduced by only 10 to 20 percent.

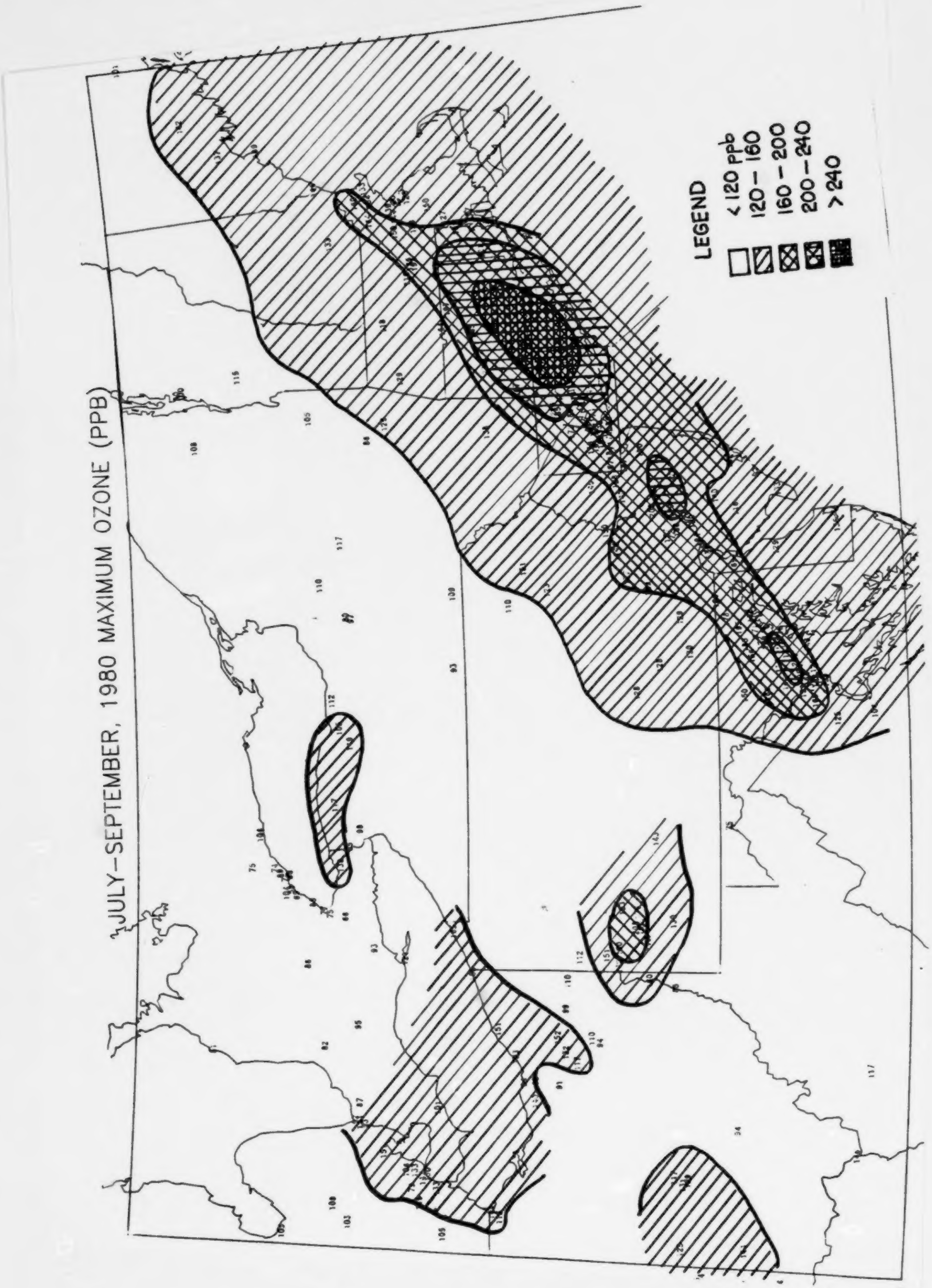
JULY–SEPTEMBER, 1980 MAXIMUM OZONE (PPB)
LEGEND
< 120 ppb
120 – 160
160 – 200
200 – 240
> 240

Figure 3-1. Maximum hourly averaged ozone concentration (ppb) observed during July - September 1980.

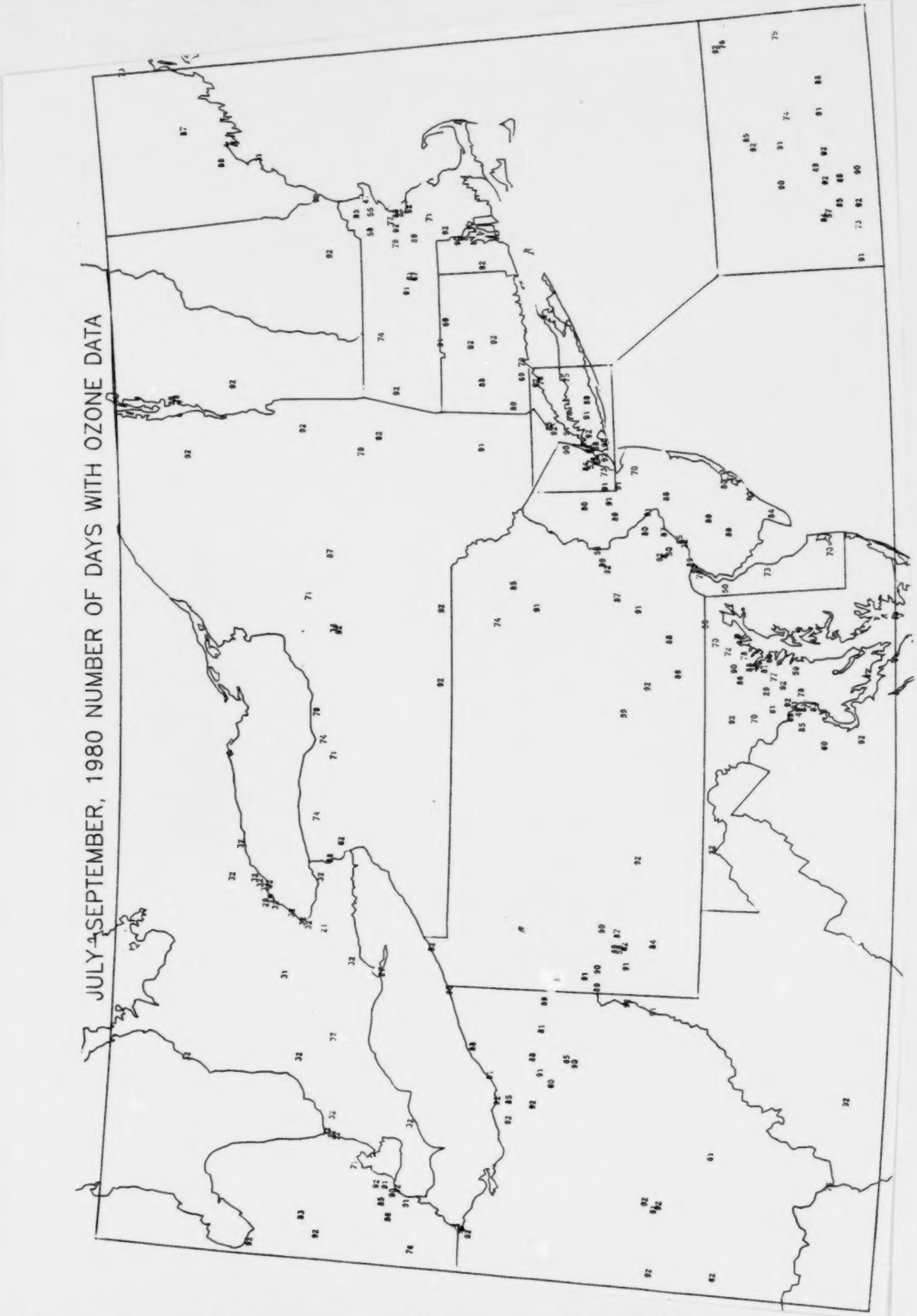
JULY-SEPTEMBER, 1980 NUMBER OF DAYS WITH OZONE DATA

Figure 3-2. Locations and record lengths (in days) of hourly averaged ozone measurements during July - September 1980.

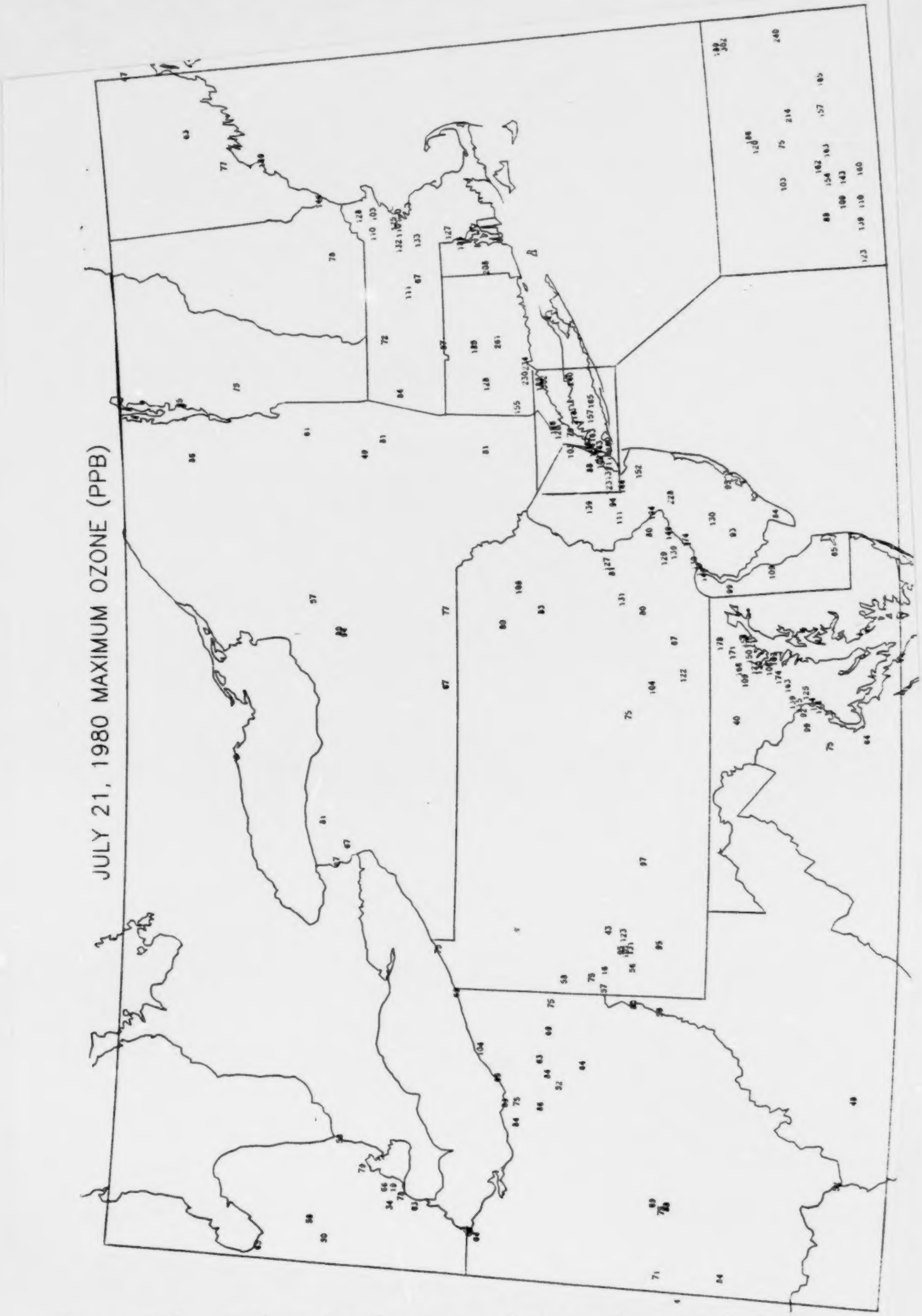
JULY 21, 1980 MAXIMUM OZONE (PPB)

Figure 3-3. Maximum hourly averaged ozone observed during an episode on 21 July 1980.

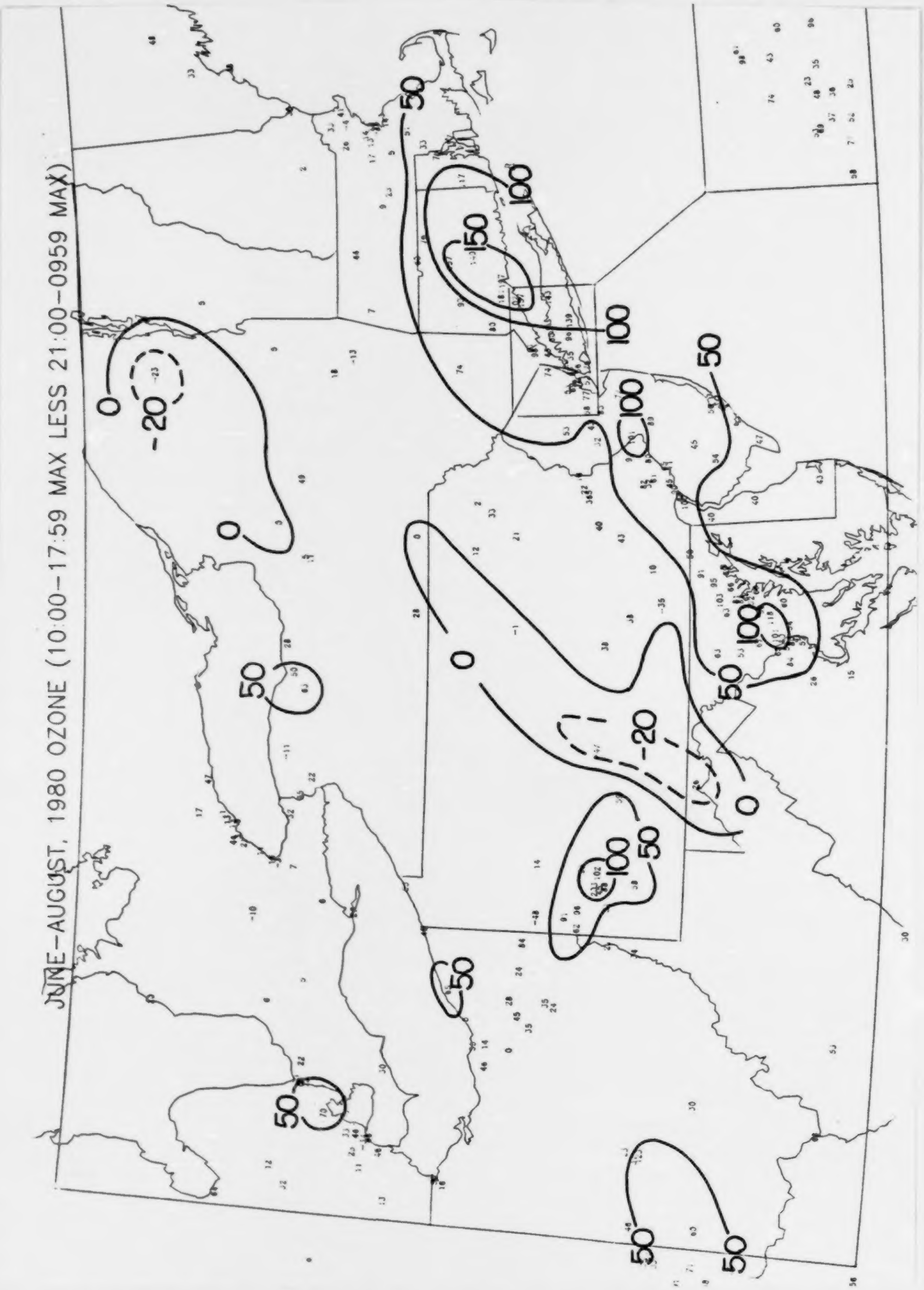
JUNE-AUGUST, 1980 OZONE (10:00-17:59 MAX LESS 21:00-0959 MAX)
0
-20
50
100
150
100
50
0
-20
0
100
50
50
100
0
50
50
50
50

Figure 3-4. Difference (ppb) between the maximum hourly averaged ozone concentration observed during the daytime (1000-1759 LST) at each monitoring station during June-August 1980 and the maximum value observed at night (2100-0959 LST) at the same station over the same 3-month period.

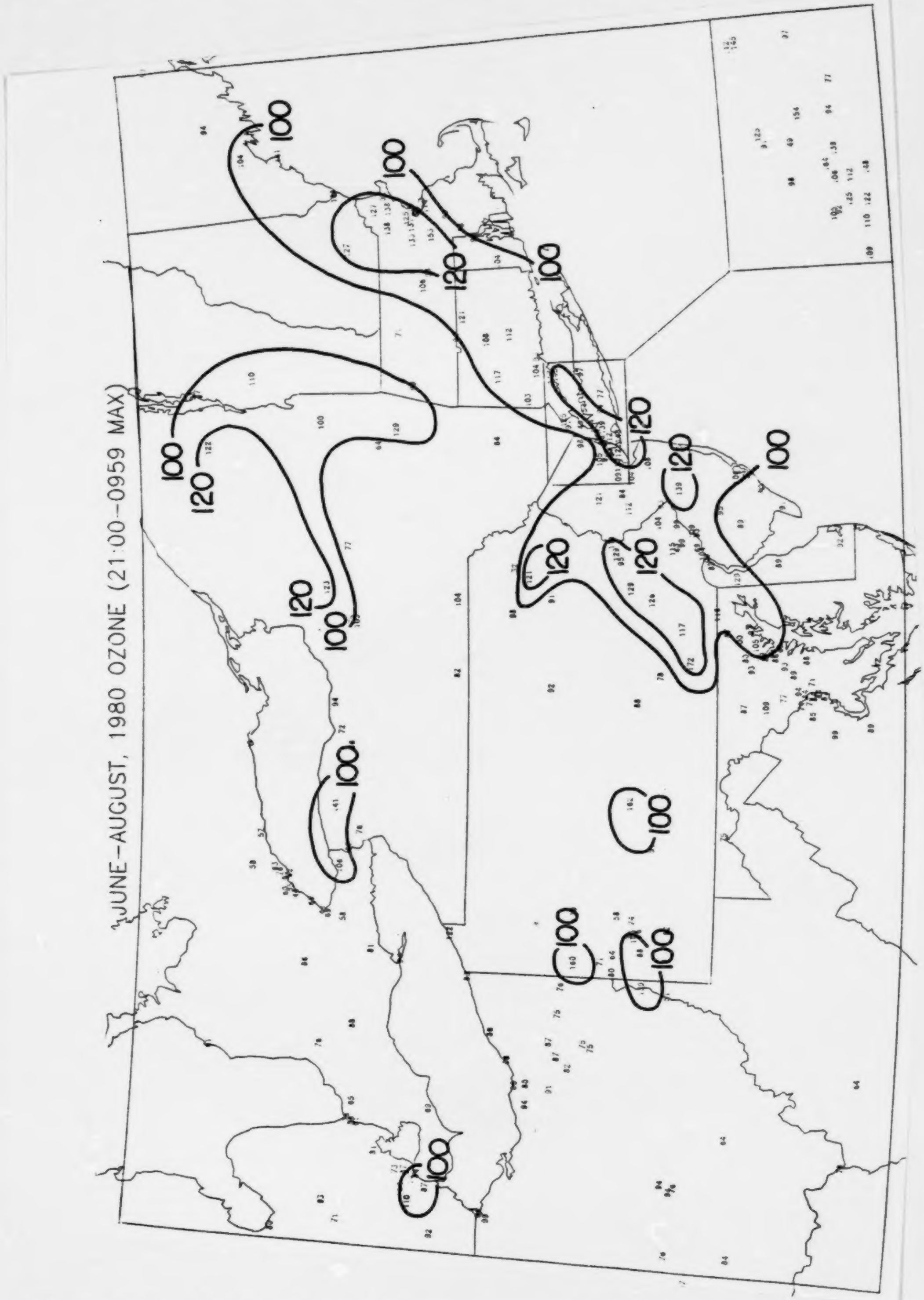
JUNE-AUGUST, 1980 OZONE (21:00-0959 MAX)
100
120
100
120
100
100
120
100
120
120
120
100
120
120
100
100
100
100
100
100

Figure 3-5. Maximum hourly averaged ozone (ppb) observed during the nighttime hours (2100-0959 LST) during June - August 1980.

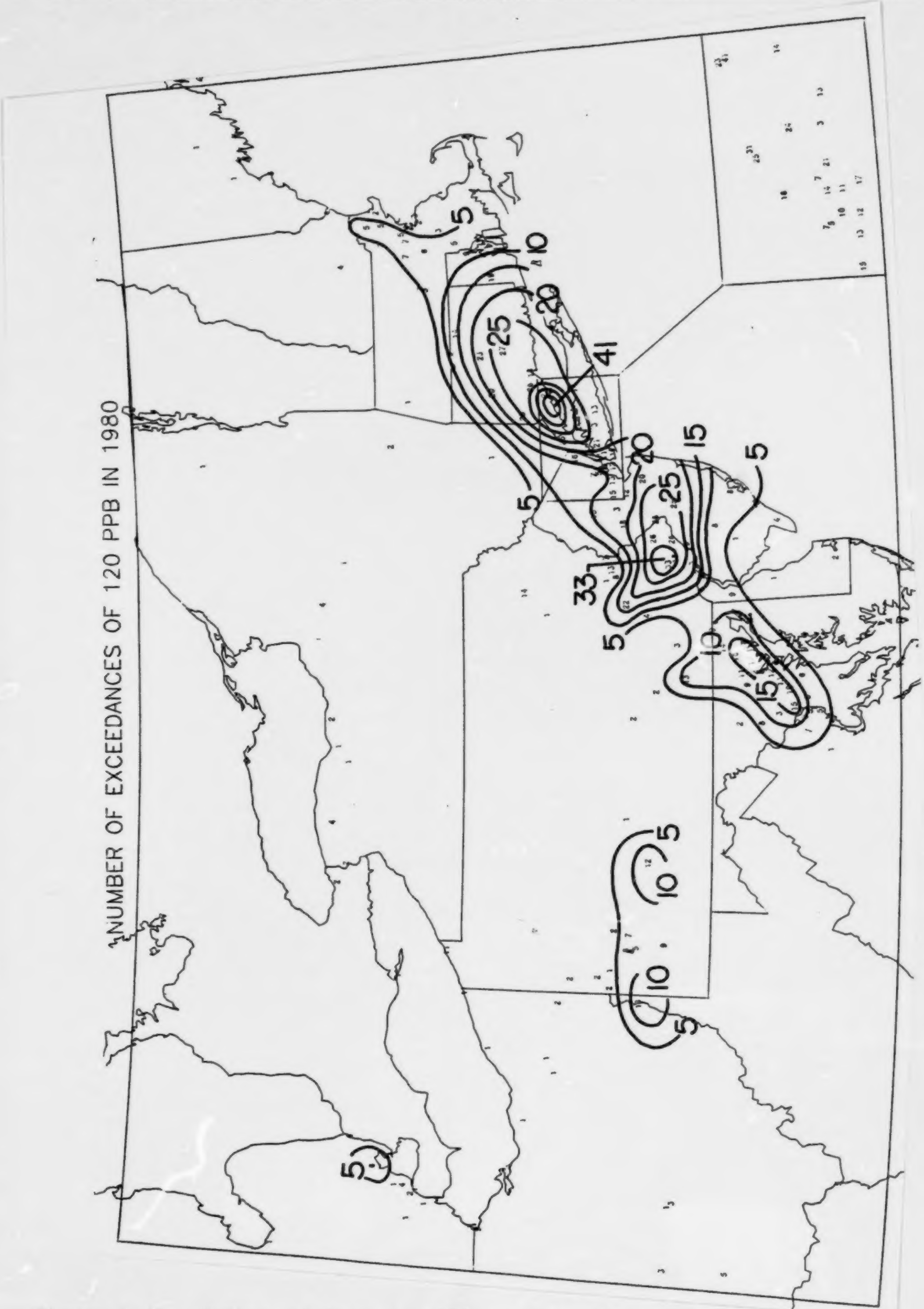
NUMBER OF EXCEEDANCES OF 120 PPB IN 1980
5
10
20
25
41
5
20
15
25
33
5
5
10
15
5
10
5
10
5
5

Figure 3-6. Number of days in 1980 in which the maximum hourly averaged ozone exceeded 120 ppb.

SECTION 4

THE SOURCES OF OZONE PRECURSOR SPECIES IN THE NORTHEASTERN UNITED STATES

As we pointed out in the previous section the only atmospheric source of ozone is the composite reaction

$$NO_2 + O_2 + h\nu \xrightarrow{k_1} NO + O_3 \qquad (4.1)$$

(see reactions 1 and 2 in the Demerjian/Schere mechanism described in Table 2-1, page 9). Hydrocarbons enter the picture in a rather subtle way that is linked to the chemical sinks of ozone, in particular its reaction with NO:

$$NO + O_3 \xrightarrow{k_2} NO_2 + O_2 \qquad (4.2)$$

In full sun conditions reactions (4.1) and (4.2) are so fast that the two achieve a quasi-photostationary state in which the concentration of ozone is given approximately by

$$O_3 \simeq \frac{k_1}{k_2} \cdot \frac{NO_2}{NO} . \qquad (4.3)$$

The ratio (k_1/k_2) is determined solely by the intensity of sunlight. It has a value of zero at night and a maximum of order 10 ppb at ground level at noon on a clear summer day along the 35° latitude circle.

By contrast the ratio (NO_2:NO) is sensitive to the presence of hydrocarbons, because these species are sources of free radicals that are capable of oxidizing NO to NO_2. In this action hydrocarbons are doubly effective in amplifying ozone levels because they remove an ozone sink, NO, at the same time that they create a source, NO_2. Reactions of NO with alkylperoxy RO_2 and peroxy radicals R_2O_2 (reactions 25 and 33 in Table 2-1, page 9) are two of the pathways in which NO is converted to NO_2.

Not all of the radicals produced by hydrocarbons act to accentuate the (NO_2:NO) ratio. The alkoxyl radical, RO, for example, depletes NO_2 concentrations by transforming this species into a stable end product, alkyl nitrate (see reaction 28, Table 2-1). Nitrogen dioxide is also removed from the ozone production cycle by reactions with hydroxyl radical, which produce nitric acid. Thus, according to the the Demerjian-Schere chemical mechanism, all nitrogen oxide emissions are eventually converted into nitrate compounds and in the process ozone is produced.

Likewise, all hydrocarbon emissions are converted ultimately into CO_2. An important aspect of the fate of the hydrocarbons is that three of the four lumped species, namely olefin (OLEF), paraffin (PARAF) and aromatics (AROM) disappear monotonically because there are no chemical sources of any of these species. The fourth lumped species, aldehydes (ALD), is produced by olefins and aromatics (see reactions 19-21 and 32 in Table 2-1, page 8), by the oxidation of certain organic free radicals (reactions 26 and 34), and it is emitted by some anthropogenic sources. Aldehydes are destroyed by photolysis and by reactions with OH. Both processes generate free radicals that are capable of converting NO to NO_2.

These aspects of hydrocarbon behavior suggest the following general scenario. In the daytime urban plume, concentrations of all the hydrocarbons decrease downwind of the city as a result of chemical reactions that produce free radicals. These, in turn, cause ozone concentrations to rise by converting the ozone scavenger NO into an ozone source, NO_2. (Model simulations indicate that over 90 percent of the olefins and aromatics initially present are consumed within 8 hours exposure to sunlight.)

After sundown aldehyde concentrations in the plume may begin to rise due to the oxidation of excess radicals left over from the daytime and to reactions of residual olefins with ozone. (The chief mechanisms of aldehyde decay, namely photolysis and reaction with OH, are absent at night.) Thus, by the beginning of the second day, olefins and aromatics will have virtually disappeared from the plume but aldehyde and paraffin levels might still be high enough to cause enhanced ozone formation from fresh emissions of nitrogen oxides that the plume might encounter during the day.

In regulatory studies the current practice is to lump all hydrocarbons except methane together and treat the sum as a single entity referred to as non-methane hydrocarbon (NMHC), or volatile organic compounds (VOC). This practice simplifies the treatment of emissions but it fails to distinguish between the ozone production potentials of the individual hydrocarbon species. Although the model simulations that we describe later in this report are based on emissions data in which hydrocarbons are split into the four lumped species OLEF, PARAF, AROM and ALD, it is convenient in the present section, where we are concerned only with qualitative features of ozone precursor sources, to look only at VOC emissions. In the context of the Demerjian-Schere chemical mechanism that is presently used in the model (see Table 2-1, page 8), VOC is defined as follows:

$$\begin{aligned}\mathrm{VOC} = 3.57 \times \mathrm{OLEF} + 4.56 \times \mathrm{PARAF} + 1.50 \times \mathrm{ALD} \\ + 7.56 \times \mathrm{AROM} + 1.02 \times (\text{Non reactives})\end{aligned} \qquad (4.4)$$

where the units of VOC, OLEF, and all remaining species are moles or ppb. Similarly, we consider nitrogen oxides emissions in the combined form

$$NO_x = NO + NO_2. \qquad (4.5)$$

Our main objective in this Section is to determine the strengths and locations of the major sources of ozone precursor, i.e., VOC and NO_x. We are especially interested in seeing where these sources lie in relation to the virtual ozone sources that we mapped out earlier in Figure 3-4 (page 23). Our motivation is the belief that once the major sources of precursor species have been identified, one can utilize controls on those particular sources as a means of achieving maximal changes in ozone concentrations.

The U.S. emissions data used in this study are from version 4.2 of the NAPAP inventory, documented by Toothman et al., 1984. Canadian emissions were estimated from data provided by Environment Canada. Due to differences between the source classification schemes used by the U.S. and Canada and to the availability of only annual Canadian emission, it was necessary to apply U.S. temporal and species allocation factors to the Canadian data to acquire the necessary model inputs. Also, Canadian population, housing and land use data were used as surrogate indicators for spatial distribution of emissions into the ROM grid network.

In this section we will adopt the practice commonly used in regulatory analyses of dealing with emissions on a county basis. We wish to emphasize, however, that in the model simulations the emissions have been apportioned to the model's grid cells, whose dimensions are 1/4° longitude x 1/6° latitude, or roughly 18 x 18 km (see Figure 2-1, page 5). Most of the counties within the model domain contain several grid cells.

To identify the major sources of NO_x and VOC we are guided by the simple, basic relationship

$$C = \frac{Q}{\overline{u}h} \tag{4.6}$$

which expresses the concentration C (mass/volume) of material from an area source of strength Q [mass/(area.time)] emitting into a mixing layer of depth h and wind speed $\overline{u}$. In other words, the ability of a source to cause high concentrations is measured by its emission density Q rather than its mass release rate $\dot{m}$ (mass/time). Thus, we determined the VOC and NO_x emissions densities Q_{VOC} and Q_{NOx} of each of the 439 counties within the model domain, and then ordered each set with the largest Q value first and the smallest last. Tables 4-1 and 4-2 (pages 41 and 42) list the counties with the top 50 values of Q_{VOC} and Q_{NOx}, respectively.

On examining these lists, one finds that 30 counties, designated by asterisks in each table, are common to both sets. As a result, the top 50 NO_x and VOC sources consist of only 70 counties rather than 100. For purposes of discussion we shall divide these 70 counties into three groups designated as follows:

(1) "High VOC" = listed in Table 4-1 but not Table 4-2;
(2) "High NO_x" = listed in Table 4-2 but not Table 4-1;
(3) "High NO_x and high VOC" = listed in both Tables (and indicated by asterisks in each).

Figure 4-1 (page 43) shows the locations of these sources. An important property of this set is that together these sources generate about 50% of all VOC and NO_x emitted in the Northeastern United States (excluding Canada). We will discuss other properties of these and the entire set of sources later in this section.

For purposes of discussion, we will refer to the 70 counties listed in Tables 4-1,2, and shown in Figure 4-1, as the major source counties. Comparing the locations of these 70 counties with the virtual ozone source distribution plotted earlier in Figure 3-4 (page 23), we see a distinct correlation. The area of high ozone generation along the East Coast apparent in Figure 3-4 surrounds the major source counties of the Eastern Corridor shown in Figure 4-1. The smaller zones of ozone generation apparent in Figure 3-4 in the Pittsburgh, Cleveland and Detroit areas lie in the immediate vicinity of major source counties, but they do not engulf the counties as is the case along the Eastern seaboard. We also see that the areas of ozone destruction lying along the Appalachian Mountains of Pennsylvania and the Adirondack Mountains of New York fall within a gap separating the major sources of the Eastern seaboard from the major sources of the Ohio Valley and Michigan areas.

The two chief discrepancies between the areas of ozone generation and the major ozone precursor species sources are first, the absence of an area of ozone production around the major source counties of southern Ohio and western West Virginia; and second, the absence of major sources in the vicinity of the high ozone production areas apparent in Figure 3-4 in southwestern Ohio. The latter discrepancy is attributable to emissions from the Cincinatti and Dayton areas which are just outside the western boundary of the model domain. The fact that high ozone production is not indicated in Figure 3-4 in the vicinity of the major sources in southern Ohio and West Virginia is due to the paucity of ozone data in this area rather than to a known absence of ozone production.

Our primary purpose in comparing our so-called major source counties with the areas of apparent ozone production is to substantiate the significance of the role that these particular sources play. One of the things that the comparison has revealed is that the major sources within the Eastern Corridor are significantly more effective in producing ozone than those west of the Appalachians. We believe that there are four main reasons for this.

First, the sources along the East Coast are considerably stronger than those west of the Appalachians. Table 4-1 indicates that all but one of the top 20 VOC sources is in the East and Table 4-2 shows that all but 4 of the top 20 NO_x sources are east of the Appalachians.

Second, the VOC:NO_x ratios of the eastern sources are generally higher than those of the west. This is evident in Figure 4-1 (page 43), where we see that the Eastern Corridor consists almost entirely of "high VOC" and "high VOC and NO_x" sources. Our modeling studies have shown that the ozone production potential of a given mixture of precursor species is realized fastest when the VOC:NO_x ratio is high. This is important in the production of ozone in the atmosphere; because if emissions are mixed with relatively clean ambient air at a rate faster than ozone is produced, the total amount of ozone generated will be diminished. The time scale of mixing of an urban plume with its environment is of the order of 1 day, because the principal mechanism of mixing at spatial scales of the order of an urban area is the vertical wind shear present in the nocturnal boundary layer. Thus, if the emissions of VOC and NO_x of a given source were in a ratio such that the maximum ozone concentration would not occur until the second day, the ozone production potential of that source would generally not be realized. Our studies with the Demerjian-Schere chemical mechanism described in Table 2-1 indicates that the critical VOC:NO_x ratio of the emissions is around 5. That is, if the ratio $Q_{VOC} : Q_{NOx} < 5$, maximum ozone levels do not occur until the second day. Otherwise, peak levels occur during the first day of travel. This is perhaps a good point to comment on why the VOC:NO_x ratios of the major sources listed in Table 4-1,2 (pages 41, 42) are so much lower than the ratios observed in air samples collected in and around major cities. Measured VOC:NO_x ratios reported by Allwine and Westberg (1977) are generally larger than 10 whereas the ratios of the emissions of the major sources listed in Tables 4-1, 2 are for the most part smaller than 5 and in many cases are smaller than 1. The higher ratios observed in the atmosphere are probably due to the fact that NO_x is transformed to product species such as HNO_3, HONO, PAN and others more rapidly than VOC is converted into products. Hence, the VOC:NO_x ratio increases with travel distance from the source. Another contributing factor is the apparently high degree of uncertainty that currently exists in gridded emissions data. We will discuss this point in some detail later in this section.

A third reason for the higher ozone generation around the eastern sources is the arrangement of these sources in a line parallel to the prevailing wind direction in the months of highest ozone potential. As a result of this arrangement air arriving in Connecticut during southwesterly winds contains not only emissions from the strong New York City sources but also ozone and precursor species arising from all the Eastern Corridor sources between New York and Washington, DC. It is not surprising, therefore, that the highest ozone concentrations lie in Connecticut (see Figures 3-1, 4, pages 20 and 23). A dramatic example of air flow moving in virtually a straight line along the Eastern Corridor cities was reported by Clark, et al (1984), who tracked the air motion with a marker balloon and conducted aircraft sampling of air at various points along the balloon's path.

A final contributing factor to the higher ozone production of the eastern sources is their proximity to the ocean. The model has predicted, and field observations have confirmed (see Siple et al., 1977; Lyons and Cole, 1976), that when air carrying fresh VOC and NO_x emissions moves from the warm land over colder water the mixture becomes trapped in a relatively shallow layer next to the water due to the loss of the surface sensible heat flux that drives convective mixing. If the sky is clear over the water -- and this is often the case since convective clouds are absent -- high concentrations of ozone can be generated. Often this ozone-rich air moves back on shore causing high ozone levels along the shoreline and progressively lesser concentrations inland as the shallow layer of air is mixed upward by convection into cleaner air. Later in this report we discuss a meteorological scenario observed in the Northeast in which air picks up emissions from the Eastern Corridor sources, moves out over the Atlantic Ocean, and after a period of one to two days returns to land crossing the same line of sources.

We have presented evidence that the 70 major sources shown in Figure 4-1, and detailed in Tables 4-1, 2, play a dominant part in causing the high ozone concentrations observed in the Northeastern United States. Consequently, these sources will form a focal point of the analysis of the model simulations that we present later in this report.

Before leaving this discussion of the sources, we want to examine two additional important points: the spatial scale of the sources vis-a-vis model grid size requirements; and the current level of uncertainty in the gridded VOC and NO_x emissions inventories.

The spatial scales of the VOC and NO_x sources

As we noted earlier the major sources shown in Figure 4-1 (page 43) are responsible for about one-half of all the VOC and NO_x emissions in the Northeast. However, it is evident in Figure 4-1 that all these sources combined cover only a small fraction of the land area contained within the model domain. Together, these facts suggest that the characteristic length scale of the emissions is small. In order to model ozone accurately, it is necessary for the model's grid size to be small enough to resolve the "granularity" of the VOC and NO_x source distributions. If the grid size is so large that major sources that are actually separated from each other in space are mixed together within a single grid cell, essential nonlinear characteristics of the chemical processes that act upon the emissions will be lost and systematic errors in predicted ozone levels will result. (See Lamb, 1986 for further details). There are two basic ways of handling the source resolution problem. First, one can use a coarse grid network and parameterize the nonlinear, subgrid scale chemistry phenomena that otherwise would not be simulated. This approach is attractive because the number of grid cells used in the model can be kept small enough to hold the computer time and memory requirements to acceptable levels. Its major drawback is that there does not exist a parameterization scheme of the kind required that is both accurate and universally valid. The second method of mitigating the source resolution problem is to make the model grid cells small enough to resolve the dominant features of the source granularity. This method is computationally expensive; but it imposes no assumptions on the model and therefore it adds no additional sources of error. This is the approach to model design that we have adopted in the ROM. Here we would like to quantify the scale of the VOC and NO_x source granularity in order to obtain an idea of how much subgrid scale variation in concentration exists in a model of given grid cell dimensions.

For this purpose we have compiled in Figure 4-2 (page 44) plots of the cumulative emissions densities Q of both VOC and NO_x as a function of cumulative area. The plots were created as follows.

Consider, for example, VOC; and let $Q_{VOC}(i)$ denote the emissions density (moles km^{-2} day^{-1}) of the i-th source. Let A(i) be the area (km^2) of the i-th source. And let the sources be numbered such that i = 1 represents the source (county) with the largest value of Q_{VOC}; i = 2 represents the second strongest source; and so on, with i = 439 representing the weakest source. (The numbering assignments are different when considering NO_x emissions.) In reference now to the plot of cumulative Q_{VOC} given in Figure 4-2, i.e., the upper curve, the ordinate Q and abscissa A of any point on that curve are given by

$$Q = \sum_{i=1}^{I} Q_{VOC}(i)A(i) / \sum_{i=1}^{I} A(i) \qquad (4.8a)$$

where I is the largest integer such that

$$\sum_{i=1}^{I} A(i) < A \qquad (4.8b)$$

For example, the left edge of the upper curve in Figure 4-2 has ordinate Q_{VOC} = 53457 moles km^{-2} day^{-1}, which one can see in the first entry in Table 4-1 (page 41) is the emissions density of the strongest VOC source. The abscissa of this point is $A = 58.1$ km^2. This is the area of the strongest VOC source. Thus, our model would need a mesh size of order $\Delta = \sqrt{A} \simeq 7.6$ km to resolve the strongest VOC source in the emissions inventory. Using the terminology we introduced earlier, we say that the smallest "grain" size of the VOC sources is of the order of 7 km.

Obviously, the actual sources of hydrocarbons have dimensions much smaller than this, but in compiling the emission inventory it is impossible to describe the full microstructure of the emissions distribution. However, sources that emit more than 100 tons per year of pollutant are considered to be significant enough to warrant detailed specification of their location, effective height, and so on. In the emissions inventory used in this study, over 50,000 sources fall into this category. In the model these sources are treated as point sources and their emissions are placed in the proper layer based upon plume rise calculations performed using meteorological conditions prevailing at the source site each hour. However, within each layer the emissions of all point sources that fall within a single grid cell are mixed together and treated as an area source. Thus, the spatial resolution of the source distribution is limited in the model by the grid size, which is about 18 km in the case of the ROM. We have just seen that the grain size of the strongest area source of VOC in the inventory is of the order of 7 km, so we wonder how large the subgrid scale variations in source strength would be in a model with an 18 km grid. The answer can be found from the curves plotted in Figure 4-2. Reading the ordinate of the VOC curve at the abscissa Δ = 18 km, we find that at best, an 18 km grid can capture only 83% of the actual peak source strength; and, from the NO_x curve, we see that only 78% of the peak NO_x emissions density is resolved. In other words, if the highest gridded VOC source strength Q were 83 units, the largest actual value in the field would be at least 100 units. The percentage value represents an upper bound, because the gridded emissions would achieve this level only if all the top sources that together fill an area A = $(18)^2$ km^2 happened to lie within a single grid. For example, the two top VOC sources listed in Table 4-1 together cover 317 km^2, which is just under the area (18^2) = 324 km^2 of a single grid cell, and both happen to fall within the same cell. So in the case of the ROM, 83% of the peak VOC source strength is resolved. The same is not true of the NO_x sources, however, because as we can see in Table 4-2 (page 42), one of the top sources does not lie in the same grid cell as the others. Therefore, the ROM's resolution of the NO_x source strengths is somewhat less than the maximum achievable, 78%.

Figure 4-2 indicates that a model with 80 km resolution captures less than 33% of the strengths of both NO_x and VOC sources, and that a model with 450 km grid cells is practically no better than one in which the entire domain is treated as a single cell. As we pointed out earlier, when a model is unable to resolve the strengths Q of the actual sources, errors can occur in simulated concentrations of photochemical species. Just how much resolution is necessary is not clear. It has been shown

(Lamb, 1986) that compared to a model with 18 km resolution, models with 80 km grid cells or larger underpredict ozone concentrations by significant margins. One would expect that the 18 km grid model also underpredicts because it, too, is unable to resolve details of the VOC and NO_x emissions. We surmise that the grid resolution necessary to obliterate subgrid scale effects altogether is determined jointly by the rate of turbulent mixing, the time scales of the dominant chemical reactions, and the sizes of the clusters in which individual emitters are grouped. Until this question has been resolved, we must rely on comparisons of model predictions and observed ozone concentrations to assess the significance of subgrid scale phenomena.

Uncertainty in gridded NO_x and VOC emissions

In the course of changing from the 1979 NECRMP emissions inventory to the more recent 1980 NAPAP data, version 4.2, we discovered considerable differences between the gridded VOC and NO_x emissions values. Figures 4-3 and 4-4 (pages 45 and 46) show scatter plots of the 200 largest VOC and NO_x grid values, respectively, comparing the NAPAP and NECRMP data. The regression lines in both cases show that the NAPAP inventory has effectively reduced the estimated strengths of sources that were strongest in the NECRMP data set and raised the estimated strengths of weaker sources. For the most part the NAPAP values are within a factor of 3 of the corresponding NECRMP estimates. The uncertainties are largest in the NO_x data where discrepancies as large as a factor of 100 occur. As we shall see later, this "noise" in the emissions data is over 10 times larger than the changes in emissions that the control strategies would cause. This brings into question the significance of the model calculations themselves. Because the response of ozone concentrations to changes in VOC and NO_x emissions is a function of the base emission levels. Therefore, if the estimated base emissions are in error, the simulated response of ozone concentrations to emissions controls will also be in error. We are pursuing the cause of these discrepancies in the emissions inventory and hopefully it will lead to refined estimates of the true source strengths.

	State	County	County ID	Moles/day			VOC:NOX Ratio	Moles/km^2· day	
				CO	NOX	VOC		Q_{nox}	Q_{voc}
1	*NEW YORK	NEW YORK	334660	10065683	1012122	3184314	3.1462	16991.1	53457.1
2	*NEW YORK	QUEENS	335660	39364248	3024665	11881457	3.9282	10813.6	42477.9
3	*MARYLAND	BALTIMORE CITY	210120	17534614	812678	6706234	8.2520	4022.9	33197.2
4	*PENNSYLVANIA	PHILADELPHIA	397160	35772168	2245221	8308535	3.7005	6720.3	24868.6
5	*NEW YORK	RICHMOND	335720	10379752	695094	3455118	4.9707	4627.4	23001.3
6	*NEW JERSEY	UNION	315440	26695066	1932289	5632339	2.9149	7243.6	21113.9
7	*NEW JERSEY	HUDSON	312240	10992423	1726337	2568909	1.4881	14182.2	21104.2
8	*MASSACHUSETTS	SUFFOLK	228013	22485598	792897	3028011	3.8189	5467.0	20877.9
9	*NEW JERSEY	ESSEX	311380	33041914	1494144	6957026	4.6562	4437.8	20663.2
10	*NEW YORK	BRONX	330600	6857337	257354	2094203	8.1374	2423.6	19722.0
11	*NEW YORK	KINGS	333440	11722983	605681	3384794	5.5884	3340.9	18670.3
12	*NEW JERSEY	BERGEN	310300	48335268	2535695	11022022	4.3467	4184.1	18187.1
13	RHODE ISLAND	BRISTOL	410060	3028159	98055	1043692	10.6439	1514.4	16119.4
14	*MICHIGAN	WAYNE	235320	91528528	7571925	20737222	2.7387	4832.5	13234.6
15	*NEW YORK	NASSAU	334520	57521000	2089855	9130554	4.3690	2792.1	12198.8
16	*VIRGINIA	ARLINGTON	480200	5842543	202274	750922	3.7124	3254.2	12080.9
17	*NEW JERSEY	MIDDLESEX	313060	38036068	2581421	9537064	3.6945	3194.6	11802.6
18	*PENNSYLVANIA	DELAWARE	392360	25666810	2001089	5396931	2.6970	4199.2	11325.2
19	*DIST. COLUMBIA	DISTRICT OF COLUMBIA	90020	13100474	538043	1693277	3.1471	3405.7	10718.0
20	*MASSACHUSETTS	NORFOLK	228011	66063576	2131636	9929761	4.6583	2089.0	9731.0
21	*OHIO	CUYAHOGA	361600	57908668	3134743	11491107	3.6657	2654.3	9730.0
22	*NEW JERSEY	PASSAIC	314120	21015488	914425	4660920	5.0971	1838.9	9373.2
23	NEW JERSEY	CAMDEN	310740	16463954	800888	4363231	5.4480	1399.3	7623.1
24	PENNSYLVANIA	VENANGO	399140	2813720	195897	12853225	65.6122	111.6	7319.8
25	*MARYLAND	BALTIMORE	210140	35517040	2560884	11068580	4.3222	1653.5	7146.7
26	*MARYLAND	ANNE ARUNDEL	210080	24252476	1880201	7376027	3.9230	1716.3	6732.9
27	MASSACHUSETTS	MIDDLESEX	228009	48352864	2685719	14280815	5.3173	1257.0	6683.7
28	PENNSYLVANIA	MONTGOMERY	396000	40792352	1970227	8431594	4.2795	1533.7	6563.6
29	DELAWARE	NEW CASTLE	80180	16798494	1667715	6816126	4.0871	1466.8	5995.0
30	*PENNSYLVANIA	ALLEGHENY	390100	57341156	5049063	11024519	2.1835	2677.9	5847.2
31	NEW YORK	WESTCHESTER	337320	31524084	1359415	6691209	4.9221	1184.9	5832.0
32	NEW JERSEY	GLOUCESTER	311760	17428882	1099198	4804490	4.3709	1290.0	5638.6
33	*MASSACHUSETTS	DUKES	228004	14518997	447507	1515017	3.3855	1661.4	5624.7
34	MICHIGAN	OAKLAND	233980	57593680	2162042	11916965	5.5119	962.9	5307.2
35	*OHIO	SUMMIT	366500	23226908	2098513	5573228	2.6558	1976.3	5248.6
36	MICHIGAN	MACOMB	233140	27493968	1016808	6397227	6.2915	817.9	5146.0
37	CONNECTICUT	FAIRFIELD	70265	27439008	1683430	8269351	4.9122	1038.3	5100.5
38	CONNECTICUT	NEW HAVEN	70705	31563138	1378849	7952039	5.7672	881.4	5083.5
39	RHODE ISLAND	PROVIDENCE	410320	20378564	893263	5339668	5.9777	829.1	4956.1
40	*NEW YORK	ROCKLAND	335780	12373977	1154893	2251644	1.9497	2533.6	4939.7
41	OHIO	FRANKLIN	362220	38795072	1935449	6709903	3.4668	1389.0	4815.4
42	*VIRGINIA	FAIRFAX	481060	33041542	2135011	4826945	2.2609	2066.1	4671.1
43	NEW JERSEY	MORRIS	313260	28841766	1042782	5333787	5.1150	860.3	4400.5
44	*NEW JERSEY	MERCER	312980	14287335	1541153	2533543	1.6439	2609.9	4290.5
45	CONNECTICUT	HARTFORD	70425	33701216	1349847	8092153	5.9949	705.3	4228.0
46	*OHIO	LUCAS	363720	13949960	1895811	3720422	1.9624	2134.1	4188.1
47	RHODE ISLAND	KENT	410140	7172443	246287	1766590	7.1729	549.7	3942.8
48	PENNSYLVANIA	BUCKS	391200	26960526	1360517	6005847	4.4144	855.6	3776.8
49	MICHIGAN	GENESEE	231700	20231098	888794	6266397	7.0504	534.5	3768.5
50	NEW YORK	ALBANY	330060	11628486	1085358	5098686	4.6977	796.7	3742.7

Table 4-1. Major county sources of VOC ranked in order of source strength Q (= mass per area per time). Counties marked with an asterisk (*) are also major sources of NO_x (listed in Table 4-2).

	State	County	County ID	Moles/day CO	NOX	VOC	VOC:NOX Ratio	Moles/km² day Q_{nox}	Q_{voc}
1	* NEW YORK	NEW YORK	334660	10065683	1012122	3184314	3.14618	16991.1	53457.1
2	* NEW JERSEY	HUDSON	312240	10992423	1726337	2568909	1.48807	14182.2	21104.2
3	* NEW YORK	QUEENS	335660	39364248	3024665	11881457	3.92819	10813.6	42477.9
4	* NEW JERSEY	UNION	315440	26695066	1932289	5632339	2.91485	7243.6	21113.9
5	PENNSYLVANIA	MONTOUR	396020	903412	2387224	190889	0.07996	7090.3	567.0
6	* PENNSYLVANIA	PHILADELPHIA	397160	35772168	2245221	8308535	3.70054	6720.3	24868.6
7	OHIO	GALLIA	362320	1679810	7154637	269301	0.03764	5865.2	220.8
8	WEST VIRGINIA	MARSHALL	501020	2094859	4440680	394826	0.08891	5640.2	501.5
9	* MASSACHUSETTS	SUFFOLK	228013	22485598	792897	3028011	3.81892	5467.0	20877.9
10	WEST VIRGINIA	PUTNAM	501560	2583423	4528822	504502	0.11140	5024.8	559.8
11	* MICHIGAN	WAYNE	235320	91528528	7571925	20737222	2.73870	4832.5	13234.6
12	* NEW YORK	RICHMOND	335720	10379752	695094	3455118	4.97072	4627.4	23001.3
13	MICHIGAN	MONROE	233600	10879483	6570619	2295234	0.34932	4554.8	1591.1
14	* NEW JERSEY	ESSEX	311380	33041914	1494144	6957026	4.65620	4437.8	20663.2
15	OHIO	JEFFERSON	363160	9764820	4538728	1221784	0.26919	4263.9	1147.8
16	* PENNSYLVANIA	DELAWARE	392360	25666810	2001089	5396931	2.69700	4197.2	11325.2
17	* NEW JERSEY	BERGEN	310300	48335268	2535695	11022022	4.34675	4184.1	18187.1
18	* MARYLAND	BALTIMORE CITY	210120	17534614	812678	6706234	8.25202	4022.9	33197.2
19	* DIST. COLUMBIA	DISTRICT OF COLUMBIA	90020	13100474	538043	1693277	3.14710	3405.7	10718.0
20	* NEW YORK	KINGS	333440	11722983	605681	3384794	5.58841	3340.9	18670.3
21	* VIRGINIA	ARLINGTON	480200	5842543	202274	750922	3.71240	3254.2	12080.9
22	* NEW JERSEY	MIDDLESEX	313060	38036068	2581421	9537064	3.69450	3194.6	11802.6
23	PENNSYLVANIA	BEAVER	390560	11025830	3442666	1966525	0.57122	3021.1	1725.7
24	OHIO	LAKE	363280	5463210	1783642	1635356	0.91686	2981.3	2733.5
25	WEST VIRGINIA	HANCOCK	500620	3765022	600557	568036	0.94585	2793.8	2642.5
26	* NEW YORK	NASSAU	334520	57521000	2089855	9130554	4.36899	2792.1	12198.8
27	PENNSYLVANIA	NORTHAMPTON	396580	13920917	2682753	2328365	0.86790	2754.9	2391.0
28	PENNSYLVANIA	INDIANA	394240	4151229	5831975	1140277	0.19552	2729.5	533.7
29	* PENNSYLVANIA	ALLEGHENY *	390100	57341156	5049063	11024519	2.18348	2677.9	5847.2
30	* OHIO	CUYAHOGA	361600	57908668	3134743	11491107	3.66573	2654.3	9730.0
31	* NEW JERSEY	MERCER	312980	14287335	1541153	2533543	1.64393	2609.9	4290.5
32	* NEW YORK	ROCKLAND	335780	12373977	1154893	2251644	1.94966	2533.6	4939.7
33	WEST VIRGINIA	HARRISON	500660	2713556	2657376	575741	0.21666	2454.7	531.8
34	* NEW YORK	BRONX	330600	6857337	257354	2094203	8.13744	2423.6	19722.0
35	* OHIO	LUCAS	363720	13949960	1895811	3720422	1.96244	2134.1	4188.1
36	OHIO	ADAMS	360040	1778439	3187405	325759	0.10220	2096.6	214.3
37	* MASSACHUSETTS	NORFOLK	228011	66063576	2131636	9929761	4.65828	2089.0	9731.0
38	* VIRGINIA	FAIRFAX	481060	33041542	2135011	4826945	2.26085	2066.1	4671.1
39	PENNSYLVANIA	ARMSTRONG	390260	3403191	3510334	707705	0.20161	2059.9	415.3
40	* OHIO	SUMMIT	366500	23226908	2098513	5573228	2.65580	1976.3	5248.6
41	MICHIGAN	BAY	230400	5547095	2183170	750525	0.34378	1885.8	648.3
42	MARYLAND	PRINCE GEORGES	211300	28559394	2309877	3947869	1.70913	1842.7	3149.4
43	* NEW JERSEY	PASSAIC	314120	21015488	914425	4660920	5.09710	1838.9	9373.2
44	WEST VIRGINIA	MONONGALIA	501140	2373645	1715912	478245	0.27871	1815.2	505.9
45	OHIO	WASHINGTON	367100	5358478	3008603	894350	0.29726	1812.3	538.7
46	* MARYLAND	ANNE ARUNDEL	210080	24252476	1880201	7376027	3.92300	1716.3	6732.9
47	OHIO	LORAIN	363640	14491698	2130922	3683211	1.72846	1662.2	2873.0
48	* MASSACHUSETTS	DUKES	228004	14518997	447507	1515017	3.38546	1661.4	5624.7
49	WEST VIRGINIA	MASON	501060	6647384	1859526	306202	0.16467	1658.2	273.0
50	* MARYLAND	BALTIMORE	210140	35517040	2560884	11068580	4.32217	1653.5	7146.7

Table 4-2. Major county sources of NO_x ranked in order of source strength Q (= mass per area per time). Counties marked with an asterisk (*) are also major sources of VOC (listed in Table 4-1).

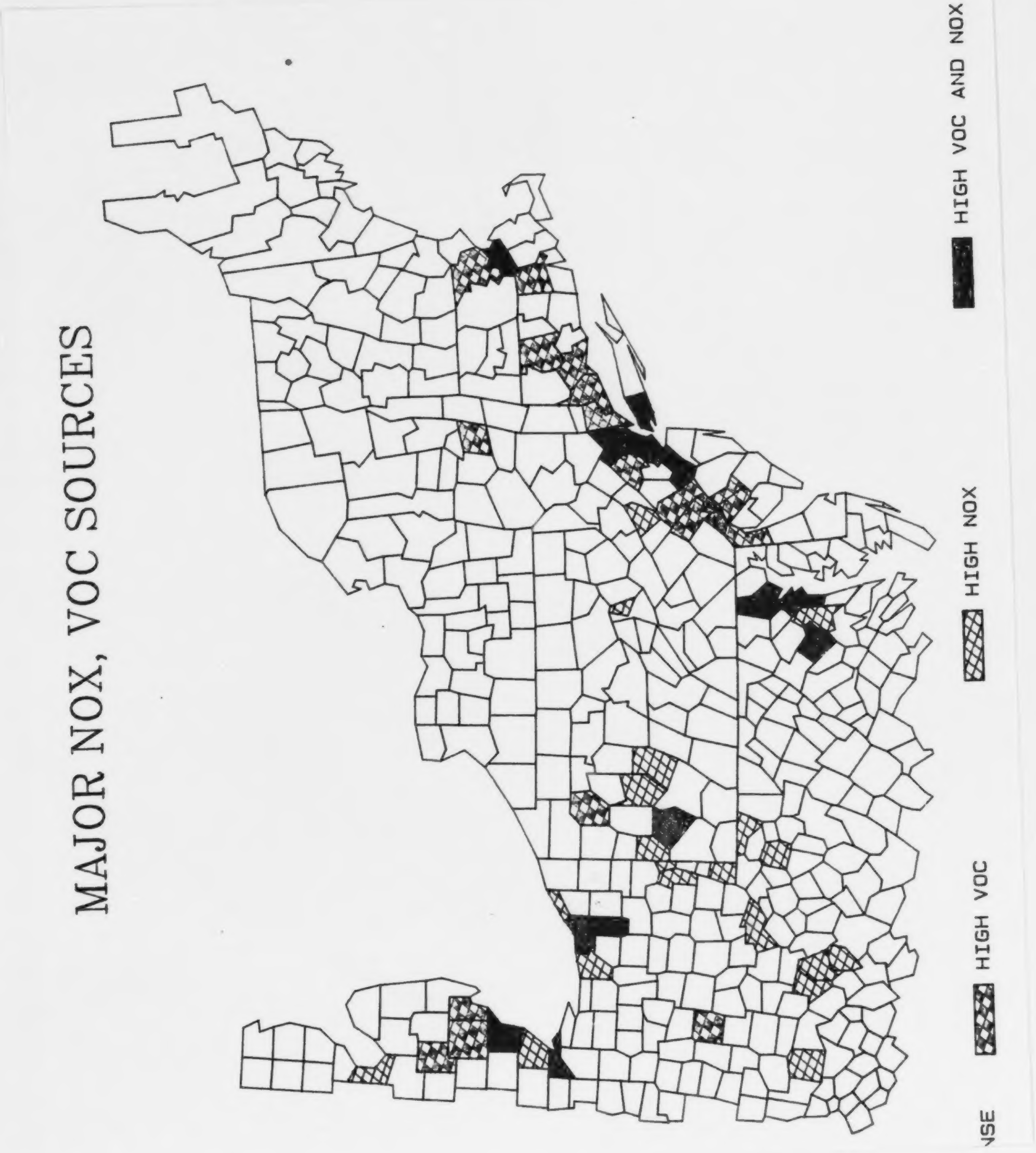
MAJOR NOX, VOC SOURCES
HIGH VOC AND NOX
HIGH NOX
HIGH VOC

Figure 4-1. Locations of the 70 major source counties listed in Tables 4-1,2. See Eq. 4.7 for definitions of "high VOC", "high NO_x", and "high VOC and NO_x".

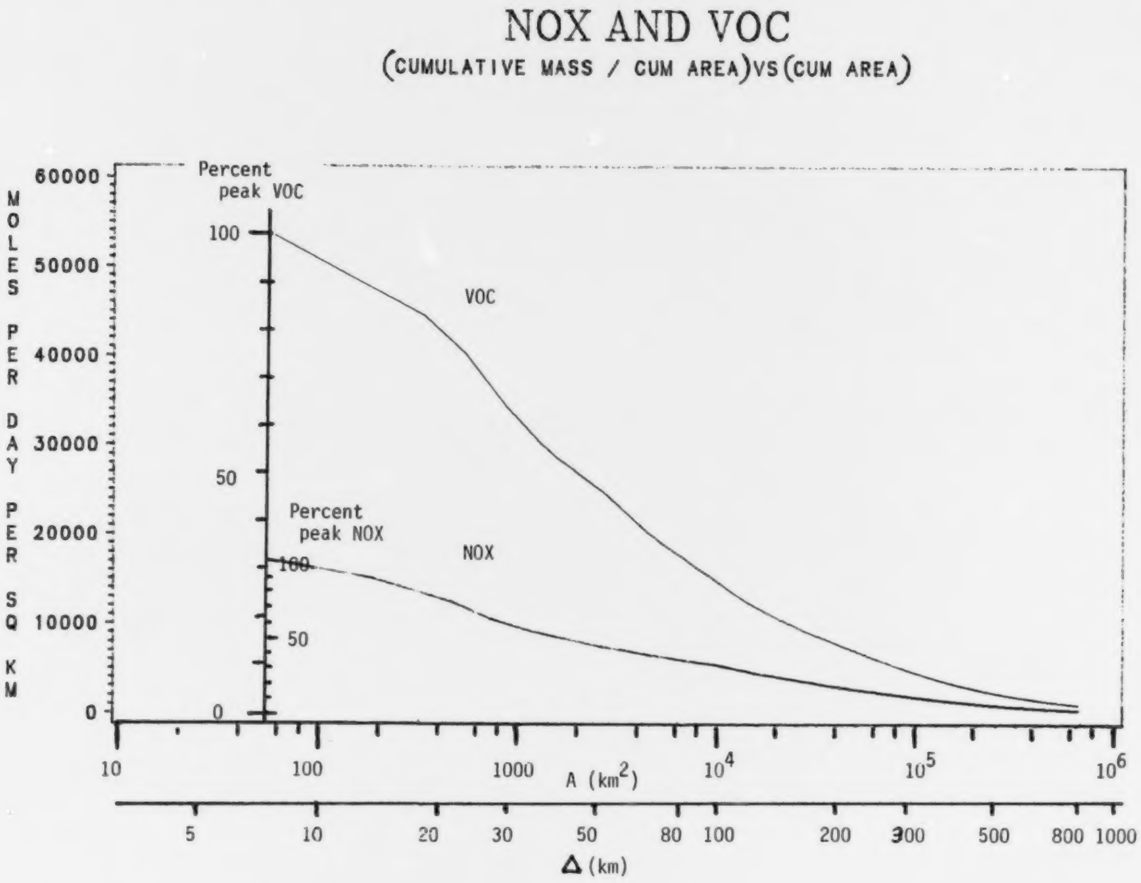

Figure 4-2. Cumulative VOC and NO_x emissions densities vs. cumulative source area and characteristic length scale. See text, pages 36 - 37, for details.

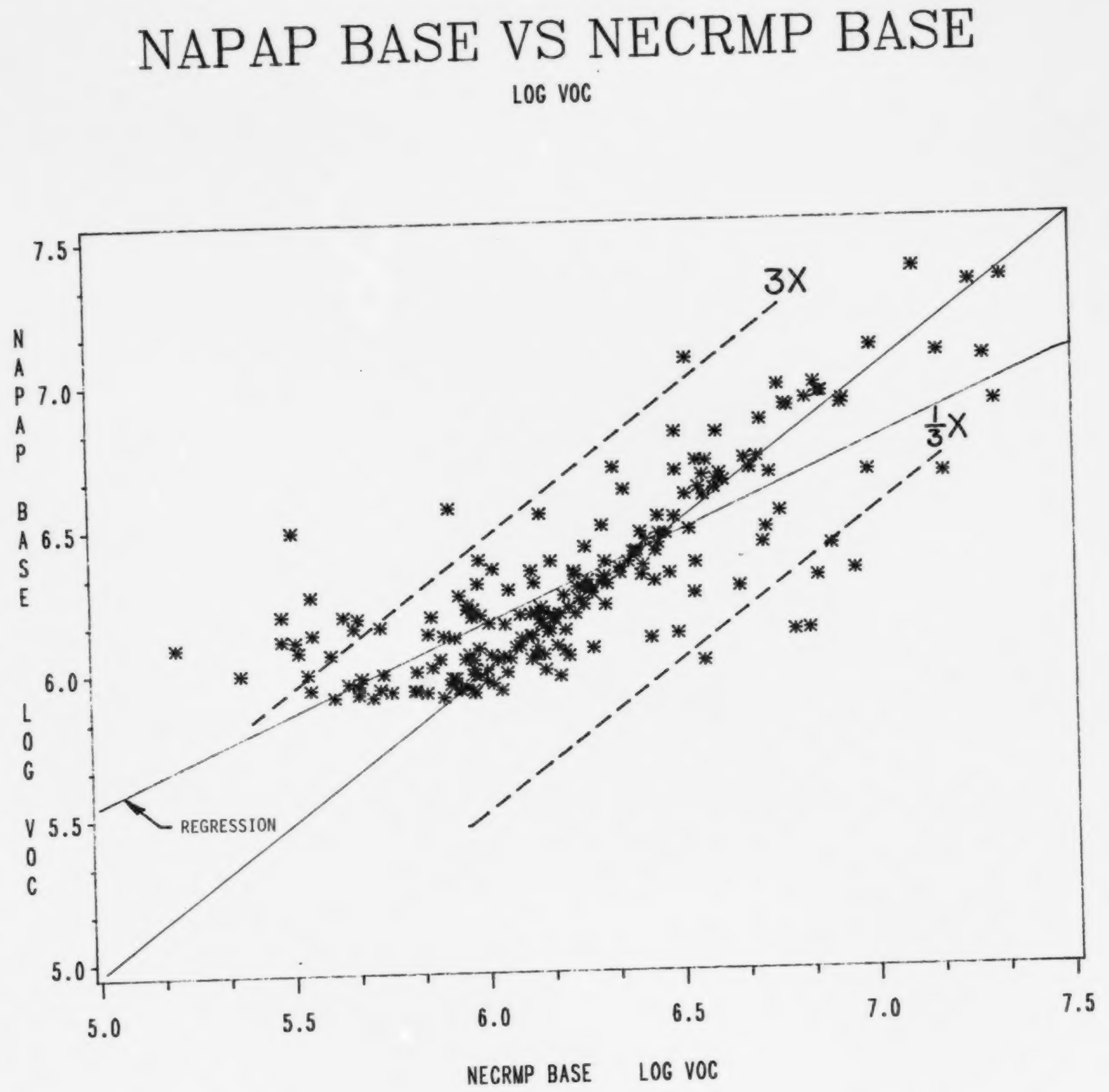

Figure 4-3. Comparison of NAPAP and NECRMP estimates of gridded VOC emissions for the 200 strongest source cells in the ROM grid network.

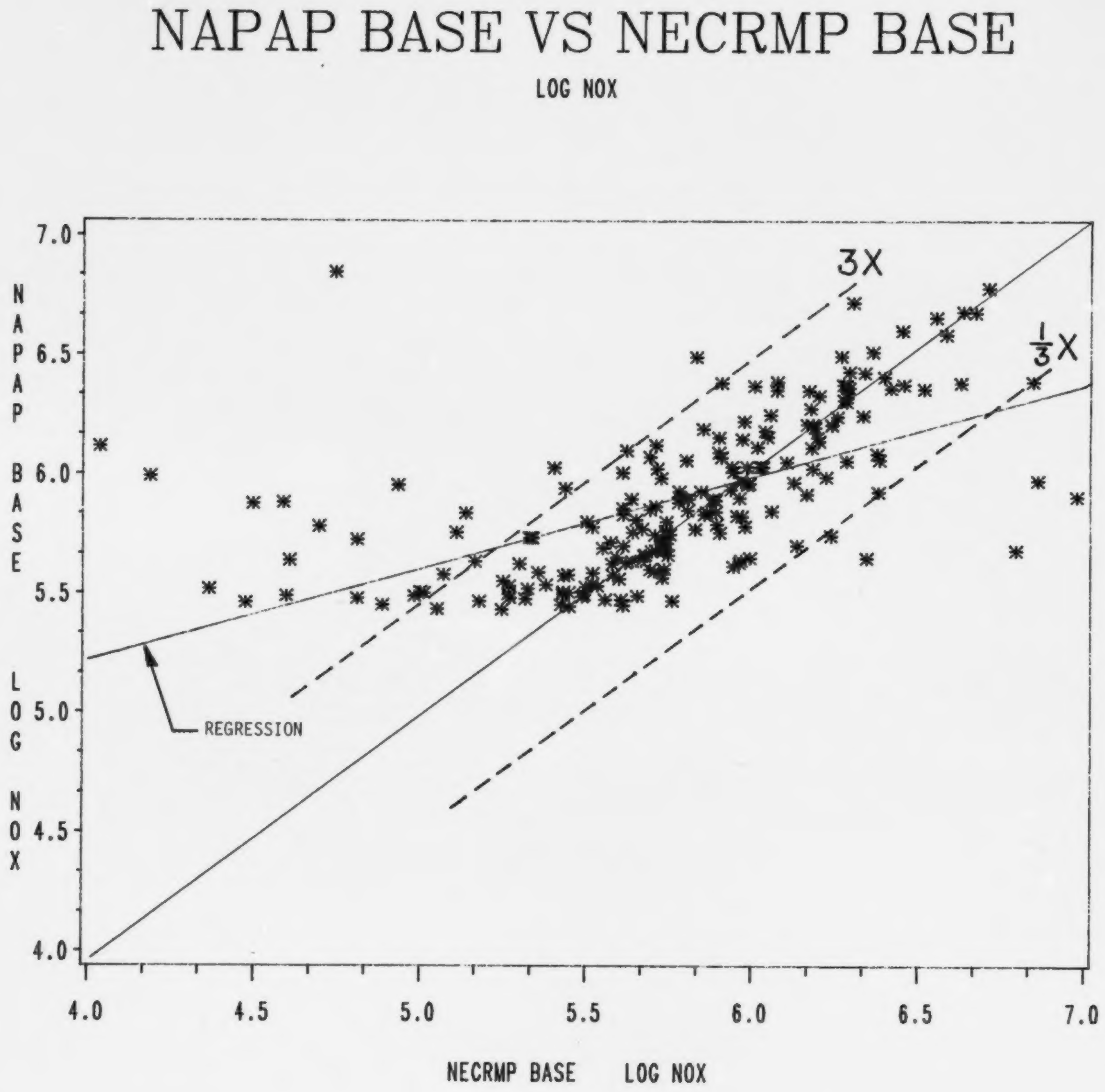

Figure 4-4. Comparison of NAPAP and NECRMP estimates of gridded NO_x emissions for the 200 strongest source cells in the ROM grid network.

SECTION 5

DEFINITIONS OF RECEPTOR CLASSES FOR USE IN ANALYZING SIMULATED CONCENTRATIONS

In several earlier reports (Lamb, 1983a, b; 1984) the author pointed out that the concentrations predicted by a regional scale model using a discrete set of meteorological data and a given source inventory are stochastic rather than deterministic variables. In the following paragraphs we will review the basic concepts behind this premise. They are important to the manner in which models should be employed in decision making roles and they form the basis of the technique we use in this report to analyze model results.

The root of the premise is the mathematical fact that a discrete set of meteorological data do not uniquely define the atmospheric flow field. Rather, they delineate an infinite set, or ensemble, of flow fields any member of which is a possible description of the flow that actually existed at the time the meteorological measurements were made (see Lamb and Hati, 1986). Hence, for a given source distribution specification, the equations governing species concentration in the atmosphere define a one-to-one mapping of members of the ensemble of flow fields to members of an ensemble of concentrations.

The network of processors that compose the ROM framework (see Figure 2-3, page 7) was designed to produce the information necessary to simulate the ensemble of concentration fields associated with a given set of meteorological and emissions conditions. From the simulated concentration ensemble one can derive probabilities, expectations or any desired statistical property of concentration at a single site or group of sites. We refer to this as the "probabilistic mode" of ROM operation. Strictly speaking this is the operating mode that should be employed both in model verification studies and in any control strategy assessments in which one is interested in effects at one or more specific receptor sites.

Complementing the probabilistic mode is the "quasi-deterministic mode" in which the ROM generates a single concentration field for each species. This single field, or realization, is computed by the ROM using a procedure designed to select from the concentration ensemble the member that has the highest probability of occurrence. Despite the fact that this is the most likely concentration field, the significance of values at any given point in space and time is limited in the same sense that the most probable outcome of a random process is not necessarily the outcome that one would observe on any given occasion. In this case one might wonder what point there is in running the model in the quasi-deterministic mode.

One reason is that useful information may exist in certain aggregate properties of individual realizations of the concentration field, as opposed to the value of concentration at a specific site. Based largely on theoretical arguments, Lamb (1983b) hypothesized that receptor sites can be grouped into classes, determined by the distances to the nearest meteorological station and major emissions sources, such that concentration averaged over all sites in a given receptor class at a given hour is a quantity that is approximately the same for all realizations in the concentration ensemble. If this is true, then with respect to the receptor class average (RCA), the concentration field is a quasi-deterministic variable, and we can interpret model simulations of single realizations in the conventional deterministic manner. Although this hypothesis has not yet been tested, all applications of the ROM in the foreseeable future will proceed under the assumption that it is correct. Because if the hypothesis is false, that is, if there does not exist any useful aggregate property of the concentration field that is relatively invariant across the ensemble, then meaningful results can be derived only from probabilistic mode operations of the model. And at present this mode of operation is prohibitively expensive. As an example, analysis of a n-day period requires only a single run of the ROM in the quasi-deterministic mode but five to ten runs in the probabilistic mode. Thus, the latter mode is five to ten times more expensive. In the case of the ROM in its current form the difference in costs in the two modes of operation for a 5-day simulation period could be of the order of $100K.

Our digression on the model's operating modes was intended to give the reader the proper basis for interpreting the results of the control strategy simulations that we are reporting here. In this study we applied the ROM in the quasi-deterministic mode, once to the 23-31 July 1980 time period using the base case source emissions as inputs, and then a second time to the same period using the modified emissions. According to the points we raised above, the only aspect of the model results that we can use to assess the effects of the control strategy is statistical properties of concentration over receptors of the same class. Comparing the concentrations predicted at a single receptor using the base emissions with the corresponding value computed with the control emissions is not meaningful because we are examining only a single realization of the concentration ensemble and the relationship between the two concentration values could vary radically from one member of the ensemble to another. By contrast, differences in the receptor class average (RCA) concentration obtained for the base and control emissions do not vary appreciably within the ensemble, according to our untested hypothesis, and therefore we can use differences in the RCA's as a measure of the impact of the emissions control strategy.

Since the ROM is a grid model that simulates concentration averaged over the volume of each grid cell, rather than concentration at individual points in space, our analyses of the model results must be done in terms of receptor cells rather than receptor points. Thus, in analogy with the receptor classes mentioned earlier, we will define cell classes. For the purposes of the present report, we define four cell classes -- urban, suburban, rural and wilderness -- as follows:

urban cell	=>	70 strongest VOC and NO_x cells in the model domain, excluding Canada;
suburban cell	=>	"urban" land useage U > 10% and cell is within 50 km of any cell of the "urban" class;
rural cell	=>	$0 < U < 10\%$, distance d to the nearest cell of the "urban" class is in the range $50 < d < 100$ km, and "agricultural" land useage > 10%;
wilderness cell	=>	U = 0 and distance d to the nearest cell of the "urban" class is greater than 100 km.

These definitions are largely heuristic and are meant mainly to illustrate applications of the ROM in the quasi-deterministic mode. In a future study we will test the hypothesis concerning the determinism of receptor class average concentrations and at that point rigorous specifications of class definitions will be developed, assuming that the hypothesis is validated.

In selecting specific cells from the ROM's domain for inclusion in each of the four classes, we began by finding all cells that satisfied the "urban class" criterion. A total of 70 cells in the 60 x 42 cell domain were found to meet these conditions. (Most of the 70 major source counties listed in Table 4-1, 2 (pages 41, 42) are represented by at least one of the urban cells.) Next, we searched for cells fulfilling the "suburban" class criteria. More than 70 cells met these requirements so we selected 70 at random from the candidate set. This procedure was repeated for the "rural" and "wilderness" classes, resulting finally in sets of 70 cells of each of the four categories. Having equal numbers of cells in each group helps minimize sampling aberrations. In the selection process only the land area within the United States was considered. Figure 5-1 (page 53) shows the locations of each of the cells in all four receptor classes. We emphasize that some grid cells do not fall within any of the four receptor types.

The criteria that we used to define the receptor classes were designed to satisfy what we believe are necessary conditions for the validity of the ensemble invariance hypothesis that we discussed earlier. However, the characteristics of the receptors that meet these criteria are not necessarily best suited to the needs of regulatory analyses where one is concerned with exposures of population, crops, and forest. Furthermore, regulatory studies must consider all locations rather than just subsets of randomly chosen sites. To serve these needs we have defined four county types analogous to the four receptor classes defined above. These are as follows:

major source county = any one of the 70 major source counties listed in Tables 4-1, 2 (pages 41, 42);

non-major source SMSA = Standard Metropolitan Statistical Area (SMSA) other than major source counties;

agricultural county = not a county of either of the above types agricultural land useage exceeds the sum of forested land plus unforested wetlands;

natural county = all counties not falling into any of the above categories.

The counties in each of these four groups are listed in Appendix C and illustrated in Figures 5-2, 3, 4 and 5 (pages 54-57). In our analyses of the model results in Section 8, we will make use of both the receptor cell and receptor county classes defined above.

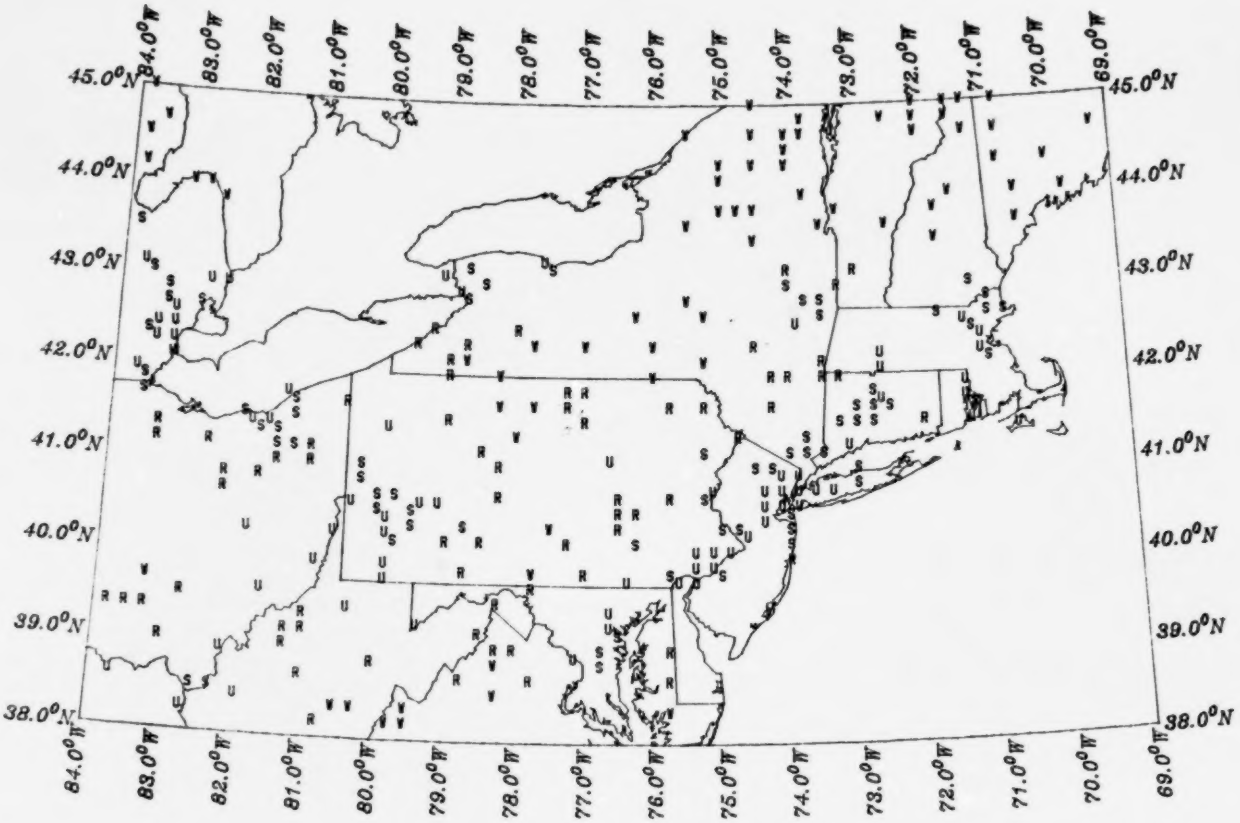
84.0°W
83.0°W
82.0°W
81.0°W
80.0°W
79.0°W
78.0°W
77.0°W
76.0°W
75.0°W
74.0°W
73.0°W
72.0°W
71.0°W
70.0°W
69.0°W
45.0°N
44.0°N
43.0°N
42.0°N
41.0°N
40.0°N
39.0°N
38.0°N

Figure 5-1. Locations of the 70 cells selected in each of the four receptor classes urban (U), suburban (S), rural (R) and wilderness (W).

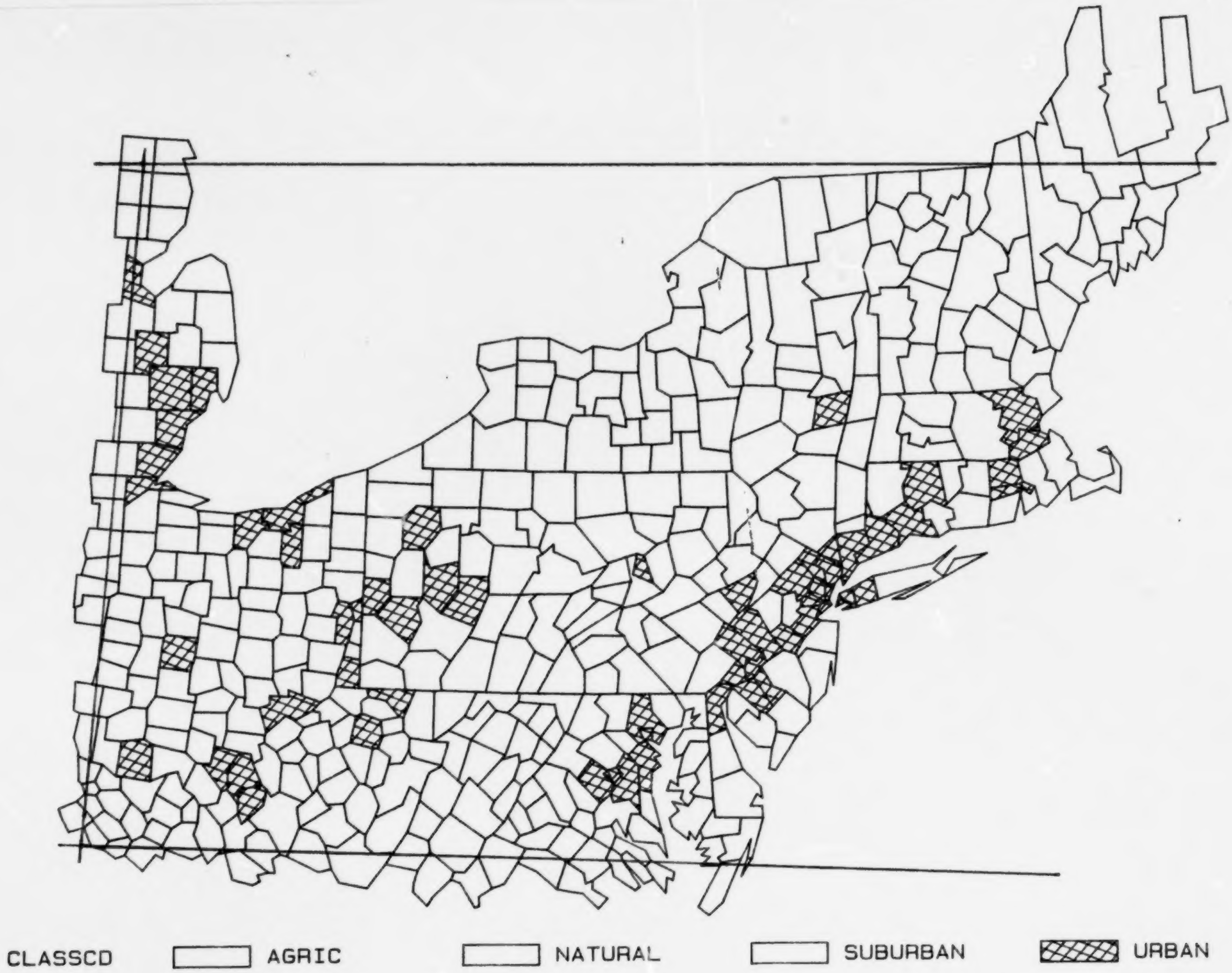
CLASSCD
AGRIC
NATURAL
SUBURBAN
URBAN

Figure 5-2. Locations of the 70 major source counties, defined as "urban" type receptors.

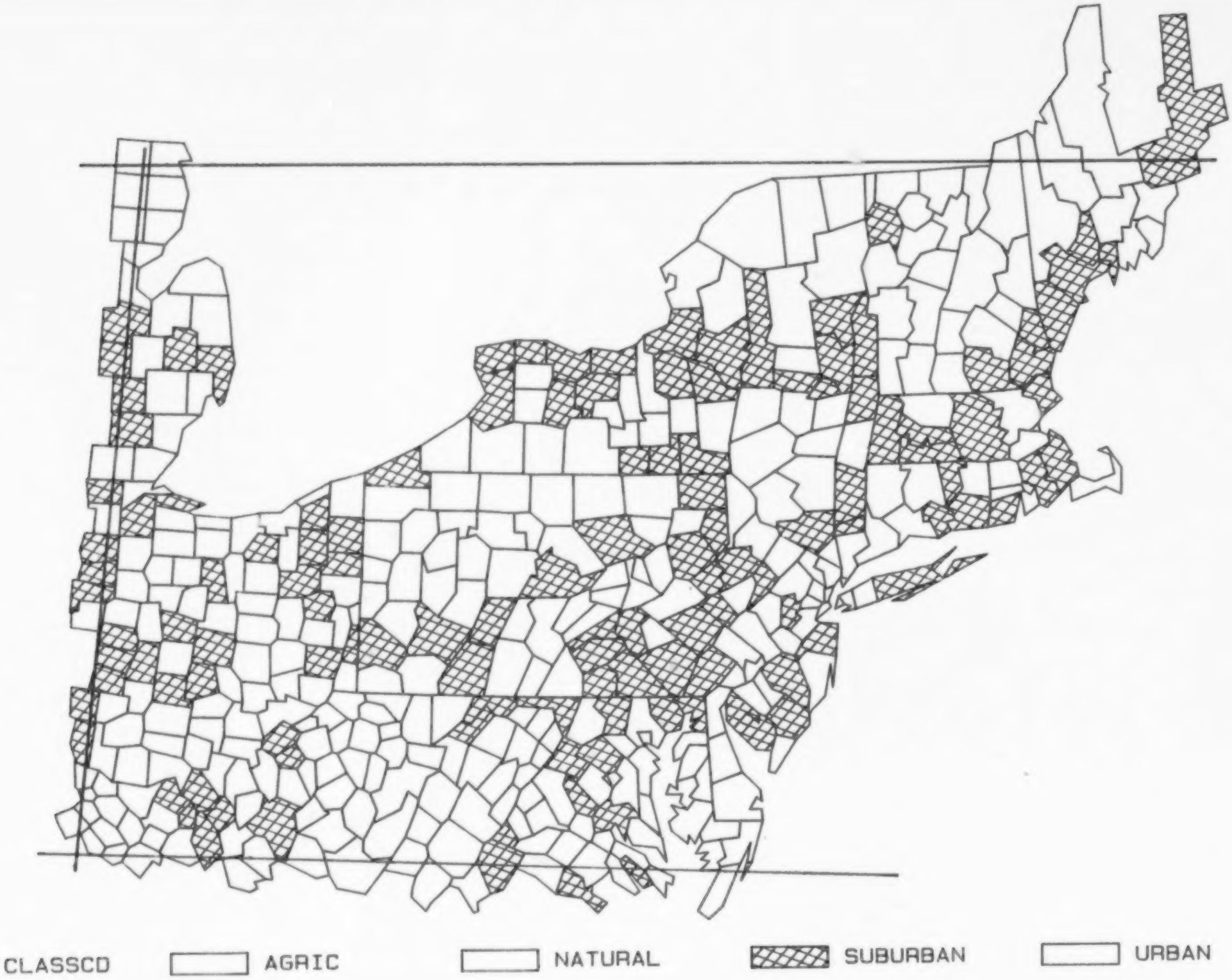
CLASSCD
AGRIC
NATURAL
SUBURBAN
URBAN

Figure 5-3. Non-major source Standard Metropolitan Statistical Areas (SMSAs) defined here as "suburban" type receptors.

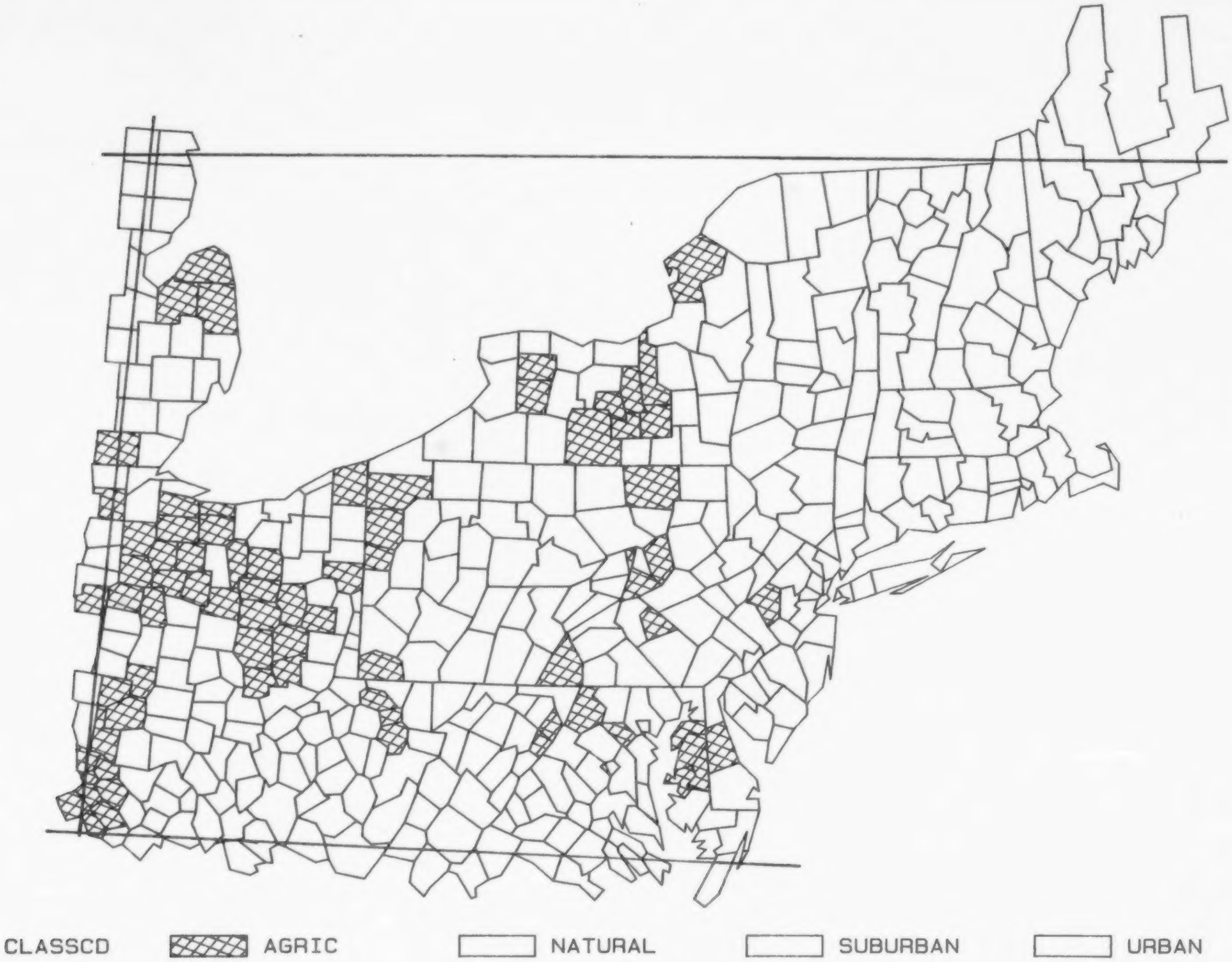
CLASSCD
AGRIC
NATURAL
SUBURBAN
URBAN

Figure 5-4. Non-major source, non-SMSA counties in which the predominant land use is in agricultural activities, defined here as "agricultural" type receptors.

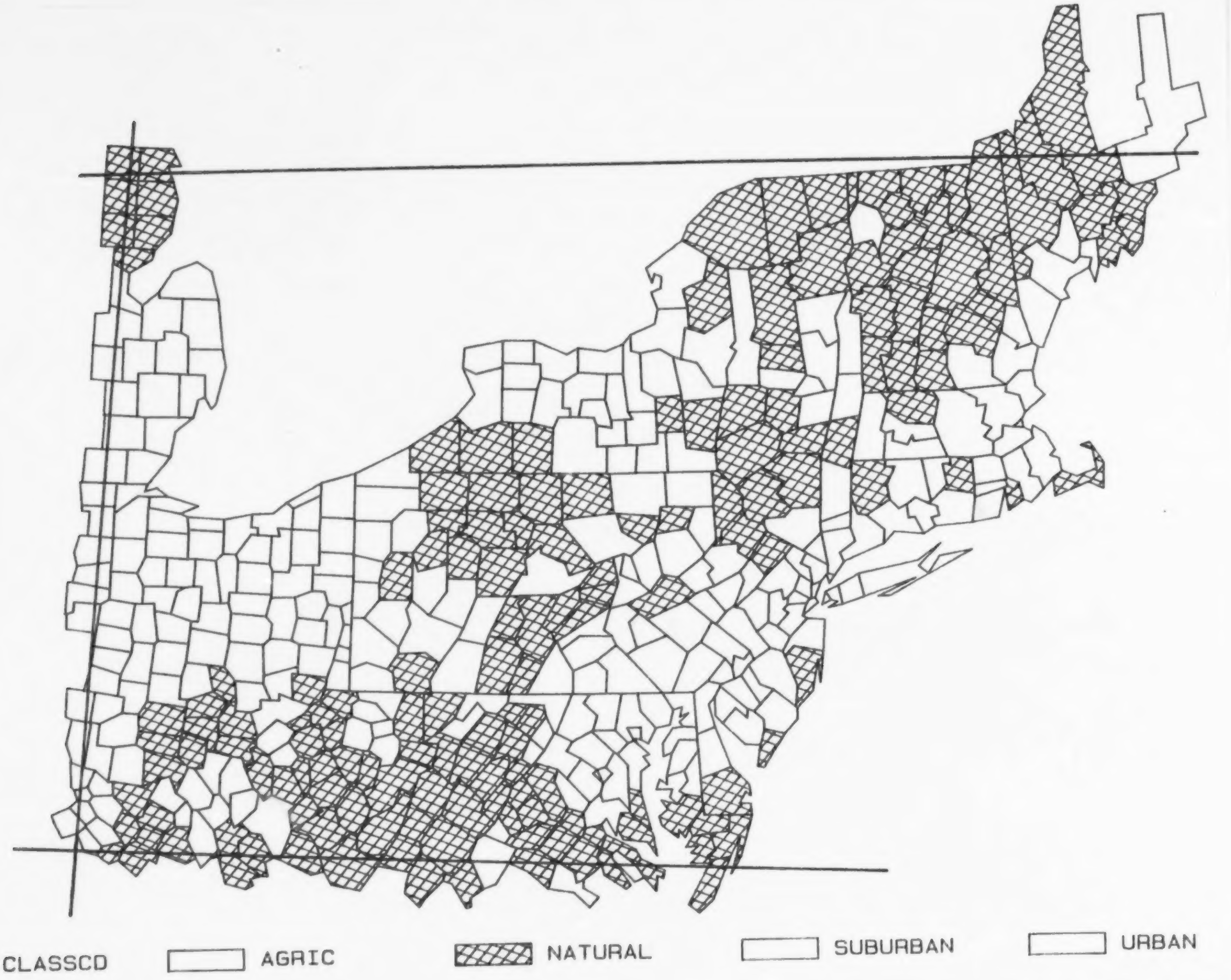
CLASSCD
AGRIC
NATURAL
SUBURBAN
URBAN

Figure 5-5. Counties in which forest and/or wetlands are the predominant land use, defined here as "natural" type receptors.

SECTION 6

METEOROLOGY OF THE TEST PERIOD: 23 - 31 JULY 1980

It is customary in air pollution modeling studies to specify the meteorological conditions used in performing the simulations, i.e., wind speed and direction, mixing depth, cloud cover, and the like. In urban modeling this task is rather straightforward because one is concerned with the limited spatial domain of a single city and with a time period of only one or two days, usually days in which meteorological conditions were stagnant. Therefore, in these particular applications meteorological conditions are quite well defined.

However, in regional scale studies that extend over 1000 km areas and periods of a week or more, "meteorology" in the sense in which it is used in urban studies is not well defined; because conditions vary from site to site within the spatial domain at any instant and from time to time within the simulated period at any site. One can discuss the passage of fronts through the simulated area or meteorological conditions at selected times and locations, but for the most part these discussions are of little or no value because they do not describe the cumulative effects of transport and mixing over time that affect concentrations over a regional area, particularly concentrations in rural and remote areas. Moreover, discussions of the meteorological variables themselves provide no perspective from which to judge the significance of the results of the model simulations. For example, if the model is being used to assess the effectiveness of emissions control strategies, one needs to know whether the predicted effects can be regarded as applicable to other seasons or other years; or whether, due to the use of meteorological data from an anomalous period, the results represent conditions that rarely occur.

These considerations have led us to the conclusion that in regional scale, multi-day modeling studies the focus of the meteorological discussions should not be on the variables themselves but rather on the effect the meteorology had on species concentrations observed during the period of interest. In particular, we believe that the most relevant indicator of the air pollution potential of the meteorological scenario selected, and the best index for judging how applicable the model results are likely to be to other times within a season or to different years, is the frequency distribution of observed concentration values, principally ozone, during the scenario period and the extent to which this distribution differs from that observed over the entire season or over the same season in a number of years combined. Detailed analyses of the meteorological variables can be useful in understanding why particular concentration phenomena occur. We will present an example of an analysis of this type later in this section.

Figure 6-1 (page 67) shows one of the concentration frequency distributions that provides information about the effects of the meteorology used in the model simulation. The figure shows a quartile plot of the maximum hourly ozone concentrations observed each day at all SAROAD monitoring sites in the model domain, some 200 sites altogether, during the three summer months June, July and August of 1980. (June through September is the period in which the highest ozone levels are generally observed each year in the Northeastern U.S.) Below is an explanation of the symbols used in the quartile plot shown in Figure 6-1.

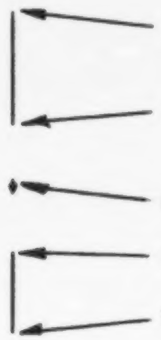

largest maximum hourly ozone observed at all SAROAD sites on the day indicated by the abscissa

75-percentile of maximum hourly ozone observed at all SAROAD sites this day

median value

25-percentile value

minimum of all maximum hourly ozone values observed at all SAROAD sites this day.

The data presented in Figure 6-1 indicate that the meteorological conditions that are to be used in the model simulations, namely data from the period 23-31 July 1980, are not capable of producing ozone concentrations as high as those that were observed on other occasions in 1980. However, this particular meteorological scenario did manage to drive the median value of the daily maximum ozone values to a level almost as high as it achieved at any other time during the summer.

Note that at the beginning of the chosen period ozone concentrations throughout the model area were as low as at any other time during the season. This aspect of the concentrations was the principal reason for selecting 23 July as the beginning of the simulation period. Because as we have already discovered in our earlier model applications, attempts to initialize a simulation at a time when significant amounts of ozone or precursor species are present in the domain introduce considerable error into the calculations because monitoring data are not available in sufficient density to specify the concentrations of all the simulated chemical species accurately. The simplest way to minimize the initialization errors is to begin the calculations at a time shortly after a "clean" air mass has moved across the model domain and concentrations are near tropospheric background levels at a majority of the monitoring sites. Consequently, in our model applications we have adopted a policy of using meteorological scenarios that begin at times when the median value of the observed hourly maximum ozone concentrations over the entire model domain is minimal.

One might argue that if the only purpose of the model simulations is to compare concentrations that would result from different source fields, it should make no difference when the meteorological scenario begins. But this is not true because the concentrations that occur at certain locations, particularly those remote from the major source areas, may be the result of the cumulative effects of transport, mixing and emissions over a period of several days. For example, if we started the meteorological scenario at an arbitrary hour and assumed, for the purposes of initializing the model that "clean" conditions existed at that hour, we might easily underpredict the peak concentrations that a given set of emissions would cause if the starting hour happened to be in the midst of a developing air pollution episode. However, the chances of such an error are greatly reduced by starting the meteorology at a time when concentrations were observed to be near minimum values.

The data presented in Figure 6-1 provide a measure of how well the chosen meteorological scenario represents the air pollution modeling region as a whole. Similar information pertaining to individual locations within the region is provided by quantile-quantile plots such as those shown in Figure 6-2a,b,c (pages 68-70) for selected monitoring sites. These graphs compare the cumulative frequency distribution of hourly averaged ozone concentrations observed during the scenario period 23-31 July at a given monitoring station with the corresponding distribution observed over the whole season, June - August, at the same site. The graphs are read as follows. Let (x_7, y_7) be the coordinates (abscissa, ordinate) of the point marked "7" in Figure 6-2a (or 6-2b or c). Then 70% of the hourly averaged ozone concentrations observed during the season at the given site were below x_7(ppb) while 70% of those observed during the scenario period were below y_7(ppb). The same interpretation applies to the point marked "5" except in this case reference is to the 50% decile rather than 70%. Points marked by asterisks refer to quantiles other than the decile points explicitly noted.

If the concentration distribution observed during the scenario period were identical to that observed over the entire season, the points in the quantile-quantile plots would all lie on the "45-degree" line (drawn in each figure). Looking at each of the graphs in Figure 6-2 we see that below about the 90 percentile, the scenario and seasonal concentration distributions are in surprisingly close agreement at each of the three stations represented (named below), while above the 90 percentile point significant differences occur.

In the case of Figure 6-2a (page 68), which represents ozone data collected at a rural site in Connecticut about 150 km northeast of New York City, the top 10% of the concentrations observed during the 9-day scenario period ranged from about 100 ppb to a high of 159 ppb, whereas the top 10% of the values measured during the season span an interval nearly 3 times as wide -- 100 ppb to 262 ppb. Since this particular site is in the heart of the area where the highest ozone concentrations observed in the Northeastern U.S. occur (see Figure 3-1, page 20), we might conclude that the meteorological scenario that we have chosen for the model simulations is not the best for testing emissions control strategies in this region. (As we have stated before, formal applications of the Regional Oxidant Model for regulatory studies will not be undertaken until the final version of the model is complete, and we have resolved issues such as the one in question here regarding the relevance of short-period simulations to the ozone problem in general.)

Figure 6-2b (page 69) compares the seasonal and scenario ozone frequency distributions measured at Whiteface Mountain, a remote, high-altitude site in upstate New York. Again the distributions are in good agreement up to the 90-th percentile. Beyond that point the extreme concentrations observed during the scenario are smaller than those seen over the entire summer.

Finally, in Figure 6-2c (page 70) we have an instance in which concentrations higher than the 90-th percentile value occurred more frequently during the scenario period than during the season -- just the reverse of the situation at the other two monitoring stations. The data represented in Figure 6-2c were collected at a New Jersey site about 50 km east of Philadelphia.

In summary, the ozone observations indicate that:

(1) over the modeling area as a whole meteorological conditions that occurred during the scenario period 23-31 July 1980 were not adequate to cause extreme concentrations, although at isolated locations values equal to the seasonal peak were observed;

(2) At seven representative receptor locations, three of which we discussed (see Figure 6-2), concentration values below the 90-th percentile level were observed at each station with about the same frequency during the 9-day scenario period as during the whole season, June-August. However, concentrations higher than the 90-th percentile value at any station occur with significantly different frequencies during the scenario than during the season.

We infer from the latter finding that 90 percent of the time, concentrations at any location are dominated by processes whose time scales are much shorter than 9 days. We have already pointed out that there is a strong diurnal variation in ozone at surface sites with a net production of ozone occurring during daylight hours and net destruction occurring at night. So we suspect that it is diurnal variations in wind speed, turbulent mixing and sunlight that determine concentrations 90 percent of the time. The highest concentrations observed at any site, namely those seen less than 10 percent of the time, appear to be caused by processes whose periods are longer than 9 days. This conjecture is based on the following reasoning. Suppose the period of the events in question is less than 9 days. In this case the 9-day sample window will capture several events which would tend to cause the scenario frequency of high concentrations to approach the frequency observed over a long period. However, if the event cycle is longer than 9 days, the scenario frequency of high concentration will either exceed or fall below the corresponding long-term frequency depending on whether the 9-day sample window captured or missed, respectively, one of the events in questions. It is the latter behavior that we observe in the ozone frequency data.

The fact that so much of the seasonal frequency distribution of ozone concentrations is emulated by a distribution based on only 9 days of observations suggest that quite reliable estimates of seasonal mean concentrations could be derived from 9 day model simulations. The same is not true, however, of peak concentrations. We are presently studying the ozone data in detail in an effort to determine criteria for selecting meteorological scenarios that will yield model outputs that can be used to infer estimates of all seasonal concentration statistics.

At the beginning of this section we stated that analyses of meteorological variables performed in the conventional way could be useful in understanding why particular concentration phenomena occur. Air parcel trajectory analyses in particular are often helpful in diagnosing causes of air quality events because it is the Lagrangian characteristics of the wind field that govern concentration distributions. Figure 6-3 (page 71) shows trajectories computed from the 9-day meteorological scenario wind fields. The trajectories begin at hour 0000 of day 206, i.e., the second day (July 24) of the 9-day period, at a number of major urban centers in the Northeast. The trajectories terminate on day 211, with the exception of those that pass outside the model boundaries before this day. Day 206 is significant because a cold front had just crossed the

East Coast by the beginning of this day (see Appendix A), and a new, clean air mass had established itself over the region.

The trajectories from the Eastern Corridor cities are especially interesting. They indicate that air that crossed the Eastern Corridor cities on day 206 returned to the same general area after 2 to 3 days of travel and crossed the cities a second time traveling in roughly the opposite direction. According to the simulations, air that originated over cities between Philadelphia and Boston spent a large part of its travel over the ocean where, as we have explained before, sunlight conditions and weak vertical mixing are highly conducive to ozone formation from VOC and NO_x emissions. The recirculatory nature of the trajectories is a consequence of the latitude of the cities in question relative to that of the path of the anticyclone that moved across the region following the frontal passages. Thus, we are led to wonder whether the combination of latitude and proximity to the ocean makes the Eastern Corridor cities more susceptible to air quality problems than other geographical areas of the country. We are investigating this question in our present studies because it has important bearing on the formulation of effective emissions control plans for this area.

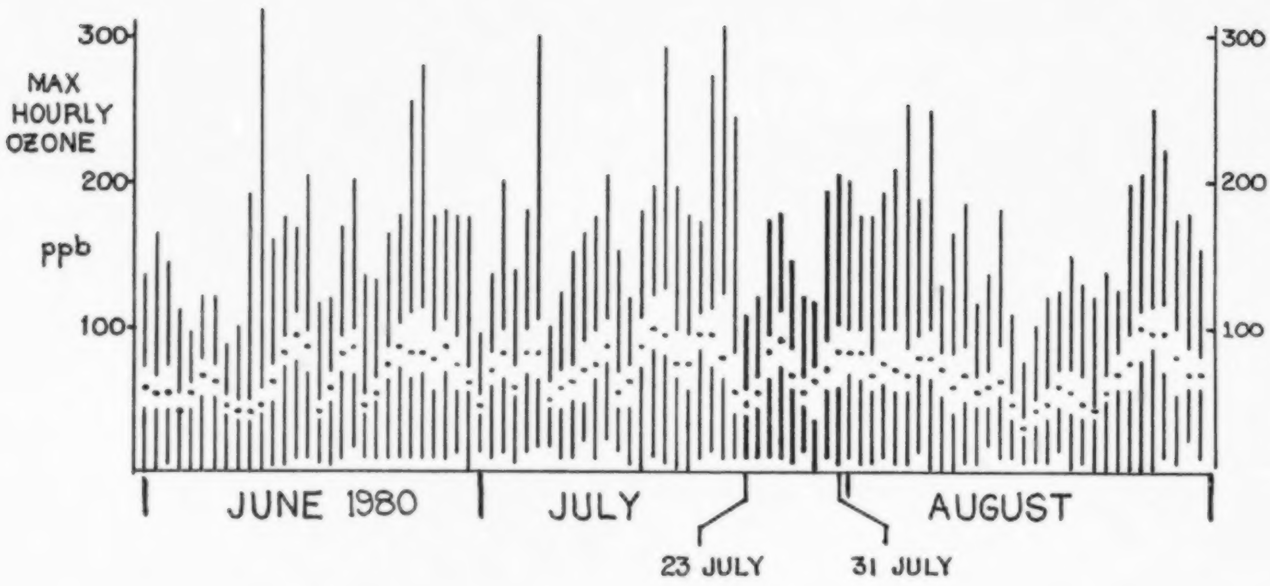

Figure 6-1. Quartile plot of the maximum hourly averaged ozone concentrations observed at some 200 SAROAD monitoring stations each day during the period June - August 1980. See text, page 60, for explanation of symbols.

Figure 6-2a. Quantile - quantile comparisons of the cumulative frequency distributions of hourly ozone concentrations at a rural site in Connecticut (070570007). The ordinate (y-axis) represents the distribution observed during the meteorological scenario period 23-31 July 1980 while the abscissa (x-axis) represents the distribution observed over the entire summer, June - August.

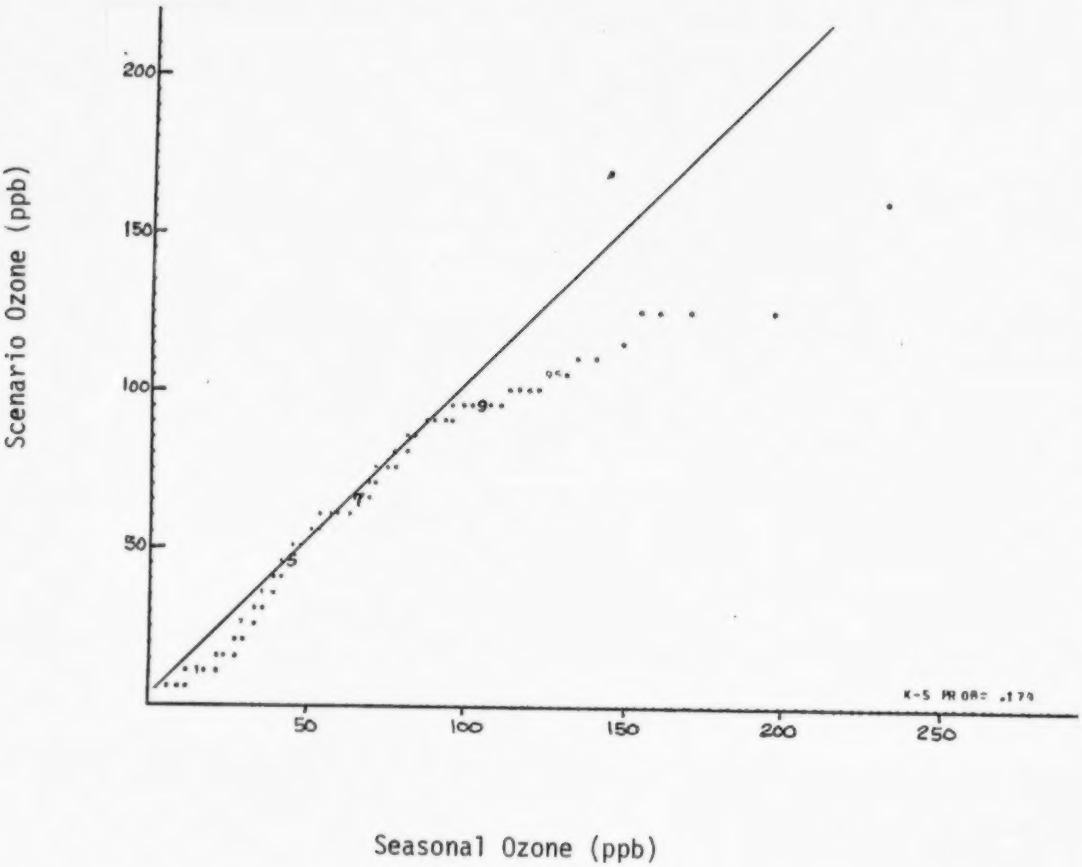

Figure 6-2b. Same as 6-2a except data are from Whiteface Mountain, New York (33020002).

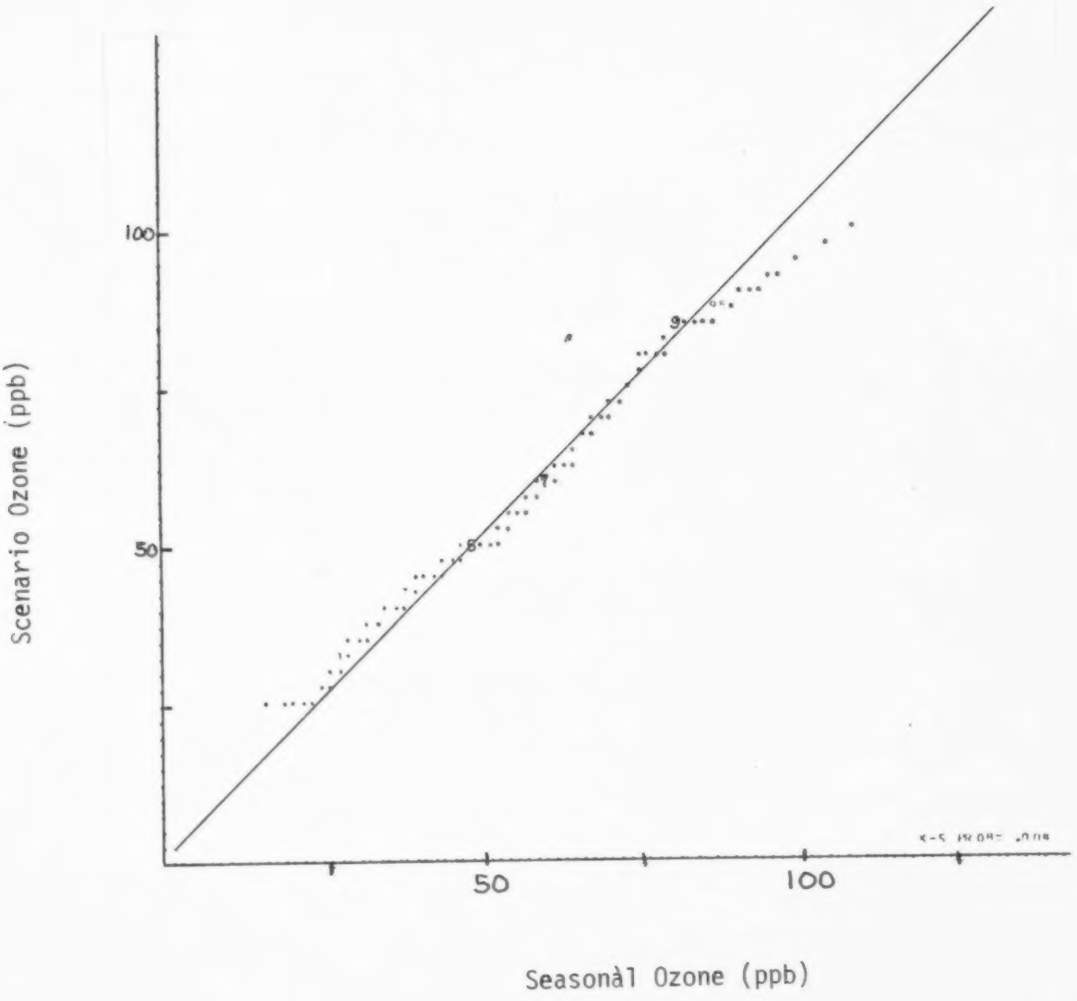

Figure 6-2c. Same as 6-2a except data are from a New Jersey site (312750001) about 50 km east of Philadelphia.

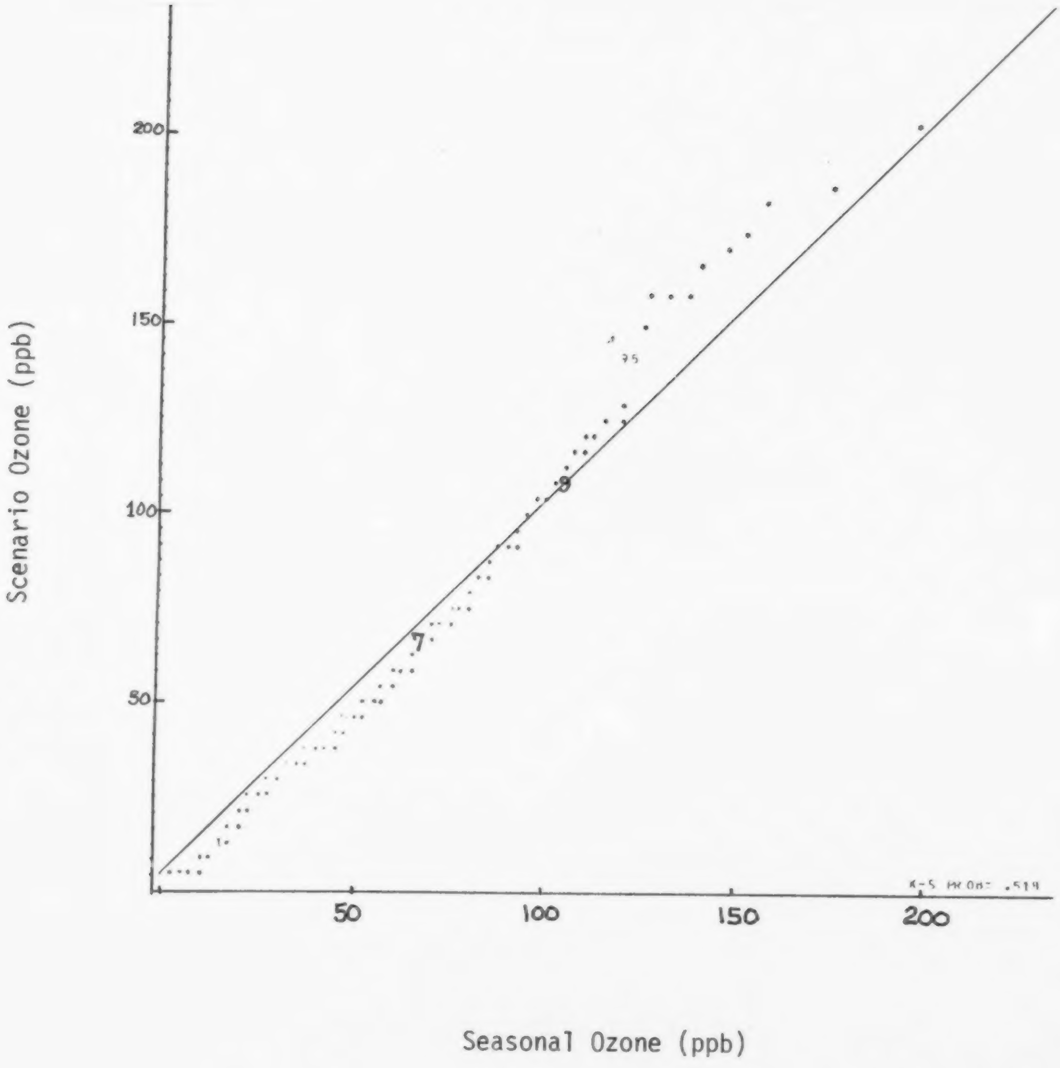

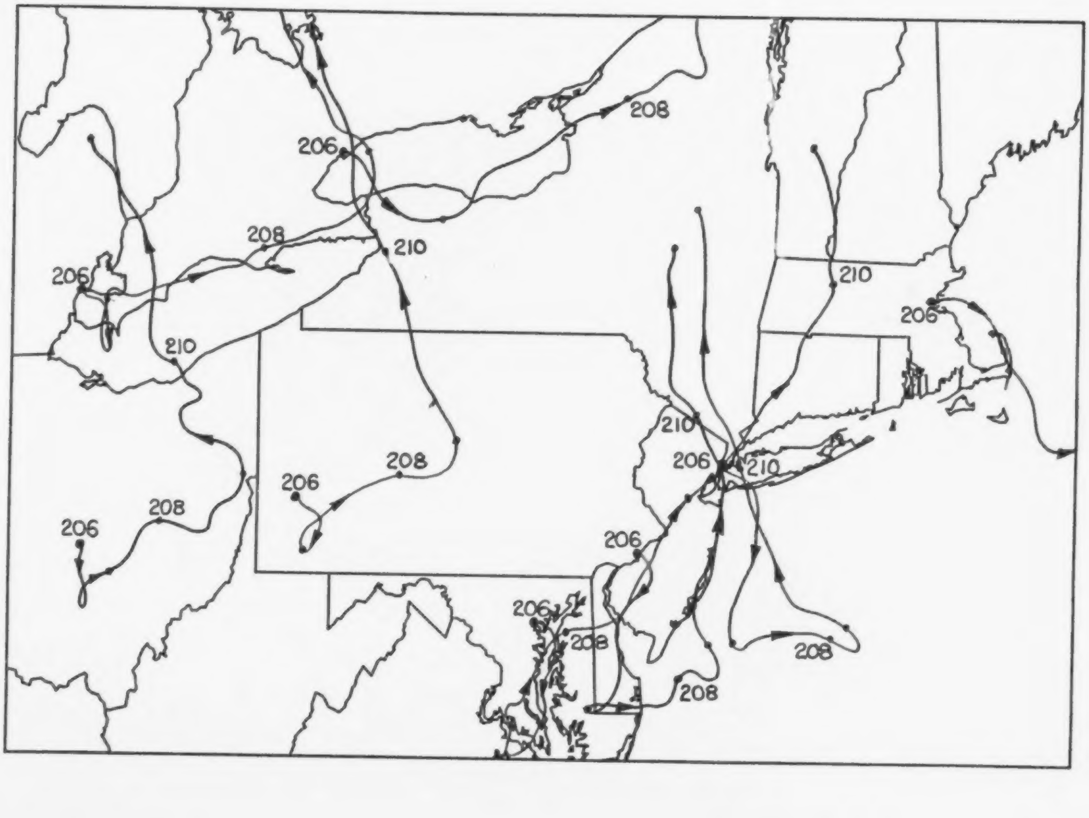
206
208
206
208
210
206
210
206
208
206
208
206
208
210
206
210
210
206
206
208
208
208
210

Figure 6-3. Trajectories calculated from wind fields used in Layer 1 of the ROM for the 9-day meteorological scenario 23-31 July 1980 (Julian dates 205-213). Numbers along the trajectories refer to Julian date.

SECTION 7

THE CONTROL STRATEGY EMISSIONS INVENTORY

The control strategy inventory was specified by the Strategies and Air Standards Division of OAQPS in the form of county-by-county changes in total hydrocarbon and NO_x emissions. The control inventory represents projected 1987 emissions based on controls contained in the 1982 SIPs. No control measures proposed after 1982 are included. The specified change in hydrocarbon was applied equally to each of the simulated hydrocarbon species -- paraffin, olefin, aldehyde and aromatic -- and the change in NO_x was applied to both NO and NO_2. Figure 7-1 (pages 75 and 76) shows isopleths of the hydrocarbon and NO_x emissions changes. Details are provided in Appendix B. The most significant aspect of the control emissions is that hydrocarbons are reduced everywhere from the base case levels whereas NO_x is decreased in some counties and increased in others. For the most part hydrocarbon emissions are reduced by 32% and NO_x is reduced by 8%.

A different perspective on the character of the emissions reductions is provided by the scatter plots in Figures 7-2,3 (pages 77 and 78) which compare the base and control VOC and NO_x emissions, respectively, of the 200 strongest source cells in the ROM domain. The regression line (dashed) in each figure shows that in the case of both the VOC and NO_x controls, there is a slight tendency to reduce the emissions of the strongest sources by smaller percentages than the weaker ones. For example, a source (in this case a grid cell roughly 18x18 km) emitting 10^7 moles VOC per day is reduced 22% on the average whereas one emitting 10^6 moles/day is reduced 35% on the average.

Earlier, in Section 4, we alluded to the high level of error that apparently exists at present in the base emissions inventories. Comparing Figure 7-2 with 4-3 (page 45) and 7-3 with 4-4 (page 46) one gets the impression that the effects of the emissions reductions that we are trying to assess are likely to be overshadowed by the system "noise" in the base emissions inventory. Until the causes of the uncertainties in the emissions data have been diagnosed and corrected, we must interpret the results of the model simulations with caution.

We argued in Section 3 that the emissions reductions imposed on the major sources of VOC and NO_x would have a proportionately greater impact on ozone levels than the changes made in lesser sources. Thus, it is instructive to examine the effects of the proposed control strategy on the 70 major source counties identified earlier in Tables 4-1,2 (pages 41 and 42). Figures 7-4 and 7-5 (pages 79 and 80) show scatter plots of the base and controlled VOC and NO_x emissions, respectively, of these 70 counties. The data presented in Figure 7-4 indicate that about 40% of the major sources have little or no VOC reductions at all -- the remainder have 30% to 40% reductions. Figure 7-5 indicates that on the average the NO_x emissions of these sources remain virtually unchanged, as is evident in the regression line.

We should emphasize that the emissions that we refer to here as the "controlled" emissions actually represent the projected 1987 baseline emissions. Thus, the model simulations that we have performed comparing the ozone concentrations simulated with the 1980 "base" emissions with the ozone levels simulated using the "controlled" inventory are intended to assess the magnitude of the ozone problem that one could expect in 1987 if no further controls beyond those in the 1982 SIPs are placed in effect. As we shall see in the next section, the model predicts that 1987 ozone levels will still exceed the primary standard in many parts of the Northeast. Consequently, one of our future modeling tasks will be to test various control strategies in an attempt to find the most cost effective one.

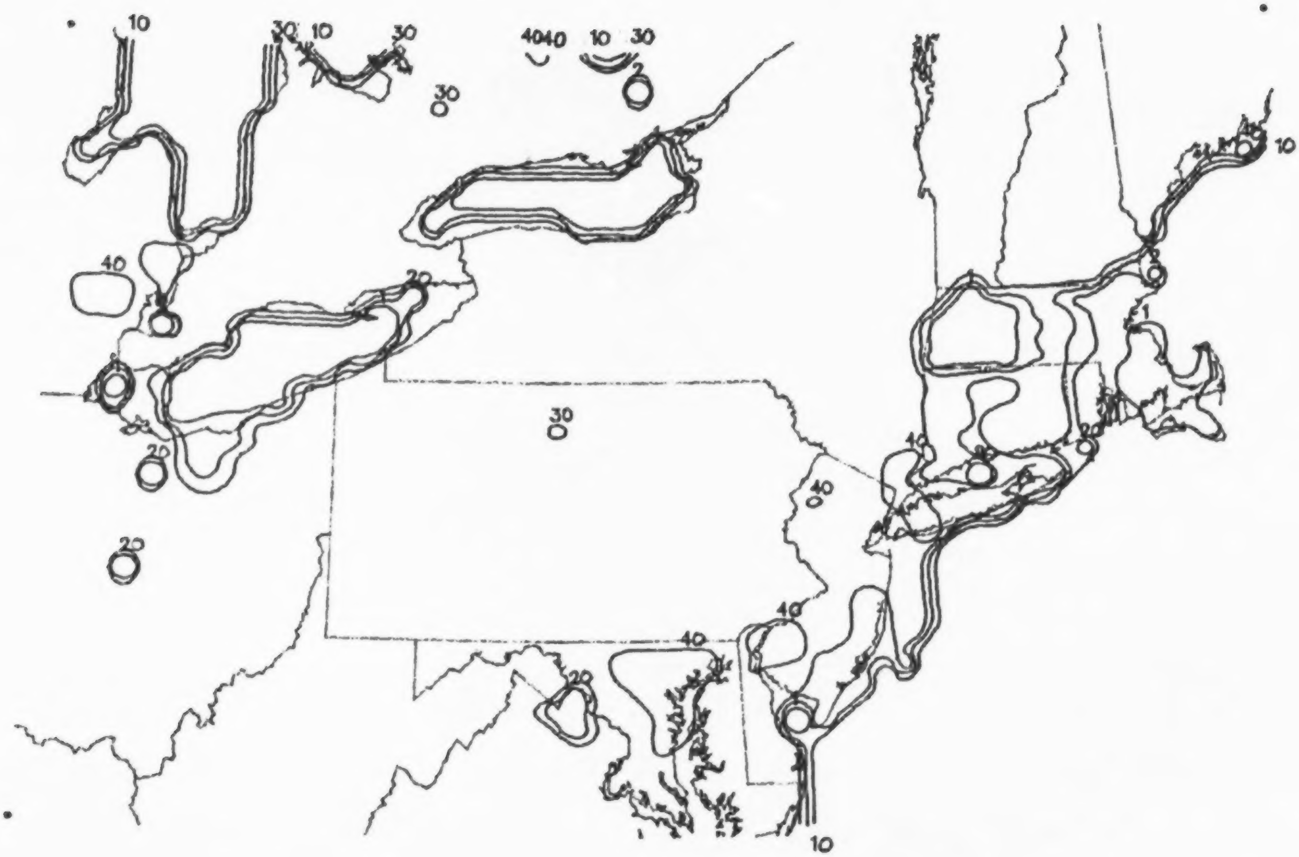
10
30
10
30
4040
10
30
30
10
40
20
30
20
40
20
40
40
20
10

Figure 7-1a. VOC emissions in the control strategy expressed as a percentage reduction in the base emissions. (See Appendix B for details.)

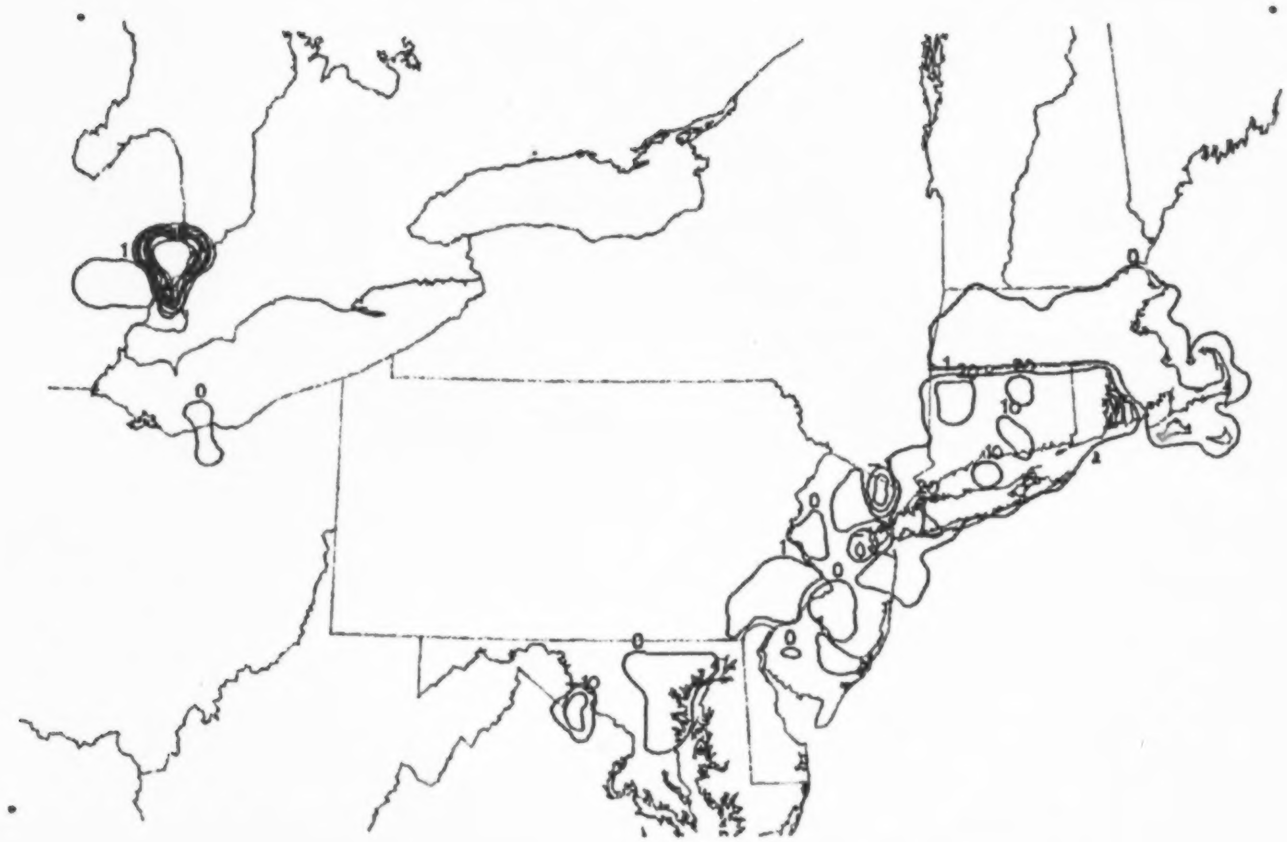

Figure 7-1b. NO_x emissions in the control strategy expressed as a percentage reduction in the base emissions. (See Appendix B for details.)

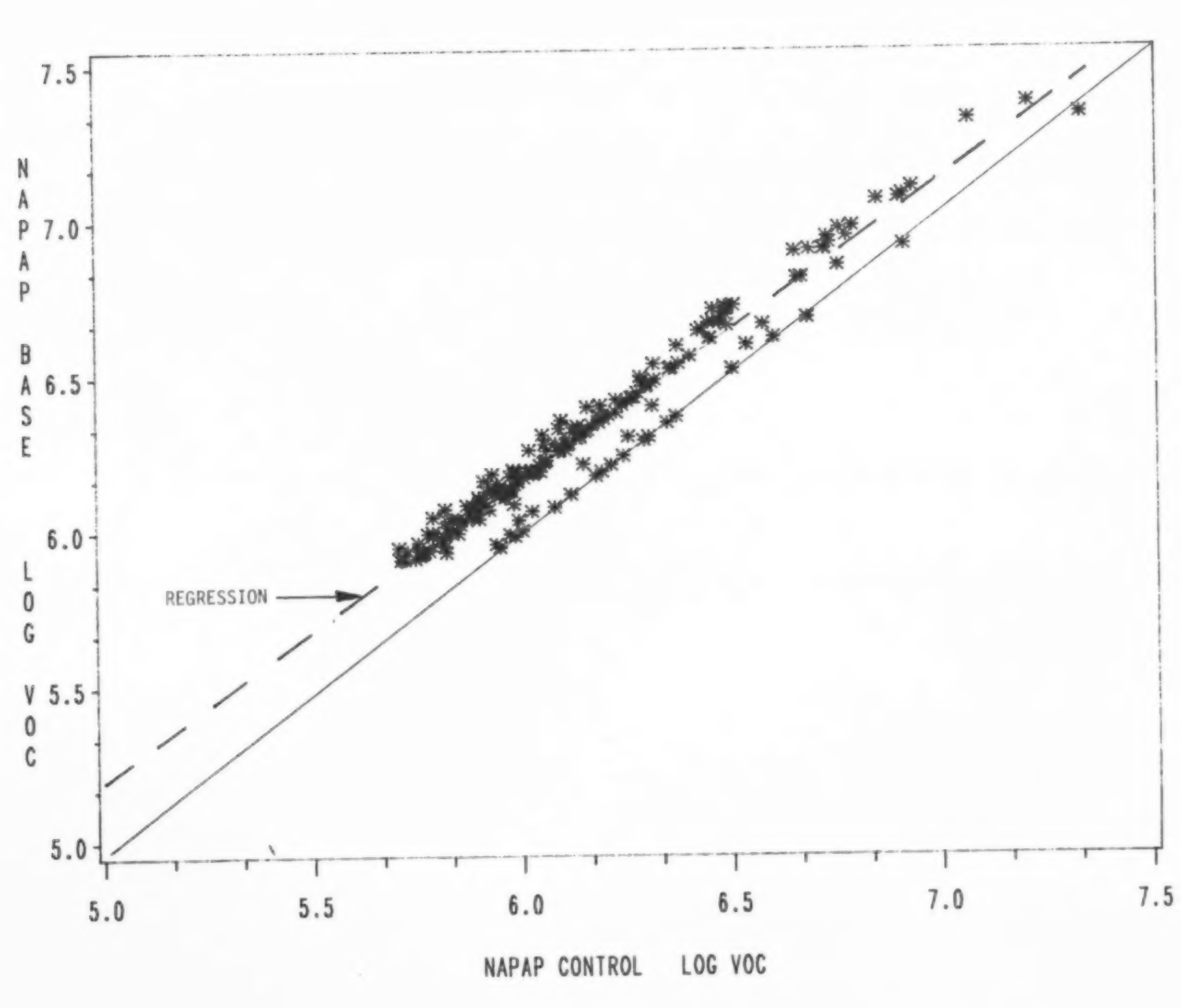

Figure 7-2. Comparison of base and controlled emissions of VOC (moles/day) of the 200 strongest VOC emitting cells in the ROM domain, Canada excluded. (All point and area sources within each cell are combined.)

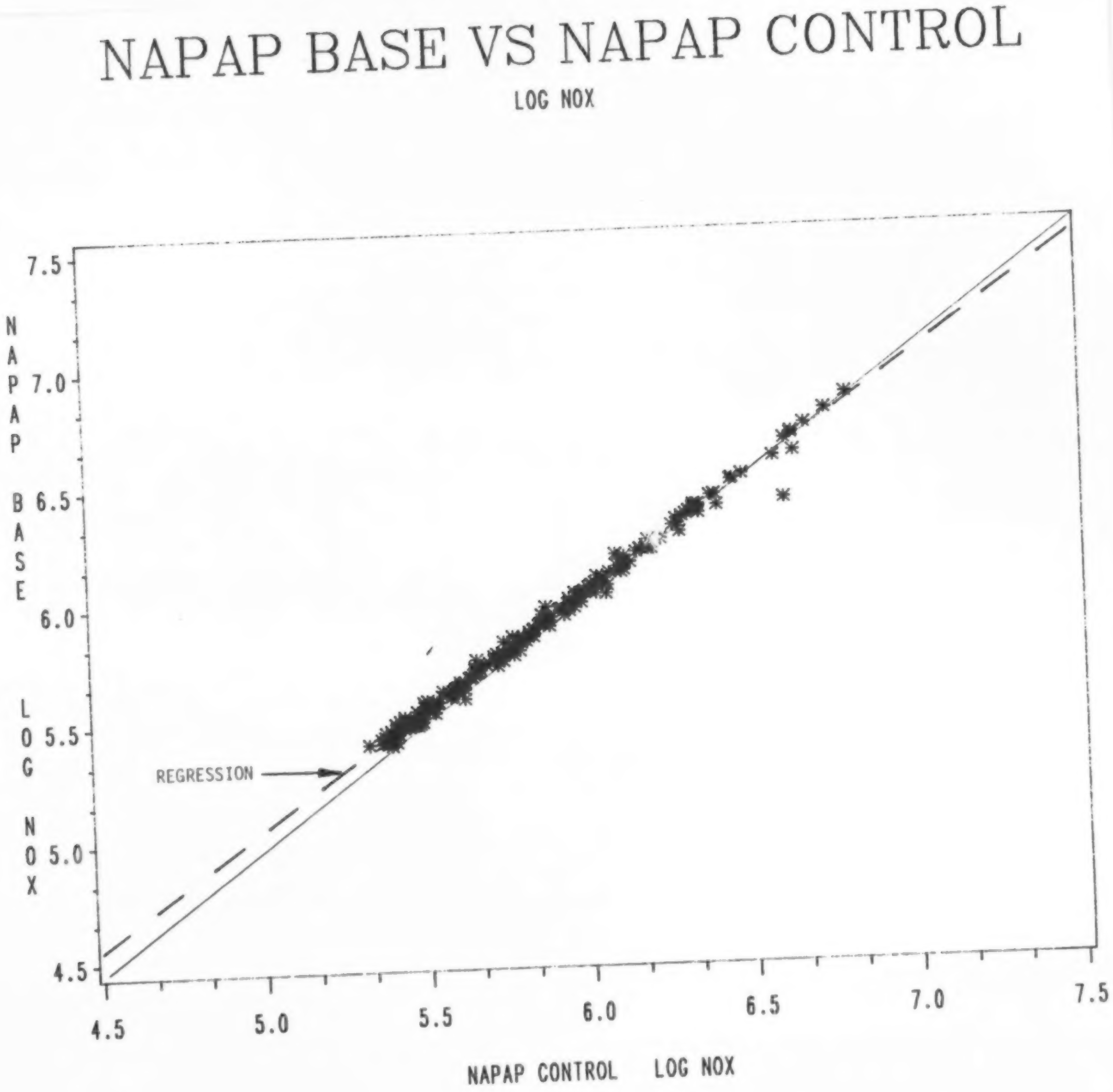

Figure 7-3. Comparison of base and controlled emissions of NO_x (moles/day) of the 200 strongest NO_x emitting cells in the ROM domain, Canada excluded. (All point and area sources within each cell are combined.)

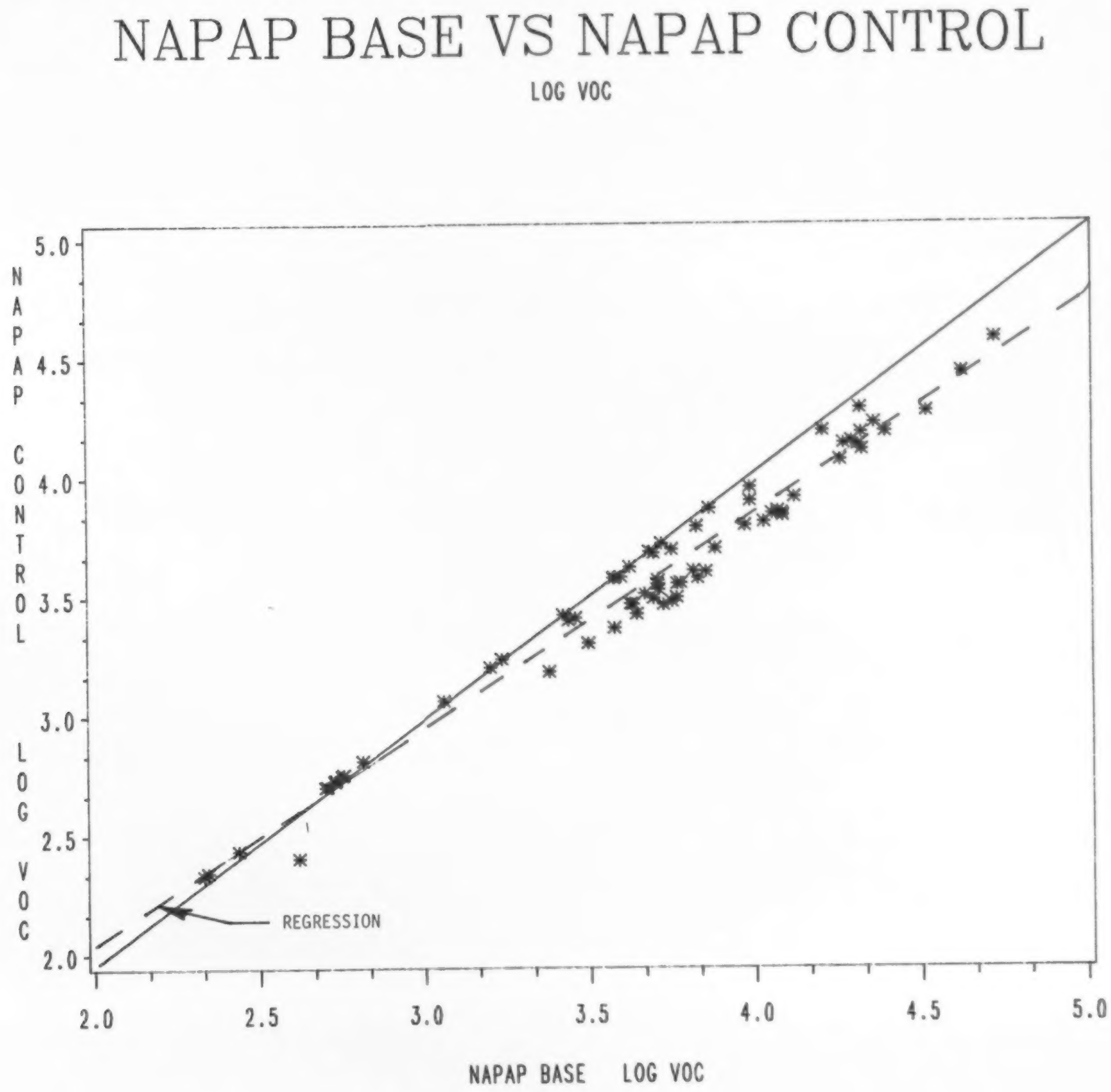

Figure 7-4. Base vs. controlled VOC emissions (moles per km^2 per day) of the 70 major source counties listed in Tables 4-1,2.

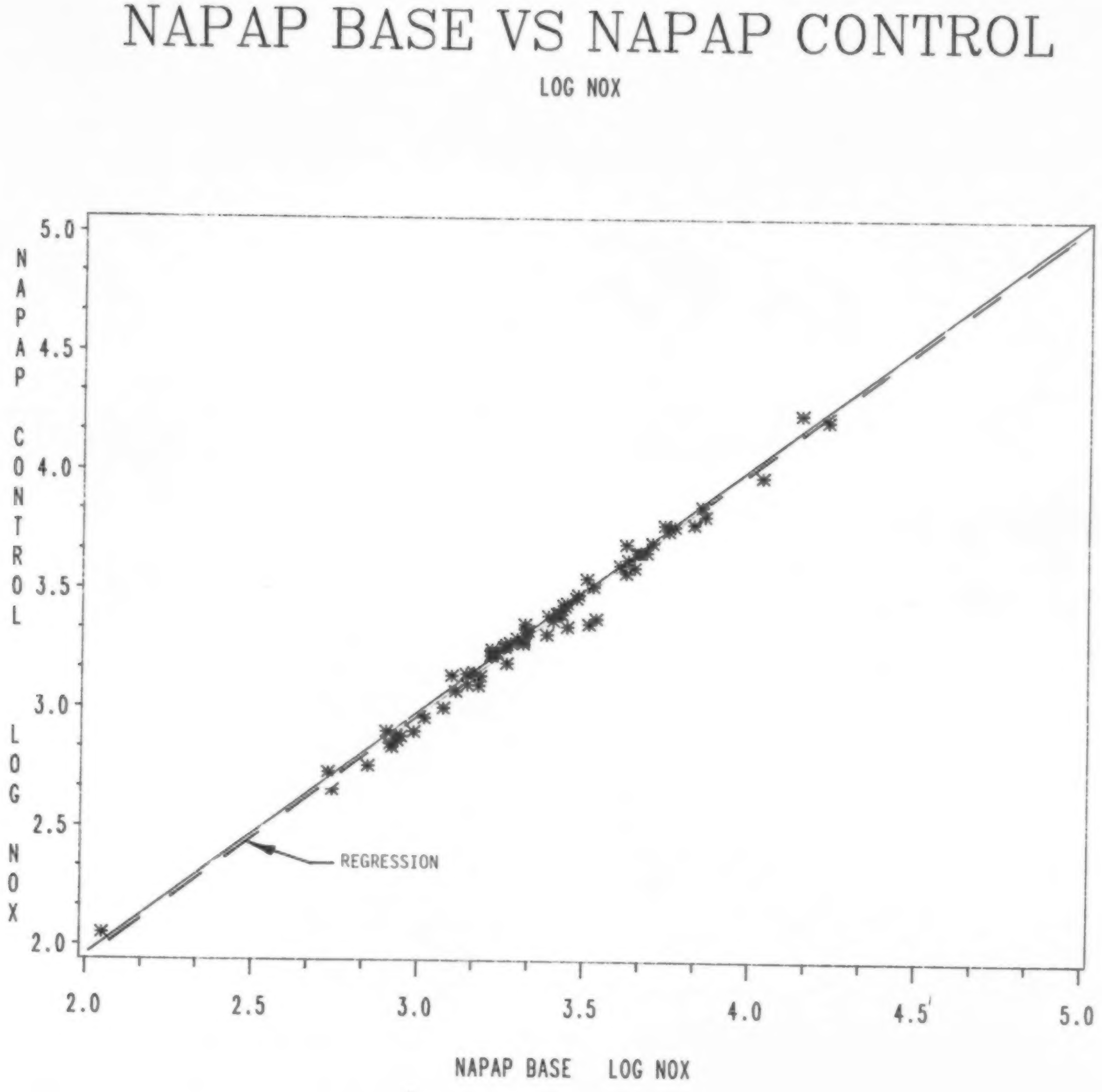

Figure 7-5. Base vs. controlled NO_x emissions (moles per km^2 per day) of the 70 major source counties listed in Tables 4-1,2.

SECTION 8

RESULTS OF MODEL SIMULATIONS

In this section we present the results of model simulations that were performed to assess the effects of projected VOC and NO_x emissions reductions on ozone levels in the Northeast. The presentation is divided into three parts. In the first we describe the input parameters used in each simulation. Following that we provide a limited comparison of the ozone predicted in the "base" case simulation with measured ozone data to give at least a qualitative overview of the model's accuracy. In the final subsection we discuss the predicted ozone concentrations from both the base and control runs.

SPECIFICATION OF INPUT PARAMETERS FOR THE MODEL SIMULATIONS

Two, 9-day model runs were made in this study. One, referred to as the "base" case, used the 1980 NAPAP version 4.2 emissions data discussed earlier in Section 4. The second run, referred to as the "control" case, used emissions fields derived by multiplying the base emissions by the projected 1987 VOC and NO_x changes described in Section 7 and specified in Appendix B. Both the base and the control runs used identical values of all other model inputs including the meteorological fields, which we discussed in Section 6 (see also Appendix A). Following we elaborate on our choice of initial and boundary conditions for the simulations, and other parameter fields that we have not yet mentioned.

Initial and Boundary Conditions

In every model application, regardless of its purpose, one must specify the 3-D spatial distribution of the concentrations of each of the simulated species at the initial instant of the simulated period. In the case of the ROM in its current form, this means specifying values of the concentration of each of 23 chemical compounds in each of some 7500 grid cells. Unfortunately, this requirement vastly exceeds the information content of presently available air monitoring data bases. Within the present ROM domain, measured hourly ozone concentrations are available at about 150 surface sites; lower quality data are available for NO_x at fewer sites; and no measurements are available for any of the remaining 23 species. Moreover, no data are available on the concentrations of any species above ground-level.

In preliminary studies, we attempted to devise a scheme for generating estimates of the concentrations of all the required species from the few ozone and NO_x data available. In order to appreciate the difficulty, and indeed futility, of this task, keep in mind that the objective of this scheme is to reconstruct the 3-D spatial structure of the concentration fields of 23 compounds given the concentration of only two of the species at a few surface locations. If the nature of the pollutant chemistry were such that the concentrations of all species were unique functions of the concentrations of the two given species, then initialization would not be a problem. But this is not the case. In fact, it appears that the ozone concentration that evolves from a given initial mix of species is quite sensitive to the initial levels assumed for hydrocarbon and NO_x, and as a consequence anomalous ozone concentrations may arise in the course of the simulation that are merely artifacts of the initialization. This problem is made all the more acute in the regional model by the prolonged residence time, 4-5 days or more, of the initially present species within the model domain. We have concluded from our studies that there is presently no initialization technique available that will allow consistently accurate simulations of historical air pollution episodes unless the period is selected so that it begins at a time when species concentrations are at minimum levels throughout the modeling region.

A related modeling problem is that of specifying the concentrations of all species at inflow boundaries. Most of our model simulations run long enough that species that enter the domain through the inflow boundaries eventually permeate the model area to nearly the same extent that the initial concentration field does. When we defined the ROM domain originally we attempted to mitigate the effects of uncertainty in the lateral fluxes of species by making the domain large enough to encompass the majority of the pollutant sources that affect air quality in the Northeast. The rationale was that if we treat the majority of the sources explicitly, the influence of transboundary fluxes on species concentrations at receptors in the interior of the domain will be at most a second-order effect and well below the level of tolerable error in the predictions.

Specifying the initial and boundary conditions accurately is necessary only if one plans to compare the predicted concentrations with observed values for model verification purposes. If the model application is for emissions control strategy assessment, meaningful results can be obtained by using hypothetical initial and boundary values with meteorological data associated with historical pollution episodes. In fact, one could argue that a polluted state of air quality observed in the past is irrelevant in control strategy development because if emissions are changed, that state of air quality might not be seen again in the future. The same argument does not apply, however, to the meteorology associated with historical episodes.

The hypothetical initial and boundary conditions that are most appropriate in emissions strategy studies are those regarded as representing the clean troposphere. Simulating the effects of emissions changes in this context makes the task of interpreting the model results particularly easy because all the computed ozone and product species in excess of the initial values can be attributed to emissions rather than the initial and/or boundary conditions. The ROM applications that we will report here were conducted using the "clean" species values given in Table 8-1 (next page) for both the initial and boundary conditions.

Deposition Velocities

In the first-generation ROM, deposition of each chemical species is treated using the same state-of-the-art technique that the second generation model will employ. In this method each land use type is assigned an uptake resistance for each chemical species simulated by the model. The value of the resistance is a function of atmospheric stability which is in part a surrogate of relative humidity and sunlight, both of which influence the rate at which plants absorb gasous material. The deposition resistances are converted in turn to deposition velocities using the local friction velocity, Obukhov length, and surface roughness. The resulting distributions of deposition velocities have highly complicated

Table 8-1. Values used for the initial and boundary concentrations in both the base and control ROM applications.

Species	Concentration (ppm) value used for initial and boundary conditions in all model layers
NO	6.58 10^{-6}
NO_2	1.82 10^{-3}
O_3	.037
Olefin	3.09 10^{-4}
Paraffin	3.92 10^{-4}
Aldehyde	4.32 10^{-5}
Aromatic	1.22 10^{-4}
CO	0.100
HNO_2	1.94 10^{-6}
HNO_3	1.53 10^{-4}
PAN	4.93 10^{-8}
RNO_3	1.80 10^{-11}
H_2O_2	1.80 10^{-11}
O	2.18 10^{-12}
NO_3	1.34 10^{-5}
HO	7.95 10^{-9}
HO_2	3.54 10^{-6}
HO4N	2.11 10^{-6}
RO	1.25 10^{-12}
RO2	1.72 10^{-6}
R2O	1.19 10^{-13}
R1O2	7.09 10^{-10}
R2O2	1.52 10^{-7}

spatial patterns and they undergo radical variations in magnitude between night and day. In the case of ozone, the largest daytime deposition velocity anywhere in the model domain is of the order of 1 cm/sec. At night the largest value is less than .1 cm/sec and in most locations it is two orders of magnitude below the daytime levels.

The principal weakness in the parameterization of species deposition is the paucity of resistence data. In applications of the second-generation ROM we may be able to update the empirical data base that we presently use.

Miscellaneous Fields

In the first-generation ROM that we used in the present study:

- the terrain is flat;
- the thicknesses of each of the three layers is constant in space and time with Layer 1 = 400 meters, Layer 2 = 800 m and Layer 3 = 800 m (these values were selected on the basis of vertical sounding data);
- horizontal diffusivity is everywhere zero;
- vertical fluxes between layers are based on turbulence estimates and vary in space and time;
- vertical exchange between layers 2 and 3 occurs only where cumulus clouds are present;
- the mean vertical air speed is everywhere zero.

COMPARISON OF PREDICTED AND OBSERVED OZONE CONCENTRATIONS

In order to give the reader a basis for judging the credibility of the emissions control simulations that we will present later in this section, we provide here a very limited comparison of the ozone concentrations predicted during the 9-day base case simulation with ozone levels observed during the same period. More detailed analyses of the model's performance can be found in Schere (1986). Our model verification studies have been limited thus far because the first-generaion verison of the ROM that we are currently using will soon be replaced by the more advanced second-generaton model.

Figure 8-1 (page 104) shows contours of the maximum, hourly averaged base case ozone concentrations predicted within the model domain over the entire 9-day simulation. Figure 8-2 (page 105) shows the corresponding concentrations measured at the SAROAD sites during the 9-day period from which the meteorological parameters used in the model were taken, namely 23-31 July 1980. Comparing the patterns and magnitudes of the concentration distributions shown in the two figures reveals the following.

First, the simulated concentration field exhibits distinct maxima in four areas. Three of these lie over the Great Lakes -- Huron, Erie and Ontario -- while the fourth occurs over the Atlantic Ocean just south of Long Island. In each case the high concentrations are the result of the limited mixing and generally cloud free conditions that exist in the summertime marine layers over the Great Lakes and the Atlantic Ocean. The simulations indicate that the Lake Huron and Erie maxima are attributable to emissions from the Detroit area while the Lake Ontario maximum is a part of the Toronto plume. The high concentrations over the Atlantic are the results of emissions from the New York City area. Confirmation of the existence of peak ozone concentrations in these four areas is not provided by the SAROAD data because only land based observations are available.

However the measurements shown in Figure 8-2 that were made around the periphery of Lake Erie tend to support the prediction that ozone concentrations are higher over the water than inland. In this particular area the model predicts a peak value of about 140 ppb along the Pennsylvania-New York shoreline of Lake Erie, and in fact a measured peak of 122 ppb was reported in that area. (One should keep in mind when comparing predicted and observed concentrations that predicted extreme values will generally exceed the corresponding observed value because the latter are available at only a limited number of sites.) Measured ozone concentrations in and around the New York City area tend to support the model predictions in this area as well. A peak value of 184 ppb was reported in southwestern Long Island, an area where the predicted maximum was 187 ppb. A concentration of 230 ppb was predicted just offshore. Peak ozone concentrations of 130 to 175 ppb were measured in southeastern and central Connecticut where the predicted values ranged from 140 to 187 ppb. There are not enough ozone data around Lake Huron and Lake Ontario to assess the accuracy of the high concentrations predicted over those areas.

There is general disagreement between the observed data plotted in Figure 8-2 (page 105) and the model predictions (Figure 8-1) in four regions: the Pittsburgh vicinity, the Washington-Baltimore corridor, the Toronto area, and the northern portions of Vermont and New Hampshire. In the first of these areas, measurements show ozone levels as high as 120 to 130 ppb within a radius of about 40 km of Pittsburgh but the highest computed values in this area are of the order of 90 ppb. Underprediction is also evident in the Washington-Baltimore area. The ozone measurements show a narrow zone in which concentrations range between 120 and 165 ppb, but no similar area appears in the simulated ozone values. It is possible that the underprediction in both this and the Pittsburgh areas is due to errors in the emissions data that we noted earlier. Errors in the meteorological inputs are another possible cause of the discrepancies, particularly errors in the cloud cover values. Since the concentrations shown in Figure 8-2 are observed maximum ozone values over a 9-day period, failure of the model to have accurate cloud cover data at the proper location and hour can cause the model to grossly underestimate the ozone that would be generated in a mixture of VOC and NO_x emissions. At this point we cannot say why the model underpredicts ozone in the two areas that we have just cited.

The opposite problem occurs in the Toronto area where peak ozone concentrations of 200 ppb are predicted but values no larger than 100 ppb are observed. Since our simulations have consistently shown high ozone levels in the Toronto plume, we suspect problems with the emissions data.

In northern Vermont and New Hampshire we find on comparing Figures 8-1 and 8-2 that the model overpredicts peak ozone values by a considerable margin -- 100 ppb observed vs 140 ppb predicted. In this case we are quite certain that the problem is due to the constant thickness of the layers in the first-generation model. The top surface of the model in the simulations presented here had an elevation of 2000 meters above ground. However, at the time the simulated pollutant cloud passed through the area in question, the meteorological data show that widespread shower activity was present which could have transported ozone and other pollutants to altitudes of 5000 m or higher. The second-generation ROM will eliminate this source of error.

In summary, the ozone observations suggest that the model overpredicts ozone concentrations in areas remote from the major precursor pollutant source areas. We also found that it underestimated concentrations near the Pittsburgh, Washington, DC, and Baltimore urban areas, but overpredicted ozone by a wide margin around Toronto.

RESULTS OF THE BASE EMISSIONS SIMULATION

Since the primary goal of this study is to examine the effects that projected 1987 emissions are likely to have on ozone concentrations, we will focus our analysis of the model results exclusively on ozone and on the differences between the predicted concentrations in the base and control cases. Analyses of a broader scope will be performed in later studies, primarily in connection with the second generation ROM.

We will present the results of the ozone simulations in four separate formats:

(1) Averages over each of the 439 counties in the model domain (Appendix D);

(2) Isopleths of concentration over the entire model area at selected times during the 9-day simulation;

(3) Statistics of county averages within each of the four receptor county categories defined in Section 5, (pages 51 and 52, see also Figures 5-2, 3, 4, 5, pages 54-57);

(4) Statistics of cell averaged concentrations within each of the receptor cell classes defined in Section 5, (page 50, see also Figure 5-1, page 53).

We also consider a variety of averaging times: 1-hour, 3-hour, 7- hour (the so-called daily daylight average, from 0900 - 1600 LST), 12-hour and 24-hour averages. The 1-hour averaged ozone concentration is regulated by the current primary National Ambient Air Quality Standard (NAAQS); and the 7-hour daily daylight average is presently being considered as a basis for specifying a new secondary standard which would protect agriculture, forests and public welfare in general.

The predicted county averaged ozone concentrations for the base emissions are tabulated in Appendix D for each of the 439 counties in the model domain. Results are given for both the 7-hour and 1-hour averaged concentrations. The corresponding values obtained using the controlled emissions are given in the same table for comparison. Examples are also given at the end of Appendix D of the type of model results that are available for other averaging times. The entire set of results is too lengthy to include in the report. The data contained in Appendix D are provided for use by others in making cost-benefit analyses of the emissions controls described in Section 7, and we will not discuss them further in this report.

The simulated distributions of ozone over the model domain at hour 1600 EST of each day of the nine day scenario are shown in Figures 8-3 through 8-11 (pages 106-114). The concentration patterns seen in these plots give an idea of the spatial size of the simulated urban plumes, the areas influenced by ozone produced from the emissions of given sources, and the temporal behavior of the ozone distribution that accompanies changes in meteorology. One should keep in mind when examining these data that unlike inert chemical species whose spatial distributions are determined chiefly by transport, ozone is created and destroyed by chemical reactions which may cause concentration patterns to change in seemingly erratic ways. For example, a "cloud" of ozone may vanish upon crossing a strong area source of NO_x and then reappear downwind.

Figure 8-3 (page 106) shows the simulated ozone distribution in Layer 1 at hour 1600 EST of the first day of the scenario, i.e., 23 July 1980 (Julian date 205). (The model was initialized at hour 00 of this day.) Concentration maxima occur over southern Lake Ontario -- the result of Toronto's VOC and NO_x sources; to the southeast of Detroit; and over the Atlantic offshore of Long Island and Massachusetts. The next figure in the sequence shows that by 1600 of the next day, the Toronto emissions are influencing ozone levels as far south as the New York-Pennsylvania border. At this point concentrations are just over 60 ppb, as compared with the background level of 37 ppb. The highest concentrations in what appears to be the Toronto plume are between 120 and 140 ppb just east of Buffalo. At this same hour we see that the previous day's ozone from Detroit has merged with ozone generated from Ohio's source emissions to elevate concentrations over northern and eastern Ohio. By the third day of the period, shown in Figure 8-5, the areas of elevated ozone associated with both the Toronto and Detroit emissions have reversed direction, and moved northward. Over the next two days these areas of high ozone continue their northward motion and by day 210, the sixth day of the simulation, they pass through the northern boundary of the model. The trajectories shown earlier in Figure 6-3 (page 71) are consistent with the motions of the Detroit and Toronto ozone plumes seen in Figures 8-3 through 8-8. A significant aspect of the simulation is that during the 9-day scenario, ozone generated in the Detroit, Toronto and northern Ohio emissions stays west of the Appalachians. It affects a zone stretching from the Adirondack Mountains through western New York into northern Ohio, as well as nearly all of the portion of Ontario that lies within the model area. The boundaries of the impact area and the maximum concentration levels produced are readily apparent in Figure 8-1 (page 104).

During the first four days of the simulation, the bulk of the ozone generated in the Eastern Corridor emissions remains just offshore of the East Coast, but edges of the polluted air mass extend inland into all the states bordering the Atlantic from Massachusetts to Delaware. By day 210, July 28, a strong southerly flow has developed over New England in advance of an approaching cold front (see Figure A-6, page 133) and the entire ozone laden air mass has been swept northward across Connecticut and Massachusetts, into northern New York, Vermont, New Hampshire and Maine. This is strikingly evident in Figure 8-8 (page 111). It is during this period, as we noted earlier, that the model overpredicts ozone concentrations by a factor of two or more due to its failure to account for the deep vertical mixing and precipitation that occurred in the southerly flow. This problem will be corrected in the second-generation model.

The area influenced by the Eastern Corridor sources and the associated maximum ozone concentrations can be seen in Figure 8-1. (When examining this figure, keep in mind the tendency of the model to overpredict concentrations far downwind of the major VOC and NO_x sources. Remember also that the isopleths are of maximum ozone concentration during the 9 days, not the mean concentration.) The concentration isopleths shown in the figure outline two broad plumes, one eminating from the Eastern Corridor sources and the other from the Detroit/Ohio area. Both plumes appear to be oriented in roughly a southwest-northeast direction with the Detroit/Ohio plume overrunning the Toronto plume. The Eastern Corridor plume and the combined Detroit-Toronto plumes intersect in northeastern New York. This indicates that on some occasions during the 9-day scenario, ozone in the Adirondack Mountains, for example, originated in the emissions of the major sources around the Great Lakes and on other occasions it arose from emissions of the major sources along the Eastern Seaboard. It is not clear whether the broad features of these two major plumes are indicative of the patterns one would find from longer term simulations. We suspect that somewhat different plume shapes would be found from, say, a 30-day simulation because as we discovered earlier in Section 6, the meteorological processes associated with extreme ozone levels appear to have periods longer than 9 days. We also anticipate changes in the ozone plume characteristics when biogenic hydrocarbon emissions are added to the source inventory. A likely result of this addition will be enhanced ozone concentrations in the Appalachian regions of West Virginia, Maryland and Pennsylvania due to reactions of NO_x from major sources in Ohio and West Virginia (see Figure 4-1, page 43) with hydrocarbons from the mountain forests. In any event we expect to find relatively well defined influence zones which should provide valuable information in the design of emissions control plans aimed at lowering concentrations in specific areas.

Information useful in performing cost/benefit studies of emissions controls is contained in the statistics of the concentrations in each of the four receptor county classes defined in Section 5 (see pages 51-52 and Figures 5-2 through 5-5, pages 54-57). Here we will examine only the predicted daily daylight (7-hour) averaged ozone values, leaving discussions of the hourly averaged values until later when we analyze the model output in the context of the receptor cells. The statistics of the simulated 7-hour averaged ozone concentrations are presented in Figure 8-12 (page 115) for each of the four county classes. A guide to the symbols used in the figure is given below:

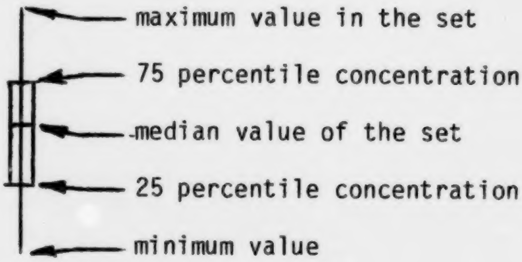

There are different numbers of counties in each of the four groups. The Major Source Counties contain the least number, 70; and the Natural Counties contain the most, 169; and the Suburban and Agricultural Counties include 104 and 96, respectively.

The quartile plots in Figure 8-12 reveal no striking, systematic differences in the simulated concentrations in each of the four county groups. This is perhaps due in part to the definitions of the groups which emphasize demographic and land use characteristics of counties rather than their proximity to major source areas. An important feature of the model output that we cited earlier in this section is the prolonged influence of the initial concentrations on the model predictions. On the first day of the simulation, i.e., 80205, the frequency distribution of ozone concentrations is virtually the same in all four county classes. It appears that it is not until the third day of the model run that significant differences begin to appear in the concentration statistics in each area. The data show that the extreme and median ozone values in natural areas can be as high as those in the major source and SMSA counties. This is probably due in part to model overprediction in remote areas and in part to the close proximity of some of the counties classified as "natural" to major sources. In the next subsection we will compare the base case quartile plots shown in Figure 8-12 with the corresponding statistics obtained using the controlled emissions.

Better insight into the nature of the processes of ozone formation and transport can be derived from the quartile plots of the simulated hourly concentrations in each of the four receptor cell classes defined in Section 5. Recall that there are 70 cells in each of the four categories and that three of the groups, namely the Suburban, Rural and Wilderness cells, are defined to be within given distance ranges of the Urban cells -- which represent the major VOC and NO_x sources (see page 50). The quartiles of the simulated base case ozone concentrations are plotted in Figure 8-13 (page 116) for each hour of the 9-day scenario for each of the four cell classes. The format is the same as that used in Figure 8-12 (described on page 96), but it appears different because the vertical boxes and lines are so close together that they give the appearance of dark and light shading.

On comparing the data presented in Figure 8-13 for each of the four receptor classes, we see again that the initial concentration field dominates the model predictions during the first three to four days of the simulation. This implies that a regional scale (1000 km) model must be run for at least four days before the predicted concentration levels in areas remote from the major sources are free of artifacts of the initial field.

We see also in Figure 8-13 a strong diurnal modulation of the 25, 50, and 75 percentile concentrations superposed on longer scale variations that are apparently associated with changes in meteorology. Based on the chemistry of ozone production that we described earlier, we interpret the diurnal variations to be evidence of ozone formation in these areas. In the Rural and Wilderness areas, which are progressively farther from the major VOC and NO_x sources, the magnitude of the diurnal component of the ozone variations is progressively smaller. Let us emphasize that the 0 and 100 percentile concentrations, i.e., the minimum and maximum values, respectively, may reflect conditions at only one of the 70 cells in a given group, whereas the 25, 50 and 75 percentile points represent more sites and hence are more representative of conditions as a whole.

We see in Figure 8-13 (page 116) that the 75 percentile concentration in the Urban cells peaks on the fourth day of the scenario, i.e., day 80208. It peaks the next day, 80209, in the Rural cells; and it is a maximum still later, day 80210, in the Wilderness sites. The ozone concentrations measured at the SAROAD sites during the scenario peaked on the first of these days (see Figure 6-1, page 67). Thus, the predicted concentrations are consistent with the observations inasmuch as a majority of the monitoring stations are in the major source areas represented by the Urban cells. The phase lag between high ozone levels in the urban and remote areas is particularly evident in Figure 8-13 at the 150 hour point (day 80211) where the median concentrations in the Urban and Suburban areas are near their minimum values while the Wilderness concentrations are near their peak.

The presence of strong NO_x sources in at least some of the Urban cells is evident in the fact that during most nighttime periods in the 9-day scenario, ozone concentrations in about 25 percent of these cells drop to values near zero. By contrast, the 25 percentile concentrations at Wilderness sites seldom drop below about 30 ppb. Note also that the extreme concentrations predicted in the Wilderness areas vary in a smoother manner with time than in the Urban or Suburban areas, suggesting, as one would expect, that ozone plumes broaden with distance from their source. The highest ozone concentration predicted at any of the 70 Wilderness sites is about 150 ppb compared to a peak of just over 200 ppb in each of the other three receptor areas.

In summary, we see evidence in the simulated concentration statistics presented in Figure 8-13 (page 116) that the bulk of the ozone generated by VOC and NO_x emissions is produced within about 100 km of the areas that we have identified as major source areas. This is suggested by the fact that the magnitude and time variation of the extreme concentrations, and the amplitude of the diurnal modulation of the median concentrations are all larger in the Urban, Suburban and Rural cell groups than in the Wilderness sites. Recall that the last group are, by definition, farther than 100 km from the nearest major source area. In a future report we plan to compute from the model output the quantity of ozone generated in each model cell at each time step. From this information we can map the virtual ozone source distribution, which will show where and in what quantities ozone is produced from VOC and NO_x emissions. We believe that this information will be especially valuable in assessing the impact of various emissions controls on ozone formation.

SIMULATED EFFECTS OF EMISSIONS CONTROLS ON OZONE CONCENTRATIONS IN THE NORTHEAST

The model results from the 9-day scenario that we just discussed used the 1980 NAPAP version 4.2 emissions inventory which we discussed in some detail in Section 4. These data are what we have referred to as the base case emissions. We ran the model a second time using identical values for all input parameters except the emissions, which were replaced by the projected 1987 inventory described in Section 7 (see also Appendix B). These are the emissions data that we have referred to as the controlled emissions. Here we will compare the ozone concentrations produced by this simulation with those obtained from the base case run described earlier. Detailed, county-by-county comparisons of the base and control ozone values are provided in Appendix D. We will limit our discussion of the results in this section to qualitative assessments of the general effects of the emissions controls.

We found that the ozone concentrations from the controlled emissions simulation were everywhere and at all times less than or equal to the corresponding values predicted in the base case simulation. We add, however, that biogenic hydrocarbon emissions were not treated in the model and their presence could alter our findings, especially in the western portion of the model region where NO_x emissions of some sources were increased in the "controlled" inventory. Due to this and other deficiencies in the first generation ROM which we discussed earlier, one should view the results of the emissions control simulations that we report here as preliminary.

Let us look first at the effect of the controls on the 7-hour, daily daylight averaged ozone. Figure 8-14 (page 117) compares the extreme and median statistics obtained in the base case and control simulations in each of the four county receptor groups. An explanation of the graphical notation used in the figure is given below.

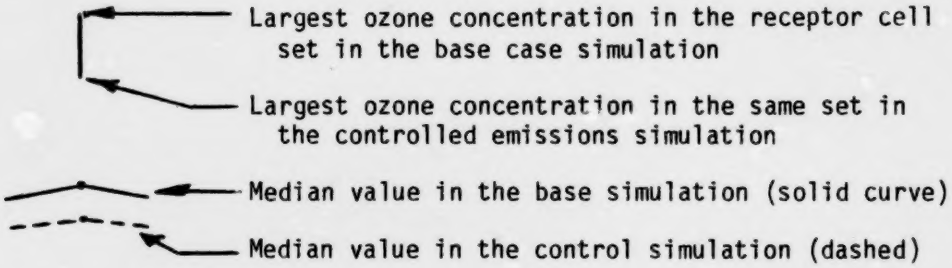

Largest ozone concentration in the receptor cell set in the base case simulation

Largest ozone concentration in the same set in the controlled emissions simulation

Median value in the base simulation (solid curve)

Median value in the control simulation (dashed)

To avoid cluttering the graph, we compare only the extreme and median values of the 7-hour average. One effect of the emissions changes that is readily apparent is that the extreme values of the 7-hour averaged concentration have been reduced in general by much larger percentages than the median values. For example, on day 80207, the maximum daily daylight averaged ozone in SMSA (suburban) counties was about 135 ppb in the base case simulation but only 80 ppb with the controlled emissions -- a reduction of 40%. At the same time the median value fell by only 15%. The degree of reduction of the maximum value varies widely from day to day in a single receptor group and from receptor to receptor on the same day. Note, too, that the controlled emissions lowered the median 7-hour averages most in the major source counties and by progressively less degrees in the SMSA, Agricultural, and Natural counties. A final interesting effect of the emissions changes is alterations in the time of occurrence of the maximum concentration. For example, in the SMSA and Natural counties, the largest values of the 7-hour average occurred on day 80209 in the base case simulation, but one day later with the controlled emissions.

These and other effects of the emissions changes are more clearly evident in the comparisons of the simulated hourly averaged concentrations in each of the four receptor cell categories shown in Figure 8-15 (page 118). The graphical representation used here is the same as that described above. Looking first at the beginning of the 9-day scenario we note that it is not until the second day of the simulation that significant differences in the median concentrations begin to appear in the Urban and Suburban areas, and it is only after four days that differences develop in the Wilderness cells. This result re-emphasizes the point we made earlier, that regional scale models must be run for periods of at least a week to produce meaningful results.

A curious feature of the early development of the concentration fields in both the base and controlled emissions simulations is the near equality of the extreme values in the Urban and Suburban areas during the first two days. It may be that during this time the highest concentrations occur near sources whose base and controlled emissions are nearly the same. Notice that extreme concentrations in the Wilderness sites are unaffected by the emissions changes until the fifth day of the simulation. This may be caused by the influence of the Toronto plume which, as we discussed earlier, affects concentrations as far south as Northern Pennsylvania. We assumed that Canadian emissions were the same in the base and controlled inventories. Therefore, the Toronto ozone plume will be identical in the two simulations up until the time that it becomes mixed with significant amounts of pollutants from U.S. sources.

The data presented in Figure 8-15 show rather clearly that in the Urban, Suburban and Rural areas, the emissions changes have the largest effects on the extreme and median concentrations during the development of the episode that peaks about 110 hours into the simulation (day 80209). Beyond that point the differences between the base and control simulations decline reaching a minimum at about hour 150. In fact, at that point the median concentrations in Urban and Suburban cells are the same for both emissions inventories. As before, the response of concentrations in remote areas to the emissions changes is radically different. No effect is evident here until after 110 hours, apparently because the ozone that built up in the urban and suburban areas does not arrive in the Wilderness areas until this time. When it does arrive, the reductions in the peak and median concentrations are smaller than those that were seen in the Urban and Suburban areas as the episode developed. The hourly data shown in Figure 8-15 also reveal the phenomenon that we saw earlier in Figure 8-14 (page 117) in connection with the 7-hour averaged concentrations, namely that the time of occurrence of the extreme concentration may be changed by changes in the emissions. This is dramatically evident in the Rural data of Figure 8-15 where we see that the peak concentration occurs near hour 110 with the base emissions but three days later, near hour 180, with the controlled sources. This suggests that the meteorological conditions that favor the highest ozone concentrations are different depending on the relationship of VOC to NO_x emissions within a spatially fixed set of sources.

In the next, and last, section we summarize our findings.

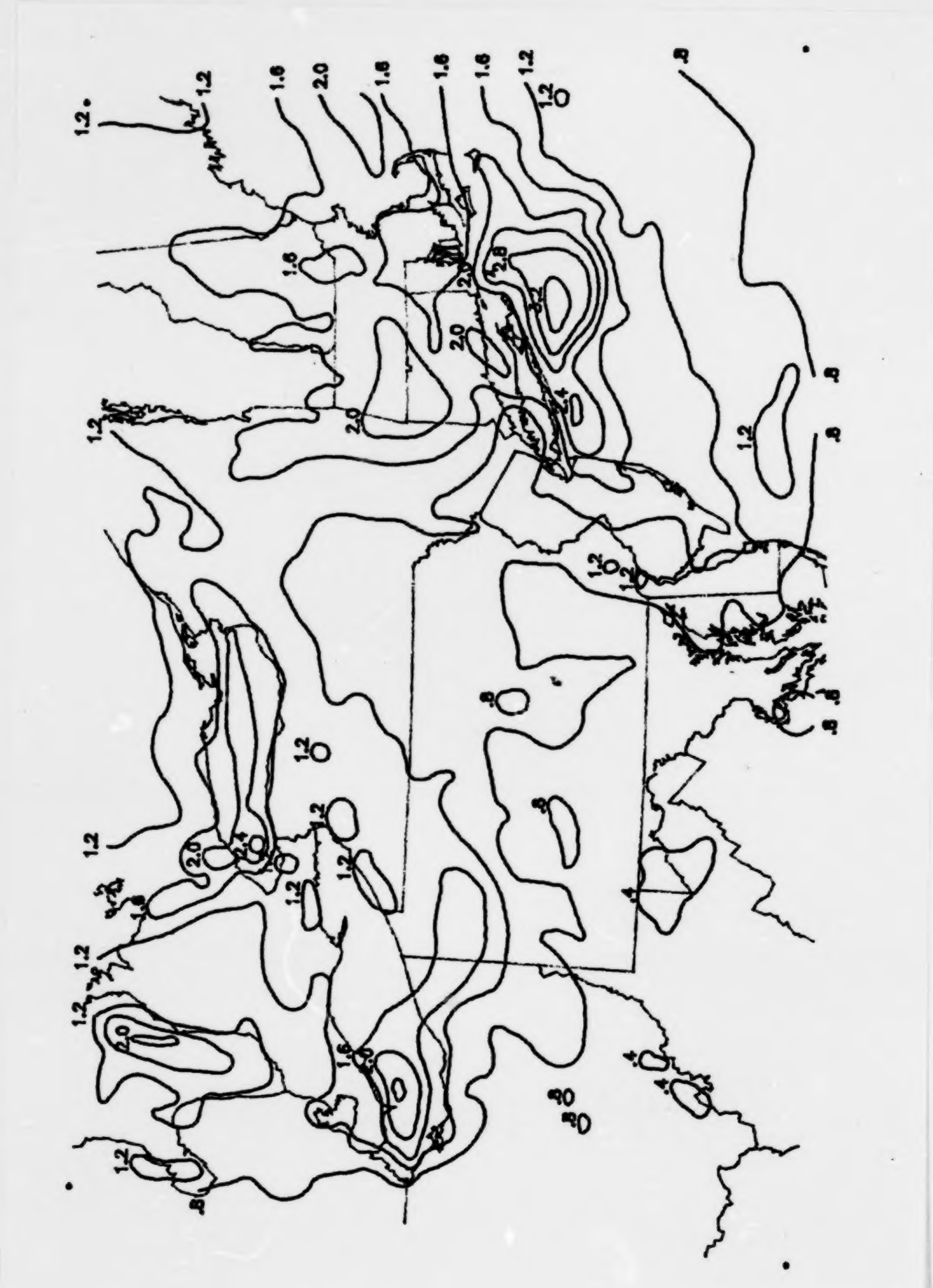

1.2
1.2
1.6
2.0
1.8
1.6
1.6
1.2
1.2
.8
1.6
2.8
3.2
2.0
2.0
2.0
2.4
1.2
1.2
.8
.8
1.2
1.2
.8
1.2
2.0
2.4
1.2
1.2
1.2
1.6
1.2
1.2
2.0
1.6
.8
.8
1.2
.8
.8
.8

Figure 8-1. Maximum ozone concentration during the 9-day scenario simulated using the base emissions inventory. Isopleths are drawn at intervals of 40 ppb. Numbers beside isopleths are ppb/100.

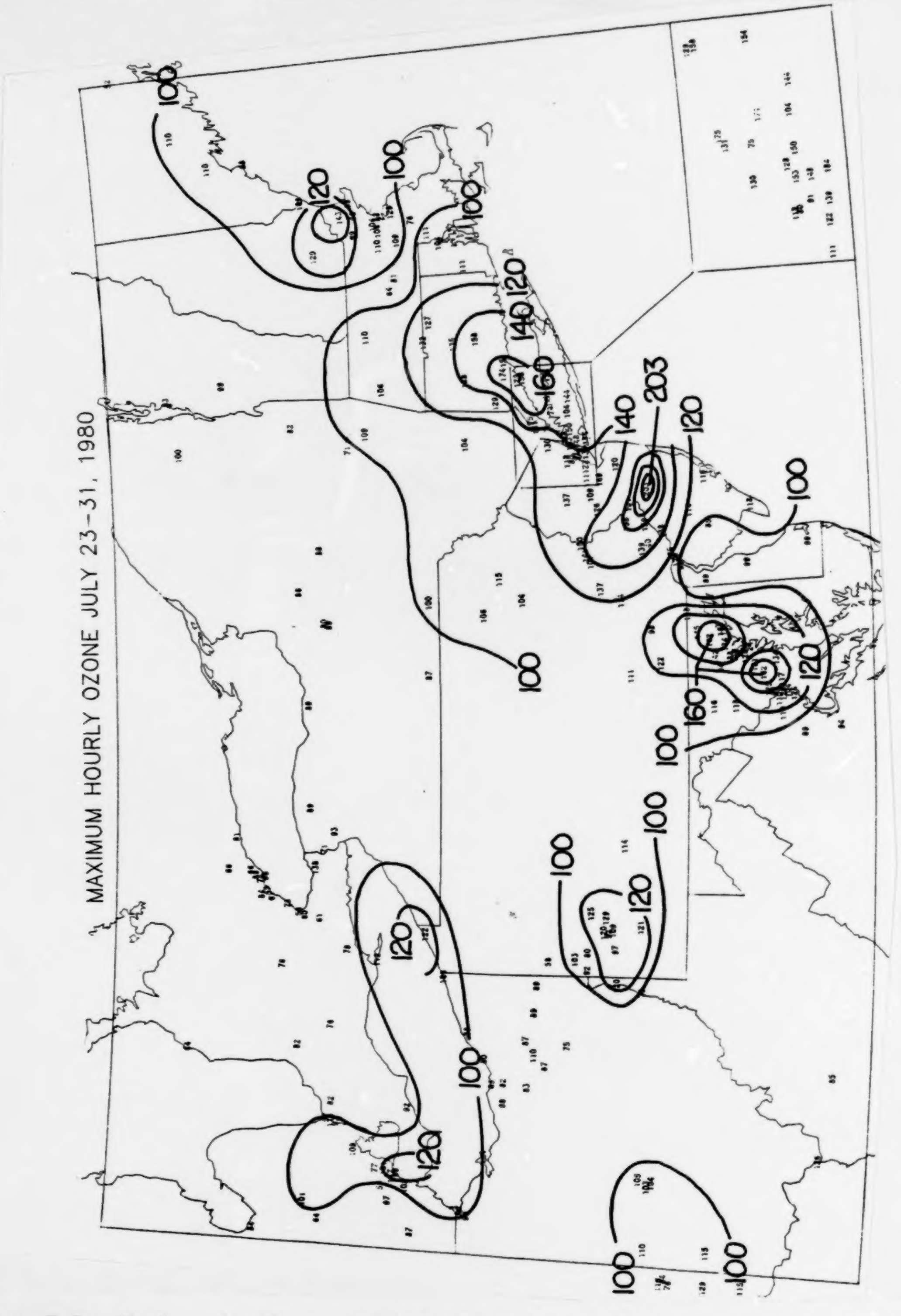
MAXIMUM HOURLY OZONE JULY 23-31, 1980
100
120
140
160
203

Figure 8-2. Maximum hourly averaged ozone concentration observed at SAROAD monitoring sites during the scenario period 23 - 31 July 1980.

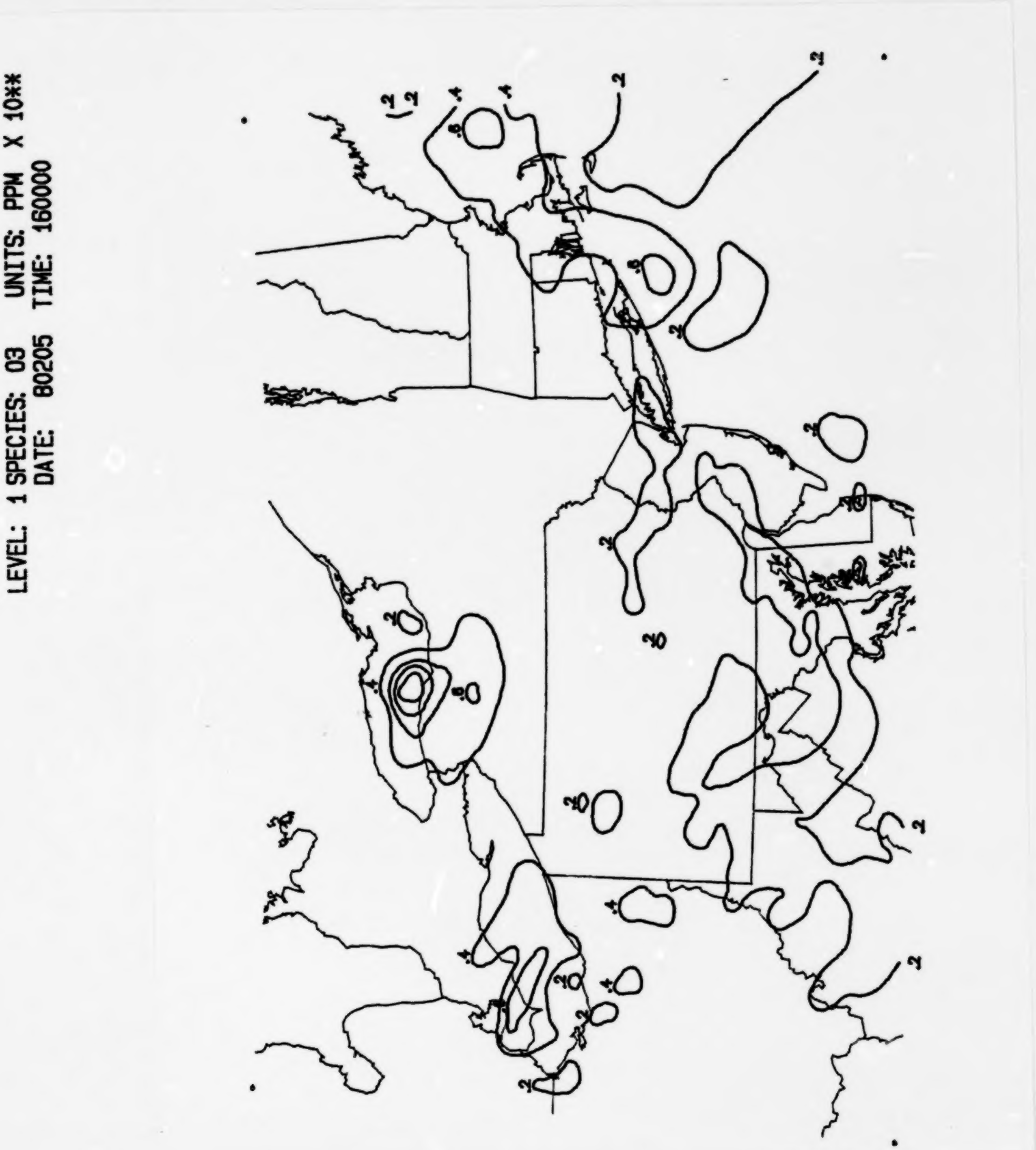
LEVEL: 1 SPECIES: O3 UNITS: PPM X 10**
DATE: 80205 TIME: 160000

Figure 8-3. Simulated ozone in Layer 1 at hour 1600 EST on the first day of the 9-day scenario, using the base emissions inventory.

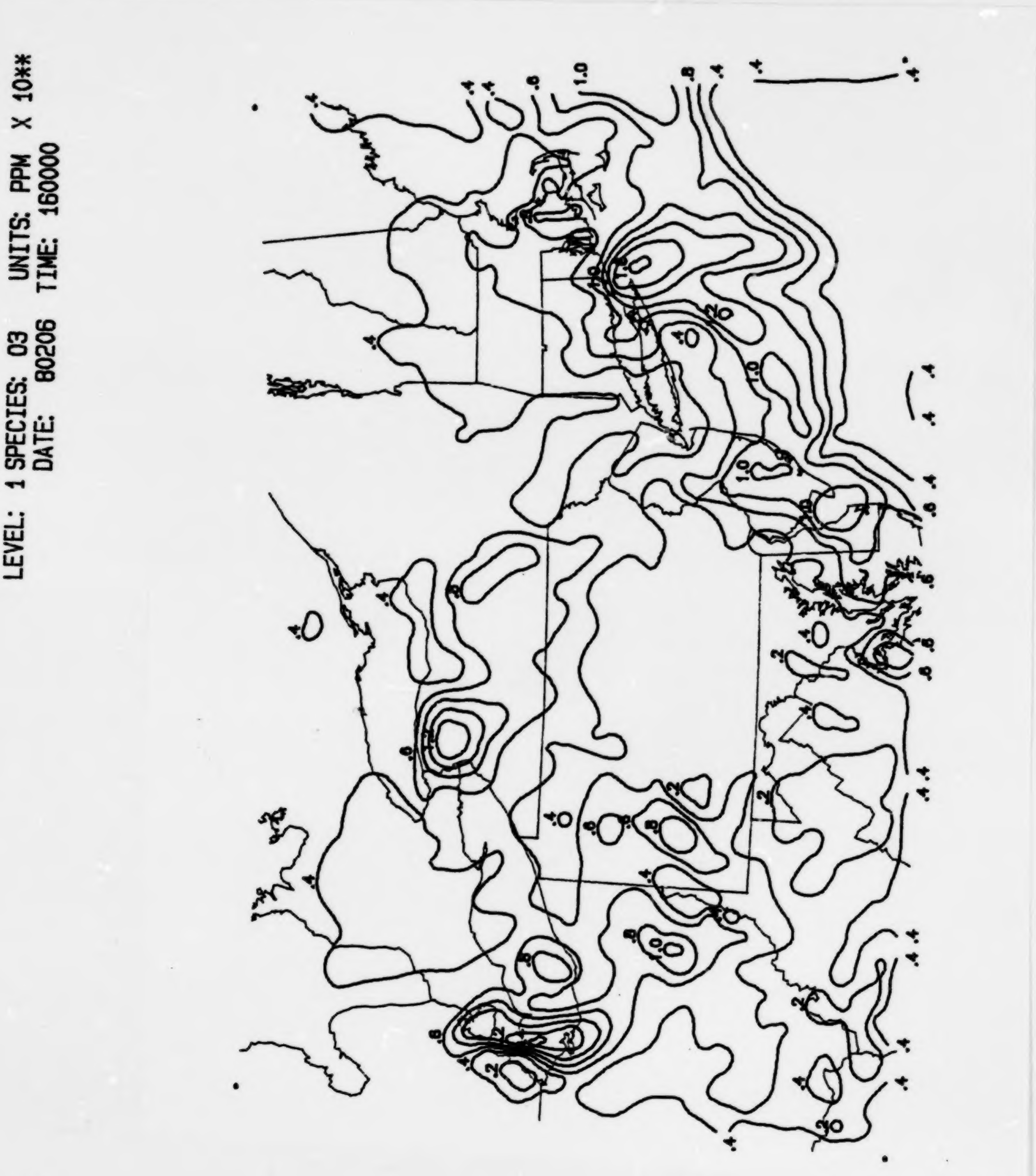
LEVEL: 1 SPECIES: O3 UNITS: PPM X 10**
DATE: 80206 TIME: 160000

Figure 8-4. Same as 8-3 except hour 1600 of day 2 of the scenario.

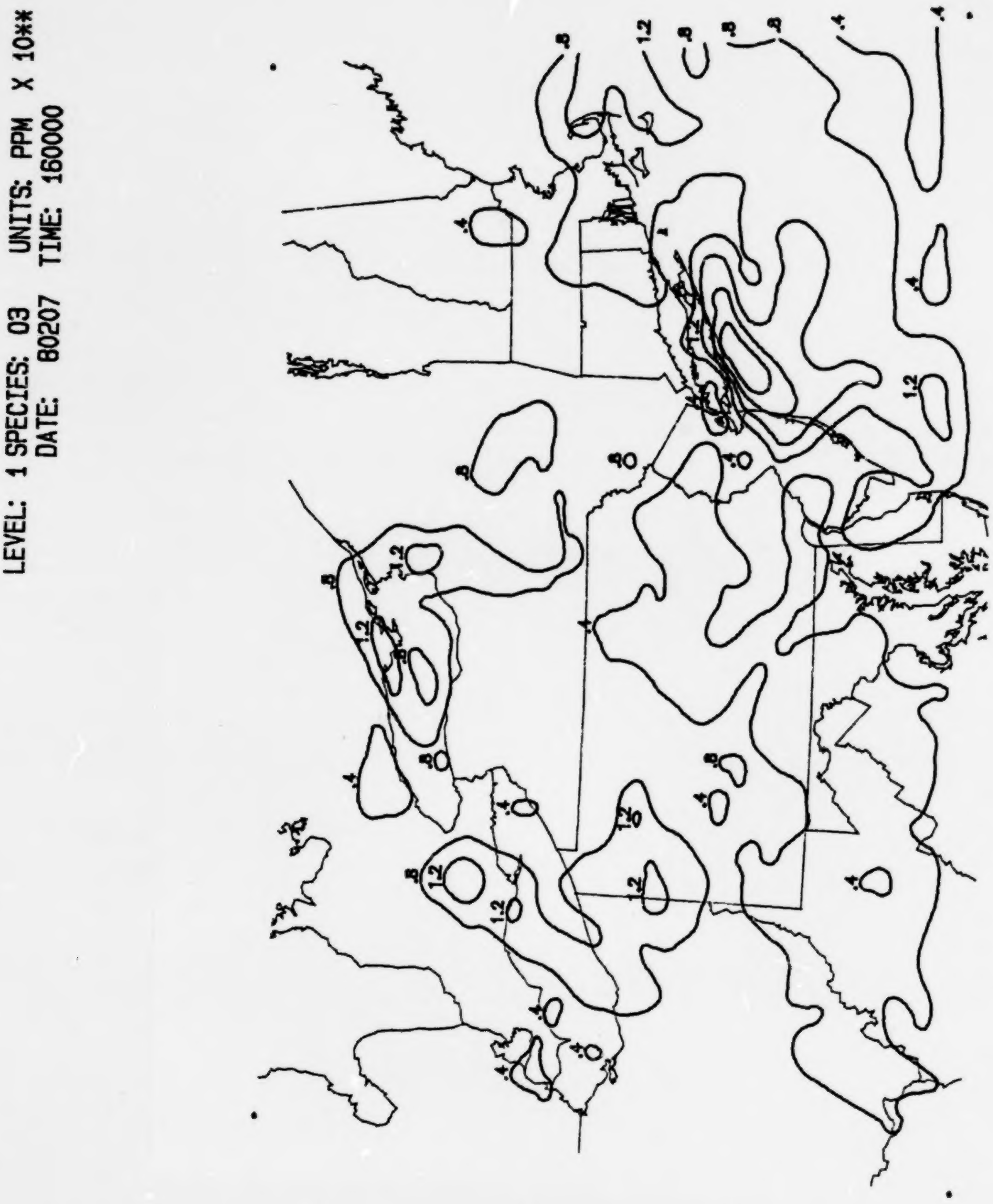
LEVEL: 1 SPECIES: 03 UNITS: PPM X 10**
DATE: 80207 TIME: 160000
.4
.8
1.2
1

Figure 8-5. Same as 8-3 except hour 1600 of day 3 of the scenario.

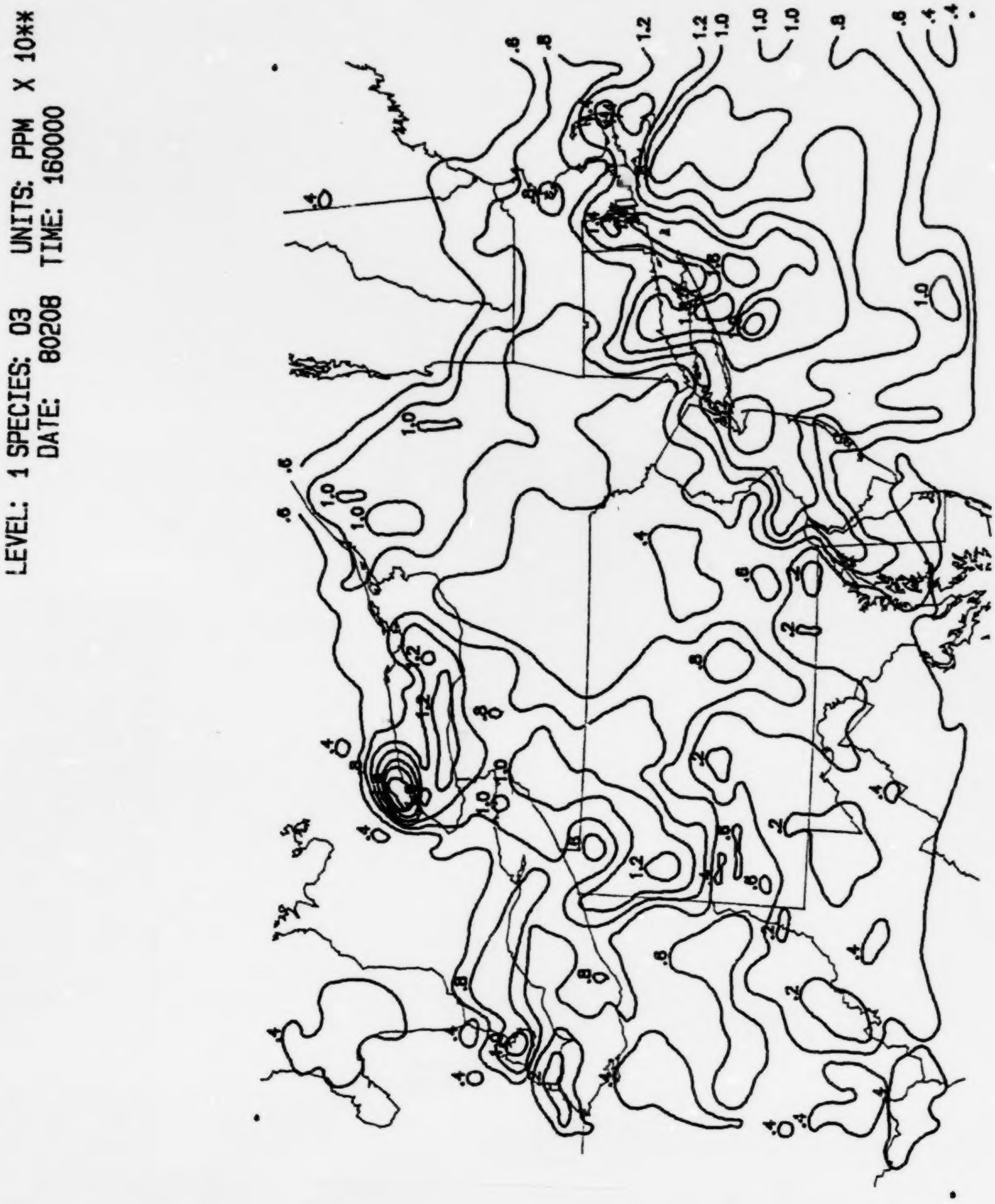
LEVEL: 1 SPECIES: O3 UNITS: PPM X 10**
DATE: 80208 TIME: 160000

Figure 8-6. Same as 8-3 except hour 1600 of day 4 of the scenario.

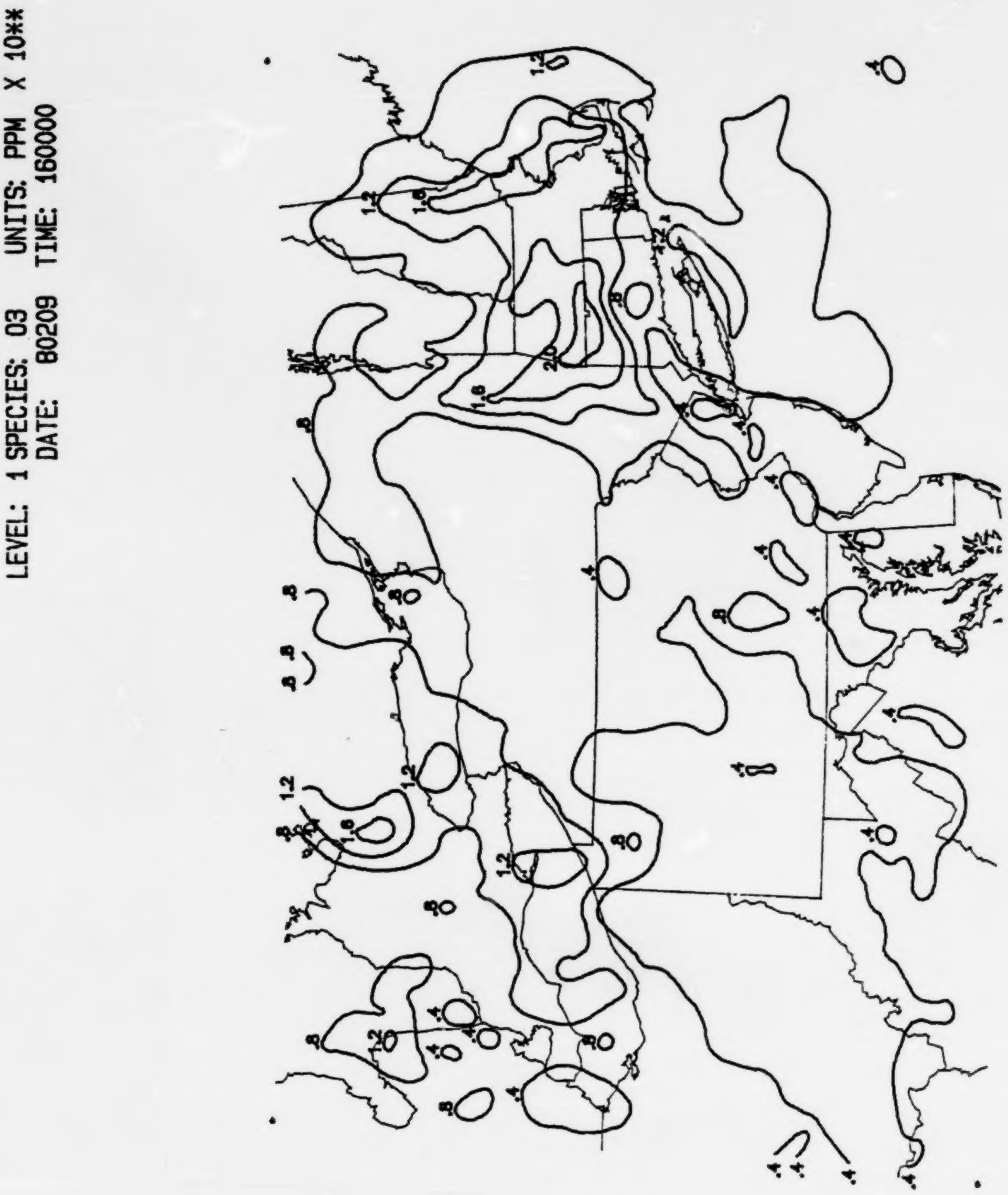
LEVEL: 1 SPECIES: O3 UNITS: PPM X 10**
DATE: 80209 TIME: 160000
.4
.8
1.2
1.6
2.0

Figure 8-7. Same as 8-3 except hour 1600 of day 5 of the scenario.

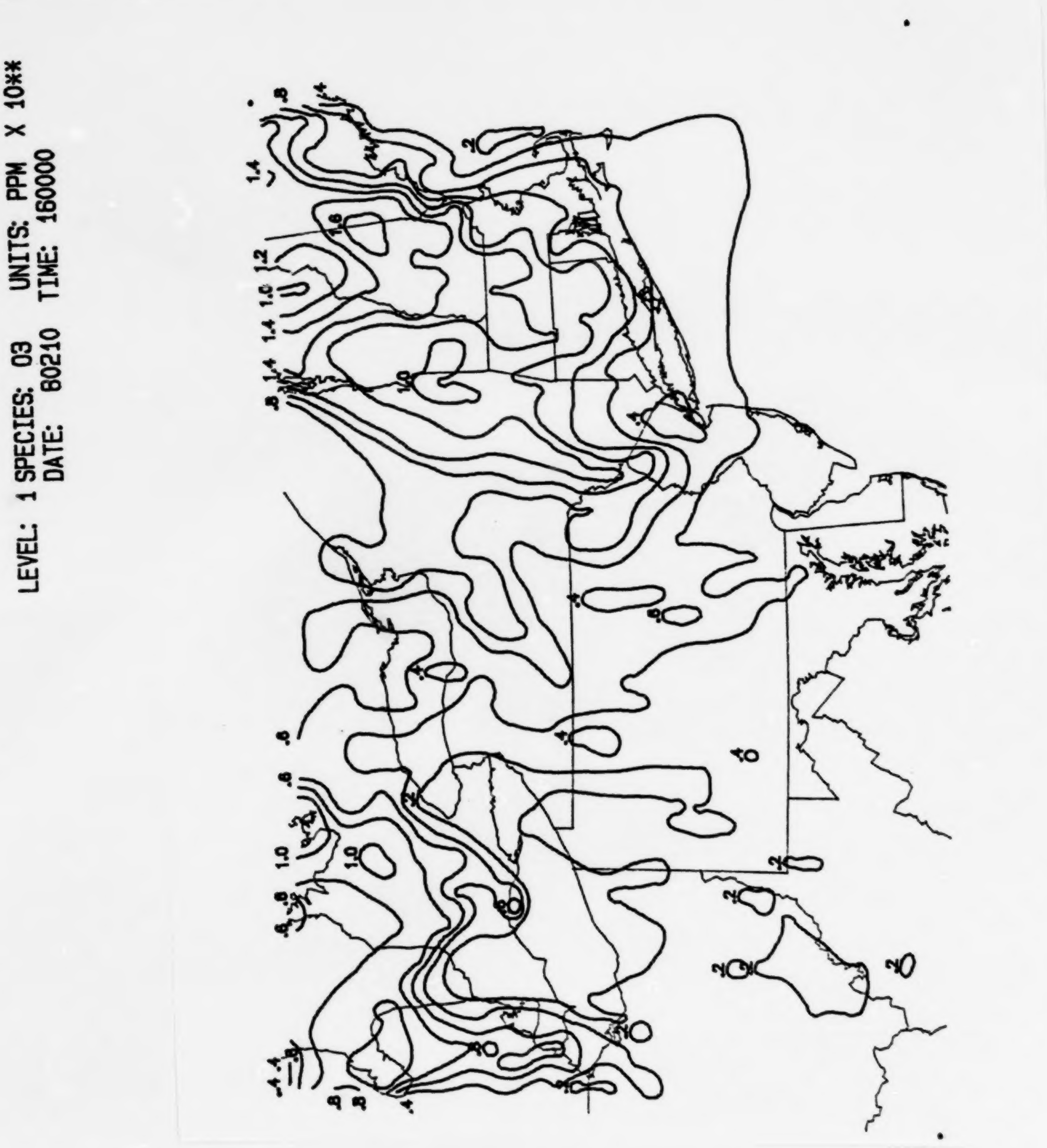
LEVEL: 1 SPECIES: 03 UNITS: PPM X 10**
DATE: 80210 TIME: 160000

Figure 8-8. Same as 8-3 except hour 1600 of day 6 of the scenario.

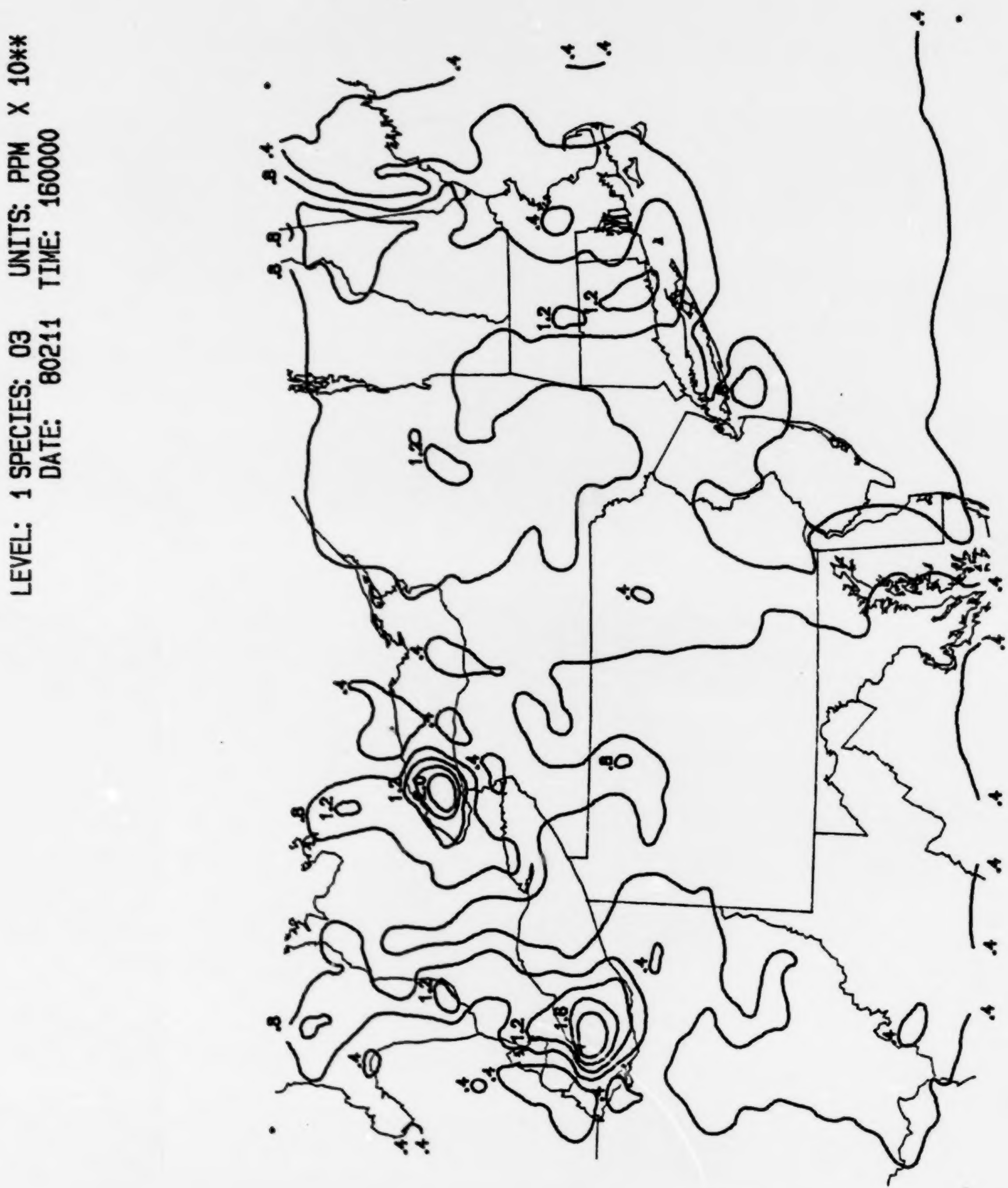
LEVEL: 1 SPECIES: O3 UNITS: PPM X 10**
DATE: 80211 TIME: 160000
.4
.8
1.2
1.6
1.8

Figure 8-9. Same as 8-3 except hour 1600 of day 7 of the scenario.

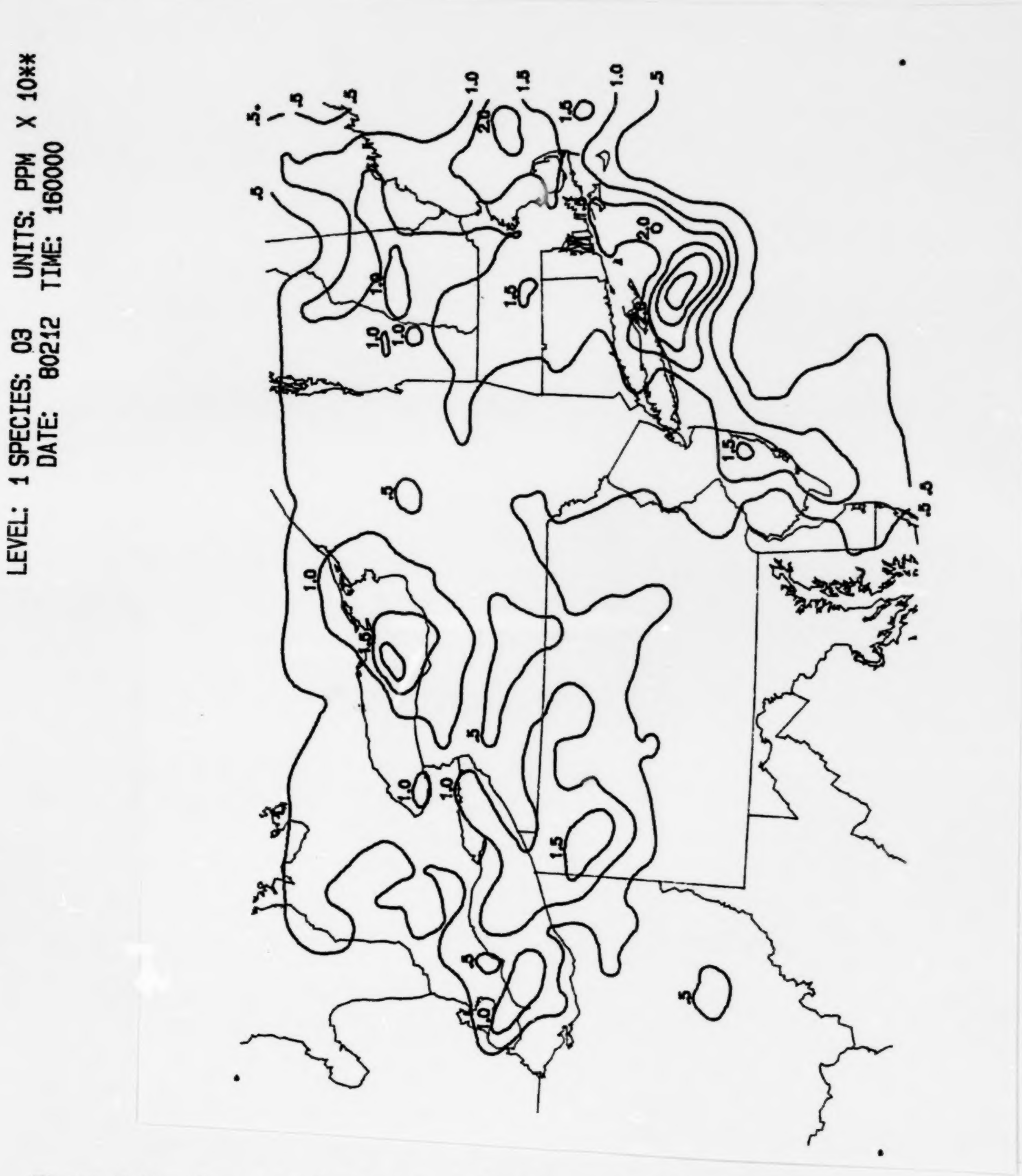
LEVEL: 1 SPECIES: 03 UNITS: PPM X 10**
DATE: 80212 TIME: 160000
.5
1.0
1.5
2.0

Figure 8-10. Same as 8-3 except hour 1600 of day 8 of the scenario.

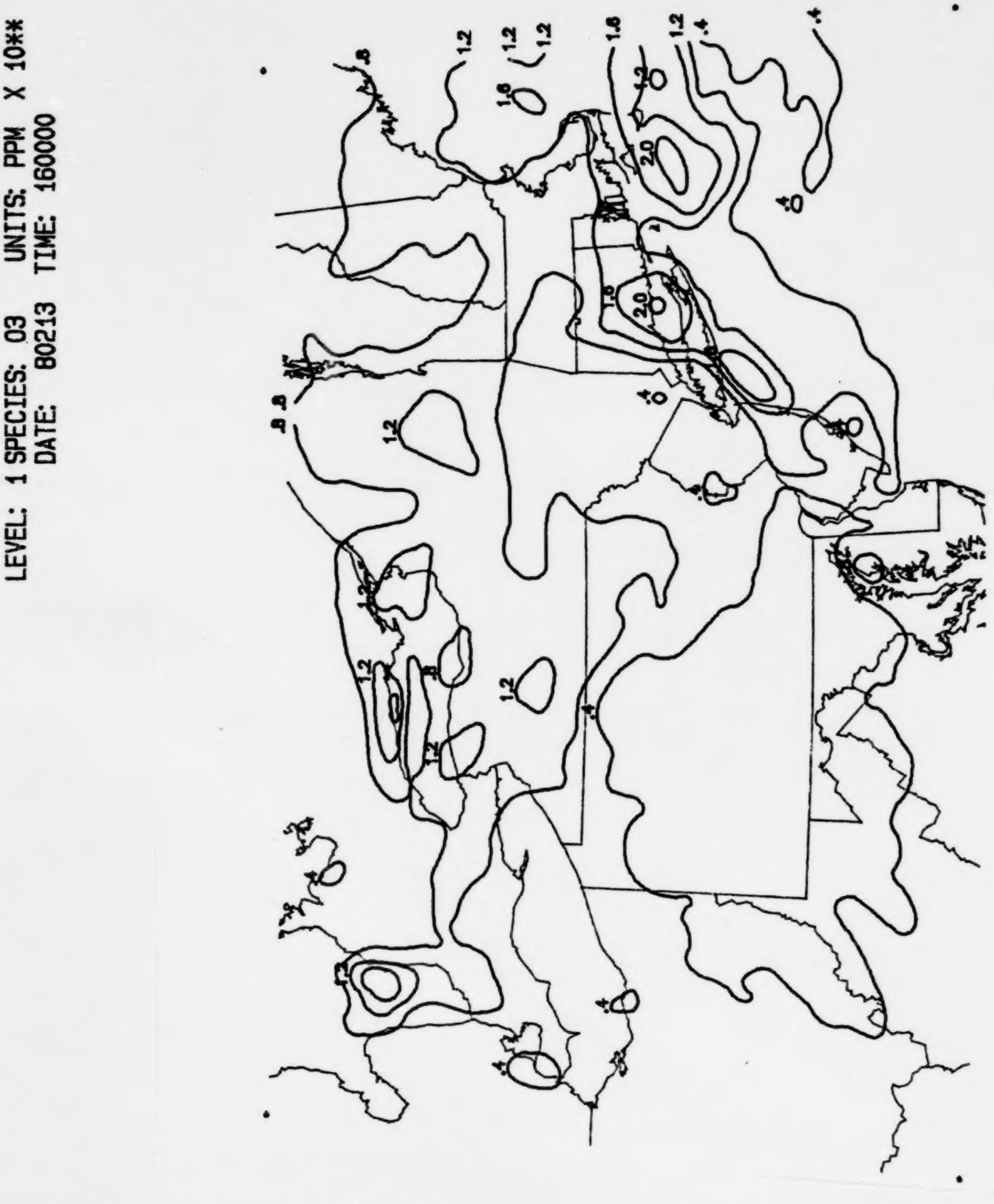
LEVEL: 1 SPECIES: O3 UNITS: PPM X 10**
DATE: 80213 TIME: 160000
.8
1.2
1.6
2.0
.4
.0

Figure 8-11. Same as 8-3 except hour 1600 of day 9 of the scenario.

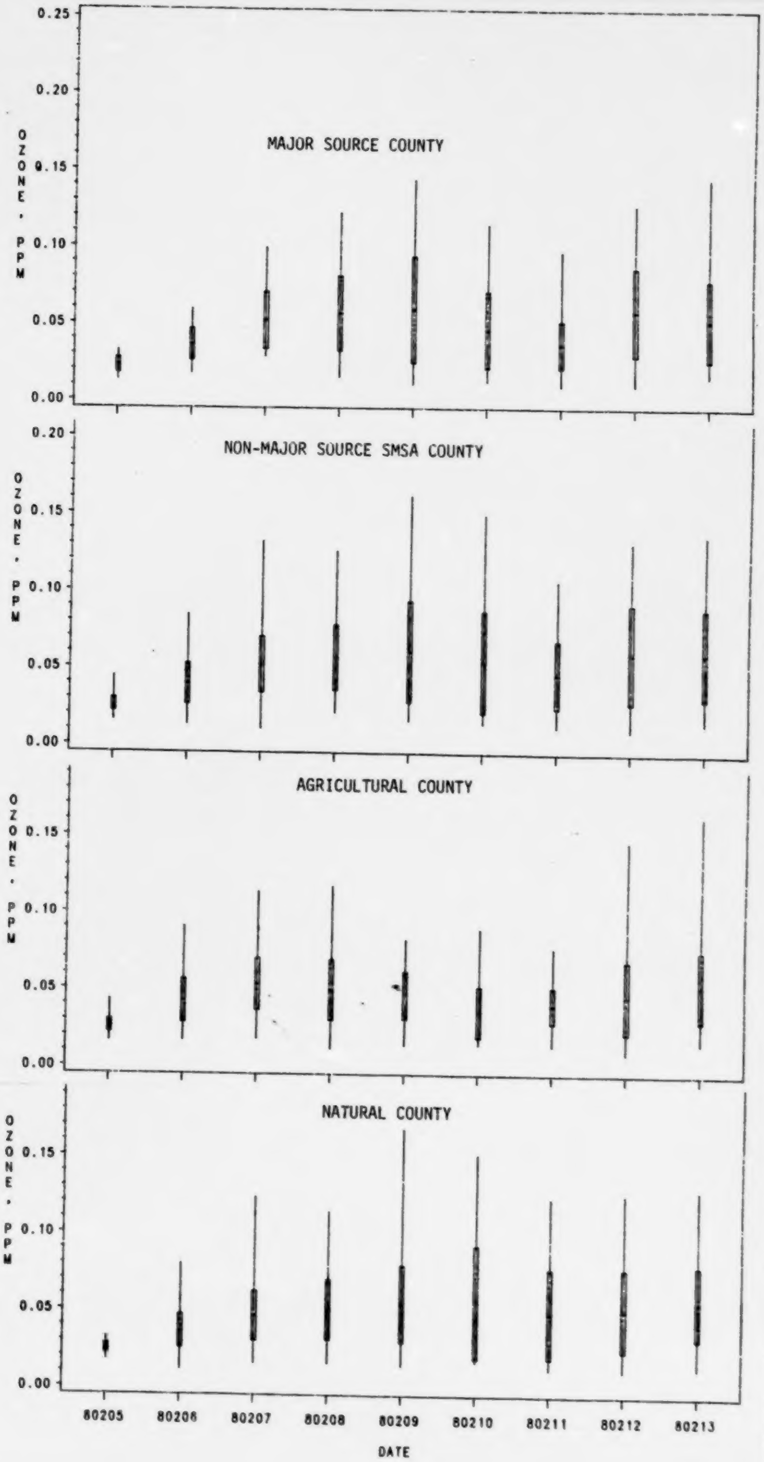

Figure 8-12. Quartile plots of simulated base case daily daylight averaged (0900-1600 LST) ozone concentrations in each of the four county receptor classes defined in Section 5. See page 96 for explanation of symbols.

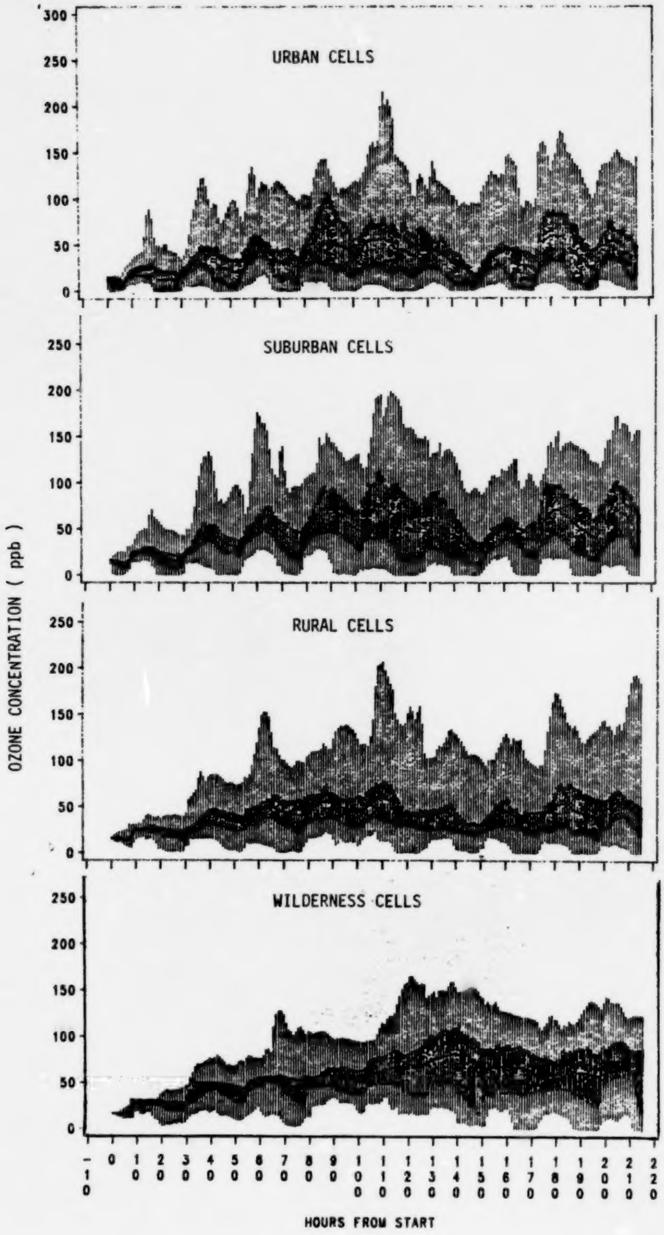

Figure 8-13. Quartile plots of simulated base case hourly ozone concentration in each of the four receptor cell classes defined in Section 5. See page 96 for an explanation of the graphs.

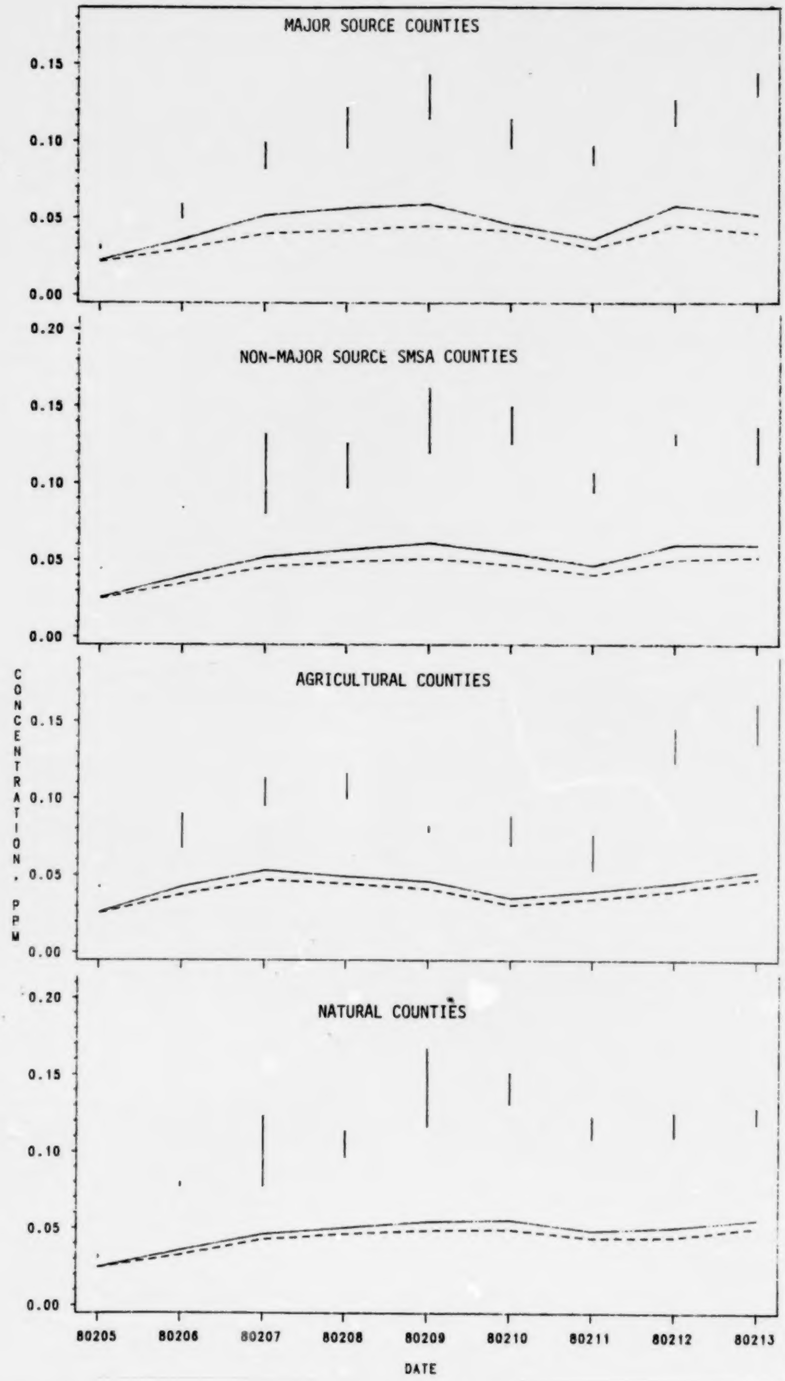

Figure 8-14. Simulated effects of emissions controls on daily daylight (0900-1600 LST) averaged ozone concentrations in each of the four county receptor classes. See page 101 for an explanation of the symbols.

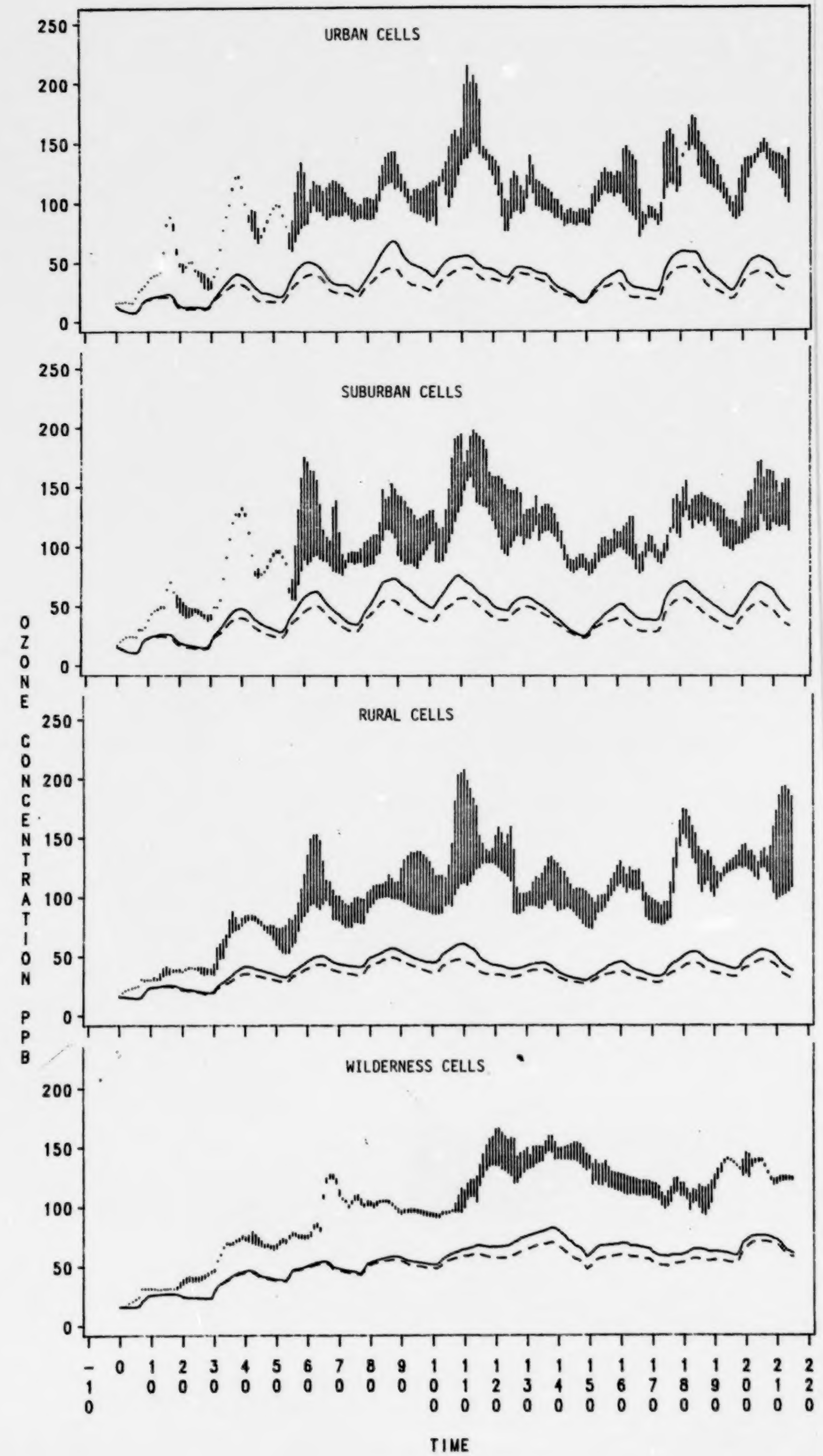

Figure 8-15. Simulated effect of emission controls on hourly averaged ozone concentrations in each of the four receptor cell classes. See page 101 for an explanation of the symbols.

SECTION 9

CONCLUSIONS

Following is a summary of the main points that we made in each of the previous sections.

- The first-generation Regional Oxidant Model (ROM1) used in this study is weak in four basic areas: (1) the chemistry scheme employed is not considered to be the best description currently available, (2) the emissions inventory does not include biogenic hydrocarbons, (3) the model's 3 and one-half layers have constant thicknesses throughout the 9-day simulation, and (4) the wind fields are non-divergent. (Problems may also exist in other aspects of the model, such as the technique used to treat major point sources.) These four weaknesses will be eliminated in the second-generation model (ROM2) which we hope to have operational in mid-1986. (See Table 2-2, page 10.)

- Based on the 1980 NAPAP version 4.2 emissions inventory, we identified 70 counties in the Northeastern U.S. as major sources of VOC and NO_x (see Tables 4-1, 2, pages 41 and 42). These counties have the highest emissions densities (moles per area per day) of VOC and NO_x of all counties in the region, and together they produce about one-half of all VOC and NO_x emissions. The areas of highest measured ozone concentrations are closely associated with the locations of these 70 counties (compare Figure 4-1, page 43, with Figure 3-1, page 20).

- The characteristic spatial scale of VOC and NO_x sources in the Northeast is estimated to be a few tens of kilometers (see Figure 4-2, page 44). This means that if a model with a grid size much larger than this, say $\Delta > 50$ km, is used to simulate photochemical air pollution in this region, significant systematic errors can occur not only in the predicted peak concentrations of secondary species, such as ozone, but also in the predicted response of the concentrations of these species to changes in VOC and NO_x emissions. The latter point is of critical importance in the use of models in regulatory studies and requires further detailed analysis.

- On comparing the 1980 NAPAP version 4.2 emissions inventory with the earlier 1979 NECRMP inventory, we found differences of 300 percent and more in the gridded (~18x18 km) VOC and NO_x emission rates (see Figures 4-3, 4, pages 45, 46). This represents a level of uncertainty in the base emissions that is roughly ten times the magnitude of the changes in emissions that are contemplated in present control strategies. The origin of this uncertainty is being investigated.

- Air quality models that treat regional scale and larger areas, i.e., domains > 1000 km in extent, can be operated in either of two modes, which we called the probabilistic mode and the quasi-deterministic mode. In the former the model predicts the probabilities, expectations and other statistical properties of concentrations at specific sites at specific times. In the quasi-deterministic mode, the model provides statistics of concentrations at given times or integrated over given periods within given receptor classes rather than at specific sites. In the present study the model is run only in the quasi-deterministic mode, yielding information on the concentrations of 23 different chemical species in four receptor classes -- Urban, Suburban, Rural, and Wilderness -- defined on page 50.

- We have tentatively proposed two criteria for selecting historical meteorological data for use in regional scale modeling studies of photochemical oxidant: (1) the meteorological scenario should begin on a day when the median value of the maximum hourly ozone concentrations observed at all measuring sites in the model domain is near the seasonal minimum value; (2) the scenario should be long enough that the frequency distribution of measured hourly ozone values during the scenario period approximates the corresponding seasonal distribution closely enough to give the results of the model simulations broad applicability. We showed that the scenario must be more than about 5 days long, to minimize the effects of the initialization procedure on predicted concentrations, and that a 9-day scenario is not long enough to model the processes that control concentrations above the 90-th percentile level at any site (see Figure 6-2a, b, c; pages 68-70).

- We performed 9-day simulations comparing ozone concentrations produced by 1980 emissions (base case) with those produced by projected 1987 emissions (control case). (See Sections 4 and 7 for discussions of the emissions inventories.) The simulations were performed using ROM1 which has the following basic limitations: "outdated" chemical mechanism; biogenic hydrocarbon emissions are ignored; model layers have constant thicknesses; horizontal winds are nondivergent. On comparing the results of the base case run with measured ozone data we found that the model underpredicted the scenario maximum ozone concentration in the Pittsburgh area -- 90 ppb predicted vs. 120 ppb observed -- and in the Washington-Baltimore area -- 90 predicted vs. 150 observed. It overpredicted near Toronto -- 200 vs. 90 -- and in northern New England -- 130 vs 100. Better agreement was found in the Detroit and New York areas (compare Figures 8-1 and 2, pages 104 and 105). The most likely causes of the errors near the urban areas are believed to be errors in the emissions data or cloud cover or both.

- Comparing the predicted ozone concentrations for the base case with corresponding values in the control case we found the following:

  (1) In general, at any given location and hour the concentration in the control case is less than or equal to that in the base case;

  (2) Within each receptor group, peak concentrations are reduced by larger percentages than the median values are reduced.

Reductions of 0 to 50% occur in the peak compared to to 0 to 25% reductions in the median (see Figure 8-15, page 118). This is true of all concentration averaging times.

(3) Ozone is reduced more at sites near the major VOC and NO_x sources than at locations far away. For example, median ozone levels at Suburban locations (defined to be within 50 km of major source centers) were reduced up to 25% whereas in Wilderness areas (greater than 100 km from major sources) reductions were less than 15% (see Figure 8-15).

(4) The maximum ozone concentrations in Rural and Wilderness areas occurred on different days in the control case than in the base case, even though meteorological conditions were identical in both simulations. This suggests that the source-receptor relationship between VOC/NO_x sources and remote sites is strongly nonlinear.

(5) Overall, the 1987 emissions reductions appear to have two basic effects on ozone: they cause a delay in ozone formation, and they reduce the total quantity produced. The former effect is evident in Figure 9-1 (next page) which shows the counties in which the simulated hourly ozone level exceeded 120 ppb in the base and control cases. The figure shows that reduction of the peak value to levels below 120 ppb occurred primarily in the upwind counties only.

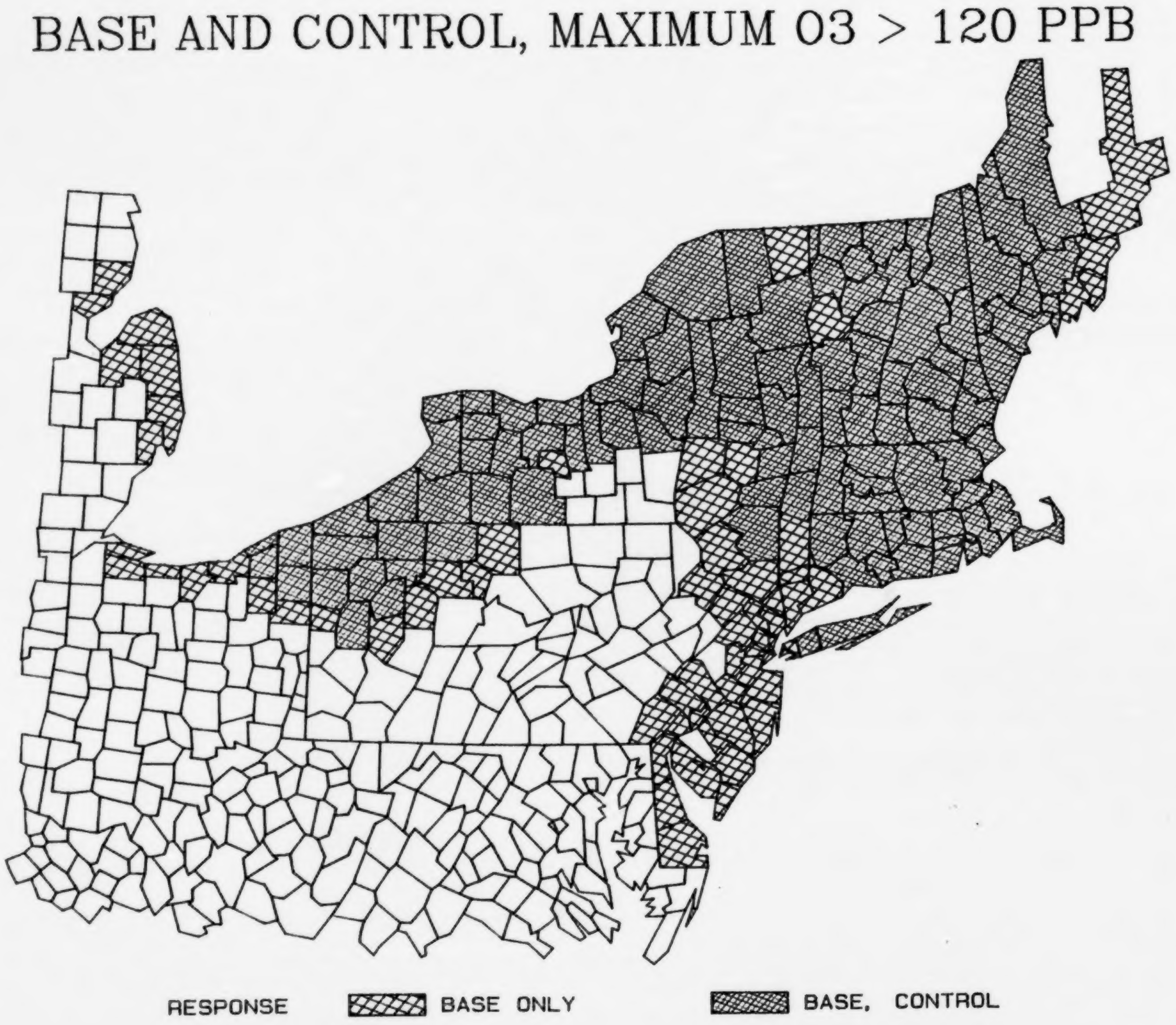
BASE AND CONTROL, MAXIMUM O3 > 120 PPB
RESPONSE
▨ BASE ONLY
▨ BASE, CONTROL

Figure 9-1. Counties in which simulated one-hour averaged ozone concentrations exceeded 120 ppb during the 9-day scenario. Light shading denotes counties in which exceedance occurred only in the base case simulation. Dark shading indicates areas where exceedance occurred in both the base and control runs.

References

1. Alkezweeny, A., K. M. Busness, R. C. Easter and J. S. Wetzel, (1981): "Northeast Corridor Regional Modeling Project: Aircraft Measurements -- New York and Vicinity. EPA-450/4-81-012. 229 pages.

2. Allwine, K. J. and H. H. Westberg, (1977): "Potential Impact of Coal-Fired Power Plants on Ground-Level Ozone Concentrations in Wisconsin", Final Report to Wisconsin Public Service Commission, Madison, Wisconsin.

3. Clark, T. L. and J. F. Clarke, (1984): "A Lagrangian Study of the Boundary Layer Transport of Pollutants in the Northeastern United States", Atmos. Envir., Vol. 18, pp 287-297.

4. Demerjian, K. L., and K. L. Schere, (1979): "Applications of a Photochemical Box Model for Ozone Air Quality in Houston, Texas. Proceedings, Ozone/Oxidants: Interactions with the Total Environment II, Houston, TX, 14-17 Oct 1979, APCA, Pittsburgh, Pa., pp. 329-352.

5. Demerjian, K. L., K. L. Schere, and J. T. Peterson, (1980): "Theoretical estimates of actinic (spherically integrated) flux and photolytic rate constants of atmospheric species in the lower troposphere." In Advances in Environmental Science and Technology - Vol. 10, J. N. Pitts et al., eds., John Wiley and Sons, New York, pp. 369-459.

6. Lamb, R. G., (1977): "A Case Study of Stratospheric Ozone Affecting Ground-Level Oxidant Concentrations" J. Appl. Meteor., Vol. 16, 780-794.

7. Lamb, R. G., (1986): "The Effects of Model Grid Size on Predicted Regional Scale Ozone Concentrations". In preparation.

8. Lamb, R. G., and S. K. Hati, (1986): "The Representation of Atmospheric Motion in Models of Regional Scale Air Pollution", submitted to J. Climate and Appl. Meteor.

9. Lamb, R. G., (1983a): "A Regional Scale (1000 km) Model of Photochemical Air Pollution: Part 1. Theoretical Formulation". EPA-600/3-83-035. 237 pages.

10. Lamb, R. G., (1983b): "Theoretical Issues in Long Range Transport Modeling". Extended Abstract Volume. Sixth Symposium on Turbulence and Diffusion. Boston, Mass. Published by the American Meteorological Society.

11. Lamb, R. G., (1984): "A Regional Scale (1000 km) Model of Photochemical Air Pollution: Part 2. Input Processor Network Design". EPA-600/3-84-085. 310 pages.

12. Lamb, R. G., and G. F. Laniak (1985): "A Regional Scale (1000 km) Model of Photochemical Air Pollution: Part 3. Tests of the Numerical Algorithms". EPA/600/3-85-037. 289 pages.

13. Lyons, W. A., and H. S. Cole, (1976): "Photochemical Oxidant Transport: Mesoscale Lake Breeze and Synoptic-Scale Aspects. J. Appl. Meteor., Vol. 15, 733-743.

14. Schere, K. L., (1986): "The EPA Regional Oxidant Model: ROM1 Evaluation for 3-4 August 1979" EPA Report.

15. Siple, G. W., G. K. Fitzsimmons, J. J. Van Ee and K. F. Zeller, (1977): "Air Quality Data for the Northeast Oxidant Transport Study, 1975", EPA-600/4-77-020, 92 pages.

16. Toothman, D. A., J. C. Yates and E. J. Sabo, (1984): "Status Report on the Development of the NAPAP Emission Inventory for the 1980 Base Year and Summary of Preliminary Data. EPA/600/7-84-01.

17. Viezee, W., W. B. Johnson and H. B. Singh, (1983): "Stratospheric Ozone in the Lower Troposphere. II. Assessment of Downward Flux and Ground-Level Impact. Atmos. Environ., Vol. 17, 1979-1993.

18. Westberg, H., (1985): "Ozone Behavior in the Combined Baltimore-Washington Plume". EPA Report.

Appendix A

Daily weather maps for the scenario period 23-31 July 1980

WEDNESDAY, JULY 23, 1980

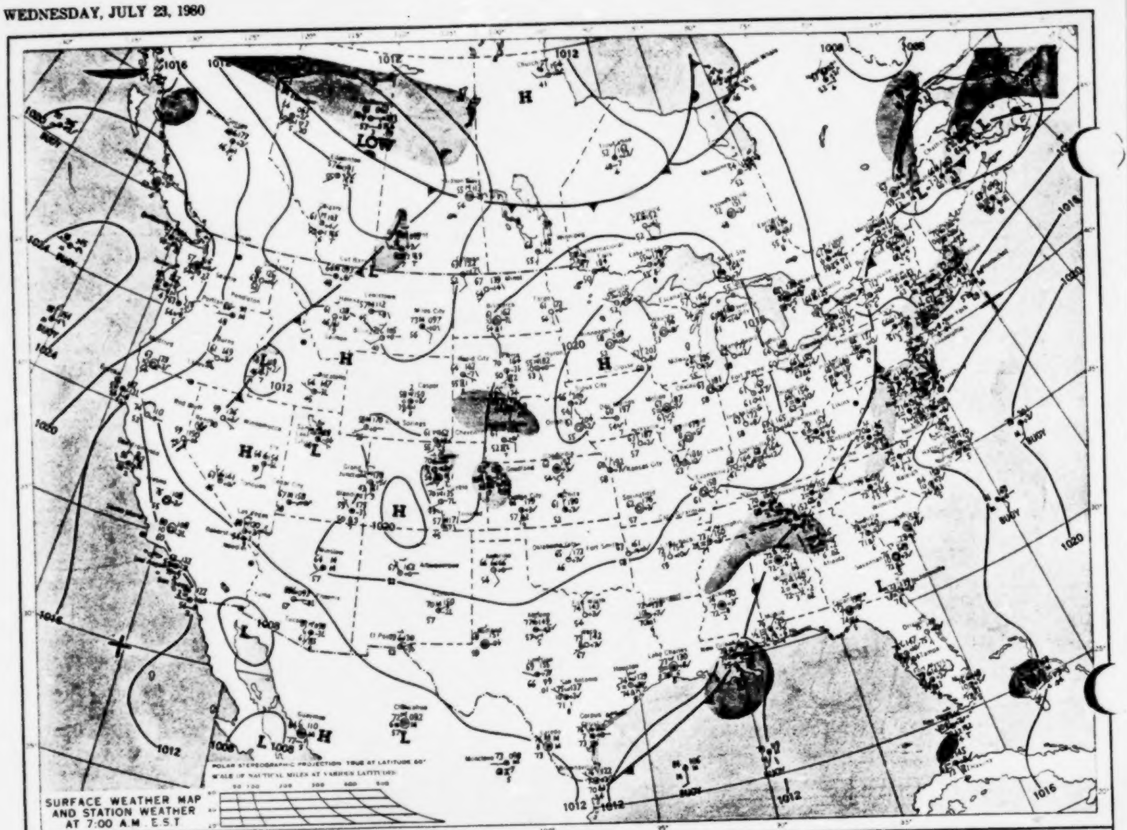
LOW
H
L
1012
1016
1020
1008
BUOY
POLAR STEREOGRAPHIC PROJECTION TRUE AT LATITUDE 60°
SCALE OF NAUTICAL MILES AT VARIOUS LATITUDES

SURFACE WEATHER MAP AND STATION WEATHER AT 7:00 A.M. E.S.T

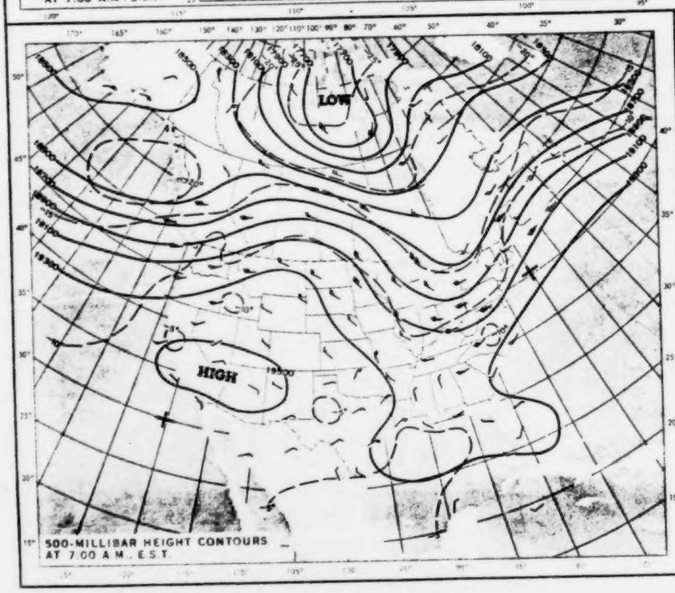

500-MILLIBAR HEIGHT CONTOURS AT 7:00 A.M., E.S.T.

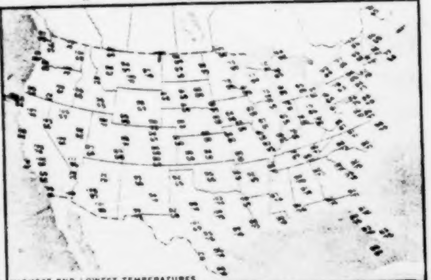

HIGHEST AND LOWEST TEMPERATURES

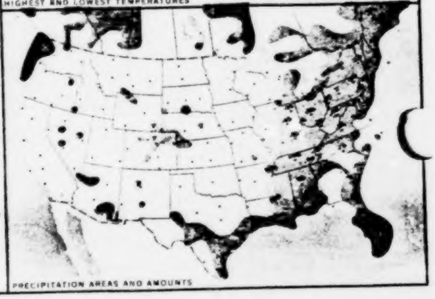

PRECIPITATION AREAS AND AMOUNTS

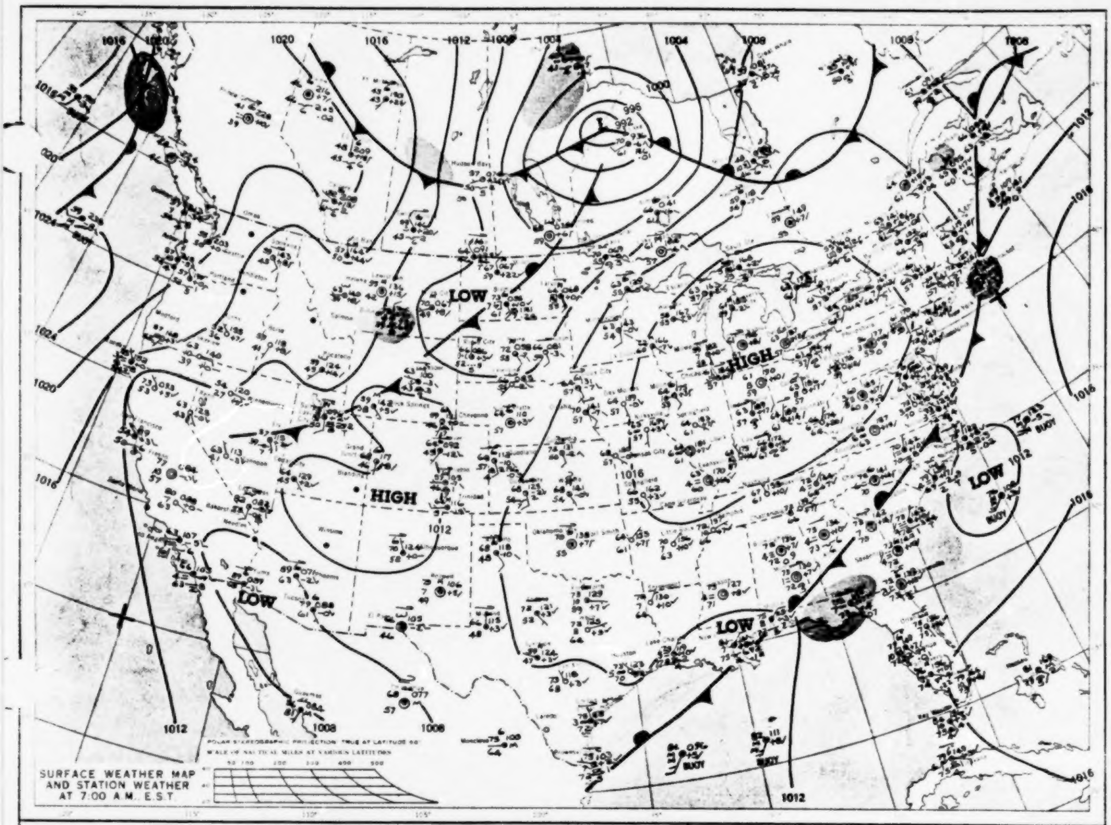
HIGH
HIGH
LOW
LOW
LOW
LOW
L
1016
1020
1024
1012
1008
1004
1000
996
992
POLAR STEREOGRAPHIC PROJECTION TRUE AT LATITUDE 60°

SURFACE WEATHER MAP AND STATION WEATHER AT 7:00 A.M. E.S.T.

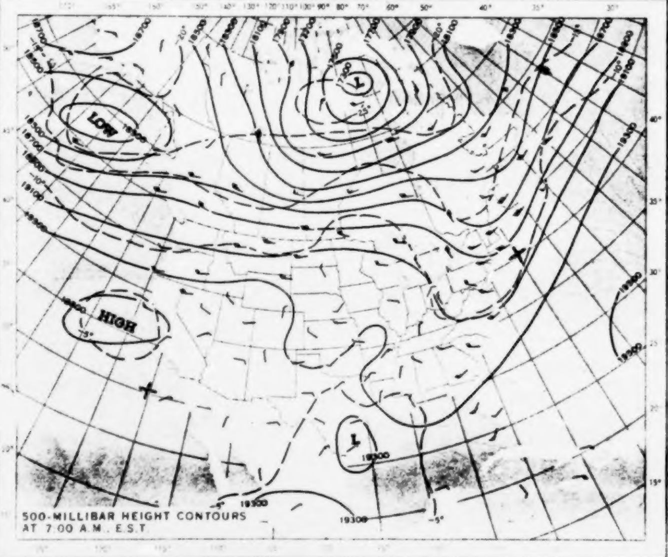
LOW
HIGH
L
L
19300

500-MILLIBAR HEIGHT CONTOURS AT 7:00 A.M., E.S.T.

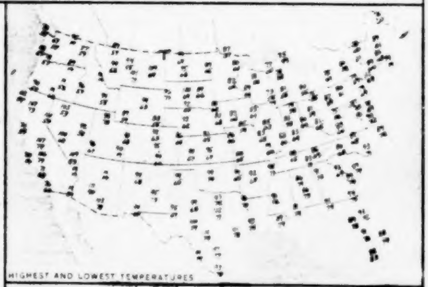

HIGHEST AND LOWEST TEMPERATURES

PRECIPITATION AREAS AND AMOUNTS

FRIDAY, JULY 25, 1980

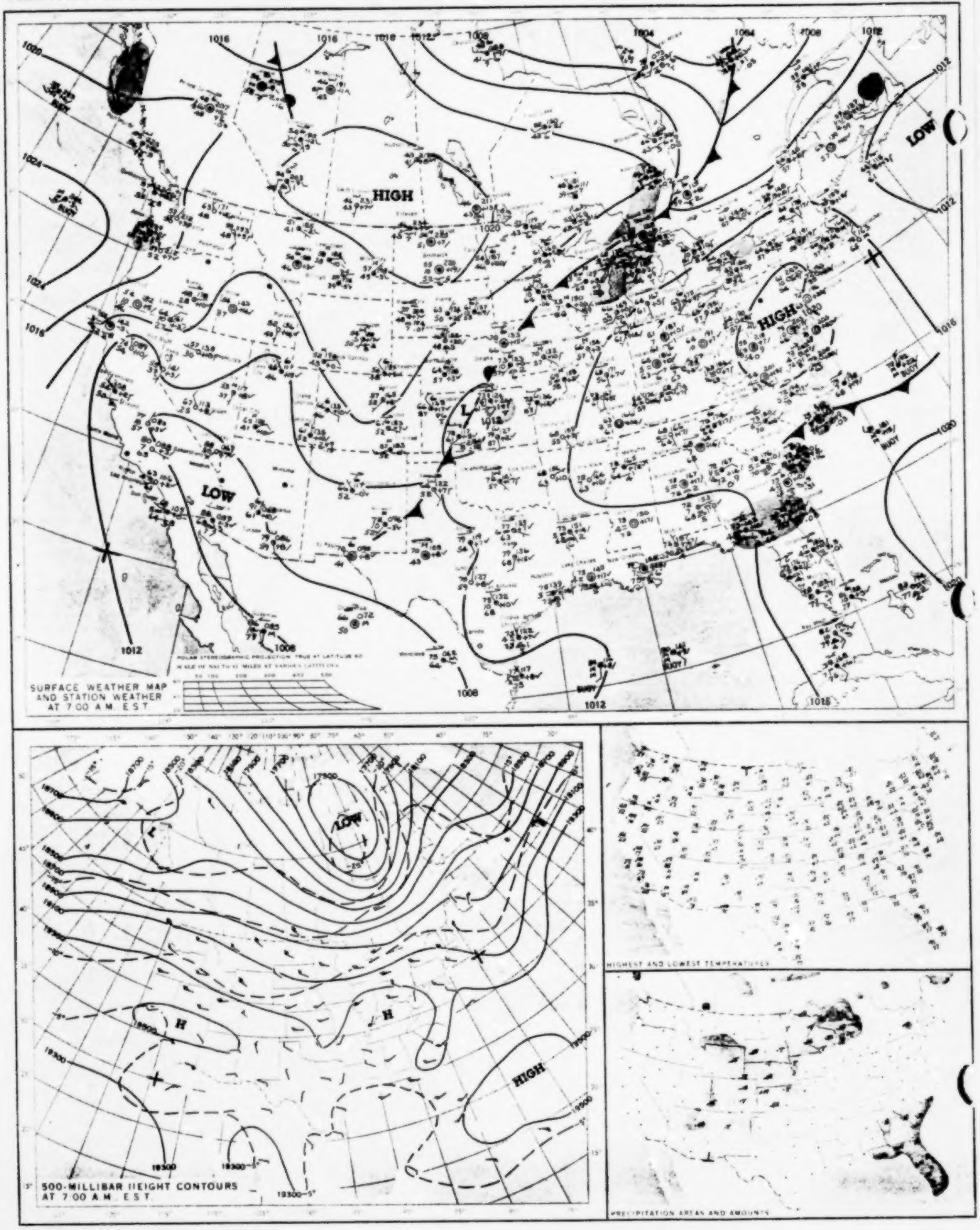

SURFACE WEATHER MAP AND STATION WEATHER AT 7:00 A.M. EST
HIGH
HIGH
LOW
LOW
L
1004
1008
1012
1016
1020
1024
500-MILLIBAR HEIGHT CONTOURS AT 7:00 A.M. EST
LOW
H
H
HIGH
L
17500
18300
HIGHEST AND LOWEST TEMPERATURES
PRECIPITATION AREAS AND AMOUNTS

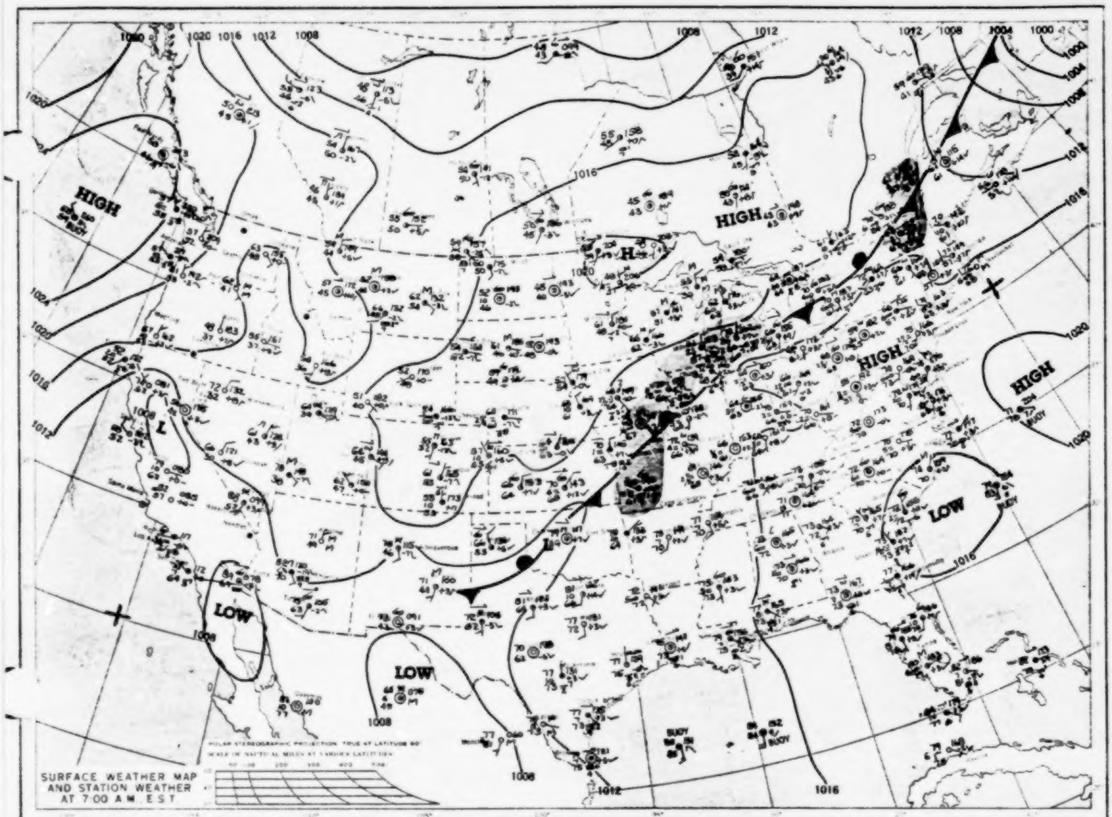
HIGH
HIGH
H
HIGH
HIGH
LOW
LOW
LOW
L
1020
1016
1012
1008
1004
1000
POLAR STEREOGRAPHIC PROJECTION TRUE AT LATITUDE 60°
SCALE OF NAUTICAL MILES AT VARIOUS LATITUDES

SURFACE WEATHER MAP AND STATION WEATHER AT 7:00 A.M., E.S.T.

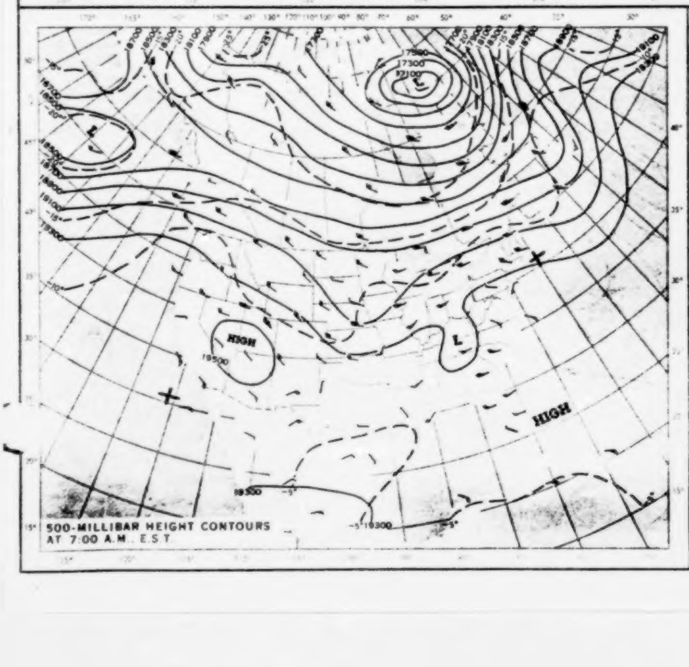
HIGH
HIGH
L
L
17300
17100
19500
19300

500-MILLIBAR HEIGHT CONTOURS AT 7:00 A.M., E.S.T.

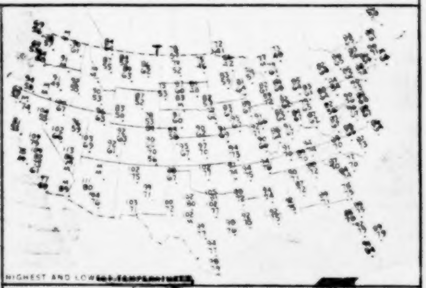

HIGHEST AND LOWEST TEMPERATURES

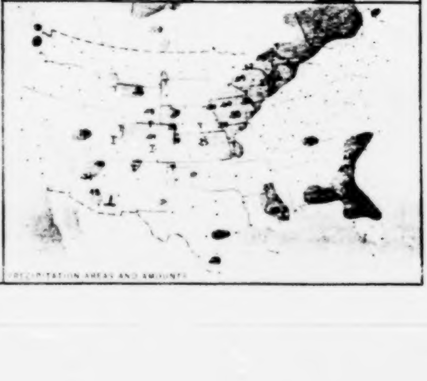

PRECIPITATION AREAS AND AMOUNTS

SUNDAY, JULY 27, 1980

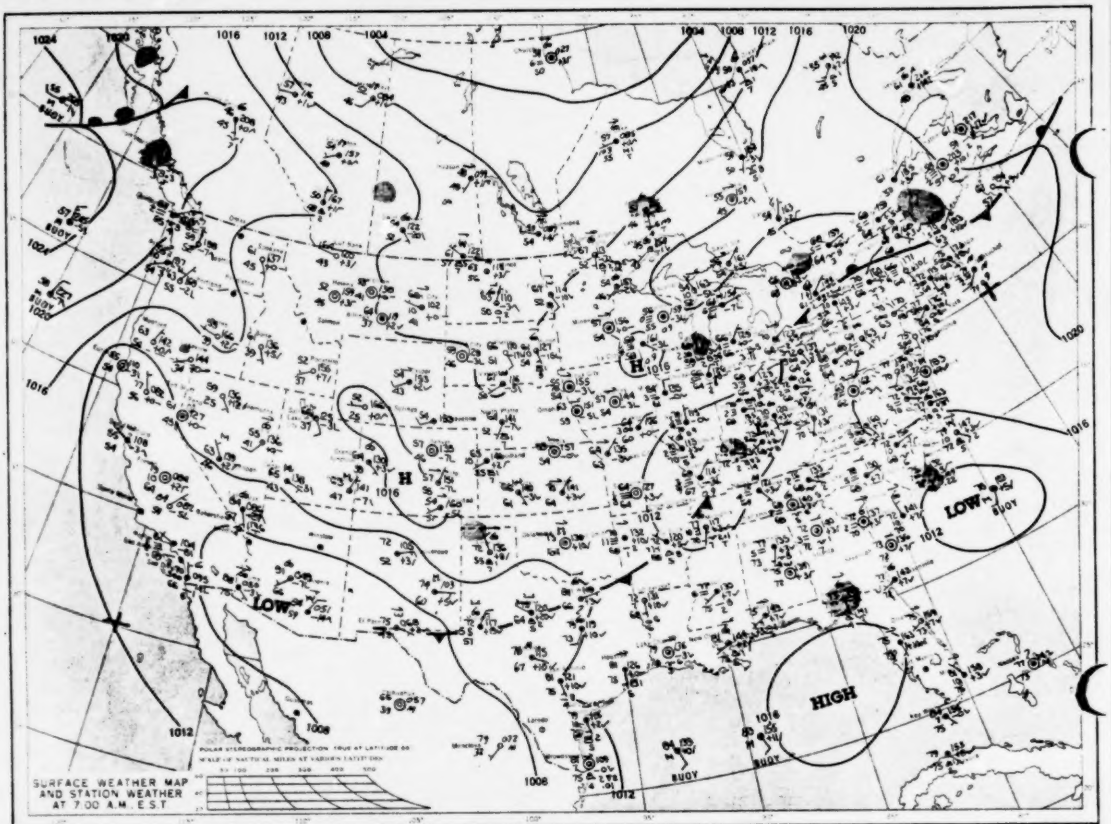
1024
1020
1016
1012
1008
1004
1004
1008
1012
1016
1020
1020
1016
1016
1012
1008
1008
1012
1024
1020
1016
1012
H
H
LOW
LOW
HIGH
BUOY
BUOY
BUOY
BUOY
POLAR STEREOGRAPHIC PROJECTION TRUE AT LATITUDE 60

SURFACE WEATHER MAP AND STATION WEATHER AT 7:00 A.M., E.S.T.

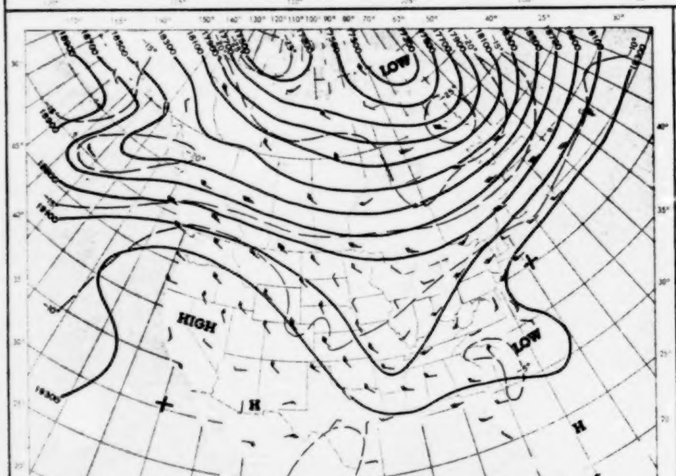
LOW
LOW
HIGH
H
H
19300
19200
18300
18900

500-MILLIBAR HEIGHT CONTOURS AT 7:00 A.M., E.S.T.

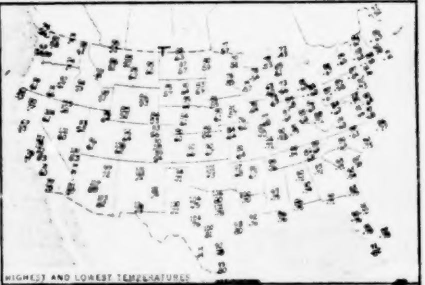

HIGHEST AND LOWEST TEMPERATURES

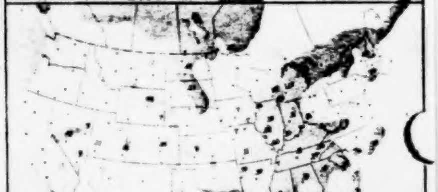

PRECIPITATION AREAS AND AMOUNTS

MONDAY, JULY 28, 1980

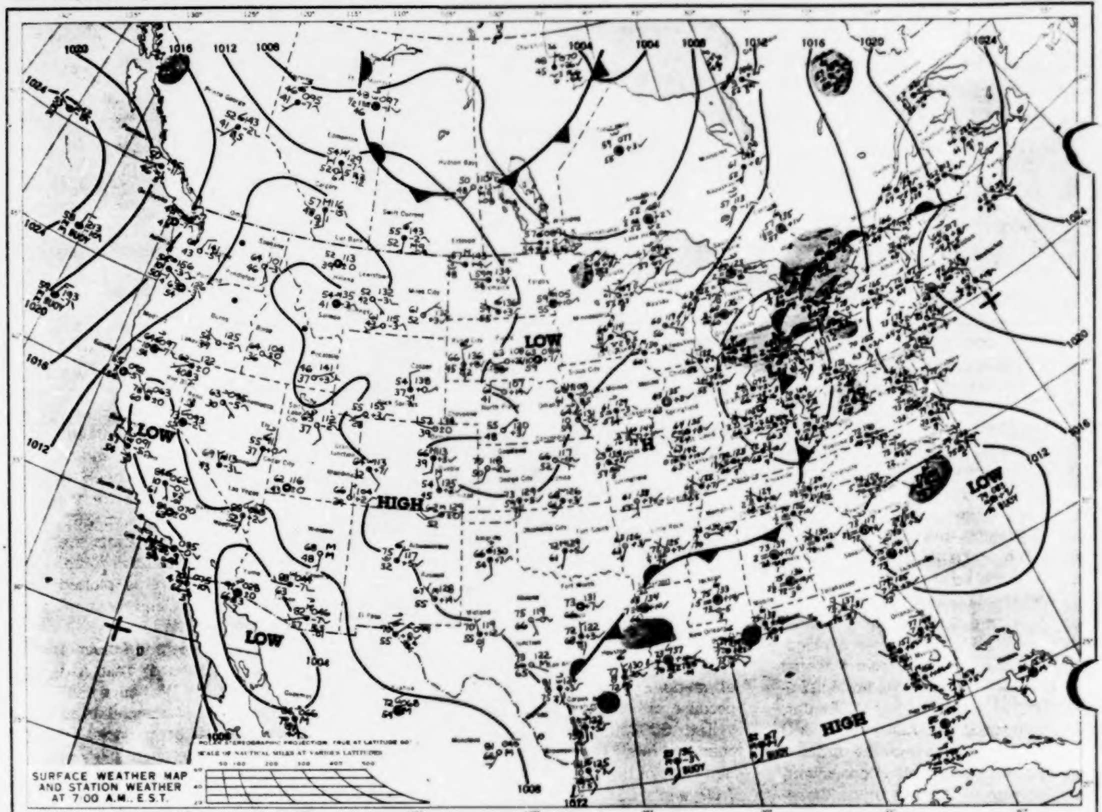
LOW
LOW
LOW
LOW
HIGH
HIGH
H
1020
1016
1012
1008
1004
1024

SURFACE WEATHER MAP AND STATION WEATHER AT 7:00 A.M., E.S.T.

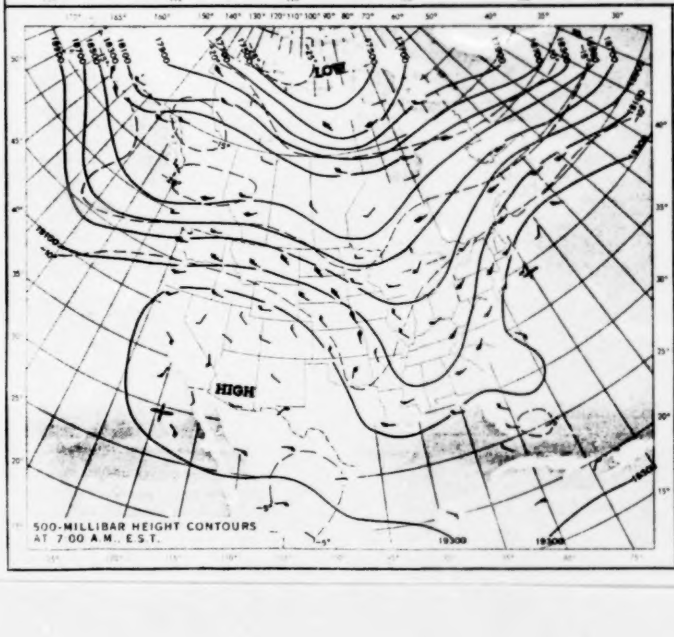

500-MILLIBAR HEIGHT CONTOURS AT 7:00 A.M., E.S.T.

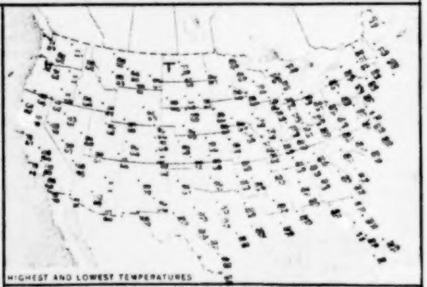

HIGHEST AND LOWEST TEMPERATURES

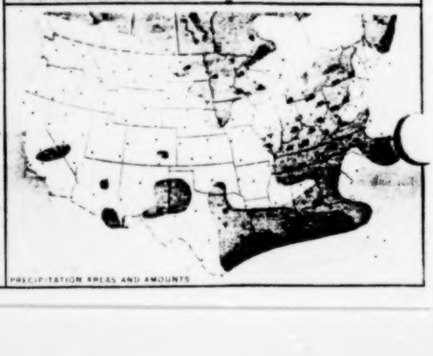

PRECIPITATION AREAS AND AMOUNTS

TUESDAY, JULY 29, 1980

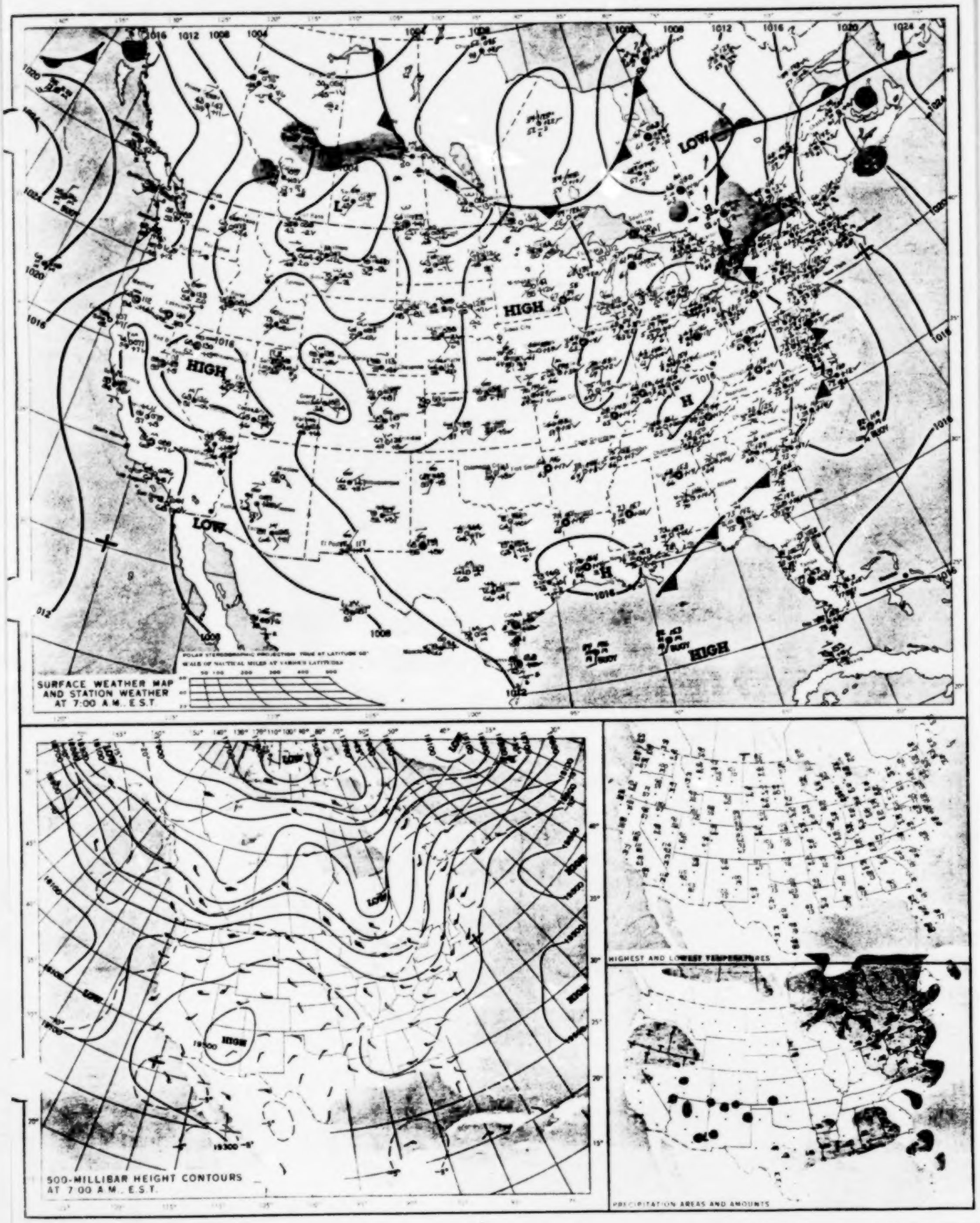
SURFACE WEATHER MAP AND STATION WEATHER AT 7:00 A.M., E.S.T.
POLAR STEREOGRAPHIC PROJECTION TRUE AT LATITUDE 60°
SCALE OF NAUTICAL MILES AT VARIOUS LATITUDES
HIGH
LOW
HIGH
HIGH
LOW
H
H
L
LOW
HIGH
1008
1012
1016
1020
1024
500-MILLIBAR HEIGHT CONTOURS AT 7:00 A.M., E.S.T.
LOW
LOW
LOW
HIGH
19500
HIGHEST AND LOWEST TEMPERATURES
PRECIPITATION AREAS AND AMOUNTS

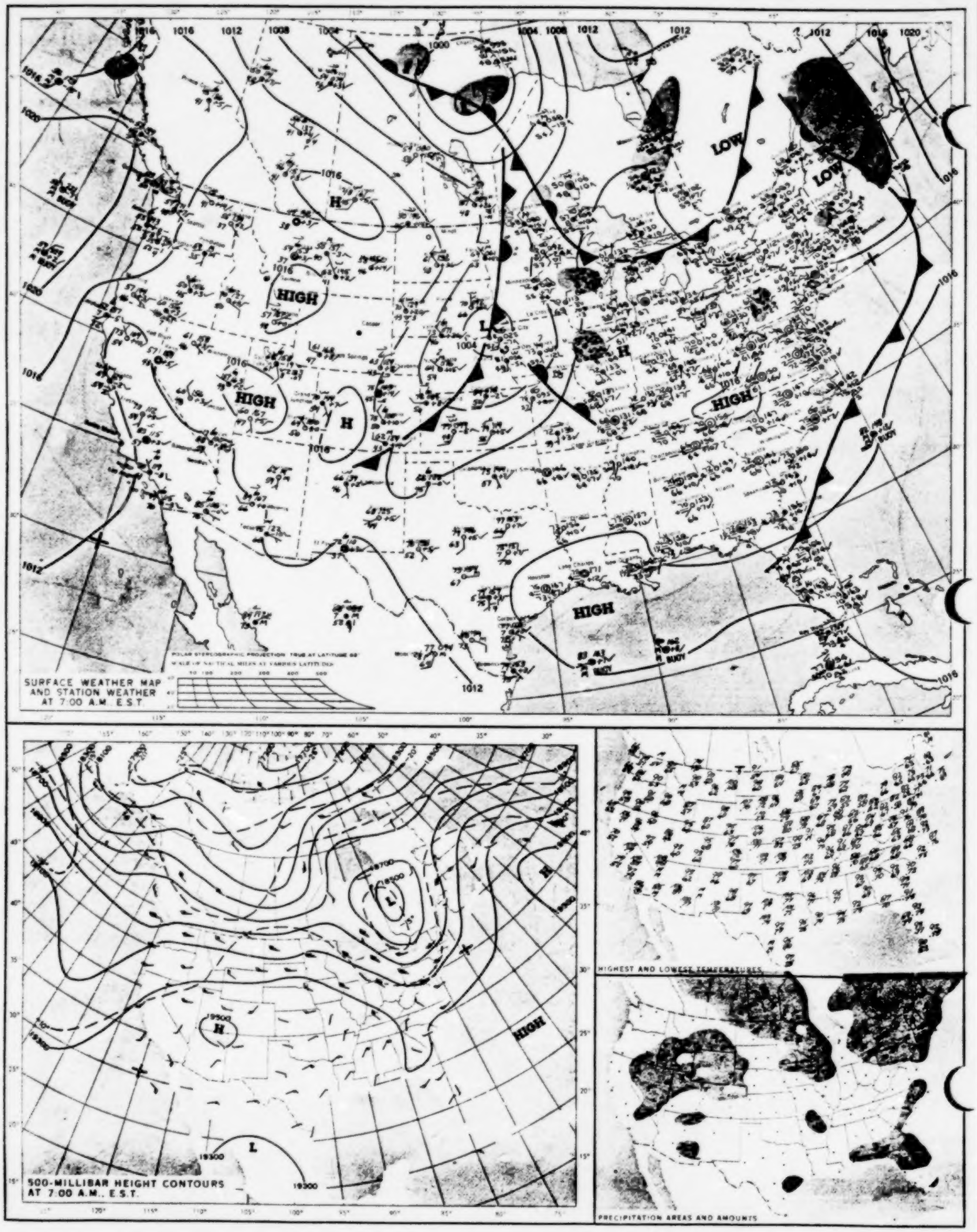
SURFACE WEATHER MAP AND STATION WEATHER AT 7:00 A.M. E.S.T.
HIGH
HIGH
HIGH
HIGH
LOW
LOW
H
H
H
L
1016
1012
1008
1004
1000
1020
POLAR STEREOGRAPHIC PROJECTION TRUE AT LATITUDE 60°
500-MILLIBAR HEIGHT CONTOURS AT 7:00 A.M., E.S.T.
HIGH
H
L
L
19500
19300
HIGHEST AND LOWEST TEMPERATURES
PRECIPITATION AREAS AND AMOUNTS

THURSDAY, JULY 31, 1980

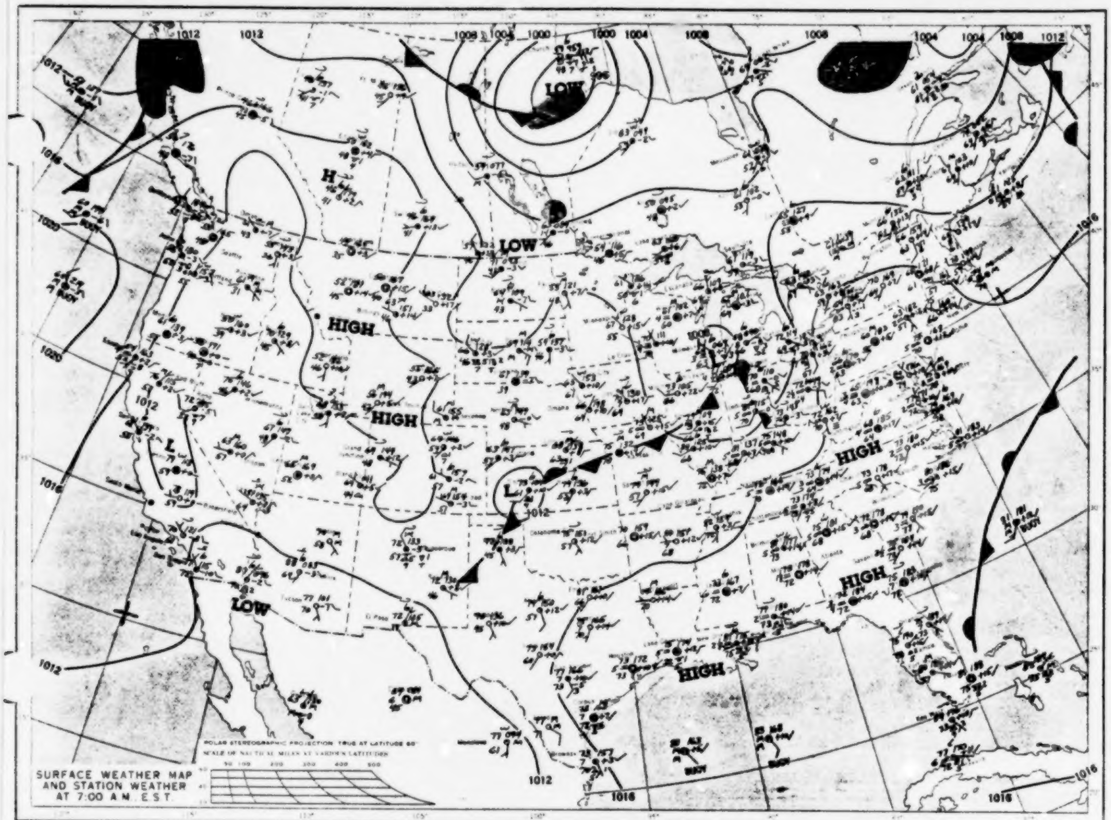
SURFACE WEATHER MAP AND STATION WEATHER AT 7:00 A.M. E.S.T.
1012
1008
1004
1000
1016
1020
LOW
HIGH
H
L
POLAR STEREOGRAPHIC PROJECTION TRUE AT LATITUDE 60°

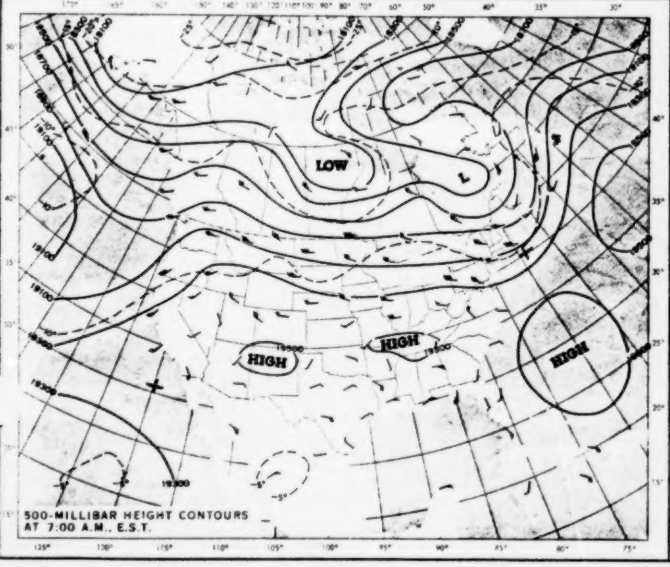
500-MILLIBAR HEIGHT CONTOURS AT 7:00 A.M., E.S.T.
LOW
L
HIGH
19500
19300

HIGHEST AND LOWEST TEMPERATURES

PRECIPITATION AREAS AND AMOUNTS

Appendix B

The county-by-county control strategy emissions inventory expressed as precentage change in hydrocarbon and NO_x emissions from the 1979 base emissions rates. Emissions changes represent 1987 projections based on 1982 SIPs.

Notes:

(1) Unspecified changes in hydrocarbon (HC) or nitrogen oxides (NO) indicate that the default values apply, namely -32% for HC and -8% for NO_x.

(2) Six digit numbers before county names are the NEDS county ID's. The first two of the six digits identify the state as follows:

07	Connecticut
08	Delaware
09	District of Columbia
18	Kentucky
20	Maine
21	Maryland
22	Massachusetts
23	Michigan
30	New Hampshire
31	New Jersey
33	New York
36	Ohio
39	Pennsylvania
41	Rhode Island
47	Vermont
48	Virginia
50	West Virginia

```
@DATA,L NEROS*CNTYEMISFORM.
DATA 9R1Q1 SL74T9 06/24/85 11:05:00 (1)
    1.           070265    FAIRFIELD CO            HC -28.4      NO -12.6
    2.           070425    HARTFORD CO             HC -30.8      NO -18.9
    3.           070478    LITCHFIELD CO           HC -27.7      NO -21.3
    4.           070565    MIDDLESEX CO            HC -28.1      NO -8.7
    5.           070705    NEW HAVEN CO            HC -30.3      NO -13.9
    6.           070725    NEW LONDON CO           HC -28.7      NO -15.5
    7.           071155    TOLLAND CO              HC -30.1      NO -22.7
    8.           071505    WINDHAM CO              HC -23.0      NO -15.0
    9.           080060    KENT CO                 HC            NO
   10.           080180    NEW CASTLE CO           HC -40.2      NO -3.3
   11.           080240    SUSSEX CO               HC            NO
   12.           090020    WASHINGTON              HC -39.7      NO -29.4
   13.           180180    BATH CO                 HC            NO
   14.           180300    BOURBON CO              HC            NO
   15.           180340    BOYD CO                 HC            NO
   16.           180380    BRACKEN CO              HC            NO
   17.           180620    CARTER CO               HC            NO
   18.           180720    CLARK CO                HC -38.1      NO
   19.           181060    ELLIOTT CO              HC            NO
   20.           181200    FLEMING CO              HC            NO
   21.           181540    GREENUP CO              HC            NO
   22.           182140    LAWRENCE CO             HC            NO
   23.           182280    LEWIS CO                HC            NO
   24.           182640    MASON CO                HC            NO
   25.           182720    MENIFEE CO              HC            NO
   26.           182860    MONTGOMERY CO           HC            NO
   27.           182900    MORGAN CO               HC            NO
   28.           183040    NICHOLAS CO             HC            NO
   29.           183520    ROBERTSON CO            HC            NO
   30.           183560    ROWAN CO                HC            NO
   31.           200027    ANDROSCOGGIN CO         HC            NO
   32.           200277    CUMBERLAND CO           HC            NO
   33.           200445    FRANKLIN CO             HC            NO
   34.           200547    KENNEBEC CO             HC            NO
   35.           200595    KNOX CO                 HC            NO
   36.           200645    LINCOLN CO              HC            NO
   37.           200885    OXFORD CO               HC            NO
   38.           200907    PENOBSCOT CO            HC            NO
   39.           201065    SAGADAHOC CO            HC            NO
   40.           201125    SOMERSET CO             HC            NO
   41.           201183    WALDO CO                HC            NO
   42.           201325    YORK CO                 HC            NO
   43.           210040    ALLEGANY CO             HC            NO
   44.           210080    ANNE ARUNDEL CO         HC -44.2      NO 0.5
   45.           210120    BALTIMORE               HC -44.2      NO 0.5
   46.           210140    BALTIMORE CO            HC -44.2      NO 0.5
   47.           210280    CALVERT CO              HC            NO
   48.           210340    CAROLINE CO             HC            NO
   49.           210360    CARROLL CO              HC -44.2      NO 0.5
   50.           210420    CECIL CO                HC            NO
   51.           210440    CHARLES CO              HC            NO
   52.           210600    DORCHESTER CO           HC            NO
   53.           210740    FREDERICK CO            HC            NO
   54.           210800    GARRETT CO              HC            NO
   55.           210920    HARFORD CO              HC -44.2      NO 0.5
```

56.	210960	HOWARD CO	HC	-44.2	NO	0.5
57.	211000	KENT CO	HC		NO	
58.	211160	MONTGOMERY CO	HC	-34.9	NO	-7.5
59.	211300	PRINCE GEORGES CO	HC	-36.6	NO	0.5
60.	211320	QUEEN ANNES CO	HC		NO	
61.	211400	ST MARYS CO	HC		NO	
62.	211500	SOMERSET CO	HC		NO	
63.	211600	TALBOT CO	HC		NO	
64.	211680	WASHINGTON CO	HC		NO	
65.	211740	WICOMICO CO	HC		NO	
66.	211800	WORCESTER CO	HC		NO	
67.	228001	BARNSTABLE	HC	-12.4	NO	6.6
68.	228002	BERKSHIRE	HC	-9.0	NO	4.0
69.	228003	BRISTOL	HC	-12.4	NO	6.6
70.	228004	DUKES	HC	-12.4	NO	6.6
71.	228005	ESSEX	HC	-7.8	NO	8.5
72.	221291	ESSEX	HC	-7.8	NO	8.5
73.	228006	FRANKLIN	HC	-8.7	NO	5.1
74.	228007	HAMPDEN	HC	-8.7	NO	5.1
75.	221798	HAMPDEN	HC	-8.7	NO	5.1
76.	228008	HAMPSHIRE	HC	-8.7	NO	5.1
77.	228009	MIDDLESEX	HC	-7.8	NO	8.5
78.	221274	MIDDLESEX	HC	-7.8	NO	8.5
79.	228010	NANTUCKET	HC	-12.4	NO	6.6
80.	228011	NORFOLK	HC	-7.8	NO	8.5
81.	228012	PLYMOUTH	HC	-12.4	NO	6.6
82.	222121	PLYMOUTH	HC	-12.4	NO	6.6
83.	228013	SUFFOLK	HC	-7.8	NO	8.5
84.	228014	WORCHESTER	HC	-20.0	NO	6.0
85.	220369	WORCHESTER	HC	-20.0	NO	6.0
86.	230060	ALCONA CO	HC		NO	
87.	230220	ALPENA CO	HC		NO	
88.	230280	ARENAC CO	HC		NO	
89.	230400	BAY CO	HC		NO	
90.	231700	GENESEE CO	HC		NO	
91.	232340	HURON CO	HC		NO	
92.	232440	IOSCO CO	HC		NO	
93.	232880	LAPEER CO	HC		NO	
94.	232960	LENAWEE CO	HC		NO	
95.	233020	LIVINGSTON CO	HC		NO	
96.	233140	MACOMB CO	HC	-34.7	NO	-13.9
97.	233600	MONROE CO	HC		NO	
98.	233640	MONTMORENCY CO	HC		NO	
99.	233980	OAKLAND CO	HC	-45.2	NO	-17.1
100.	234040	OGEMAW CO	HC		NO	
101.	234100	OSCODA CO	HC		NO	
102.	234620	ST CLAIR CO	HC	-41.8	NO	61.1
103.	234780	SAGINAW CO	HC		NO	
104.	234800	SANILAC CO	HC		NO	
105.	234860	SHIAWASSEE CO	HC		NO	
106.	235160	TUSCOLA CO	HC		NO	
107.	235280	WASHTENAW CO	HC		NO	
108.	235320	WAYNE CO	HC	-38.3	NO	-5.3
109.	300020	BELKNAP CO	HC		NO	
110.	300060	CARROLL CO	HC		NO	
111.	300080	CHESHIRE CO	HC		NO	
112.	300140	COOS CO	HC		NO	

113.	300240	GRAFTON CO	HC	NO
114.	300300	HILLSBOROUGH CO	HC	NO
115.	300440	MERRIMACK CO	HC	NO
116.	300580	ROCKINGHAM CO	HC	NO
117.	300640	STRAFFORD CO	HC	NO
118.	300660	SULLIVAN CO	HC	NO
119.	310080	ATLANTIC CO	HC -29.5	NO -10.4
120.	310300	BERGEN CO	HC -35.9	NO 18.4
121.	310660	BURLINGTON CO	HC -34.9	NO 9.8
122.	310740	CAMDEN CO	HC -34.5	NO -10.5
123.	310780	CAPE MAY CO	HC -24.8	NO -0.8
124.	311050	CUMBERLAND CO	HC -31.6	NO -2.0
125.	311380	ESSEX CO	HC -34.7	NO -10.9
126.	311760	GLOUCESTER CO	HC -46.8	NO -8.4
127.	312240	HUDSON CO	HC -28.0	NO 22.2
128.	312260	HUNTERDON CO	HC -35.3	NO 4.3
129.	312980	MERCER CO	HC -32.2	NO -3.2
130.	313060	MIDDLESEX CO	HC -39.6	NO 10.9
131.	313180	MONMOUTH CO	HC -37.2	NO -16.1
132.	313260	MORRIS CO	HC -39.7	NO -15.3
133.	313900	OCEAN CO	HC -27.5	NO -7.2
134.	314120	PASSAIC CO	HC -33.5	NO -15.4
135.	314900	SALEM CO	HC -49.2	NO 0.3
136.	315020	SOMERSET CO	HC -33.8	NO -8.1
137.	315300	SUSSEX CO	HC -33.4	NO -8.6
138.	315440	UNION CO	HC -39.1	NO -10.4
139.	315660	WARREN CO	HC -41.0	NO -2.4
140.	330060	ALBANY CO	HC	NO
141.	330120	ALLEGANY CO	HC	NO
142.	330600	BRONX CO	HC -28.9	NO -15.0
143.	330640	BROOME CO	HC	NO
144.	330840	CATTARAUGUS CO	HC	NO
145.	330860	CAYUGA CO	HC	NO
146.	331000	CHAUTAUQUA CO	HC	NO
147.	331060	CHEMUNG CO	HC	NO
148.	331080	CHENANGO CO	HC	NO
149.	331120	CLINTON CO	HC	NO
150.	331220	COLUMBIA CO	HC	NO
151.	331400	CORTLAND CO	HC	NO
152.	331520	DELAWARE CO	HC	NO
153.	331620	DUTCHESS CO	HC	NO
154.	332000	ERIE CO	HC	NO
155.	332020	ESSEX CO	HC	NO
156.	332240	FRANKLIN CO	HC	NO
157.	332340	FULTON CO	HC	NO
158.	332400	GENESEE CO	HC	NO
159.	332660	GREENE CO	HC	NO
160.	332820	HAMILTON CO	HC	NO
161.	332960	HERKIMER CO	HC	NO
162.	333340	JEFFERSON CO	HC	NO
163.	333440	KINGS CO	HC -26.7	NO -1.7
164.	333740	LEWIS CO	HC	NO
165.	333880	LIVINGSTON CO	HC	NO
166.	334040	MADISON CO	HC	NO
167.	334380	MONROE CO	HC	NO
168.	334400	MONTGOMERY CO	HC	NO
169.	334520	NASSAU CO	HC -44.2	NO -20.3

170.	334660	NEW YORK CO	HC -29.4	NO -4.1
171.	334720	NIAGARA CO	HC	NO
172.	335060	ONEIDA CO	HC	NO
173.	335100	ONONDAGA CO	HC	NO
174.	335120	ONTARIO CO	HC	NO
175.	335140	ORANGE CO	HC	NO
176.	335180	ORLEANS CO	HC	NO
177.	335240	OSWEGO CO	HC	NO
178.	335260	OTSEGO CO	HC	NO
179.	335640	PUTNAM CO	HC	NO
180.	335660	QUEENS CO	HC -36.0	NO -12.2
181.	335700	RENSSELAER CO	HC	NO
182.	335720	RICHMOND CO	HC -27.6	NO -1.5
183.	335780	ROCKLAND CO	HC -37.6	NO -7.1
184.	335930	ST. LAWRENCE CO	HC	NO
185.	335965	SARATOGA CO	HC	NO
186.	336040	SCHENECTADY CO	HC	NO
187.	336060	SCHOHARIE CO	HC	NO
188.	336080	SCHUYLER CO	HC	NO
189.	336160	SENECA CO	HC	NO
190.	336500	STEUBEN CO	HC	NO
191.	336580	SUFFOLK CO	HC -37.3	NO -12.1
192.	336600	SULLIVAN CO	HC	NO
193.	336700	TIOGA CO	HC	NO
194.	336720	TOMPKINS CO	HC	NO
195.	336840	ULSTER CO	HC	NO
196.	337040	WARREN CO	HC	NO
197.	337100	WASHINGTON CO	HC	NO
198.	337240	WAYNE CO	HC	NO
199.	337320	WESTCHESTER CO	HC -46.7	NO -15.2
200.	337580	WYOMING CO	HC	NO
201.	337600	YATES CO	HC	NO
202.	360040	ADAMS CO	HC	NO
203.	360080	ALLEN CO	HC	NO
204.	360180	ASHLAND CO	HC	NO
205.	360220	ASHTABULA CO	HC	NO
206.	360260	ATHENS CO	HC	NO
207.	360280	AUGLAIZE CO	HC	NO
208.	360540	BELMONT CO	HC	NO
209.	360820	BROWN CO	HC	NO
210.	361040	CARROLL CO	HC	NO
211.	361140	CHAMPAIGN CO	HC	NO
212.	361260	CLARK CO	HC	NO
213.	361280	CLERMONT CO	HC -24.9	NO -6.7
214.	361340	CLINTON CO	HC	NO
215.	361440	COLUMBIANA CO	HC	NO
216.	361520	COSHOCTON CO	HC	NO
217.	361540	CRAWFORD CO	HC	NO
218.	361600	CUYAHOGA CO	HC -18.9	NO -4.7
219.	361760	DELAWARE CO	HC	NO
220.	362000	ERIE CO	HC	NO
221.	362080	FAIRFIELD CO	HC	NO
222.	362140	FAYETTE CO	HC	NO
223.	362220	FRANKLIN CO	HC	NO
224.	362260	FULTON CO	HC	NO
225.	362320	GALLIA CO	HC	NO
226.	362380	GEAUGA CO	HC	NO

227.	362580	GREENE CO	HC	NO
228.	362680	GUERNSEY CO	HC	NO
229.	362740	HANCOCK CO	HC	NO
230.	362760	HARDIN CO	HC	NO
231.	362800	HARRISON CO	HC	NO
232.	362820	HENRY CO	HC	NO
233.	362860	HIGHLAND CO	HC	NO
234.	362940	HOCKING CO	HC	NO
235.	362960	HOLMES CO	HC	NO
236.	363020	HURON CO	HC	NO
237.	363120	JACKSON CO	HC	NO
238.	363160	JEFFERSON CO	HC	NO
239.	363260	KNOX CO	HC	NO
240.	363280	LAKE CO	HC -8.6	NO -1.9
241.	363380	LAWRENCE CO	HC	NO
242.	363440	LICKING CO	HC	NO
243.	363580	LOGAN CO	HC	NO
244.	363640	LORAIN CO	HC -10.7	NO 2.3
245.	363720	LUCAS CO	HC	NO
246.	363800	MADISON CO	HC	NO
247.	363820	MAHONING CO	HC	NO
248.	363960	MARION CO	HC	NO
249.	364160	MEDINA CO	HC -19.6	NO -0.1
250.	364180	MEIGS CO	HC	NO
251.	364460	MONROE CO	HC	NO
252.	364540	MORGAN CO	HC	NO
253.	364560	MORROW CO	HC	NO
254.	364640	MUSKINGUM CO	HC	NO
255.	364900	NOBLE CO	HC	NO
256.	365260	OTTAWA CO	HC	NO
257.	365440	PERRY CO	HC	NO
258.	365480	PICKAWAY CO	HC	NO
259.	365500	PIKE CO	HC	NO
260.	365580	PORTAGE CO	HC	NO
261.	365660	PUTNAM CO	HC	NO
262.	365740	RICHLAND CO	HC	NO
263.	365840	ROSS CO	HC	NO
264.	365980	SANDUSKY CO	HC	NO
265.	366020	SCIOTO CO	HC	NO
266.	366060	SENECA CO	HC	NO
267.	366220	SHELBY CO	HC	NO
268.	366400	STARK CO	HC	NO
269.	366500	SUMMIT CO	HC	NO
270.	366700	TRUMBULL CO	HC	NO
271.	366720	TUSCARAWAS CO	HC	NO
272.	366780	UNION CO	HC	NO
273.	366960	VINTON CO	HC	NO
274.	367040	WARREN CO	HC -35.0	NO -4.0
275.	367100	WASHINGTON CO	HC	NO
276.	367160	WAYNE CO	HC	NO
277.	367580	WOOD CO	HC	NO
278.	367680	WYANDOT CO	HC	NO
279.	390040	ADAMS CO	HC	NO
280.	390100	ALLEGHENY CO	HC -39.3	NO -6.4
281.	390260	ARMSTRONG CO	HC -39.3	NO -6.4
282.	390560	BEAVER CO	HC	NO
283.	390620	BEDFORD CO	HC	NO

284.	390720	BERKS CO	HC		NO	
285.	390820	BLAIR CO	HC		NO	
286.	391000	BRADFORD CO	HC		NO	
287.	391200	BUCKS CO	HC	-38.5	NO	-10.7
288.	391260	BUTLER CO	HC	-39.3	NO	-6.4
289.	391300	CAMBRIA CO	HC		NO	
290.	391320	CAMERON CO	HC		NO	
291.	391380	CARBON CO	HC		NO	
292.	391520	CENTRE CO	HC		NO	
293.	391660	CHESTER CO	HC	-38.5	NO	-10.7
294.	391760	CLARION CO	HC		NO	
295.	391820	CLEARFIELD CO	HC		NO	
296.	391860	CLINTON CO	HC		NO	
297.	391960	COLUMBIA CO	HC		NO	
298.	392140	CRAWFORD CO	HC		NO	
299.	392180	CUMBERLAND CO	HC		NO	
300.	392340	DAUPHIN CO	HC		NO	
301.	392360	DELAWARE CO	HC	-38.5	NO	-10.7
302.	392940	ELK CO	HC		NO	
303.	393080	ERIE CO	HC		NO	
304.	393220	FAYETTE CO	HC		NO	
305.	393320	FOREST CO	HC		NO	
306.	393480	FRANKLIN CO	HC		NO	
307.	393540	FULTON CO	HC		NO	
308.	393720	GREENE CO	HC		NO	
309.	394200	HUNTINGDON CO	HC		NO	
310.	394240	INDIANA CO	HC		NO	
311.	394340	JEFFERSON CO	HC		NO	
312.	394480	JUNIATA CO	HC		NO	
313.	394640	LACKAWANNA CO	HC		NO	
314.	394700	LANCASTER CO	HC		NO	
315.	394840	LAWRENCE CO	HC		NO	
316.	394900	LEBANON CO	HC		NO	
317.	394940	LEHIGH CO	HC	-36.1	NO	-2.4
318.	395220	LUZERNE CO	HC		NO	
319.	395240	LYCOMING CO	HC		NO	
320.	395360	MC KEAN CO	HC		NO	
321.	395660	MERCER CO	HC		NO	
322.	395760	MIFFLIN CO	HC		NO	
323.	395960	MONROE CO	HC		NO	
324.	396000	MONTGOMERY CO	HC	-38.5	NO	-10.7
325.	396020	MONTOUR CO	HC		NO	
326.	396580	NORTHAMPTON CO	HC	-36.1	NO	-2.4
327.	396700	NORTHUMBERLAND CO	HC		NO	
328.	397120	PERRY CO	HC		NO	
329.	397160	PHILADELPHIA CO	HC	-38.5	NO	-10.7
330.	397220	PIKE CO	HC		NO	
331.	397460	POTTER CO	HC		NO	
332.	397960	SCHUYLKILL CO	HC		NO	
333.	398320	SNYDER CO	HC		NO	
334.	398360	SOMERSET CO	HC		NO	
335.	398740	SULLIVAN CO	HC		NO	
336.	398800	SUSQUEHANNA CO	HC		NO	
337.	399000	TIOGA CO	HC		NO	
338.	399070	UNION CO	HC		NO	
339.	399140	VENANGO CO	HC		NO	
340.	399180	WARREN CO	HC		NO	

341.	399200	WASHINGTON CO	HC -39.3	NO -6.4
342.	399220	WAYNE CO	HC	NO
343.	399330	WESTMORELAND CO	HC -39.3	NO -6.4
344.	399530	WYOMING CO	HC	NO
345.	399570	YORK CO	HC	NO
346.	410060	BRISTOL CO	HC -3.9	NO -17.4
347.	410140	KENT CO	HC -3.9	NO -17.4
348.	410200	NEWPORT CO	HC -3.9	NO -17.4
349.	410320	PROVIDENCE CO	HC -3.9	NO -17.4
350.	410380	WASHINGTON CO	HC -3.9	NO -17.4
351.	470020	ADDISON CO	HC	NO
352.	470100	BENNINGTON CO	HC	NO
353.	470160	CALEDONIA CO	HC	NO
354.	470180	CHITTENDEN CO	HC	NO
355.	470200	ESSEX CO	HC	NO
356.	470240	FRANKLIN CO	HC	NO
357.	470260	GRAND ISLE CO	HC	NO
358.	470280	LAMOILLE CO	HC	NO
359.	470360	ORANGE CO	HC	NO
360.	470380	ORLEANS CO	HC	NO
361.	470420	RUTLAND CO	HC	NO
362.	470500	WASHINGTON CO	HC	NO
363.	470580	WINDHAM CO	HC	NO
364.	470620	WINDSOR CO	HC	NO
365.	480040	ACCOMACK CO	HC	NO
366.	480060	ALBEMARLE CO	HC	NO
367.	480200	ARLINGTON CO	HC -42.4	NO -30.0
368.	480260	AUGUSTA CO	HC	NO
369.	480300	BATH CO	HC	NO
370.	480600	CAROLINE CO	HC	NO
371.	480760	CLARKE CO	HC	NO
372.	480880	CULPEPER CO	HC	NO
373.	481000	ESSEX CO	HC	NO
374.	481060	FAIRFAX CO	HC -30.9	NO -9.0
375.	480080	FAIRFAX CO	HC -30.9	NO -9.0
376.	481120	FAUQUIER CO	HC	NO
377.	481220	FREDERICK CO	HC	NO
378.	481380	GREENE CO	HC	NO
379.	481460	HANOVER CO	HC	NO
380.	481540	HIGHLAND CO	HC	NO
381.	481640	KING GEORGE CO	HC	NO
382.	481760	LOUDOUN CO	HC -10.5	NO 10.2
383.	481780	LOUISA CO	HC	NO
384.	481860	MADISON CO	HC	NO
385.	482080	NELSON CO	HC	NO
386.	482200	NORTHUMBERLAND CO	HC	NO
387.	482300	ORANGE CO	HC	NO
388.	482320	PAGE CO	HC	NO
389.	482520	PRINCE WILLIAM CO	HC -33.5	NO -5.9
390.	482620	RAPPAHANNOCK CO	HC	NO
391.	482680	RICHMOND CO	HC	NO
392.	482740	ROCKBRIDGE CO	HC	NO
393.	482760	ROCKINGHAM CO	HC	NO
394.	482880	SHENANDOAH CO	HC	NO
395.	483000	SPOTSYLVANIA CO	HC	NO
396.	483040	STAFFORD CO	HC	NO
397.	483260	WARREN CO	HC	NO

```
   398.          483340   WESTMORELAND CO         HC            NO
   399.          500020   BARBOUR CO              HC            NO
   400.          500100   BERKELEY CO             HC            NO
   401.          500140   BOONE CO                HC            NO
   402.          500160   BRAXTON CO              HC            NO
   403.          500200   BROOKE CO               HC            NO
   404.          500240   CABELL CO               HC            NO
   405.          500260   CALHOUN CO              HC            NO
   406.          500380   CLAY CO                 HC            NO
   407.          500400   DODDRIDGE CO            HC            NO
   408.          500460   FAYETTE CO              HC            NO
   409.          500520   GILMER CO               HC            NO
   410.          500560   GRANT CO                HC            NO
   411.          500580   GREENBRIER CO           HC            NO
   412.          500600   HAMPSHIRE CO            HC            NO
   413.          500620   HANCOCK CO              HC            NO
   414.          500640   HARDY CO                HC            NO
   415.          500660   HARRISON CO             HC            NO
   416.          500720   JACKSON CO              HC            NO
   417.          500740   JEFFERSON CO            HC            NO
   418.          500760   KANAWHA CO              HC            NO
   419.          500840   LEWIS CO                HC            NO
   420.          500860   LINCOLN CO              HC            NO
   421.          500900   LOGAN CO                HC            NO
   422.          500980   MARION CO               HC            NO
   423.          501020   MARSHALL CO             HC            NO
   424.          501060   MASON CO                HC            NO
   425.          501100   MINERAL CO              HC            NO
   426.          501140   MONONGALIA CO           HC            NO
   427.          501200   MORGAN CO               HC            NO
   428.          501320   NICHOLAS CO             HC            NO
   429.          501380   OHIO CO                 HC            NO
   430.          501440   PENDLETON CO            HC            NO
   431.          501460   PLEASANTS CO            HC            NO
   432.          501480   POCAHONTAS CO           HC            NO
   433.          501520   PRESTON CO              HC            NO
   434.          501560   PUTNAM CO               HC            NO
   435.          501600   RANDOLPH CO             HC            NO
   436.          501680   RITCHIE CO              HC            NO
   437.          501700   ROANE CO                HC            NO
   438.          501840   TAYLOR CO               HC            NO
   439.          501860   TUCKER CO               HC            NO
   440.          501880   TYLER CO                HC            NO
   441.          501900   UPSHUR CO               HC            NO
   442.          501960   WAYNE CO                HC            NO
   443.          501980   WEBSTER CO              HC            NO
   444.          502100   WETZEL CO               HC            NO
   445.          502200   WIRT CO                 HC            NO
   446.          502220   WOOD CO                 HC            NO
END DATA. ERRORS: NONE. TIME:  2.101 SEC. IMAGE COUNT: 446
```

APPENDIX C

Lists of counties in each of the four receptor county classes

Major Source Counties

STATENM	COUNTYNM
CONNECTICUT	FAIRFIELD
CONNECTICUT	HARTFORD
CONNECTICUT	NEW HAVEN
DELAWARE	NEW CASTLE
DIST. COLUMBIA	DISTRICT OF COLUMBIA
MARYLAND	ANNE ARUNDEL
MARYLAND	BALTIMORE CITY
MARYLAND	BALTIMORE
MARYLAND	PRINCE GEORGES
MASSACHUSETTS	DUKES
MASSACHUSETTS	MIDDLESEX
MASSACHUSETTS	NORFOLK
MASSACHUSETTS	SUFFOLK
MICHIGAN	BAY
MICHIGAN	GENESEE
MICHIGAN	MACOMB
MICHIGAN	MONROE
MICHIGAN	OAKLAND
MICHIGAN	WAYNE
NEW JERSEY	BERGEN
NEW JERSEY	CAMDEN
NEW JERSEY	ESSEX
NEW JERSEY	GLOUCESTER
NEW JERSEY	HUDSON
NEW JERSEY	MERCER
NEW JERSEY	MIDDLESEX
NEW JERSEY	MORRIS
NEW JERSEY	PASSAIC
NEW JERSEY	UNION
NEW YORK	ALBANY
NEW YORK	BRONX
NEW YORK	KINGS
NEW YORK	NASSAU
NEW YORK	NEW YORK
NEW YORK	QUEENS
NEW YORK	RICHMOND
NEW YORK	ROCKLAND
NEW YORK	WESTCHESTER

STATENM	COUNTYNM
OHIO	ADAMS
OHIO	CUYAHOGA
OHIO	FRANKLIN
OHIO	GALLIA
OHIO	JEFFERSON
OHIO	LAKE
OHIO	LORAIN
OHIO	LUCAS
OHIO	SUMMIT
OHIO	WASHINGTON
PENNSYLVANIA	ALLEGHENY
PENNSYLVANIA	ARMSTRONG
PENNSYLVANIA	BEAVER
PENNSYLVANIA	BUCKS
PENNSYLVANIA	DELAWARE
PENNSYLVANIA	INDIANA
PENNSYLVANIA	MONTGOMERY
PENNSYLVANIA	MONTOUR
PENNSYLVANIA	NORTHAMPTON
PENNSYLVANIA	PHILADELPHIA
PENNSYLVANIA	VENANGO
RHODE ISLAND	BRISTOL
RHODE ISLAND	KENT
RHODE ISLAND	PROVIDENCE
VIRGINIA	ARLINGTON
VIRGINIA	FAIRFAX
WEST VIRGINIA	HANCOCK
WEST VIRGINIA	HARRISON
WEST VIRGINIA	MARSHALL
WEST VIRGINIA	MASON
WEST VIRGINIA	MONONGALIA
WEST VIRGINIA	PUTNAM

Non-Major Source SMSA Counties
(Suburban Counties)

STATENM	COUNTYNM
CONNECTICUT	MIDDLESEX
CONNECTICUT	NEW LONDON
CONNECTICUT	TOLLAND
KENTUCKY	BOYD
KENTUCKY	GREENUP
MAINE	ANDROSCOGGIN
MAINE	CUMBERLAND
MAINE	PENOBSCOT
MAINE	SAGADAHOC
MAINE	YORK
MARYLAND	ALLEGANY
MARYLAND	CARROLL
MARYLAND	CECIL
MARYLAND	CHARLES
MARYLAND	HARFORD
MARYLAND	MONTGOMERY
MARYLAND	WASHINGTON
MASSACHUSETTS	BERKSHIRE
MASSACHUSETTS	BRISTOL
MASSACHUSETTS	ESSEX
MASSACHUSETTS	HAMPDEN
MASSACHUSETTS	HAMPSHIRE
MASSACHUSETTS	PLYMOUTH
MASSACHUSETTS	WORCESTER
MICHIGAN	LAPEER
MICHIGAN	LIVINGSTON
MICHIGAN	SAGINAW
MICHIGAN	ST CLAIR
MICHIGAN	SHIAWASSEE
MICHIGAN	WASHTENAW
NEW HAMPSHIRE	HILLSBOROUGH
NEW HAMPSHIRE	ROCKINGHAM
NEW HAMPSHIRE	STRAFFORD
NEW JERSEY	ATLANTIC
NEW JERSEY	BURLINGTON
NEW JERSEY	CUMBERLAND
NEW JERSEY	MONMOUTH
NEW JERSEY	SALEM
NEW JERSEY	SOMERSET
NEW JERSEY	WARREN
NEW YORK	BROOME
NEW YORK	CHEMUNG
NEW YORK	DUTCHESS
NEW YORK	ERIE
NEW YORK	HERKIMER
NEW YORK	LIVINGSTON
NEW YORK	MADISON
NEW YORK	MONROE
NEW YORK	MONTGOMERY
NEW YORK	NIAGARA
NEW YORK	ONEIDA
NEW YORK	ONONDAGA
NEW YORK	ONTARIO
NEW YORK	ORANGE
NEW YORK	ORLEANS
NEW YORK	OSWEGO
NEW YORK	PUTNAM
NEW YORK	RENSSELAER
NEW YORK	SARATOGA
NEW YORK	SCHENECTADY
NEW YORK	SUFFOLK
NEW YORK	TIOGA
NEW YORK	WARREN
NEW YORK	WASHINGTON
NEW YORK	WAYNE
OHIO	ALLEN
OHIO	AUGLAIZE
OHIO	BELMONT
OHIO	CARROLL
OHIO	CHAMPAIGN
OHIO	CLARK
OHIO	CLERMONT
OHIO	DELAWARE
OHIO	FAIRFIELD
OHIO	FULTON
OHIO	GEAUGA
OHIO	GREENE
OHIO	LAWRENCE
OHIO	LICKING
OHIO	MADISON
OHIO	MAHONING
OHIO	MEDINA
OHIO	OTTAWA
OHIO	PICKAWAY
OHIO	PORTAGE
OHIO	PUTNAM
OHIO	RICHLAND
OHIO	STARK
OHIO	TRUMBULL
OHIO	WARREN
OHIO	WOOD
PENNSYLVANIA	ADAMS
PENNSYLVANIA	BERKS
PENNSYLVANIA	CAMBRIA
PENNSYLVANIA	CARBON
PENNSYLVANIA	CENTRE
PENNSYLVANIA	CHESTER
PENNSYLVANIA	CUMBERLAND
PENNSYLVANIA	DAUPHIN
PENNSYLVANIA	ERIE
PENNSYLVANIA	LACKAWANNA
PENNSYLVANIA	LANCASTER
PENNSYLVANIA	LEHIGH
PENNSYLVANIA	LUZERNE
PENNSYLVANIA	LYCOMING
PENNSYLVANIA	MONROE
PENNSYLVANIA	PERRY
PENNSYLVANIA	SOMERSET
PENNSYLVANIA	SUSQUEHANNA
PENNSYLVANIA	WASHINGTON
PENNSYLVANIA	WESTMORELAND
PENNSYLVANIA	YORK
RHODE ISLAND	WASHINGTON
VERMONT	CHITTENDEN
VIRGINIA	ALBEMARLE
VIRGINIA	GREENE
VIRGINIA	HANOVER
VIRGINIA	LOUDOUN
VIRGINIA	PRINCE WILLIAM
VIRGINIA	RICHMOND
WEST VIRGINIA	BROOKE
WEST VIRGINIA	CABELL
WEST VIRGINIA	KANAWHA
WEST VIRGINIA	MINERAL
WEST VIRGINIA	OHIO
WEST VIRGINIA	WAYNE
WEST VIRGINIA	WIRT
WEST VIRGINIA	WOOD

Agricultural Counties

STATENM	COUNTYNM
DELAWARE	KENT
KENTUCKY	BATH
KENTUCKY	BOURBON
KENTUCKY	BRACKEN
KENTUCKY	FLEMING
KENTUCKY	MASON
KENTUCKY	MONTGOMERY
KENTUCKY	NICHOLAS
KENTUCKY	ROBERTSON
MARYLAND	CAROLINE
MARYLAND	FREDERICK
MARYLAND	HOWARD
MARYLAND	KENT
MARYLAND	QUEEN ANNES
MARYLAND	TALBOT
MASSACHUSETTS	NANTUCKET
MICHIGAN	HURON
MICHIGAN	LENAWEE
MICHIGAN	SANILAC
MICHIGAN	TUSCOLA
NEW JERSEY	HUNTERDON
NEW YORK	CAYUGA
NEW YORK	GENESEE
NEW YORK	JEFFERSON
NEW YORK	SCHUYLER
NEW YORK	SENECA
NEW YORK	STEUBEN
NEW YORK	TOMPKINS
NEW YORK	WYOMING
NEW YORK	YATES
OHIO	ASHLAND
OHIO	ASHTABULA
OHIO	BROWN
OHIO	CLINTON
OHIO	COLUMBIANA
OHIO	COSHOCTON
OHIO	CRAWFORD
OHIO	ERIE
OHIO	FAYETTE
OHIO	GUERNSEY
OHIO	HANCOCK
OHIO	HARDIN
OHIO	HARRISON
OHIO	HENRY
OHIO	HIGHLAND
OHIO	HOLMES
OHIO	HURON
OHIO	KNOX
OHIO	LOGAN
OHIO	MARION
OHIO	MORGAN
OHIO	MORROW
OHIO	MUSKINGUM
OHIO	NOBLE
OHIO	SANDUSKY
OHIO	SENECA
OHIO	SHELBY
OHIO	TUSCARAWAS
OHIO	UNION
OHIO	WAYNE
OHIO	WYANDOT
PENNSYLVANIA	BRADFORD
PENNSYLVANIA	COLUMBIA
PENNSYLVANIA	CRAWFORD
PENNSYLVANIA	FRANKLIN
PENNSYLVANIA	GREENE
PENNSYLVANIA	LAWRENCE
PENNSYLVANIA	LEBANON
PENNSYLVANIA	MERCER
PENNSYLVANIA	NORTHUMBERLAND
VIRGINIA	CLARKE
WEST VIRGINIA	BARBOUR
WEST VIRGINIA	JEFFERSON
WEST VIRGINIA	MARION
WEST VIRGINIA	TAYLOR

Natural Counties

STATENM	COUNTYNM
CONNECTICUT	LITCHFIELD
CONNECTICUT	WINDHAM
DELAWARE	SUSSEX
KENTUCKY	CARTER
KENTUCKY	ELLIOTT
KENTUCKY	LAWRENCE
KENTUCKY	LEWIS
KENTUCKY	MENIFEE
KENTUCKY	MORGAN
KENTUCKY	ROWAN
MAINE	FRANKLIN
MAINE	KENNEBEC
MAINE	KNOX
MAINE	LINCOLN
MAINE	OXFORD
MAINE	SOMERSET
MAINE	WALDO
MARYLAND	CALVERT
MARYLAND	DORCHESTER
MARYLAND	GARRETT
MARYLAND	ST MARYS
MARYLAND	SOMERSET
MARYLAND	WICOMICO
MARYLAND	WORCESTER
MASSACHUSETTS	BARNSTABLE
MASSACHUSETTS	FRANKLIN
MICHIGAN	ALCONA
MICHIGAN	ALPENA
MICHIGAN	ARENAC
MICHIGAN	IOSCO
MICHIGAN	MONTMORENCY
MICHIGAN	OGEMAW
MICHIGAN	OSCODA
NEW HAMPSHIRE	BELKNAP
NEW HAMPSHIRE	CARROLL
NEW HAMPSHIRE	CHESHIRE
NEW HAMPSHIRE	COOS
NEW HAMPSHIRE	GRAFTON
NEW HAMPSHIRE	MERRIMACK
NEW HAMPSHIRE	SULLIVAN
NEW JERSEY	CAPE MAY
NEW JERSEY	OCEAN
NEW JERSEY	SUSSEX
NEW YORK	ALLEGANY
NEW YORK	CATTARAUGUS
NEW YORK	CHAUTAUQUA
NEW YORK	CHENANGO
NEW YORK	CLINTON
NEW YORK	COLUMBIA
NEW YORK	CORTLAND
NEW YORK	DELAWARE
NEW YORK	ESSEX
NEW YORK	FRANKLIN
NEW YORK	FULTON
NEW YORK	GREENE
NEW YORK	HAMILTON
NEW YORK	LEWIS
NEW YORK	OTSEGO
NEW YORK	ST LAWRENCE
NEW YORK	SCHOHARIE
NEW YORK	SULLIVAN
NEW YORK	ULSTER
OHIO	ATHENS
OHIO	HOCKING
OHIO	JACKSON
OHIO	MEIGS
OHIO	MONROE
OHIO	PERRY
OHIO	PIKE
OHIO	ROSS
OHIO	SCIOTO
OHIO	VINTON
PENNSYLVANIA	BEDFORD
PENNSYLVANIA	BLAIR
PENNSYLVANIA	BUTLER
PENNSYLVANIA	CAMERON
PENNSYLVANIA	CLARION
PENNSYLVANIA	CLEARFIELD
PENNSYLVANIA	CLINTON

Natural Counties, continued

STATENM	COUNTYNM
PENNSYLVANIA	ELK
PENNSYLVANIA	FAYETTE
PENNSYLVANIA	FOREST
PENNSYLVANIA	FULTON
PENNSYLVANIA	HUNTINGDON
PENNSYLVANIA	JEFFERSON
PENNSYLVANIA	JUNIATA
PENNSYLVANIA	MC KEAN
PENNSYLVANIA	MIFFLIN
PENNSYLVANIA	PIKE
PENNSYLVANIA	POTTER
PENNSYLVANIA	SCHUYLKILL
PENNSYLVANIA	SNYDER
PENNSYLVANIA	SULLIVAN
PENNSYLVANIA	TIOGA
PENNSYLVANIA	UNION
PENNSYLVANIA	WARREN
PENNSYLVANIA	WAYNE
PENNSYLVANIA	WYOMING
RHODE ISLAND	NEWPORT
VERMONT	ADDISON
VERMONT	BENNINGTON
VERMONT	CALEDONIA
VERMONT	ESSEX
VERMONT	FRANKLIN
VERMONT	GRAND ISLE
VERMONT	LAMOILLE
VERMONT	ORANGE
VERMONT	ORLEANS
VERMONT	RUTLAND
VERMONT	WASHINGTON
VERMONT	WINDHAM
VERMONT	WINDSOR
VIRGINIA	ACCOMACK
VIRGINIA	AUGUSTA
VIRGINIA	BATH
VIRGINIA	CAROLINE
VIRGINIA	CULPEPER
VIRGINIA	ESSEX
VIRGINIA	FAUQUIER
VIRGINIA	FREDERICK
VIRGINIA	HIGHLAND
VIRGINIA	KING GEORGE
VIRGINIA	LOUISA
VIRGINIA	MADISON
VIRGINIA	NELSON
VIRGINIA	NORTHUMBERLAND
VIRGINIA	ORANGE
VIRGINIA	PAGE
VIRGINIA	RAPPAHANNOCK
VIRGINIA	ROCKBRIDGE
VIRGINIA	ROCKINGHAM
VIRGINIA	SHENANDOAH
VIRGINIA	SPOTSYLVANIA
VIRGINIA	STAFFORD
VIRGINIA	WARREN
VIRGINIA	WESTMORELAND
WEST VIRGINIA	BERKELEY
WEST VIRGINIA	BOONE
WEST VIRGINIA	BRAXTON
WEST VIRGINIA	CALHOUN
WEST VIRGINIA	CLAY
WEST VIRGINIA	DODDRIDGE
WEST VIRGINIA	FAYETTE
WEST VIRGINIA	GILMER
WEST VIRGINIA	GRANT
WEST VIRGINIA	GREENBRIER
WEST VIRGINIA	HAMPSHIRE
WEST VIRGINIA	HARDY
WEST VIRGINIA	JACKSON
WEST VIRGINIA	LEWIS
WEST VIRGINIA	LINCOLN
WEST VIRGINIA	LOGAN
WEST VIRGINIA	MORGAN
WEST VIRGINIA	NICHOLAS
WEST VIRGINIA	PENDLETON
WEST VIRGINIA	PLEASANTS
WEST VIRGINIA	POCAHONTAS
WEST VIRGINIA	PRESTON
WEST VIRGINIA	RANDOLPH
WEST VIRGINIA	RITCHIE
WEST VIRGINIA	ROANE
WEST VIRGINIA	TUCKER
WEST VIRGINIA	TYLER
WEST VIRGINIA	UPSHUR
WEST VIRGINIA	WEBSTER
WEST VIRGINIA	WETZEL

Appendix D

County-by-county comparisons of base case vs. control case ozone concentrations. Mean and standard deviation values are for the 9-day scenario period. All concentrations are in ppm.

		BASE CASE				CONTROL CASE			
COUNTYNM	STATENM	MEAN7HR	STD7HR	MEANMAX	STDMAX	MEAN7HR	STD7HR	MEANMAX	STDMAX
FAIRFIELD	CONNECTICUT	.065	.030	.076	.033	.048	.017	.057	.020
HARTFORD	CONNECTICUT	.083	.036	.095	.042	.067	.025	.073	.027
LITCHFIELD	CONNECTICUT	.074	.043	.085	.051	.059	.025	.065	.027
MIDDLESEX	CONNECTICUT	.087	.030	.111	.047	.066	.023	.079	.027
NEW HAVEN	CONNECTICUT	.080	.030	.096	.040	.059	.019	.069	.022
NEW LONDON	CONNECTICUT	.093	.029	.110	.041	.071	.023	.081	.027
TOLLAND	CONNECTICUT	.087	.033	.099	.039	.070	.025	.078	.027
WINDHAM	CONNECTICUT	.088	.031	.102	.034	.071	.024	.082	.026
KENT	DELAWARE	.048	.018	.063	.024	.034	.008	.041	.008
NEW CASTLE	DELAWARE	.041	.017	.054	.021	.030	.009	.035	.011
SUSSEX	DELAWARE	.046	.017	.059	.023	.036	.008	.043	.009
DISTRICT OF COLUMBIA	DIST. COLUMBIA	.028	.006	.037	.008	.025	.006	.033	.008
BATH	KENTUCKY	.045	.009	.046	.009	.045	.009	.046	.009
BOURBON	KENTUCKY	.045	.009	.047	.009	.045	.009	.047	.009
BOYD	KENTUCKY	.035	.010	.038	.010	.035	.010	.038	.010
BRACKEN	KENTUCKY	.045	.010	.048	.009	.045	.010	.048	.009
CARTER	KENTUCKY	.038	.010	.043	.011	.038	.010	.043	.011
ELLIOTT	KENTUCKY	.043	.011	.046	.010	.043	.011	.046	.010
FLEMING	KENTUCKY	.043	.011	.046	.009	.043	.010	.046	.009
GREENUP	KENTUCKY	.037	.007	.042	.008	.036	.008	.042	.009
LAWRENCE	KENTUCKY	.041	.013	.044	.011	.041	.013	.044	.011
LEWIS	KENTUCKY	.036	.008	.042	.008	.036	.008	.042	.009
MASON	KENTUCKY	.042	.009	.045	.008	.042	.009	.046	.008
MENIFEE	KENTUCKY	.045	.010	.047	.009	.045	.010	.047	.009
MONTGOMERY	KENTUCKY	.045	.009	.047	.009	.045	.009	.047	.009
MORGAN	KENTUCKY	.044	.010	.047	.010	.044	.010	.047	.010
NICHOLAS	KENTUCKY	.045	.009	.047	.009	.045	.009	.047	.009
ROBERTSON	KENTUCKY	.045	.010	.048	.008	.045	.009	.048	.008
ROWAN	KENTUCKY	.043	.010	.046	.010	.043	.010	.046	.010
ANDROSCOGGIN	MAINE	.060	.029	.071	.036	.056	.025	.067	.031
CUMBERLAND	MAINE	.064	.033	.072	.037	.060	.029	.067	.032
FRANKLIN	MAINE	.062	.028	.069	.032	.059	.024	.065	.028
KENNEBEC	MAINE	.053	.024	.066	.033	.051	.021	.063	.029
KNOX	MAINE	.046	.015	.061	.028	.045	.014	.059	.025
LINCOLN	MAINE	.050	.023	.066	.032	.048	.020	.062	.029
OXFORD	MAINE	.067	.031	.075	.035	.063	.027	.071	.031
PENOBSCOT	MAINE	.049	.011	.062	.023	.048	.011	.060	.020
SAGADAHOC	MAINE	.054	.023	.067	.035	.052	.020	.063	.030
SOMERSET	MAINE	.055	.022	.066	.030	.054	.020	.063	.026
WALDO	MAINE	.048	.016	.063	.028	.047	.014	.060	.025
YORK	MAINE	.074	.037	.081	.040	.068	.032	.073	.034
ALLEGANY	MARYLAND	.026	.008	.029	.008	.024	.007	.027	.008
ANNE ARUNDEL	MARYLAND	.033	.008	.040	.011	.027	.006	.033	.009
BALTIMORE CITY	MARYLAND	.029	.007	.034	.009	.023	.007	.027	.008
BALTIMORE	MARYLAND	.031	.009	.035	.009	.025	.007	.028	.007
CALVERT	MARYLAND	.035	.008	.040	.010	.030	.007	.038	.010
CAROLINE	MARYLAND	.044	.013	.054	.014	.034	.006	.040	.007
CARROLL	MARYLAND	.028	.009	.034	.009	.024	.007	.028	.007
CECIL	MARYLAND	.035	.011	.048	.014	.028	.009	.032	.009
CHARLES	MARYLAND	.038	.008	.044	.012	.034	.007	.040	.010
DORCHESTER	MARYLAND	.040	.009	.051	.016	.034	.007	.040	.009
FREDERICK	MARYLAND	.026	.008	.032	.009	.023	.007	.028	.008
GARRETT	MARYLAND	.022	.006	.025	.007	.021	.005	.023	.006
HARFORD	MARYLAND	.032	.010	.038	.011	.026	.009	.029	.009

		BASE CASE				CONTROL CASE			
COUNTYNM	STATENM	MEAN7HR	STD7HR	MEANMAX	STDMAX	MEAN7HR	STD7HR	MEANMAX	STDMAX
HOWARD	MARYLAND	.028	.008	.034	.009	.025	.006	.030	.008
KENT	MARYLAND	.042	.015	.055	.022	.030	.008	.035	.008
MONTGOMERY	MARYLAND	.027	.006	.034	.007	.024	.006	.031	.007
PRINCE GEORGES	MARYLAND	.031	.007	.037	.008	.027	.006	.033	.008
QUEEN ANNES	MARYLAND	.042	.013	.054	.017	.031	.007	.037	.007
ST MARYS	MARYLAND	.039	.009	.043	.011	.035	.008	.041	.011
SOMERSET	MARYLAND	.044	.010	.048	.013	.040	.009	.044	.009
TALBOT	MARYLAND	.041	.009	.052	.013	.033	.006	.041	.009
WASHINGTON	MARYLAND	.026	.008	.032	.011	.023	.006	.028	.008
WICOMICO	MARYLAND	.042	.011	.050	.016	.036	.007	.040	.008
WORCESTER	MARYLAND	.045	.012	.051	.015	.040	.008	.043	.008
BARNSTABLE	MASSACHUSETTS	.083	.040	.097	.042	.072	.034	.084	.038
BERKSHIRE	MASSACHUSETTS	.074	.037	.086	.047	.064	.028	.071	.033
BRISTOL	MASSACHUSETTS	.086	.036	.098	.035	.074	.030	.084	.030
DUKES	MASSACHUSETTS	.085	.039	.104	.038	.075	.034	.090	.036
ESSEX	MASSACHUSETTS	.081	.043	.089	.048	.069	.035	.077	.040
FRANKLIN	MASSACHUSETTS	.081	.039	.094	.050	.071	.033	.082	.041
HAMPDEN	MASSACHUSETTS	.082	.039	.093	.053	.069	.030	.077	.035
HAMPSHIRE	MASSACHUSETTS	.082	.042	.093	.054	.070	.033	.077	.038
MIDDLESEX	MASSACHUSETTS	.075	.037	.089	.043	.065	.030	.079	.039
NANTUCKET	MASSACHUSETTS	.081	.045	.100	.055	.072	.037	.085	.045
NORFOLK	MASSACHUSETTS	.077	.038	.092	.038	.066	.032	.079	.033
PLYMOUTH	MASSACHUSETTS	.085	.037	.097	.034	.073	.031	.081	.029
SUFFOLK	MASSACHUSETTS	.071	.039	.086	.045	.060	.032	.074	.038
WORCESTER	MASSACHUSETTS	.081	.035	.099	.047	.071	.030	.082	.036
ALCONA	MICHIGAN	.051	.013	.058	.019	.049	.011	.056	.016
ALPENA	MICHIGAN	.047	.008	.056	.016	.046	.008	.054	.013
ARENAC	MICHIGAN	.049	.010	.056	.022	.047	.008	.053	.016
BAY	MICHIGAN	.045	.008	.049	.009	.044	.009	.047	.008
GENESEE	MICHIGAN	.047	.009	.053	.014	.045	.008	.049	.009
HURON	MICHIGAN	.053	.019	.063	.026	.048	.012	.056	.017
IOSCO	MICHIGAN	.049	.012	.059	.023	.047	.009	.055	.018
LAPEER	MICHIGAN	.047	.010	.053	.015	.042	.007	.046	.007
LENAWEE	MICHIGAN	.045	.012	.048	.010	.044	.012	.048	.010
LIVINGSTON	MICHIGAN	.046	.008	.049	.010	.046	.009	.047	.009
MACOMB	MICHIGAN	.047	.010	.060	.016	.041	.007	.046	.009
MONROE	MICHIGAN	.032	.008	.038	.009	.031	.009	.035	.008
MONTMORENCY	MICHIGAN	.047	.008	.056	.015	.047	.008	.054	.013
OAKLAND	MICHIGAN	.045	.008	.051	.011	.041	.006	.045	.006
OGEMAW	MICHIGAN	.048	.009	.055	.020	.047	.008	.053	.015
OSCODA	MICHIGAN	.050	.011	.057	.018	.049	.009	.055	.015
ST CLAIR	MICHIGAN	.043	.009	.056	.016	.037	.007	.043	.009
SAGINAW	MICHIGAN	.046	.009	.050	.008	.045	.009	.047	.008
SANILAC	MICHIGAN	.052	.016	.060	.017	.045	.010	.051	.009
SHIAWASSEE	MICHIGAN	.046	.010	.054	.013	.045	.009	.050	.008
TUSCOLA	MICHIGAN	.049	.012	.056	.018	.045	.007	.049	.009
WASHTENAW	MICHIGAN	.043	.008	.045	.008	.043	.008	.045	.008
WAYNE	MICHIGAN	.039	.008	.049	.013	.034	.007	.039	.008
BELKNAP	NEW HAMPSHIRE	.080	.042	.091	.052	.072	.035	.080	.041
CARROLL	NEW HAMPSHIRE	.080	.041	.091	.050	.074	.035	.082	.042
CHESHIRE	NEW HAMPSHIRE	.075	.038	.089	.044	.066	.031	.078	.036
COOS	NEW HAMPSHIRE	.067	.032	.079	.037	.063	.027	.074	.032
GRAFTON	NEW HAMPSHIRE	.074	.035	.087	.044	.068	.031	.078	.036
HILLSBOROUGH	NEW HAMPSHIRE	.077	.039	.091	.046	.068	.032	.081	.039

COUNTYNM	STATENM	BASE CASE				CONTROL CASE			
		MEAN7HR	STD7HR	MEANMAX	STDMAX	MEAN7HR	STD7HR	MEANMAX	STDMAX
MERRIMACK	NEW HAMPSHIRE	.078	.039	.086	.043	.070	.033	.077	.036
ROCKINGHAM	NEW HAMPSHIRE	.079	.045	.086	.048	.069	.035	.075	.039
STRAFFORD	NEW HAMPSHIRE	.081	.044	.089	.049	.072	.036	.079	.040
SULLIVAN	NEW HAMPSHIRE	.075	.041	.083	.041	.067	.034	.075	.034
ATLANTIC	NEW JERSEY	.054	.025	.071	.030	.038	.012	.047	.015
BERGEN	NEW JERSEY	.047	.019	.065	.026	.034	.012	.042	.014
BURLINGTON	NEW JERSEY	.059	.027	.077	.032	.039	.011	.050	.016
CAMDEN	NEW JERSEY	.050	.025	.065	.029	.033	.010	.043	.015
CAPE MAY	NEW JERSEY	.053	.024	.071	.031	.038	.012	.046	.014
CUMBERLAND	NEW JERSEY	.050	.020	.070	.026	.035	.009	.043	.010
ESSEX	NEW JERSEY	.048	.016	.064	.028	.033	.009	.040	.013
GLOUCESTER	NEW JERSEY	.046	.022	.060	.025	.032	.009	.039	.013
HUDSON	NEW JERSEY	.044	.015	.062	.030	.029	.010	.038	.015
HUNTERDON	NEW JERSEY	.048	.016	.059	.022	.034	.011	.040	.013
MERCER	NEW JERSEY	.052	.018	.068	.028	.033	.009	.041	.013
MIDDLESEX	NEW JERSEY	.056	.021	.075	.033	.035	.010	.044	.014
MONMOUTH	NEW JERSEY	.066	.038	.089	.044	.041	.015	.055	.022
MORRIS	NEW JERSEY	.051	.018	.064	.024	.037	.011	.043	.012
OCEAN	NEW JERSEY	.068	.033	.089	.040	.046	.014	.058	.020
PASSAIC	NEW JERSEY	.051	.020	.068	.025	.038	.011	.047	.013
SALEM	NEW JERSEY	.045	.019	.060	.021	.032	.009	.038	.012
SOMERSET	NEW JERSEY	.052	.015	.067	.023	.036	.009	.042	.012
SUSSEX	NEW JERSEY	.056	.020	.068	.023	.042	.012	.048	.013
UNION	NEW JERSEY	.051	.016	.068	.029	.034	.009	.041	.013
WARREN	NEW JERSEY	.046	.017	.056	.024	.033	.011	.039	.013
ALBANY	NEW YORK	.074	.030	.087	.037	.061	.021	.073	.027
ALLEGANY	NEW YORK	.057	.026	.069	.027	.050	.025	.060	.025
BRONX	NEW YORK	.044	.019	.063	.029	.032	.013	.043	.020
BROOME	NEW YORK	.057	.017	.070	.020	.048	.013	.059	.018
CATTARAUGUS	NEW YORK	.059	.031	.071	.032	.052	.027	.063	.030
CAYUGA	NEW YORK	.062	.017	.075	.020	.052	.018	.065	.019
CHAUTAUQUA	NEW YORK	.059	.030	.072	.032	.050	.024	.064	.029
CHEMUNG	NEW YORK	.059	.019	.064	.022	.050	.017	.055	.021
CHENANGO	NEW YORK	.057	.016	.070	.018	.048	.013	.059	.016
CLINTON	NEW YORK	.060	.019	.073	.030	.057	.015	.064	.021
COLUMBIA	NEW YORK	.074	.037	.087	.046	.061	.024	.071	.029
CORTLAND	NEW YORK	.058	.016	.069	.017	.048	.015	.059	.018
DELAWARE	NEW YORK	.063	.021	.072	.023	.052	.016	.059	.015
DUTCHESS	NEW YORK	.068	.042	.079	.044	.052	.021	.060	.022
ERIE	NEW YORK	.065	.028	.077	.027	.058	.025	.068	.028
ESSEX	NEW YORK	.070	.027	.082	.035	.063	.020	.072	.026
FRANKLIN	NEW YORK	.063	.021	.071	.023	.060	.020	.065	.021
FULTON	NEW YORK	.078	.033	.090	.033	.067	.026	.077	.026
GENESEE	NEW YORK	.069	.026	.091	.028	.062	.024	.083	.029
GREENE	NEW YORK	.075	.032	.084	.036	.062	.021	.070	.025
HAMILTON	NEW YORK	.076	.032	.087	.035	.068	.028	.076	.029
HERKIMER	NEW YORK	.072	.028	.079	.029	.063	.025	.069	.026
JEFFERSON	NEW YORK	.066	.021	.093	.038	.059	.021	.087	.040
KINGS	NEW YORK	.051	.021	.072	.033	.032	.011	.046	.023
LEWIS	NEW YORK	.066	.025	.088	.033	.060	.025	.080	.032
LIVINGSTON	NEW YORK	.058	.019	.075	.020	.052	.019	.068	.021
MADISON	NEW YORK	.063	.017	.071	.021	.051	.011	.061	.017
MONROE	NEW YORK	.065	.029	.088	.025	.058	.027	.082	.029
MONTGOMERY	NEW YORK	.076	.030	.087	.031	.065	.021	.075	.023

		BASE CASE				CONTROL CASE			
COUNTYNM	STATENM	MEAN7HR	STD7HR	MEANMAX	STDMAX	MEAN7HR	STD7HR	MEANMAX	STDMAX
NASSAU	NEW YORK	.056	.023	.073	.031	.038	.014	.050	.023
NEW YORK	NEW YORK	.041	.016	.058	.030	.027	.011	.039	.020
NIAGARA	NEW YORK	.075	.033	.093	.029	.069	.031	.084	.029
ONEIDA	NEW YORK	.069	.025	.080	.029	.059	.022	.070	.025
ONONDAGA	NEW YORK	.063	.016	.077	.025	.052	.014	.065	.024
ONTARIO	NEW YORK	.061	.017	.079	.020	.054	.017	.069	.020
ORANGE	NEW YORK	.056	.023	.069	.023	.043	.012	.050	.013
ORLEANS	NEW YORK	.075	.033	.094	.033	.068	.032	.089	.033
OSWEGO	NEW YORK	.066	.023	.087	.038	.057	.022	.078	.040
OTSEGO	NEW YORK	.065	.022	.073	.022	.053	.016	.061	.016
PUTNAM	NEW YORK	.060	.035	.073	.035	.045	.016	.052	.017
QUEENS	NEW YORK	.047	.019	.066	.030	.031	.011	.044	.023
RENSSELAER	NEW YORK	.072	.032	.091	.045	.063	.024	.075	.031
RICHMOND	NEW YORK	.053	.021	.074	.036	.033	.010	.045	.018
ROCKLAND	NEW YORK	.052	.024	.068	.025	.039	.012	.047	.013
ST LAWRENCE	NEW YORK	.065	.020	.077	.025	.060	.020	.072	.023
SARATOGA	NEW YORK	.072	.029	.092	.044	.062	.023	.077	.031
SCHENECTADY	NEW YORK	.073	.028	.088	.033	.062	.021	.074	.025
SCHOHARIE	NEW YORK	.072	.027	.083	.031	.059	.019	.068	.022
SCHUYLER	NEW YORK	.061	.019	.069	.022	.051	.017	.059	.022
SENECA	NEW YORK	.061	.017	.076	.020	.052	.018	.066	.018
STEUBEN	NEW YORK	.054	.020	.063	.021	.048	.019	.054	.021
SUFFOLK	NEW YORK	.077	.036	.099	.041	.054	.019	.067	.026
SULLIVAN	NEW YORK	.062	.023	.071	.026	.049	.014	.056	.016
TIOGA	NEW YORK	.058	.019	.065	.020	.049	.016	.055	.019
TOMPKINS	NEW YORK	.059	.016	.069	.019	.049	.015	.058	.020
ULSTER	NEW YORK	.067	.029	.075	.031	.054	.018	.060	.020
WARREN	NEW YORK	.073	.029	.095	.047	.063	.020	.082	.035
WASHINGTON	NEW YORK	.067	.026	.089	.043	.059	.020	.076	.030
WAYNE	NEW YORK	.062	.022	.083	.027	.055	.021	.074	.030
WESTCHESTER	NEW YORK	.054	.025	.067	.027	.040	.014	.048	.017
WYOMING	NEW YORK	.061	.023	.080	.022	.055	.023	.071	.026
YATES	NEW YORK	.059	.016	.073	.019	.051	.016	.063	.020
ADAMS	OHIO	.038	.009	.044	.009	.038	.009	.043	.009
ALLEN	OHIO	.045	.010	.050	.009	.044	.010	.048	.008
ASHLAND	OHIO	.040	.009	.046	.010	.035	.008	.040	.008
ASHTABULA	OHIO	.058	.041	.076	.036	.049	.034	.060	.033
ATHENS	OHIO	.028	.007	.032	.007	.027	.007	.031	.007
AUGLAIZE	OHIO	.045	.010	.050	.009	.045	.010	.048	.008
BELMONT	OHIO	.033	.012	.040	.015	.030	.008	.034	.009
BROWN	OHIO	.044	.009	.046	.009	.044	.009	.046	.009
CARROLL	OHIO	.041	.018	.056	.020	.035	.012	.045	.012
CHAMPAIGN	OHIO	.043	.009	.045	.009	.043	.009	.044	.009
CLARK	OHIO	.042	.009	.044	.009	.042	.009	.044	.009
CLERMONT	OHIO	.045	.009	.047	.009	.044	.009	.047	.009
CLINTON	OHIO	.044	.009	.045	.009	.044	.009	.045	.009
COLUMBIANA	OHIO	.043	.024	.055	.022	.036	.017	.044	.014
COSHOCTON	OHIO	.037	.015	.046	.015	.033	.012	.040	.011
CRAWFORD	OHIO	.036	.010	.043	.011	.034	.009	.039	.009
CUYAHOGA	OHIO	.045	.019	.062	.027	.037	.014	.050	.021
DELAWARE	OHIO	.040	.011	.047	.015	.038	.010	.043	.011
ERIE	OHIO	.049	.023	.063	.026	.040	.014	.052	.015
FAIRFIELD	OHIO	.038	.008	.041	.008	.036	.008	.038	.008
FAYETTE	OHIO	.040	.009	.043	.009	.040	.009	.042	.009

		BASE CASE				CONTROL CASE			
COUNTYNM	STATENM	MEAN7HR	STD7HR	MEANMAX	STDMAX	MEAN7HR	STD7HR	MEANMAX	STDMAX
FRANKLIN	OHIO	.038	.010	.043	.011	.036	.009	.040	.009
FULTON	OHIO	.044	.010	.047	.009	.044	.011	.047	.009
GALLIA	OHIO	.031	.007	.035	.008	.030	.008	.034	.008
GEAUGA	OHIO	.049	.025	.069	.033	.040	.017	.053	.023
GREENE	OHIO	.044	.009	.045	.009	.043	.009	.045	.009
GUERNSEY	OHIO	.035	.010	.045	.016	.032	.007	.038	.010
HANCOCK	OHIO	.042	.010	.046	.009	.041	.010	.045	.009
HARDIN	OHIO	.043	.011	.048	.010	.042	.010	.046	.008
HARRISON	OHIO	.039	.016	.050	.020	.034	.011	.041	.012
HENRY	OHIO	.046	.009	.048	.008	.046	.009	.048	.009
HIGHLAND	OHIO	.041	.009	.044	.009	.041	.009	.044	.009
HOCKING	OHIO	.034	.007	.039	.008	.033	.008	.037	.009
HOLMES	OHIO	.038	.011	.045	.010	.034	.009	.040	.008
HURON	OHIO	.041	.014	.051	.018	.035	.010	.043	.011
JACKSON	OHIO	.031	.008	.035	.008	.031	.008	.035	.008
JEFFERSON	OHIO	.036	.019	.043	.019	.031	.013	.035	.014
KNOX	OHIO	.037	.010	.045	.012	.034	.008	.040	.010
LAKE	OHIO	.051	.033	.076	.041	.041	.023	.059	.030
LAWRENCE	OHIO	.035	.008	.039	.009	.035	.009	.038	.009
LICKING	OHIO	.040	.014	.046	.016	.036	.010	.041	.011
LOGAN	OHIO	.044	.010	.048	.008	.044	.009	.047	.008
LORAIN	OHIO	.049	.017	.056	.019	.040	.012	.046	.012
LUCAS	OHIO	.040	.010	.045	.009	.039	.011	.043	.010
MADISON	OHIO	.040	.008	.042	.009	.039	.009	.041	.009
MAHONING	OHIO	.049	.028	.065	.030	.040	.020	.050	.020
MARION	OHIO	.038	.012	.044	.013	.037	.011	.041	.011
MEDINA	OHIO	.045	.015	.055	.018	.038	.012	.046	.013
MEIGS	OHIO	.025	.007	.027	.007	.024	.007	.027	.007
MONROE	OHIO	.028	.009	.035	.010	.027	.006	.032	.007
MORGAN	OHIO	.029	.008	.035	.008	.028	.007	.033	.008
MORROW	OHIO	.038	.009	.044	.012	.036	.009	.040	.010
MUSKINGUM	OHIO	.036	.011	.042	.013	.033	.009	.037	.009
NOBLE	OHIO	.030	.007	.035	.007	.028	.005	.032	.006
OTTAWA	OHIO	.044	.013	.054	.020	.038	.008	.045	.011
PERRY	OHIO	.036	.009	.040	.008	.033	.008	.037	.008
PICKAWAY	OHIO	.039	.008	.043	.008	.038	.008	.041	.008
PIKE	OHIO	.036	.008	.043	.008	.036	.008	.042	.008
PORTAGE	OHIO	.045	.019	.055	.021	.037	.014	.044	.015
PUTNAM	OHIO	.045	.009	.047	.010	.044	.009	.047	.009
RICHLAND	OHIO	.038	.008	.044	.010	.035	.008	.040	.009
ROSS	OHIO	.038	.007	.043	.008	.037	.007	.042	.008
SANDUSKY	OHIO	.040	.011	.049	.015	.035	.008	.043	.010
SCIOTO	OHIO	.035	.008	.042	.008	.035	.008	.041	.008
SENECA	OHIO	.037	.010	.045	.010	.034	.009	.042	.008
SHELBY	OHIO	.046	.010	.050	.008	.046	.010	.049	.008
STARK	OHIO	.043	.018	.052	.017	.036	.011	.043	.011
SUMMIT	OHIO	.042	.016	.054	.021	.036	.012	.044	.015
TRUMBULL	OHIO	.053	.034	.069	.041	.043	.025	.054	.030
TUSCARAWAS	OHIO	.040	.018	.052	.023	.034	.012	.042	.013
UNION	OHIO	.040	.010	.043	.010	.038	.009	.041	.009
VINTON	OHIO	.033	.007	.036	.008	.032	.008	.035	.008
WARREN	OHIO	.046	.009	.047	.010	.046	.009	.047	.010
WASHINGTON	OHIO	.024	.006	.030	.007	.023	.005	.029	.007
WAYNE	OHIO	.040	.011	.048	.011	.035	.008	.041	.007

BASE CASE

COUNTYNM	STATENM	MEAN7HR	STD7HR	MEANMAX	STDMAX
WOOD	OHIO	.041	.008	.045	.009
WYANDOT	OHIO	.039	.013	.044	.011
ADAMS	PENNSYLVANIA	.028	.007	.035	.009
ALLEGHENY	PENNSYLVANIA	.031	.017	.038	.019
ARMSTRONG	PENNSYLVANIA	.035	.015	.048	.019
BEAVER	PENNSYLVANIA	.036	.021	.045	.021
BEDFORD	PENNSYLVANIA	.027	.009	.030	.008
BERKS	PENNSYLVANIA	.036	.009	.042	.011
BLAIR	PENNSYLVANIA	.028	.009	.039	.016
BRADFORD	PENNSYLVANIA	.050	.017	.056	.017
BUCKS	PENNSYLVANIA	.047	.016	.055	.019
BUTLER	PENNSYLVANIA	.041	.021	.058	.030
CAMBRIA	PENNSYLVANIA	.028	.012	.037	.016
CAMERON	PENNSYLVANIA	.045	.019	.064	.025
CARBON	PENNSYLVANIA	.040	.012	.049	.014
CENTRE	PENNSYLVANIA	.037	.014	.045	.015
CHESTER	PENNSYLVANIA	.036	.010	.042	.014
CLARION	PENNSYLVANIA	.044	.021	.071	.032
CLEARFIELD	PENNSYLVANIA	.035	.013	.044	.015
CLINTON	PENNSYLVANIA	.045	.016	.054	.019
COLUMBIA	PENNSYLVANIA	.039	.017	.049	.021
CRAWFORD	PENNSYLVANIA	.056	.031	.081	.040
CUMBERLAND	PENNSYLVANIA	.031	.008	.038	.012
DAUPHIN	PENNSYLVANIA	.039	.012	.048	.019
DELAWARE	PENNSYLVANIA	.039	.016	.048	.027
ELK	PENNSYLVANIA	.045	.021	.067	.026
ERIE	PENNSYLVANIA	.053	.030	.077	.036
FAYETTE	PENNSYLVANIA	.023	.010	.027	.010
FOREST	PENNSYLVANIA	.051	.027	.082	.043
FRANKLIN	PENNSYLVANIA	.028	.010	.035	.012
FULTON	PENNSYLVANIA	.027	.010	.034	.010
GREENE	PENNSYLVANIA	.025	.010	.029	.011
HUNTINGDON	PENNSYLVANIA	.031	.012	.037	.012
INDIANA	PENNSYLVANIA	.027	.013	.035	.012
JEFFERSON	PENNSYLVANIA	.037	.018	.052	.018
JUNIATA	PENNSYLVANIA	.036	.014	.046	.020
LACKAWANNA	PENNSYLVANIA	.049	.013	.063	.019
LANCASTER	PENNSYLVANIA	.033	.008	.038	.010
LAWRENCE	PENNSYLVANIA	.049	.032	.068	.037
LEBANON	PENNSYLVANIA	.037	.011	.044	.016
LEHIGH	PENNSYLVANIA	.039	.014	.047	.014
LUZERNE	PENNSYLVANIA	.041	.014	.053	.019
LYCOMING	PENNSYLVANIA	.047	.016	.053	.019
MC KEAN	PENNSYLVANIA	.054	.024	.071	.032
MERCER	PENNSYLVANIA	.056	.034	.080	.047
MIFFLIN	PENNSYLVANIA	.035	.015	.044	.019
MONROE	PENNSYLVANIA	.047	.014	.056	.017
MONTGOMERY	PENNSYLVANIA	.040	.014	.050	.022
MONTOUR	PENNSYLVANIA	.037	.017	.050	.022
NORTHAMPTON	PENNSYLVANIA	.043	.017	.050	.019
NORTHUMBERLAND	PENNSYLVANIA	.040	.014	.053	.019
PERRY	PENNSYLVANIA	.035	.012	.043	.017
PHILADELPHIA	PENNSYLVANIA	.042	.019	.052	.026
PIKE	PENNSYLVANIA	.056	.017	.066	.020

CONTROL CASE

MEAN7HR	STD7HR	MEANMAX	STDMAX
.040	.009	.043	.009
.037	.011	.041	.010
.024	.006	.029	.007
.025	.012	.030	.014
.028	.011	.038	.014
.030	.014	.036	.015
.024	.007	.027	.008
.029	.006	.032	.006
.023	.008	.029	.008
.043	.015	.047	.016
.032	.009	.037	.011
.033	.015	.046	.021
.023	.008	.028	.008
.038	.017	.051	.019
.031	.007	.037	.007
.029	.007	.033	.006
.029	.007	.032	.008
.036	.016	.057	.023
.029	.009	.034	.009
.036	.010	.041	.011
.031	.010	.037	.012
.047	.025	.067	.036
.025	.006	.030	.007
.030	.006	.035	.009
.028	.007	.035	.012
.038	.017	.054	.020
.046	.024	.065	.032
.020	.007	.024	.006
.043	.024	.070	.035
.024	.005	.029	.006
.023	.006	.028	.007
.023	.008	.026	.008
.025	.007	.028	.007
.022	.008	.028	.007
.030	.013	.041	.011
.028	.007	.032	.008
.040	.008	.049	.014
.028	.007	.030	.007
.040	.023	.054	.027
.029	.006	.032	.007
.030	.009	.035	.008
.034	.009	.041	.012
.038	.010	.043	.013
.045	.019	.061	.026
.045	.025	.064	.035
.027	.006	.031	.007
.036	.008	.041	.009
.030	.007	.035	.009
.029	.010	.036	.012
.032	.010	.036	.011
.031	.007	.037	.008
.028	.007	.032	.008
.027	.008	.034	.012
.043	.009	.049	.012

		BASE CASE				CONTROL CASE			
COUNTYNM	STATENM	MEAN7HR	STD7HR	MEANMAX	STDMAX	MEAN7HR	STD7HR	MEANMAX	STDMAX
POTTER	PENNSYLVANIA	.051	.019	.063	.026	.042	.014	.055	.019
SCHUYLKILL	PENNSYLVANIA	.038	.010	.046	.014	.030	.006	.034	.006
SNYDER	PENNSYLVANIA	.040	.010	.056	.023	.031	.006	.037	.008
SOMERSET	PENNSYLVANIA	.027	.009	.031	.010	.023	.007	.027	.007
SULLIVAN	PENNSYLVANIA	.042	.018	.052	.018	.036	.015	.043	.015
SUSQUEHANNA	PENNSYLVANIA	.051	.013	.063	.019	.044	.010	.053	.017
TIOGA	PENNSYLVANIA	.051	.018	.060	.021	.043	.014	.048	.015
UNION	PENNSYLVANIA	.042	.011	.053	.017	.032	.006	.038	.007
VENANGO	PENNSYLVANIA	.055	.028	.082	.045	.045	.021	.068	.037
WARREN	PENNSYLVANIA	.055	.028	.076	.042	.046	.023	.066	.039
WASHINGTON	PENNSYLVANIA	.031	.011	.036	.013	.027	.008	.030	.008
WAYNE	PENNSYLVANIA	.055	.014	.065	.019	.044	.009	.052	.013
WESTMORELAND	PENNSYLVANIA	.028	.012	.034	.013	.023	.007	.026	.008
WYOMING	PENNSYLVANIA	.046	.015	.058	.018	.039	.012	.047	.015
YORK	PENNSYLVANIA	.033	.012	.037	.012	.026	.008	.029	.008
BRISTOL	RHODE ISLAND	.086	.037	.101	.039	.074	.030	.085	.032
KENT	RHODE ISLAND	.089	.036	.105	.037	.073	.027	.085	.028
NEWPORT	RHODE ISLAND	.088	.037	.104	.034	.075	.030	.087	.030
PROVIDENCE	RHODE ISLAND	.084	.033	.099	.035	.071	.026	.082	.028
WASHINGTON	RHODE ISLAND	.093	.037	.110	.034	.075	.027	.087	.028
ADDISON	VERMONT	.070	.031	.079	.036	.062	.022	.070	.027
BENNINGTON	VERMONT	.069	.029	.089	.040	.061	.023	.079	.033
CALEDONIA	VERMONT	.069	.030	.081	.039	.064	.026	.074	.033
CHITTENDEN	VERMONT	.070	.033	.078	.035	.064	.024	.071	.027
ESSEX	VERMONT	.063	.027	.078	.036	.060	.023	.073	.031
FRANKLIN	VERMONT	.068	.033	.074	.035	.062	.026	.068	.027
GRAND ISLE	VERMONT	.066	.028	.074	.032	.061	.022	.067	.024
LAMOILLE	VERMONT	.070	.035	.077	.036	.065	.028	.070	.029
ORANGE	VERMONT	.072	.035	.079	.039	.066	.029	.072	.032
ORLEANS	VERMONT	.062	.024	.073	.034	.059	.021	.068	.028
RUTLAND	VERMONT	.067	.030	.079	.038	.060	.023	.069	.027
WASHINGTON	VERMONT	.072	.034	.078	.036	.066	.028	.070	.028
WINDHAM	VERMONT	.071	.032	.085	.040	.061	.025	.074	.031
WINDSOR	VERMONT	.070	.036	.076	.039	.062	.029	.067	.030
ACCOMACK	VIRGINIA	.046	.009	.050	.012	.043	.010	.047	.009
ALBEMARLE	VIRGINIA	.040	.013	.044	.010	.040	.013	.044	.010
ARLINGTON	VIRGINIA	.028	.007	.037	.008	.025	.006	.033	.008
AUGUSTA	VIRGINIA	.038	.011	.042	.010	.038	.011	.041	.010
BATH	VIRGINIA	.040	.012	.045	.009	.040	.012	.045	.009
CAROLINE	VIRGINIA	.044	.008	.049	.013	.042	.009	.046	.009
CLARKE	VIRGINIA	.028	.006	.034	.007	.025	.006	.031	.007
CULPEPER	VIRGINIA	.034	.007	.039	.009	.033	.008	.038	.009
ESSEX	VIRGINIA	.045	.009	.052	.017	.043	.010	.047	.010
FAIRFAX	VIRGINIA	.029	.006	.037	.008	.026	.007	.034	.008
FAUQUIER	VIRGINIA	.029	.006	.036	.007	.028	.007	.034	.008
FREDERICK	VIRGINIA	.025	.006	.030	.008	.023	.006	.027	.008
GREENE	VIRGINIA	.036	.011	.039	.012	.035	.012	.039	.012
HANOVER	VIRGINIA	.043	.011	.047	.009	.042	.011	.047	.009
HIGHLAND	VIRGINIA	.032	.011	.036	.011	.032	.011	.035	.011
KING GEORGE	VIRGINIA	.042	.009	.049	.019	.039	.007	.044	.009
LOUDOUN	VIRGINIA	.027	.006	.035	.007	.025	.006	.032	.008
LOUISA	VIRGINIA	.042	.012	.046	.011	.041	.013	.046	.011
MADISON	VIRGINIA	.034	.009	.038	.010	.033	.009	.038	.010
NELSON	VIRGINIA	.041	.013	.046	.010	.041	.013	.046	.010

		BASE CASE				CONTROL CASE			
COUNTYNM	STATENM	MEAN7HR	STD7HR	MEANMAX	STDMAX	MEAN7HR	STD7HR	MEANMAX	STDMAX
NORTHUMBERLAND	VIRGINIA	.044	.009	.048	.010	.041	.010	.046	.010
ORANGE	VIRGINIA	.039	.011	.041	.011	.038	.011	.041	.012
PAGE	VIRGINIA	.030	.007	.035	.008	.028	.007	.033	.008
PRINCE WILLIAM	VIRGINIA	.032	.006	.038	.008	.029	.007	.036	.009
RAPPAHANNOCK	VIRGINIA	.030	.005	.037	.007	.029	.005	.035	.008
RICHMOND	VIRGINIA	.042	.010	.049	.012	.042	.011	.045	.011
ROCKBRIDGE	VIRGINIA	.043	.010	.047	.009	.043	.011	.047	.009
ROCKINGHAM	VIRGINIA	.030	.008	.034	.009	.029	.008	.033	.009
SHENANDOAH	VIRGINIA	.025	.007	.030	.008	.024	.006	.028	.008
SPOTSYLVANIA	VIRGINIA	.040	.008	.044	.009	.039	.009	.042	.010
STAFFORD	VIRGINIA	.037	.007	.043	.012	.034	.007	.038	.008
WARREN	VIRGINIA	.028	.006	.033	.007	.026	.006	.031	.007
WESTMORELAND	VIRGINIA	.043	.009	.048	.012	.041	.010	.044	.010
BARBOUR	WEST VIRGINIA	.025	.008	.030	.009	.024	.008	.028	.008
BERKELEY	WEST VIRGINIA	.026	.008	.032	.010	.023	.006	.028	.009
BOONE	WEST VIRGINIA	.044	.011	.046	.011	.044	.011	.046	.011
BRAXTON	WEST VIRGINIA	.031	.007	.036	.006	.030	.007	.034	.007
BROOKE	WEST VIRGINIA	.031	.017	.036	.019	.027	.011	.030	.013
CABELL	WEST VIRGINIA	.037	.013	.040	.011	.037	.013	.040	.011
CALHOUN	WEST VIRGINIA	.030	.009	.038	.008	.029	.009	.036	.010
CLAY	WEST VIRGINIA	.032	.010	.037	.010	.032	.010	.037	.010
DODDRIDGE	WEST VIRGINIA	.028	.007	.033	.008	.026	.007	.031	.008
FAYETTE	WEST VIRGINIA	.041	.012	.044	.011	.041	.012	.044	.011
GILMER	WEST VIRGINIA	.031	.007	.037	.008	.030	.007	.035	.009
GRANT	WEST VIRGINIA	.023	.008	.026	.008	.022	.007	.025	.008
GREENBRIER	WEST VIRGINIA	.042	.012	.046	.009	.041	.012	.046	.009
HAMPSHIRE	WEST VIRGINIA	.025	.008	.029	.008	.023	.007	.027	.007
HANCOCK	WEST VIRGINIA	.037	.023	.044	.023	.031	.016	.036	.017
HARDY	WEST VIRGINIA	.024	.007	.028	.009	.023	.007	.027	.008
HARRISON	WEST VIRGINIA	.024	.008	.028	.008	.023	.008	.027	.009
JACKSON	WEST VIRGINIA	.026	.009	.033	.009	.025	.009	.032	.010
JEFFERSON	WEST VIRGINIA	.026	.007	.034	.009	.024	.006	.031	.009
KANAWHA	WEST VIRGINIA	.033	.012	.037	.011	.033	.012	.036	.012
LEWIS	WEST VIRGINIA	.029	.007	.034	.007	.028	.006	.032	.007
LINCOLN	WEST VIRGINIA	.041	.011	.045	.010	.041	.012	.045	.010
LOGAN	WEST VIRGINIA	.045	.011	.048	.010	.045	.011	.047	.010
MARION	WEST VIRGINIA	.023	.008	.028	.011	.022	.007	.026	.009
MARSHALL	WEST VIRGINIA	.026	.010	.030	.010	.024	.008	.027	.008
MASON	WEST VIRGINIA	.028	.009	.034	.011	.027	.009	.033	.011
MINERAL	WEST VIRGINIA	.024	.009	.025	.009	.022	.008	.024	.008
MONONGALIA	WEST VIRGINIA	.024	.008	.029	.009	.022	.007	.026	.008
MORGAN	WEST VIRGINIA	.027	.009	.032	.009	.024	.007	.028	.008
NICHOLAS	WEST VIRGINIA	.037	.011	.040	.012	.036	.012	.040	.012
OHIO	WEST VIRGINIA	.034	.013	.039	.015	.030	.009	.033	.010
PENDLETON	WEST VIRGINIA	.028	.007	.033	.009	.027	.007	.032	.009
PLEASANTS	WEST VIRGINIA	.025	.007	.030	.010	.024	.006	.028	.009
POCAHONTAS	WEST VIRGINIA	.036	.010	.038	.010	.035	.010	.038	.010
PRESTON	WEST VIRGINIA	.023	.007	.026	.008	.022	.007	.024	.008
PUTNAM	WEST VIRGINIA	.031	.009	.036	.011	.031	.010	.036	.011
RANDOLPH	WEST VIRGINIA	.029	.007	.032	.009	.028	.007	.031	.009
RITCHIE	WEST VIRGINIA	.027	.007	.034	.008	.026	.007	.033	.009
ROANE	WEST VIRGINIA	.030	.010	.037	.009	.029	.009	.036	.009
TAYLOR	WEST VIRGINIA	.024	.009	.027	.010	.023	.008	.026	.009
TUCKER	WEST VIRGINIA	.026	.006	.030	.008	.025	.006	.029	.008

		BASE CASE				CONTROL CASE			
COUNTYNM	STATENM	MEAN7HR	STD7HR	MEANMAX	STDMAX	MEAN7HR	STD7HR	MEANMAX	STDMAX
TYLER	WEST VIRGINIA	.026	.008	.030	.010	.024	.007	.028	.009
UPSHUR	WEST VIRGINIA	.029	.007	.033	.007	.027	.007	.032	.007
WAYNE	WEST VIRGINIA	.039	.012	.043	.010	.039	.012	.043	.010
WEBSTER	WEST VIRGINIA	.033	.008	.037	.008	.032	.008	.036	.009
WETZEL	WEST VIRGINIA	.026	.009	.031	.011	.024	.008	.028	.009
WIRT	WEST VIRGINIA	.026	.009	.034	.009	.026	.009	.033	.010
WOOD	WEST VIRGINIA	.023	.005	.030	.008	.022	.006	.028	.008

Example of other types of concentration information provided by the simulation. Here we compare the 3, 12, and 24 hour averaged concentrations predicted at one of the 439 counties in the base and control simulations.

Base case results

```
--------------------------------COUNTYNM=LITCHFIELD   STATENM=CONNECTICUT-----------------------------

  DATE      AVG24     MAX24     MAX12S1    MAX12S2    AVG3S1    AVG3S2    AVG3S3    AVG3S4    AVG3S5

  80205     .021      .026      .026       .025       .019      .024      .026      .025      .024
  80206     .031      .039      .039       .038       .028      .033      .037      .039      .037
  80207     .043      .052      .052       .056       .041      .046      .051      .050      .046
  80208     .070      .093      .093       .089       .063      .071      .087      .093      .087
  80209     .115      .199      .199       .096       .112      .156      .194      .145      .082
  80210     .087      .106      .106       .074       .097      .104      .097      .077      .067
  80211     .063      .081      .072       .091       .070      .055      .046      .051      .063
  80212     .088      .099      .099       .080       .095      .096      .098      .087      .077
  80213     .063      .073      .073         .        .062      .064      .071      .066      .059
```

control case results

```
--------------------------------COUNTYNM=LITCHFIELD   STATENM=CONNECTICUT--------------------------------

  DATE      AVG24     MAX24     MAX12S1    MAX12S2    AVG3S1    AVG3S2    AVG3S3    AVG3S4    AVG3S5

  80205     .021      .025      .025       .024       .019      .024      .025      .025      .023
  80206     .029      .036      .036       .036       .026      .031      .034      .036      .035
  80207     .039      .047      .047       .051       .039      .044      .047      .044      .040
  80208     .056      .071      .071       .064       .057      .062      .069      .070      .061
  80209     .069      .109      .109       .080       .070      .093      .106      .079      .062
  80210     .077      .091      .091       .068       .084      .090      .085      .070      .061
  80211     .055      .068      .065       .074       .064      .052      .042      .042      .047
  80212     .072      .085      .085       .066       .081      .084      .084      .074      .064
  80213     .048      .056      .056         .        .051      .052      .055      .049      .040
```